CENTRAL LIBRARY
Birla Institute of Technology & Science
PILANI (Rajasthan)

Call No. 660.28427
E227I

Accession No. 51883

Acc. NO. 51883

ISSUE LABEL

*Not later than the latest date stamped below.*

INTRODUCTION TO

# The Transfer of Heat and Mass

# INTRODUCTION TO
# The Transfer of Heat and Mass

by E. R. G. ECKERT
*Professor of Mechanical Engineering*
*University of Minnesota*

WITH AN
APPENDIX ON PROPERTY VALUES

by Robert M. Drake, Jr.
*Instructor, Engineering Department, University of California*
*Berkeley*

McGRAW-HILL BOOK COMPANY, INC.

NEW YORK TORONTO LONDON
1950

INTRODUCTION TO THE TRANSFER OF HEAT AND MASS

Copyright, 1950, by the McGraw-Hill Book Company, Inc. Printed in the United States of America. All rights reserved. This book, or parts thereof, may not be reproduced in any form without permission of the publishers.

IV

THE MAPLE PRESS COMPANY, YORK, PA.

# PREFACE

The predecessor of this book is a German text with the same title which was written for students as an introduction to the transfer of heat and mass. I was advised that there was no book of similar scope in American literature. There are good elementary introductions on the one hand, and on the other, the excellent and widely used extensive treatment by W. H. McAdams, as well as the recently published book by M. Jakob. In addition to these, however, a short, systematic introduction, such as this book, which stresses the basic laws and at the same time presents all the fundamental knowledge existing today on this subject, should be useful on a level corresponding approximately to a course for graduate students. Since the German text was completed more than seven years ago, this book had to be written anew in many parts.

The book endeavors to arouse and widen the understanding of the physical processes and laws connected with heat and mass transfer. This, however, is not possible without analysis; therefore, formulas derived from analysis and proven by experiments are always preferred to relationships found by experiment alone. It is the opinion of the author that a physical process is understood thoroughly only where it is possible to calculate the occurrences from basic knowledge and when these calculated results are checked by experiments.

The foundation of all analysis and proper understanding of heat transfer is (in addition to the dimensional analysis introduced into this field by W. Nusselt) the boundary-layer theory by L. Prandtl. This theory is used widely in the book. For laminar flow, exact solutions of the boundary-layer equations are known. They are, however, difficult and tedious to derive; therefore, approximate solutions made possible by the use of the momentum equation as introduced by T. von Kármán and of the analogous heat- and mass-flow equations are preferred here. These solutions, when used with physical understanding, gave good results in all cases where they could be compared with experimental results or with exact solutions. The calculations following this method are much simpler than those for the exact solutions, and such calculations are possible in many cases where exact solutions are not as yet known. Laminar heat transfer is covered more extensively than usual in this book because recently interest has increased in the laminar range. For instance, heat-transfer processes in airplanes and missiles at high altitudes are very often in this region.

The analysis of turbulent heat exchange is based on Reynolds' analogy and its extension by L. Prandtl, G. I. Taylor, and T. von Kármán. This theory is now developed to such a degree that it allows the prediction of heat-transfer data from experimental friction data with fairly good accuracy. Generally, the accuracy with which heat-transfer values can be predicted should not be overestimated. An accuracy of 10 per cent is very satisfactory in heat-transfer calculations for industrial heat exchangers. Therefore, the numerical calculations in the examples have been done with a slide rule.

In the presentation of the material on heat transfer by forced convection, the usual path which first considers the flow in tubes was abandoned and was replaced by the treatment of the heat transfer from a flat plate. It is felt that in this way the student will remember more easily the fact that flow becomes fully developed only in long tubes. In short tubes the flow is more related to that over a plate.

There are so many relationships between the transfer of heat and the exchange of mass that both should be treated together. This introduction presents the laws of mass transfer only for the example of exchange of water vapor between air and surfaces. To cover the whole field of mass exchange would exceed the space available. It is hoped, however, that the knowledge of the basic laws will enable the student to read more easily the literature on special topics in this field.

The nomenclature in this book follows the recommendations as shown in ASA Z10.4—1943 "Letter Symbols for Heat and Thermodynamics Including Heat Flow." Only in a few places were deviations necessitated by the wide field covered in the book. The dimensionless moduli such as Reynolds number, had to take indices which would indicate the special way in which they were formed. To avoid congestion of indices, these moduli are designated by the first two letters of the scientist after whom they are named instead of an $N$ with the letters as indices as recommended in the above rules.

I dedicate this book to my colleagues in the field of heat transfer in this country. The reception which I found in their circle was so broadminded and cordial that it belongs among my finest reminiscences. This book would not have become a reality without the help of Robert M. Drake, Jr., and I wish to thank him especially for it. He not only prepared the Appendix on property values, the knowledge of which is necessary for heat- and mass-transfer calculations, but also read the text, corrected its English, made many suggestions which improved the understandability, and helped in many other ways. I am indebted to Dr. T. W. Jackson for his help in reading the proof.

E. R. G. ECKERT

DAYTON, OHIO
*February,* 1950

# CONTENTS

PREFACE . . . . . . . . . . . . . . . . . . . . . . . . . v

NOMENCLATURE . . . . . . . . . . . . . . . . . . . . . . xi

CHAPTER

1. FUNDAMENTAL PRINCIPLES OF HEAT TRANSFER . . . . . . . . . 1
   1. The different methods of heat transfer. . . . . . . . . . . 1
   2. Thermal conductivity, film and over-all heat transfer coefficients 3
   3. Parallel flow, counterflow, crossflow . . . . . . . . . . . . 9

2. HEAT CONDUCTION. . . . . . . . . . . . . . . . . . . . 19
   4. The basic equation of heat conduction. . . . . . . . . . . . 19
   5. The tube . . . . . . . . . . . . . . . . . . . . . 22
   6. The sphere. . . . . . . . . . . . . . . . . . . . . 25
   7. The rod. . . . . . . . . . . . . . . . . . . . . . 25
   8. Finned heating surfaces . . . . . . . . . . . . . . . . 29
   9. The wall with heat sources. . . . . . . . . . . . . . . 37
   10. The general heat-conduction equation. . . . . . . . . . . 40
   11. Unsteady heat flow. . . . . . . . . . . . . . . . . . 43
   12. The calculation of the regenerator . . . . . . . . . . . 54

3. HEAT TRANSFER BY CONVECTION. . . . . . . . . . . . . . . 59
   13. The various types of heat transfer . . . . . . . . . . . . 59

*Basic Conceptions of the Flow Theory*

14. Boundary layer and turbulence. . . . . . . . . . . . . . . 61
15. The momentum equation of the boundary layer . . . . . . . 66
16. The plane plate in longitudinal flow. . . . . . . . . . . . 68
17. The flow in a tube . . . . . . . . . . . . . . . . . . 79 ✓
18. Cylinder in crossflow . . . . . . . . . . . . . . . . . 83

*Forced Convection in Laminar Flow*

19. The heat-flow equation . . . . . . . . . . . . . . . . . 86
20. The plane plate in longitudinal flow. . . . . . . . . . . . 88
21. Cylindrical bodies in flow normal to their axes . . . . . . . . 95 ✓
22. Flow through a tube . . . . . . . . . . . . . . . . . . 98 ✓

*Forced Convection in Turbulent Flow*

23. Exchange of momentum and heat. . . . . . . . . . . . . . 106
24. Flow in a tube. . . . . . . . . . . . . . . . . . . . . 112 ✓

25. The plate in longitudinal flow . . . . . . . . . . . . . . . . 117
26. Recent improvements in the theory of turbulent heat transfer . 120
27. Dimensional analysis of heat transfer . . . . . . . . . . 128
28. Tubes and tube bundles in crossflow . . . . . . . . . . . . 140
29. Heat transfer in gases at high velocities . . . . . . . . . . . 150

*Free Convection*

30. Vertical plate and horizontal tube. . . . . . . . . . . . . . 158

*Condensation and Evaporation*

31. Condensation . . . . . . . . . . . . . . . . . . . . . . . 172
32. Evaporation. . . . . . . . . . . . . . . . . . . . . . . . 179
33. Heat transfer in gases at low densities. . . . . . . . . . . . 185

4. THERMAL RADIATION. . . . . . . . . . . . . . . . . . . . . 193
34. Basic conceptions. . . . . . . . . . . . . . . . . . . . . 193

*The Emission of Thermal Radiation*

35. The black body. . . . . . . . . . . . . . . . . . . . . . 195
36. Solid and liquid bodies . . . . . . . . . . . . . . . . . . 199
37. Gases. . . . . . . . . . . . . . . . . . . . . . . . . . 205

*Heat Exchange by Radiation*

38. Black bodies. . . . . . . . . . . . . . . . . . . . . . . 211
39. Solid, liquid, and gaseous bodies . . . . . . . . . . . . . . 215
40. Radiation of flames. . . . . . . . . . . . . . . . . . . . 219
41. The heat-transfer coefficient for radiation . . . . . . . . . . 223

5. THE EXCHANGE OF MASS . . . . . . . . . . . . . . . . . . 228
42. Basic equations for mixtures of two components . . . . . . . 228
43. The *s*-*i* diagram for moist air. . . . . . . . . . . . . . . 231
44. Diffusion . . . . . . . . . . . . . . . . . . . . . . . . 236
45. The boundary-layer equations of mass transfer. . . . . . . . 241
46. Similarity relations for mass transfer . . . . . . . . . . . . 249
47. The evaporation of water into air. . . . . . . . . . . . . . 254

APPENDIX . . . . . . . . . . . . . . . . . . . . . . . . . . 259

INDEX. . . . . . . . . . . . . . . . . . . . . . . . . . . . 279

# NOMENCLATURE

| | |
|---|---|
| $b$ | wall thickness |
| $c$ | specific heat |
| $c_p$ | specific heat at constant pressure |
| $d$ | diameter |
| $f$ | friction coefficient for flow through a tube (p. 81) |
| $f_c$ | drag coefficient of a cylinder (p. 85) |
| $f_p$ | friction coefficient of a plane plate (p. 72) |
| $g$ | acceleration of gravity |
| $h$ | film heat-transfer coefficient (p. 7) |
| $k$ | thermal conductivity |
| $l$ | length |
| $n$ | normal |
| $p$ | pressure |
| $q$ | heat flow per unit area (specific rate of heat flow) |
| $r$ | radius; heat generated by heat source per unit volume; heat of evaporation |
| $s$ | thickness, distance |
| $t$ | temperature |
| $t_B$ | bulk temperature (p. 100) |
| $t_{ad}$ | adiabatic temperature (which an unheated body assumes in an air stream of great velocity) (p. 152) |
| $u, v, w$ | velocity components |
| $v$ | specific volume |
| $v^*$ | shearing-stress velocity (p. 82) |
| $w$ | mass rate of flow |
| $x, y, z$ | coordinates |
| $A$ | area |
| $C$ | constant, circumference |
| $E$ | voltage |
| $G$ | weight flow |
| $I$ | electric current |
| $L$ | length |
| $L_e$ | entrance length (p. 65) |
| $M$ | molecular weight |
| $Q$ | heat flow |
| $R$ | electric resistance, gas constant |
| $R_c$ | thermal conduction resistance (p. 5) |
| $R_t$ | thermal convection resistance (p. 8) |
| $T$ | absolute temperature |

| | |
|---|---|
| $U$ | over-all heat-transfer coefficient (p. 8) |
| $V$ | volume flow, velocity |
| $W$ | weight, power |
| $\alpha$ | angle, thermal diffusivity (p. 42) |
| $\beta$ | expansion coefficient |
| $\gamma$ | specific weight |
| $\delta$ | boundary-layer thickness (p. 63) |
| $\delta_t$ | thermal boundary-layer thickness (p. 86) |
| $\epsilon$ | eddy diffusivity (p. 121) |
| $\zeta$ | ratio of thermal and flow boundary-layer thicknesses |
| $\theta$ | temperature difference |
| $\lambda$ | electric conductivity |
| $\mu$ | dynamic viscosity |
| $\nu$ | kinematic viscosity |
| $\rho$ | density, radius, electric resistivity |
| $\tau$ | shearing stress, time |
| $\Theta$ | temperature difference |

## ADDITIONALLY FOR HEAT RADIATION

| | |
|---|---|
| $e$ | emissive power (p. 194) |
| $i$ | radiation intensity (p. 196) |
| $F$ | geometrical factor (p. 212) |
| $L_e$ | equivalent radius (p. 210) |
| $\alpha$ | absorptivity (p. 193) |
| $\beta$ | angle |
| $\epsilon$ | emissivity (p. 195) |
| $\lambda$ | wave length |
| $\rho$ | reflectivity (p. 193) |
| $\sigma$ | Boltzmann constant (p. 198) |
| $\tau$ | transmissivity (p. 193) |
| $\omega$ | solid angle |

## ADDITIONALLY FOR MASS EXCHANGE

| | |
|---|---|
| $c$ | concentration |
| $i$ | enthalpy |
| $p$ | total pressure |
| $p_a$ | partial pressure of air |
| $p_v$ | partial pressure of vapor |
| $p_s$ | saturation pressure |
| $r$ | relative humidity (p. 229) |
| $s$ | specific humidity (p. 229) |
| $C_p$ | specific heat per unit volume |
| $D$ | diffusion coefficient |
| $M$ | molecular weight |
| $R$ | gas constant |
| $\mathcal{R}$ | universal gas constant |
| $V$ | volume |

| | |
|---|---|
| $W$ | weight |
| $\delta_p$ | diffusion boundary-layer thickness (p. 246) |
| $\rho$ | relative humidity (p. 230) |
| $\sigma$ | evaporation coefficient (p. 255) |

## DIMENSIONLESS VALUES

| | |
|---|---|
| $Re_x$ | Reynolds number, built with length $x$ (p. 71) |
| $Re_d$ | Reynolds number, built with diameter $d$ (p. 80) |
| $Nu_x$ | Nusselt number, built with length $x$ (p. 92) |
| $Nu_d$ | Nusselt number, built with diameter $d$ (p. 100) |
| $Pr$ | Prandtl number (p. 90) |
| $Gr$ | Grashof number for heat transfer (p. 137) |
| $Gr_D$ | Grashof number for mass transfer (p. 253) |
| $Ma$ | Mach number (p. 138) |
| $St$ | Stanton number (p. 113) |
| $Sc$ | Schmidt number (p. 250) |

## INDICES

| | |
|---|---|
| $w$ | values on the wall surface |
| $i$ | inlet |
| $e$ | exit |
| $m$ | mean value |
| $M$ | arithmetic mean value |
| $cr$ | critical values for transition to turbulent flow |
| $s$ | values in the stream outside the boundary layer |
| $b$ | values on the border between laminar sublayer and turbulent boundary layer |
| $t$ | turbulent |
| $0$ | values on a reference point |
| $\infty$ | values at great distance from a body |
| $st$ | static values (static pressure, etc.) |
| $T$ | total values (total pressure, etc.) |
| $dy$ | dynamic values (dynamic pressure, etc.) |

## CHAPTER 1

# FUNDAMENTAL PRINCIPLES OF HEAT TRANSFER

### 1. The different methods of heat transfer

In the course of time, temperature differences in a body are equalized by heat flowing from regions of higher temperatures to those of lower temperature. This process takes place in all substances which are found in nature, in solid bodies as well as in liquids and in gases. Knowledge of the laws and procedure governing this process is of great importance in the entire field of engineering, since by virtue of this knowledge means are available for channeling the flow of heat in a desirable manner.

For instance, one may be given the task of improving upon the flow of heat by any possible means. This, for instance, is applicable to the case of heat exchangers for heating and cooling in the chemical industry. Applied to heat engines we are confronted with this task again and again. According to the theory of thermodynamics, such a heat engine consists in principle of two heat accumulators at different temperatures, with the engine that performs the work placed in between. In such applications, the heat vehicle frequently changes in the course of the working process. The heat must then be exchanged between the individual heat vehicles using the smallest possible temperature drop. In steam power plants the heat is contained initially in the combustion gases. In the steam boiler the heat is transferred to the steam. In the condenser the steam gives off its heat to the cooling water, and the cooling water while passing through the cooling tower transfers this heat to the air. In the case of combustion engines this type of heat exchange does not exist, since the heat is produced by combustion directly in the air, performing work, and the waste heat as well as the waste gases are jointly exhausted. In spite of all this, a complete understanding of heat transmission is also of great importance for the design of combustion engines since here, by using air or water coolants, the cylinder walls must be kept at temperatures which can be safely withstood by the material. Therefore the admissible output of a cylinder of a high-performance engine is determined essentially by solution of cooling problems. For gas turbines, now entering, at an increasing rate, a stage of economical and reliable industrial application, the mastery of heat-transmission problems is likewise of fundamental significance.

On the other hand, we often face the task of preventing an undesirable amount of heat transfer in so far as is possible. This can be done by application of a heat-retaining layer of a material (insulator) with a low coefficient of thermal conductivity. The prevention of heat losses is also of far-reaching influence on the efficiency of heat engines. According to the second law of thermodynamics, a quantity of heat generally is the more valuable for use the higher its temperature. Any decrease of the temperature without performance of work increases the entropy, which means that there occurs an undesirable loss of mechanical energy.

In a solid body the flow of heat is the result of the transfer of thermal energy from one molecule to another. This process is called *conduction.* The same process takes place within liquids and gases. In these substances, however, the molecules are no longer confined to a certain point, but constantly change their places, even if the substance is in a state of rest. In this manner thermal energy is transferred. The heat transfer by this process is also included in heat transfer by conduction.

In addition there is still another mode of heat transfer in liquids and gases. Here the transfer of heat from one point to another may be effected by carrying along the heat with the flowing substance (by macroscopic motions). This process is called *heat transmission by convection.*

A third mode of heat transfer is the result of *radiation.* Solid bodies, as well as liquids and gases, are capable of radiating thermal energy in form of electromagnetic waves, and of picking up radiant energy by absorption. In industrial processes all three mechanisms often participate in the mutually superimposed transmission of heat. For a study of these phenomena, however, it is necessary to discriminate clearly between the various mechanisms since they are subject to different laws. First we consider the processes of heat conduction and convection. Heat radiation will be dealt with separately in a later section.

## 2. Thermal conductivity, film and over-all heat-transfer coefficients

In technical computations we are, above all, interested in the quantity of heat being exchanged per unit of time between two liquids or two gases at different temperatures, if the substances are separated by a wall. According to the statements made in the introduction it has already become clear that in this case a superposition of diverse processes occurs. First, the heat of one gas (or one liquid) has to be brought to the separating wall. Subsequently the heat must pass through the separating wall and, finally, from the other wall surface it flows into the cooler gas (or the cooler liquid). This section is to deal with the computation of heat flow for the simplest case, namely, a plane wall with temperatures constant with respect to time, in order thus to introduce the fundamental laws of heat transmission. The individual processes will be thoroughly investigated in the following sections.

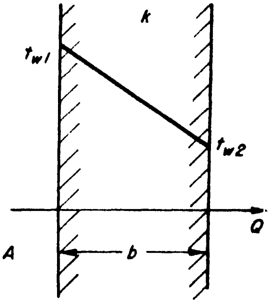

FIG. 1. Steady heat conduction through a plane wall.

Thus, we consider at first a plane wall with the thickness $b$, both surfaces of which are kept at different, but constant, temperatures $t_{w1}$ and $t_{w2}$ in steady state (Fig. 1). The quantity of heat which by this temperature difference is caused to flow through the area $A$ of the wall per unit of time is called the *rate of heat flow*, and will be designated by $Q$.[1] For this quantity of heat, Fourier's law is valid:

$$Q = \frac{k}{b} A(t_{w1} - t_{w2}) \tag{1}$$

where $k$, the *thermal conductivity*, is a property of the substance of which the wall consists. From Eq. (1) its dimension[2] can easily be derived:

---

[1] Differing from thermodynamics, where $Q$ means any amount of heat without reference to time.

[2] In the formulas of dimensions in this book the symbol ° for degree is omitted when temperatures in degrees Fahrenheit (°F), or degrees Rankine (°R), when counted from the absolute zero point, are given, since it may easily lead to confusions with power marks.

$$\mathbf{k} = \frac{\mathbf{Qb}}{\mathbf{A}(\mathbf{t}_{w1} - \mathbf{t}_{w2})} \qquad \mathrm{Btu/(hr)(ft)(F)}$$

The amount of heat penetrating a unit area of the surface per unit of time is called the *specific rate of heat flow.* For this, therefore, the following equation is valid:

$$q = \frac{Q}{A} = \frac{k}{b}(t_{w1} - t_{w2}) \tag{2}$$

As illustrated in Fig. 1 the temperature within the wall decreases linearly from the value $t_{w1}$ to $t_{w2}$, if the thermal conductivity is independent of the temperature. The thermal conductivities of a number of substances are indicated in the Appendix of this book. There it appears that, among solid bodies, metals have the highest values for thermal conductivities. For instance, iron has a thermal conductivity of approximately 30 Btu/(hr)(ft)(F); copper of approximately 200 Btu/(hr)(ft)(F). Metal alloys have substantially lower thermal conductivity values than those of the pure substances. Stainless steel, for instance, has a value for thermal conductivity of about 9 Btu/(hr)(ft)(F). Nonmetallic substances have thermal conductivity values of approximately 0.03 to 2 Btu/(hr)(ft)(F). The quantity of heat flowing through such bodies therefore is only 1/1,000 to $\frac{1}{100}$ of the quantity flowing through metals at the same temperatures and with the same dimensions. The thermal conductivity of liquids is approximately 0.06 to 0.3 Btu/(hr)(ft)(F). That of gases is only one-tenth as large. Gases, therefore, have the lowest thermal conductivity values of all substances. The low thermal conductivity of heat-insulating materials (diatomaceous earth, slag wool, peat, cork) are accounted for by their porosity. The flow of heat in these materials, therefore, is essentially a process of heat conduction through the air contained in the pores. The solid substance has only the task of preventing the air from getting into motion as a result of the temperature differences and thereby precluding deliverance of additional heat by convection. Fourier's law[1] for the heat-conduction process very much resembles Ohm's law for electric currents. This can readily be seen if Eq. (1) is stated in the following form:

---

[1] Jean Baptiste Jos. Fourier (1768–1830).

$$t_{w1} - t_{w2} = \frac{b}{kA} Q \tag{3}$$

and compared with Ohm's law:

$$E = RI \tag{4}$$

The heat flow $Q$ corresponds here to the electric current $I$. The driving force for the heat flow is the temperature difference $(t_{w1} - t_{w2})$; this corresponds to the driving force for the electric current, or the impressed voltage $E$. The expression $b/kA$ is called *the thermal resistance of the heat-conducting process* and is designated by $R_c$ (it corresponds here to Ohm's resistance $R$), or

$$R_c = \frac{b}{kA} \tag{5}$$

The inverse value of thermal conductivity, *i.e.*, the specific resistance to heat conduction, corresponds to specific resistance in electrical engineering,

$$\frac{1}{k} = R_c \frac{A}{b}$$

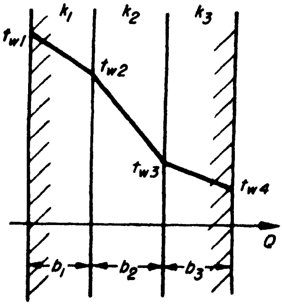

FIG. 2. Steady heat conduction through a composite plane wall.

Assuming a plane wall to be composed of several layers, *e.g.*, three, of different materials with thermal conductivities $k_1$, $k_2$, $k_3$, and designating the temperatures at the adjoining faces by $t_{w2}$ and $t_{w3}$ (Fig. 2), we can put down Eq. (3) for each layer:

$$t_{w1} - t_{w2} = \frac{b_1}{k_1 A} Q$$

$$t_{w2} - t_{w3} = \frac{b_2}{k_2 A} Q$$

$$t_{w3} - t_{w4} = \frac{b_3}{k_3 A} Q$$

By adding all the equations we obtain the expression

$$t_{w1} - t_{w4} = \left(\frac{b_1}{k_1 A} + \frac{b_2}{k_2 A} + \frac{b_3}{k_3 A}\right) Q = (R_{c1} + R_{c2} + R_{c3})Q \tag{6}$$

With this equation the heat flow $Q$ can be calculated from the temperatures of the two surfaces $t_{w1}$ and $t_{w4}$. The resistance to heat conduction of the composite wall equals the sum of the thermal resistances of the single layers. In this case, therefore, the same law can be applied as for resistors connected in series as used in electrical engineering.

As for heat exchangers in engineering practice, we are mostly concerned with walls separating liquids or gases from each other. In these cases we do not know the temperatures of both surfaces of the separating walls, but only the temperatures of the liquids on both sides of the wall. In Fig. 3 these temperatures are indicated as $t_1$ and $t_2$. By measuring the temperature field in the liquids one obtains the curves shown. The temperature gradient is confined to a relatively narrow layer of thickness $\delta$ quite close to the wall, whereas at a greater distance from the wall in most cases only small temperature differences exist. Simplified, this temperature curve can be replaced by the dashed broken line. This can be explained by assuming that a thin film of liquid (of the thickness $\delta'$) adheres to the wall, whereas outside this film all temperature differences vanish as a result of mixing motions of the liquid. This picture oversimplifies the actual process considerably as we shall see later, but it comprises the salient features and has the advantage of being explicitly clear. Within the film the heat transfer takes place by conduction, as in a solid wall. The temperature curve in the film, therefore, is again linear, and the flow of heat follows from Eq. (1), whereby the thermal conductivity $k$ of the liquid or of the gas, and the thickness of the film $\delta'$, are to be inserted.

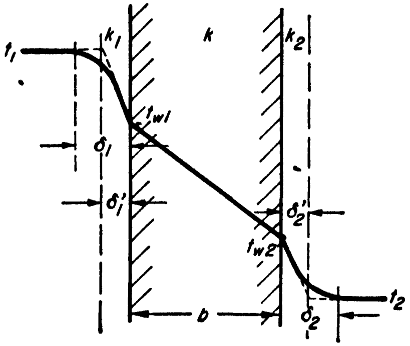

FIG. 3. Steady film heat transfer and heat conduction in a plane wall.

Thus, for the heat flow to the wall the equation

$$Q = \frac{k}{\delta'} A(t - t_w) \tag{7}$$

is obtained. From this equation the rate of heat flow $Q$ can be calculated as soon as the film thickness $\delta'$ is known. The latter, however, depends to a very great extent upon the external flow conditions, for instance, upon the velocity with which the liquid flows along the wall, upon the shape of the wall, upon the nature of the wall surface, and similar factors. In engineering practice it is the usual procedure to calculate with the expression $k/\delta'$, rather than directly with the film thickness $\delta'$. This value is called *film heat-transfer coefficient* and is designated by the letter $h$. Thus the mathematical expression

$$\mathbf{Q = hA(t - t_w)} \tag{8}$$

already established by Isaac Newton (1643–1727) is obtained. For some time in the beginning the heat-transfer coefficient $h$ was considered a property of the flowing liquid or gas. It was not until the more recent developments of the theory of heat transmission that the intricate relations became apparent which hold for this value. In this book a chapter of greater length is devoted to the evaluation of the heat-transfer coefficients. The orders of magnitude of the heat-transfer coefficients as they occur under engineering conditions have been compiled in Table 1. This indicates approximately the relative sizes of these values. Since the heat-transfer coefficient is the quotient of thermal conductivity and film thickness, it is to be expected that gases, because of their smaller thermal conductivity, have smaller heat-transfer coefficients than liquids. Table 1 confirms this conclusion.

TABLE 1. ORDER OF MAGNITUDE OF FILM HEAT-TRANSFER COEFFICIENTS

| | Btu/(hr)(ft$^2$)(F) |
|---|---|
| Flowing air | 2– 50 |
| Flowing water | 100–1000 |
| Boiling water | 500–1000 |
| Condensing water vapor | 1000–5000 |

Applying Eq. (8) to the two surfaces in Fig. 3 produces

$$Q = h_1A(t_1 - t_{w1})$$
$$Q = h_2A(t_{w2} - t_2)$$

Both these heat quantities must be of the same magnitude in steady state. These equations, too, can be put into the form corresponding to Ohm's law:

$$\begin{aligned} t_1 - t_{w1} &= \frac{1}{h_1 A} Q \\ t_{w2} - t_2 &= \frac{1}{h_2 A} Q \end{aligned} \tag{9}$$

The value $1/hA$ is called *thermal resistance* $R_t$ of the film heat-transfer process

$$R_t = \frac{1}{hA} \tag{10}$$

By adding Eq. (3) to Eqs. (9) and summing all the equations a relation is obtained between the heat flow through the separating wall and the two temperatures $t_1$ and $t_2$ (Fig. 3):

$$\begin{aligned} t_1 - t_{w1} &= \frac{1}{h_1 A} Q \\ t_{w1} - t_{w2} &= \frac{b}{kA} Q \\ t_{w2} - t_2 &= \frac{1}{h_2 A} Q \\ \hline t_1 - t_2 &= \left(\frac{1}{h_1 A} + \frac{b}{kA} + \frac{1}{h_2 A}\right) Q \\ &= (R_{t1} + R_c + R_{t2})\, Q = R_0 Q \end{aligned} \tag{11}$$

The sum of the individual resistances is the thermal resistance $R_0$ of the over-all heat-transfer process. In this case also, for the total process, the same law applies as for electric resistances connected in series. Instead of the resistances, technical calculation in most cases employ the thermal conductivities and heat-transfer coefficients. For these, the following relations are valid, which result readily from equation (11):

$$\mathbf{Q = UA(t_1 - t_2)} \tag{11a}$$

$$\mathbf{\frac{1}{U} = \frac{1}{h_1} + \frac{b}{k} + \frac{1}{h_2}} \tag{11b}$$

The value $U$ is called the *over-all heat-transfer coefficient:* it has the dimension Btu/(hr)(ft²)(F). Considering a wall, consisting of several layers with different thermal conductivities $k_i$ and the thicknesses $b_i$, the middle term in Eq. (11*b*) is replaced by the sum $\Sigma b_i/k_i$.

✓**Example 1.** A plane iron wall, 0.5 in. thick, is washed by air on both sides, the heat-transfer coefficients $h_1 = h_2$ being 2 Btu/(hr)(ft$^2$)(F) (Table 1). The values of the over-all thermal resistance and of the over-all heat-transfer coefficient are to be calculated. The heat conductivity of the wall is $k = 30$ Btu/(hr)(ft)(F). According to Eq. (11),

$$
\begin{aligned}
R_0 &= \frac{1}{A}\left(\frac{1}{h_1} + \frac{b}{k} + \frac{1}{h_2}\right) = \frac{1}{A}\left(\frac{1}{2} + \frac{1}{24 \times 30} + \frac{1}{2}\right) \\
&= \frac{721}{720}\,\frac{1}{A} \qquad \text{(hr) (F)/Btu}
\end{aligned}
$$

The over-all heat-transfer coefficient is $U = 1/AR = 1$ Btu/(hr)(ft$^2$)(F). The thermal resistance to heat conduction of the iron wall therefore is absolutely negligible for the heat passage. If it is intended to increase the heat flow, it is useless to decrease this resistance. The heat-transfer coefficients, however, must be enlarged.

**Example 2.** An iron wall, 0.5 in. thick, and an aluminum wall, 1.0 in. thick, are laid one upon another, leaving an air space of 0.0005 in. between them. The thermal resistance of this composite wall is to be calculated. According to Eq. (6) and Table 13 (Appendix),

$$
\begin{aligned}
R_C &= \frac{1}{A}\left(\frac{b_1}{k_1} + \frac{b_2}{k_2} + \frac{b_3}{k_3}\right) = \frac{1}{A}\left(\frac{1}{24 \times 30} + \frac{0.0005}{12 \times 0.014} + \frac{1}{12 \times 132}\right) \\
&= \frac{1}{A}\left(\frac{1}{720} + \frac{1}{336} + \frac{1}{1{,}584}\right) \qquad \text{(hr)(F)/Btu}
\end{aligned}
$$

The thermal resistance of the composite wall above is therefore influenced essentially by the air space, which, however small, cannot be avoided even by the most careful construction. The resistance without an air space would be

$$
\frac{1}{A}\left(\frac{1}{720} + \frac{1}{1{,}584}\right) \qquad \text{(hr)(F)/Btu}
$$

which is less than one-half the above.

## 3. Parallel flow, counterflow, crossflow

The preceding section treated heat exchange between two gases or liquids on the assumption that the temperatures on both sides of the heating surface would be constant over the surface $A$. As a matter of fact, the temperatures of the two liquids mostly change while passing along the heating surface, as a result of the heat exchange. Hence, a mean temperature difference is to be inserted into the formulas of the previous section. This mean temperature difference will now be calculated. The first case to be considered shows both liquids flowing past the heating surface in the same direction (Fig. 4); this is called *parallel flow*. Plotted also in Fig. 4 are the temperature trends of both liquids as they flow along the heating surface $A$. Now consider a surface element of the size $dA$. The temperatures of the liquids at this point are $t_1$ and $t_2$. The temperature difference between the two liquids is to be denoted by $\Delta t$. Hence, for the point considered, the equation

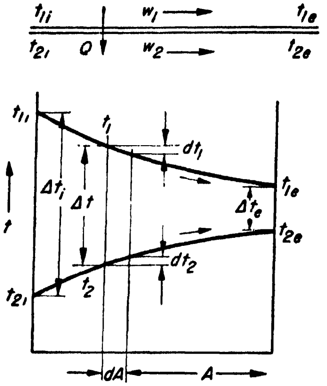

FIG. 4. Over-all heat transfer in parallel flow.

$$\Delta t = t_1 - t_2 \tag{12}$$

is valid. The heat flow $dQ$ through the area $dA$ is given by Eq. (11*a*), *i.e.*, with the symbols applied here,

$$dQ = U\,dA\,\Delta t \tag{13}$$

The over-all heat-transfer coefficient $U$ is assumed constant along the heating surface. Because of the heat exchange, the hotter liquid cools by the amount $dt_1$. For this the relation

$$dQ = -w_1c_1\,dt_1 \tag{14}$$

is valid, if $w_1$ is the weight of liquid flowing along the heating surface per unit of time (the weight rate of flow), and $c_1$ is its specific heat. The factor $w_1c_1$ represents the water equivalent or heat capacity of the weight rate of liquid flow. According to the equation

$$dQ = w_2c_2\,dt_2 \tag{15}$$

the colder fluid in the same manner is heated by the amount $dt_2$; $w_2$ and $c_2$ are the weight rate of flow and the specific heat of the second fluid respectively. By differentiating Eq. (12),

$$d(\Delta t) = dt_1 - dt_2 \tag{16}$$

If the temperature differentials from Eqs. (14) and (15) are substituted herein,

$$d(\Delta t) = -\left(\frac{1}{w_1c_1} + \frac{1}{w_2c_2}\right) dQ = -\mu\, dQ \tag{17}$$

if the symbol $\mu$ is chosen instead of the expression in parenthesis. Equation (17) can be integrated immediately. Expressing the temperature difference at the beginning (intake) of the heating surface $A$ by $\Delta t_i$, and at the end by $\Delta t_e$,

$$\Delta t_i - \Delta t_e = \mu Q \tag{18}$$

Inserting the heat flow $dQ$ from Eq. (13) into Eq. (17), the relation

$$\frac{d(\Delta t)}{\Delta t} = -\mu U\, dA \tag{19}$$

is obtained, and integration across the entire heating surface $A$, with consideration of the boundary condition ($A = 0$; $\Delta t = \Delta t_i$), gives

$$\ln \frac{\Delta t_e}{\Delta t_i} = -\mu UA \tag{20}$$

The temperature difference at the end of the heating surface, therefore, can be calculated with the aid of the equation

$$\Delta t_e = \Delta t_i e^{-\mu UA} \tag{21}$$

By replacing the value $\mu$ in Eq. (18) from Eq. (20) there is obtained for the heat flow through the entire heating surface $A$ the relation,

$$Q = UA\,\frac{\Delta t_i - \Delta t_e}{\ln \Delta t_i/\Delta t_e} \tag{22}$$

The fraction on the right-hand side of the equation represents nothing more than the mean temperature difference $\Delta t_m$ looked for. The rate of heat flow, therefore, can be calculated with the aid of the following formulas

$$\mathbf{Q = UA\,\Delta t_m} \tag{23}$$

$$\mathbf{\Delta t_m = \frac{\Delta t_i - \Delta t_e}{\ln \Delta t_i/\Delta t_e}} \tag{24}$$

Another group of heat exchangers is built in such a way that the two liquids flow in opposite directions, as shown in Fig. 5.

This arrangement is called *counterflow*. In this case, calculation of the mean temperature difference is accomplished in the same manner as in the case of parallel flow, except that in Eq. (15) there appears a minus sign, since the cooler liquid likewise cools off when proceeding along the heating surface $A$ in a positive direction. The value $\mu$ thereby is shown as follows:

$$\mu = \frac{1}{w_1c_1} - \frac{1}{w_2c_2} \tag{25}$$

Formulas (21), (22), (23), and (24) of the preceding paragraph remain unchanged and apply also to counterflow.

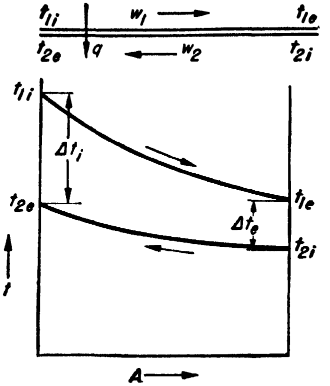

FIG. 5. Over-all heat transfer in counterflow.

The mean temperature difference calculated according to Eq. (24) is always smaller than the arithmetic mean value $\Delta t_M$ of the initial and final temperature differences:

$$\Delta t_M = \frac{\Delta t_i + \Delta t_e}{2} \tag{26}$$

The ratio $a$ of the logarithmic mean of Eq. (24) to the arithmetic mean is dependent on the ratio $\Delta t_i/\Delta t_e$ of the temperature differences as shown in Table 2. This table may be employed for

TABLE 2. RATIO $a$ OF THE LOGARITHMIC MEAN TEMPERATURE DIFFERENCE $\Delta t_m$ TO THE ARITHMETIC MEAN $\Delta t_M$ FOR PARALLEL FLOW AND COUNTERFLOW*

$$\Delta t_m = a\,\Delta t_M$$

| $\frac{\Delta t_i}{\Delta t_e}$ | $a$ | $\frac{\Delta t_i}{\Delta t_e}$ | $a$ | $\frac{\Delta t_i}{\Delta t_e}$ | $a$ | $\frac{\Delta t_i}{\Delta t_e}$ | $a$ |
|---|---|---|---|---|---|---|---|
| 1.0 | 1.000 | 2.0 | 0.962 | 3.0 | 0.910 | 6.0 | 0.798 |
| 1.2 | 0.998 | 2.2 | 0.952 | 3.5 | 0.889 | 7.0 | 0.770 |
| 1.4 | 0.991 | 2.4 | 0.942 | 4.0 | 0.867 | 8.0 | 0.748 |
| 1.6 | 0.981 | 2.6 | 0.928 | 4.5 | 0.846 | 9.0 | 0.729 |
| 1.8 | 0.971 | 2.8 | 0.918 | 5.0 | 0.829 | 10.0 | 0.710 |

* The values in the table are valid also for the reciprocal values $\Delta t_e/\Delta t_i$.

a simpler determination of the logarithmic mean value by calculating the arithmetic mean and then multiplying this value by the factor *a* indicated in the table.

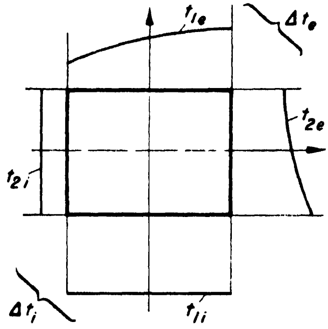

Fig. 6. Over-all heat transfer in crossflow.

A third method of guiding liquids in a heat exchanger is to cause the two liquids to flow at right angles to each other. This is called *crossflow* and is illustrated in Fig. 6. As shown there, one liquid flows in front of the heating surface, the other one behind it. The calculation of the mean temperature difference is considerably more difficult in this case than in the case of parallel flow or counterflow; such a calculation was carried out by W. Nusselt.[1] As shown in Fig. 6, the temperatures of the two liquids, when leaving the heating surface, are not uniform across the cross section of the outlet. The mean outlet temperatures are now expressed by the symbol $t_e$. The value

$$\Delta t_i = t_{1i} - t_{2i} \tag{27}$$

is to be understood as the initial temperature difference. In this equation $t_{1i}$ represents the inlet temperature of the hot fluid, and $t_{2i}$ represents the inlet temperature of the cold fluid. Accordingly, the final temperature difference is given by the expression

$$\Delta t_e = t_{1e} - t_{2e} \tag{28}$$

with $t_{1e}$ the mean outlet temperature of the substance giving off heat, and $t_{2e}$ the mean outlet temperature of the substance absorbing heat. The mean temperature difference in this case depends not only on the ratio $\Delta t_i/\Delta t_e$, but also on the ratio, $w_1c_1/w_2c_2$, of the heat capacities of the two liquids. From Table 3, calculated on the basis of the results of Nusselt's investigation, the ratio of the logarithmic mean temperature difference $\Delta t_m$ to the arithmetic mean $\Delta t_M$ can be found, and therewith the

---

[1] W. Nusselt, *Z. Ver. deut. Ing.*, **55**, 2091 (1911); and *Forsch. Gebiete Ingenieurw.*, **1**, 417 (1930).

TABLE 3. RATIO $a$ OF THE TRUE MEAN TEMPERATURE DIFFERENCE $\Delta t_m$ TO THE ARITHMETIC MEAN $\Delta t_M$ FOR CROSSFLOW (FROM VALUES CALCULATED BY W. NUSSELT)*

$$\Delta t_m = a\,\Delta t_M$$

| $w_1c_1/w_2c_2$ \ $\Delta t_e/\Delta t_i$ | 0.9 | 0.8 | 0.7 | 0.6 | 0.5 | 0.4 | 0.3 | 0.2 | 0.1 |
|---|---|---|---|---|---|---|---|---|---|
| 0 | 0.998 | 0.993 | 0.986 | 0.978 | 0.962 | 0.939 | 0.902 | 0.836 | 0.707 |
| 0.2 | 0.998 | 0.993 | 0.987 | 0.981 | 0.971 | 0.958 | 0.936 | 0.902 | 0.848 |
| 0.5 | 0.998 | 0.993 | 0.988 | 0.982 | 0.977 | 0.968 | 0.945 | 0.935 | 0.913 |
| 1 | 0.998 | 0.993 | 0.989 | 0.983 | 0.978 | 0.974 | 0.961 | 0.948 | 0.933 |

| $w_1c_1/w_2c_2$ \ $\Delta t_e/\Delta t_i$ | 0 | −0.1 | −0.2 | −0.3 | −0.4 | −0.5 | −0.6 | −0.7 | −0.8 |
|---|---|---|---|---|---|---|---|---|---|
| 0 | 0 | | | | | | | | |
| 0.2 | 0.762 | 0.630 | | | | | | | |
| 0.5 | 0.874 | 0.819 | 0.750 | 0.632 | 0.519 | | | | |
| 1 | 0.912 | 0.876 | 0.835 | 0.766 | 0.710 | 0.618 | 0.500 | 0.380 | 0.220 |

* The values in this table are valid also for the reciprocal values $w_2c_2/w_1c_1$.

mean temperature difference can be determined as was done earlier in the case of parallel flow and counterflow.

The smallest heating surface for a given rate of heat flow and at given initial and final temperature differences is obtained with the liquids flowing in counterflow. Parallel flow requires the largest heating surface. Moreover, counterflow is more favorable than parallel flow, in so far as with it, the outlet temperature $t_{2e}$ of the heated liquid can be raised to a temperature higher than the outlet temperature $t_{1e}$ of the heating liquid (Fig. 5). The same result can be attained with crossflow (in the region of the negative values of $\Delta t_e/\Delta t_i$ in Table 3). With respect to the size of the heating surface, crossflow lies between the two other possibilities. The difference in the heating surface is greatest when the heat capacities of both liquids have the same magnitude. When the heat capacity of one liquid is greater, the difference in the heating surfaces becomes smaller. If the heat capacity of one liquid becomes infinite, there exists no longer any difference in the size of the heating surface. This case is illustrated in Fig. 7. Here the temperature of the one liquid remains constant along the heating surface and, really, in this case one cannot speak of parallel flow, counterflow, or crossflow any more. Practically, the temperature curve shown in Fig. 7, for instance, occurs with the evaporation or condensation of a liquid.

If the heat capacity is the same for both liquids, the initial temperature difference $\Delta t_i$ becomes, according to Eq. (18), equal to the final temperature difference $\Delta t_e$ in case of counterflow, as Eq. (25) in this case gives $\mu = 0$. The logarithmic and the arithmetic mean likewise have the same magnitude

$$\Delta t_m = \Delta t_M = \Delta t_i \tag{29}$$

In this case, the temperatures change linearly along the heating surface. Hence, temperature curves result, as shown in Fig. 8.

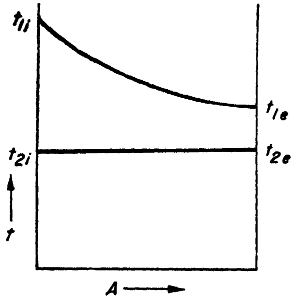

Fig. 7. Heat transfer with infinite heat capacity of one fluid.

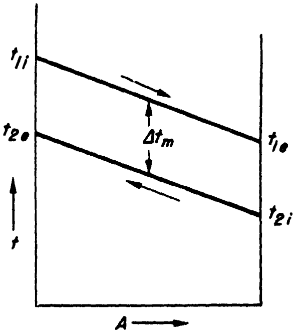

Fig. 8. Counterflow heat transfer with equal heat capacity of both fluids.

The heating surface need not have the shape of a plane wall as shown in Figs. 4 to 8. The cooling of liquids and gases while passing through a bundle of tubes can likewise be calculated with the previously derived formulas (Fig. 9). These relations, however, are strictly valid only when the number of tube rows is very large, though practically the same formulas are applied even if there is a small number of tube rows.

With the preceding calculations, the over-all heat-transfer coefficient $U$ was assumed constant along the heating surface. As this frequently is not the case, it is necessary to divide the entire heating surface into single sections, the over-all heat-transfer coefficient of each of which varies but so slightly that it can be assumed to be constant. Thus, these single sections can be calculated with the given formulas.

Heat exchange in parallel flow and counterflow has also been treated for the case in which the over-all heat-transfer coefficient varies linearly with the temperature.[1] The formula

$$Q = A \frac{U_e \, \Delta t_i - U_i \, \Delta t_e}{\ln U_e \, \Delta t_i / U_i \, \Delta t_e}$$

now takes the place of the Eqs. (23) and (24). Alternatively, we may also calculate with an average over-all heat-transfer coefficient. The reference temperature for this can be taken from diagrams.[2]

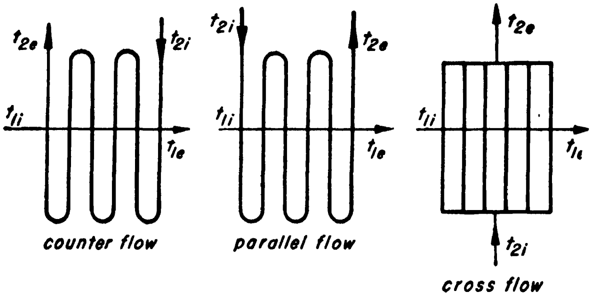

FIG. 9. Counterflow, parallel flow, and crossflow on tube bundles.

Besides the combinations dealt with in this chapter and represented in Fig. 9, others are encountered in practice, as for instance, mixed parallel flow and counterflow. The temperature differences to be inserted into Eq. (23) for a large number of these combinations were treated in an extensive investigation and plotted in diagrams by Bowman, Mueller, and Nagle.[3]

**Example.** $w_1 = 100$ lb per hr of water is to be heated from 50 to 170 F with flue gases having an initial temperature of 330 F. The quantity of the flue gases is $w_2 = 400$ lb/hr; their specific heat $c_p = 0.25$ Btu/(lb)(F); the over-all heat transfer coefficient $U = 20$ Btu/(hr)(ft$^2$)(F). The size of the heating surface $A$ is to be calculated for parallel flow, counterflow, and crossflow.

First, the cooling of the flue gases can be found for each case with the aid of a heat balance. The heat absorption of the water is

[1] J. Nikuradse, *Proc. Intern. Congr. Appl. Mech.*, 3d Congr., **1**, 239, Stockholm, 1930.

[2] A. P. Colburn, *Ind. Eng. Chem.*, **25**, 873–877 (1933).

[3] R. A. Bowman, A. C. Mueller, and W. M. Nagle, *Trans. ASME*, **62**, 283–294 (1940).

$$100(170 - 50) = 12{,}000 \text{ Btu/hr}$$

When there are no heat losses, the heat delivery of the flue gases must be equal to the heat absorbed by the water. From this relation we can calculate the final temperature of the gases:

$$12{,}000 = 400 \times 0.25(330 - t_e); \quad t_e = 210 \text{ F}$$

With *parallel* flow the following scheme is valid for the temperatures along the heating surface:

$$280 \text{ F} \left(\begin{array}{c} 330 \text{ F} \rightarrow 210 \text{ F} \\ \hline 50 \text{ F} \rightarrow 170 \text{ F} \end{array}\right) 40 \text{ F}$$

The initial temperature difference therefore is $\Delta t_i = 280$ F and the final temperature difference $\Delta t_e = 40$ F. The arithmetic mean becomes $\Delta t_M = (280 + 40)/2 = 160$ F and the ratio $\Delta t_i/\Delta t_e = 280/40 = 7$. The value $a = 0.77$ is taken from Table 2. Thus we obtain the logarithmic mean temperature difference $\Delta t_m = 0.77 \times 160 = 123$ F. From Eq. (23) it follows that

$$A = \frac{12{,}000}{(20 \times 123)} = 4.88 \text{ ft}^2$$

For *counterflow* we obtain from the scheme, $160 \text{ F} \left(\begin{array}{c} 330 \text{ F} \rightarrow 210 \text{ F} \\ \hline 170 \text{ F} \leftarrow 50 \text{ F} \end{array}\right) 160 \text{ F}$, where $\Delta t_i = \Delta t_e = 160$ F. Thus $\Delta t_i/\Delta t_e = 1$; therefore $a = 1$. Hence, the logarithmic mean is $\Delta t_m = 160$ F and

$$A = \frac{12{,}000}{(20 \times 160)} = 3.75 \text{ ft}^2$$

According to the following scheme, there is for *crossflow:*

$$\Delta t_i = 280 \text{ F} \qquad \Delta t_e = 40 \text{ F} \qquad \Delta t_M = \frac{280 + 40}{2} = 160 \text{ F}$$

$$\frac{\Delta t_e}{\Delta t_i} = 0.143 \qquad \text{and} \qquad \frac{w_1 c_1}{w_2 c_2} = 1$$

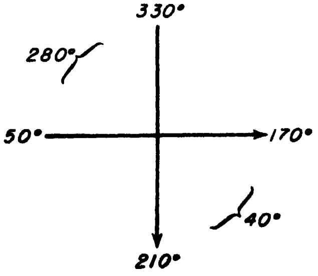

It follows by interpolation from Table 3 that $a = 0.940$ and therewith $\Delta t_m = 0.940 \times 160 = 150$ F. The size of the heating surface thereby becomes

$$= \frac{12{,}000}{20 \times 150} = 4 \text{ ft}^2$$

The results show that counterflow requires the smallest and parallel flow the largest heating surface. The size of the heating surface for parallel flow increases to a very considerable extent with greater heating of the water. At a water outlet temperature of 190 F, the final temperature difference will be $\Delta t_e = 0$ and therefore the heating surface will be infinite. Hence, it follows that an increase above this temperature cannot be obtained by parallel flow, but only by counterflow or crossflow.

# CHAPTER 2

# HEAT CONDUCTION

## 4. The basic equation of heat conduction

In this section the process of heat conduction is discussed in detail. As mentioned in the introduction, flow of heat in solid bodies takes place exclusively by this process. In liquids and gases, however, the processes of heat conduction, convection, and radiation occur simultaneously. The problems dealt with in this section may first of all be applied to solid bodies; in particular cases, however, where heat exchange by convection is prevented and heat transfer by radiation is low, they may be applied as well to gases and liquids. The basic equation for the steady-state process of heat conduction in a plane wall was given in the preceding chapter [Eq. (1)]. In steady state, a linear temperature gradient occurs in such a wall, as illustrated in Fig. 1. Strictly, however, this holds only if the thermal conductivity of the wall is independent of temperature. This linear temperature curve likewise does not exist in unsteady heating or cooling processes, so that in these cases, Eq. (1) cannot be employed. The linear course of the temperature gradient in a plane wall in steady state is due to the fact that a constant flow of heat on its way through the material has always the same cross-sectional area at its disposal or in other words that the specific rate of heat flow is constant. Generally the specific rate of heat flow varies locally and in time. Equation (1) may then be applied only to parts of the body of infinitely small dimensions. We assume a plane located in any direction within the body, and on this plane we consider the surface element $dA$. The rate of heat flow through this surface element is to be calculated. The normal to this element will be called $n$. Figure 10 shows the surface element $dA$ in a manner that makes the normal $n$ to the surface appear in the plane of the drawing. The temperature curve along this normal has likewise been shown. The temperature varies by the amount $\partial t$ within the infinitely small range $\partial n$.

The temperature curve can be considered linear within this range so that Eq. (1) may be employed again. The temperature difference ($t_{w1} - t_{w2}$) in Eq. (1) is to be replaced by the differential $\partial t$; the place of the wall thickness $b$ is taken by the differential $\partial n$, where $n$ is the line normal to the plane of the surface element $dA$. In this way, for the rate of heat flow $dQ$ through the surface $dA$, the equation

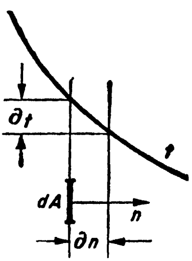

FIG. 10. General heat conduction.

$$\mathbf{dQ = -kdA \frac{\partial t}{\partial n}} \tag{30}$$

is obtained. The minus sign in this equation indicates that the heat flow proceeds in the direction of a temperature drop, that is, in the direction of a negative rise of temperature $\partial t/\partial n$.[1] For the specific rate of heat flow $q_n$ through the differential element, the equation

$$q_n = -k \frac{\partial t}{\partial n} \tag{31}$$

is obtained. Equation (30) is the mathematical expression for the physical fact that the rate of heat flow through an area $dA$, taken at random in the body, is proportional to the thermal conductivity $k$, to the size of the differential element $dA$, and to the temperature gradient in the direction of the normal to the plane of the differential element. In giving the specific rate of heat flow for any place within a body, one must also specify the location of the differential area by specifying the direction of the normal $n$ to that area. The subscript $n$ in Eq. (31) is retained to emphasize this. Equations (30) and (31) are the general equations for the process of heat conduction. The general equation for heat conduction also has its analogy in the range of electricity. Ohm's law for a conductor of any shape has the form

$$dI = -\lambda\, dA \frac{\partial E}{\partial n} \tag{32}$$

In this equation the electric current $I$ corresponds to the heat flow $Q$ in Eq. (30), the electric potential $E$ corresponds to the temperature $t$, and the electric conductivity $\lambda$ ($\lambda = 1/\rho$ where $\rho$ is the resistivity) corresponds to the thermal conductivity $k$. As Eqs. (30) and (32) have the same form, the temperature field within a heated body and the field of the electric potential in a body of the same shape correspond to one another, provided the temperature distribution on the surface is similar to the distribution of the electric potential. This analogy enables one to study heat-flow problems from electrical models. For example, let us consider the task of determining the heat loss of an insulated tube. In Fig. 11, the tube is represented by the circle $a$, the outer surface of the insulation by line $b$. It may be assumed that the outer surface cannot be circular for any reasons, but must have two grooves $c$. The temperatures along the inner and along the outer surface may be constant. It is difficult to calculate the heat loss through such an insulation. For a model test, a cross section of the insulation is cut from a thin metal sheet. The tube $a$ and the outer surface $b$ of the insulation are represented by two copper strips which must be intimately connected with the metal sheet. Then the two copper strips are connected with the two poles of an electric battery and the current $I$ is measured, which flows through this electric circuit when the potential difference of the battery is $\Delta E$. The heat $Q$ flowing through the length $L$ of the tube insulation, is derived from the equation

---

[1] The partial differential signs $\partial$ merely express that within the body the temperature curve is taken into consideration on the normal to the plane only.

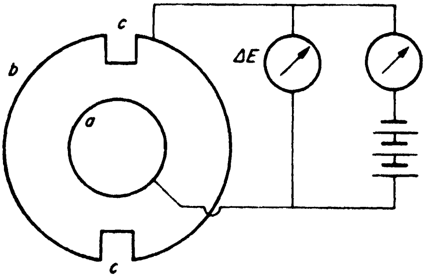

FIG. 11. Electrical model for investigating heat conduction through insulation.

$$Q = I \frac{k}{\lambda} \frac{\Delta t}{\Delta E} \frac{L}{s}$$

where $k$ is the thermal conductivity of the insulation, $\lambda$ is the electric conductivity of the metal sheet of thickness $s$, and $\Delta t$ is the temperature difference between the tube $a$ and the outer surface of the insulation. The electric potential at any point within the insulation is proportional to the temperature at the same spot. The metal sheet may be replaced by a liquid. Such a device is called an electrolytic trough.

## 5. The tube

Except for the plane wall, the tube is the most common shape in industrial installations in which heat transfer occurs. The heat flow through a tube will now be calculated when the inner and outer surface have constant but different temperatures. In Fig. 12, the cross section is depicted through such a tube with an inner radius $r_i$ and an outer radius $r_a$. For the heat flow through an element of the tube wall limited by the two cylindrical surfaces with radii $r$ and $(r + dr)$ we may use Eq. (30). As we know beforehand that the temperature is constant on cylindrical surfaces, we may insert $dA = 2\pi rl$, when $l$ is the length of the tube.

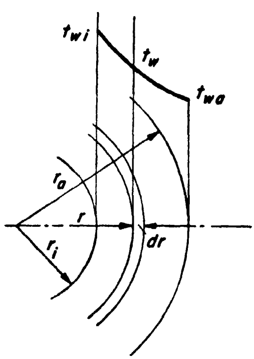

FIG. 12. Steady heat conduction in a thick-walled tube.

$$Q = -k2\pi rl \frac{dt}{dr} \tag{32a}$$

Since the temperature depends only on the radius, we may replace the sign $\partial$ for the partial differential by the sign $d$ for the total differential. The tables in the Appendix show that the thermal conductivity $k$ is a function of the temperature for all materials. In steady state, the same amount of heat flows through every cylindrical section of the tube. Therefore, the heat flow $Q$ is independent of radius $r$. For integration of Eq. (32$a$) the variables are separated:

$$\frac{dr}{r} = -\frac{2\pi l}{Q} k(t)\, dt$$

Integration between the limits $r_i$ and $r_a$ gives

$$\ln \frac{r_a}{r_i} = \frac{2\pi l}{Q} \int_{t_{wa}}^{t_{wi}} k(t)\, dt$$

If a mean value

$$k_m = \frac{1}{t_{wi} - t_{wa}} \int_{t_{wa}}^{t_{wi}} k(t)\, dt$$

is inserted, we find

$$\ln \frac{r_a}{r_i} = \frac{2\pi l k_m}{Q} (t_{wi} - t_{wa}) \qquad (32b)$$

The same expression is obtained when the thermal conductivity is assumed independent of temperature in Eq. (32*a*). It is therefore possible to calculate with $k$ as a constant magnitude, when the value of $k$ at mean temperature is inserted in the equation. The exact value of this mean temperature cannot be derived for all problems. As the temperature dependency of $k$ is not great, however, it is sufficient in most cases to use the arithmetic mean of the limiting temperatures.

The heat flow is found by solving Eq. (32*b*) for $Q$:

$$Q = k_m \frac{2\pi l}{\ln r_a/r_i} (t_{wi} - t_{wa}) \qquad (33)$$

We can give this equation a shape, which corresponds exactly to Eq. (1) for a plane wall, by introducing a mean radius $r_m$:

$$\mathbf{Q} = \mathbf{k}_m \frac{2\pi \mathbf{r}_m \mathbf{l}}{\mathbf{r}_a - \mathbf{r}_i} (\mathbf{t}_{wi} - \mathbf{t}_{wa}) \qquad (34)$$

$$\mathbf{r}_m = \frac{\mathbf{r}_a - \mathbf{r}_i}{\ln \mathbf{r}_a/\mathbf{r}_i} \qquad (35)$$

The area $A$ in Eq. (1) is replaced here by the area $2\pi r_m l$, and the plane wall thickness $b$ is replaced by the thickness $(r_a - r_i)$ of the tube wall. The mean radius $r_m$ is established by the same expression as the mean logarithmic temperature difference for parallel flow and counterflow [Eq. (24)]. It can be found, therefore, with the help of Table 2. The term $\Delta t_i$ has been replaced here by $r_a$ and $\Delta t_e$ by $r_i$.

We now take into consideration the heat transfer on the outer and inner surface of the tube. For the heat transfer on the outer surface, the equation

$$Q = h_a 2\pi r_a l (t_{wa} - t_a) \qquad (36)$$

holds, in which $h_a$ is the heat-transfer coefficient and $t_a$ the temperature of the liquid or gas surrounding the tube. In the same way,

$$Q = h_i 2\pi r_i l (t_i - t_{wi}) \qquad (37)$$

with $h_i$ as heat-transfer coefficient on the inner surface and $t_i$ as temperature of the liquid or gas in the tube. By solving Eqs.

(34), (36), and (37) for the temperature differences and adding them we get

$$t_i - t_a = \left(\frac{1}{h_a r_a} + \frac{1}{r_m}\frac{r_a - r_i}{k_m} + \frac{1}{h_i r_i}\right)\frac{Q}{2\pi l}$$

The heat flow $Q$ therefore is

$$\mathbf{Q} = \frac{2\pi \mathbf{r}_m \mathbf{l}}{\frac{\mathbf{r}_m}{\mathbf{r}_a}\frac{\mathbf{1}}{\mathbf{h}_a} + \frac{\mathbf{r}_a - \mathbf{r}_i}{\mathbf{k}_m} + \frac{\mathbf{r}_m}{\mathbf{r}_i}\frac{\mathbf{1}}{\mathbf{h}_i}}(\mathbf{t}_i - \mathbf{t}_a) \tag{38}$$

This equation corresponds to Eq. (11) for the plane wall and differs only inasmuch as each heat-transfer coefficient is multiplied by a corresponding ratio of radii.

For a thin wall, the radii $r_a$, $r_m$, and $r_i$ have practically the same magnitude. In this case the formula for the plane wall holds true. If the tube is composed of several layers with different thermal conductivities, the mean summand in the denominator of Eq. (38) must be replaced by the sum $\sum \frac{r_m}{r_{mj}}\frac{r_{aj} - r_{ij}}{k_j}$ where $k_j$, $r_{aj}$, $r_{ij}$, and $r_{mj}$ are, respectively, the conductivity, the outer, inner, and mean radius of a single layer; and $r_m$ is the mean radius of the composite tube. The equations derived in this paragraph are of special importance for calculating the heat losses of insulated tubes.

**Example.** In a tube with 3.6 in. inside diameter there flows superheated steam at 400 F. The tube is insulated with slag wool 1.8 in. thick. The temperature of the surrounding air is 40 F. The heat loss per foot length of the tube is to be calculated. The heat-transfer coefficient from the steam to the tube wall is 10 Btu/(hr)(ft$^2$)(F) (approximately, as shown for air, Table 1); the heat-transfer coefficient on the outer surface to the surrounding air is 1 Btu/(hr)(ft$^2$)(F). The arithmetic mean between the inner radius $r_i = 1.8$ in. and the outer radius $r_a = 3.6$ in. is $r_M = 2.7$ in. $= 0.225$ ft, and the ratio $r_a/r_i = 2$. From Table 2, $a = 0.962$ and, therefore, the logarithmic mean

$$r_m = ar_M = 0.962 \times 0.225 = 0.216 \text{ ft.}$$

The thermal conductivity of slag wool is $k = 0.027$ Btu/(hr)(ft)(F) at 200 F. Equation (38) gives

$$Q = \frac{2\pi \times 0.216}{0.216/0.3 \times 1 + 0.15/0.027 + 0.216/0.15 \times 10} \times 360$$
$$= 76.2 \qquad \text{Btu/(hr)(ft)}$$

As can be seen, the heat loss is influenced only slightly by the heat-transfer coefficients. It is not necessary, therefore, to know these values accurately. The thermal resistance of the iron tube wall could be neglected as being very small.

### 6. The sphere

The heat flow through the wall of a spherical vessel with an inner radius $r_i$ and an outer radius $r_a$ can be calculated in the same way as that through a tube. We use Eq. (30) for a thin layer between two spherical surfaces with radii $r$ and $(r + dr)$, respectively. The surface $dA$ is then $4\pi r^2$ and the thickness of the layer is $dr$. The solution of the differential equation, which is found very easily, is

$$Q = \frac{4\pi k}{1/r_i - 1/r_a} (t_{wi} - t_{wa}) \tag{39}$$

The heat transfer on both surfaces of the vessel can be included in the same way as in the previous paragraph.

### 7. The rod

The heat flow is to be considered through a rod which is cooled on its surface by any gas or liquid, and which is connected at its base to a heated wall. The temperature of this wall is $t_l$ (Fig. 13). The cross-sectional area of the rod may be $A$, its circumference $C$, its length $l$. The heat-transfer coefficient $h$ may have a constant value over the whole surface. Also, the area $A$ and the circumference $C$ are constant along the rod length. We consider a volume element of the rod with the length $dx$ at a distance $x$ from the wall. The heat flow through this element is given by the equation

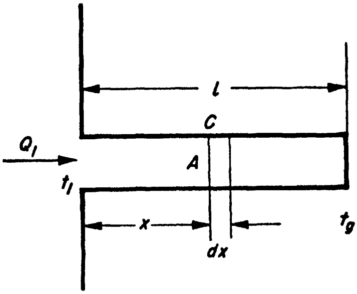

FIG. 13. Steady heat conduction in a rod.

$$Q = -kA\frac{dt}{dx} \tag{40}$$

in which $t$ denotes the temperature at the distance $x$. If the surrounding gas has a temperature $t_g$, a heat flow

$$dQ = hC\,dx(t - t_g) \tag{41}$$

leaves the volume element through the convex surface $C\,dx$. As a consequence of this the heat flowing along the rod becomes less with increasing distance $x$. Through the cross section contained in the distance $(x + dx)$ the heat flow is

$$Q' = Q + \frac{dQ}{dx}\,dx = -kA\,\frac{dt}{dx} - kA\,\frac{d^2t}{dx^2}\,dx \qquad (42)$$

In steady state the difference between the heat expressed by Eqs. (40) and (42) must equal that given by Eq. (41). Thus the differential equation

$$hC(t - t_g) = kA\,\frac{d^2t}{dx^2} \qquad (43)$$

is derived. If the symbol $\vartheta = t - t_g$ is used for the temperature difference, Eq. (43) becomes

$$\frac{d^2\vartheta}{dx^2} = \frac{hC}{kA}\,\vartheta \qquad (44)$$

A particular solution can be gained by the expression $\vartheta = e^{mx}$. By introducing it into the equation we get

$$m^2 = \frac{hc}{kA} \qquad (45)$$

and

$$\mathbf{m} = \sqrt{\frac{\mathbf{hC}}{\mathbf{kA}}} \qquad (46)$$

The general solution of the differential equation must have two constants. We get, therefore,

$$\vartheta = C_1e^{mx} + C_2e^{-mx} \qquad (47)$$

The constants $C_1$ and $C_2$ must be derived from the boundary conditions. The end of the rod, $x = 0$, which is fastened to the wall assumes the wall temperature $t_1$. The other end transmits heat to the surrounding gas. This process is described by the equation

$$-k\left(\frac{d\vartheta}{dx}\right)_{x=l} = h\vartheta_{x=l} \qquad (48)$$

To simplify the calculation, this heat flow can be disregarded, however, if the length $l$ of the rod is great compared with its thickness. The second boundary condition is then

$$\left(\frac{d\vartheta}{dx}\right)_{x=l} = 0 \tag{49}$$

The two boundary conditions introduced into the solution (47) of the differential equation give

$$\vartheta_1 = t_1 - t_g = C_1 + C_2 \tag{50}$$

$$\left(\frac{d\vartheta}{dx}\right)_{x=l} = 0 = C_1 m e^{ml} - C_2 m e^{-ml} \tag{51}$$

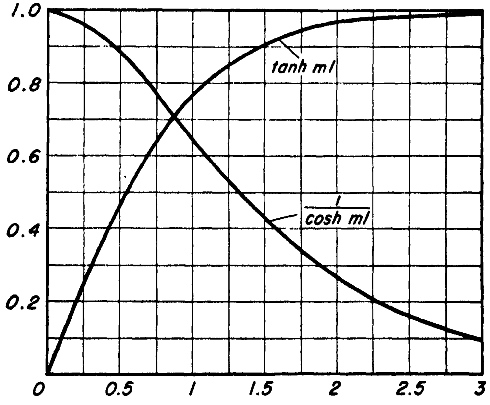

FIG. 14. Functions determining heat flow and temperature profile in a rod.

Solving these two equations for $C_1$ and $C_2$ and introducing these into (47) gives

$$\vartheta = \vartheta_1 \frac{e^{m(l-x)} + e^{-m(l-x)}}{e^{ml} + e^{-ml}} = \vartheta_1 \frac{\cosh m(l-x)}{\cosh ml} \tag{52}$$

The excess temperature of the end of the rod ($x = l$) is

$$\vartheta_2 = \frac{\vartheta_1}{\cosh ml} \tag{53}$$

and the heat flow through the base of the rod ($x = 0$) is

$$Q_1 = -kA\left(\frac{d\vartheta}{dx}\right)_{x=0} = mkA\vartheta_1\left(\frac{\sinh m(l-x)}{\cosh ml}\right)_{x=0}$$
$$= mkA\vartheta_1 \tanh ml \tag{54}$$

The two functions $1/\cosh ml$ and $\tanh ml$ are given in Fig. 14 and Table 4. In Fig. 14, it can be seen that when the length $l$ is

TABLE 4. CALCULATION OF HEAT CONDUCTION IN A ROD

| $ml$ | 0 | 0.5 | 1 | 1.5 | 2 | 3 | 4 | 5 | 6 |
|---|---|---|---|---|---|---|---|---|---|
| cosh $ml$ | 1 | 1.1276 | 1.543 | 2.352 | 3.762 | 10.07 | 27.31 | 74.21 | 201.7 |
| tanh $ml$ | 0 | 0.4621 | 0.7616 | 0.9052 | 0.9640 | 0.9951 | 0.9993 | 0.9999 | 1 |

increased beginning at zero, the heat flow $Q$ increases rapidly at first, but this increment of increase becomes smaller and smaller, and finally the heat flow approaches an asymptotic value. The excess temperature decreases to zero at the end of a very long rod.

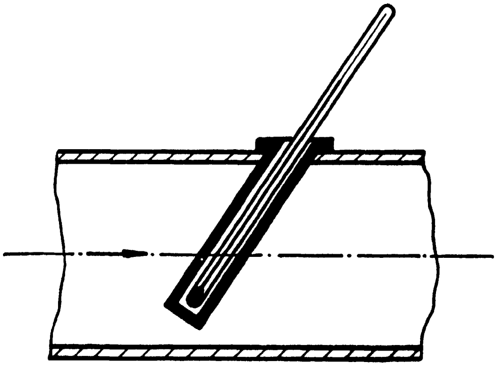

FIG. 15. Temperature measurement in flow through a tube.

The lengthy calculation with the boundary condition (48) gives the result[1]

$$Q_1 = mkA\vartheta_1 \frac{\frac{h}{k}\frac{1}{m} + \tanh ml}{1 + \frac{h}{k}\frac{1}{m}\tanh ml} \tag{55}$$

From this it can be seen under which condition the simplified Eq. (54) holds true. Equation (55) transforms into Eq. (54), when $(h/k)(1/m)$ is small compared with 1, or $h$ is small compared with $kC/A$ and $ml$ is not too small.

The following calculated example has an important technical application. The temperature of a gas flowing in a tube is measured usually by a thermometer put into a well which is welded into the tube wall as shown in Fig. 15. If the gas temperature differs greatly from the outside temperature, the tube wall has a lower temperature than the gas, and heat flows by conduction from the well to the tube wall. The end of the well where the bulb of the thermometer is placed may become colder than the gas, and the thermometer will not indicate the true gas temperature. This error can be calculated by Eq. (53). Figure 14 or Table 4 gives the necessary length of the tube when the error must be confined within a certain limit. Another application of the equations derived here is the calculation of finned heating surfaces. These are dealt with in the next section.

---

[1] See, for instance, M. ten Bosch, "Die Wärmeübertragung," 3d ed., p. 58, Springer-Verlag, Berlin, 1936.

**Example.** In a tube of 3.6 in. diameter for superheated steam there is placed an iron well (Fig. 15) with a diameter $d = 0.6$ in., for a thermometer. The steam has a pressure of 14.26 lb/in.$^2$, and a temperature of 600 F. It flows with a velocity of 65 fps. The length of the well, which gives an error in temperature measurement less than 0.5 per cent of the difference between the gas temperature and the tube-wall temperature, is to be determined. The film heat-transfer coefficient between the steam and the tube wall is $h = 18.5$ Btu/(hr)(ft$^2$)(F) as calculated according to Sec. 28. If the wall thickness of the well is $s = 0.036$ in., the cross section for the heat flow in the well is $A = d\pi s$, and the circumference is $C = d\pi$. Therefore

$$m = \sqrt{\frac{hC}{kA}} = \sqrt{\frac{h}{ks}} = \sqrt{\frac{18.5}{32 \times 0.003}} = 13.7/\text{ft}$$

With the signs used in this paragraph, the error is $\vartheta_2/\vartheta_1 = 0.005$. For this value, the product $ml$ must be 6 as is found in Table 4. Therefore, the length of the well $l = 6/m = 6/13.7 = 0.44$ ft $= 5.28$ in. As this length is greater than the tube diameter, it is necessary to locate the well obliquely in the tube (Fig. 15).

Heat radiation between the end of the well and the tube wall may originate in an additional error in temperature measurement. This will be dealt with in a later chapter.

## 8. Finned heating surfaces

It was shown in Sec. 2 that the over-all heat-transfer resistance of a plane wall is determined by the greatest partial resistance. If this is one of the convection resistances, the heat flow through the wall may be increased by placing fins on the surface where the great resistance occurs. Such finned heating surfaces are widely used, for example, as economizers in steam boilers, as radiators for steam and hot-water heating systems, on electric transformers, for the cylinders of air-cooled combustion engines, etc.

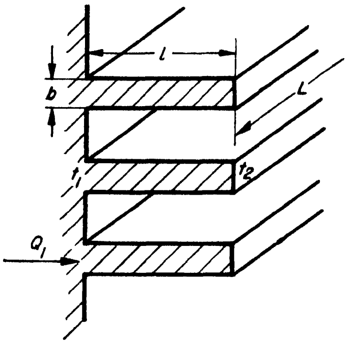

FIG. 16. Heating surface with rectangular fins.

In the following, calculations are made for the plane, finned surface, since this is the simplest case. As long as the height of the fins on a tube is comparatively small, the formulas derived for the plane wall can also be used for the cylinder. For fins of constant thickness with the height $l$, the formulas derived in Sec. 7 hold true (Fig. 16). Using the symbols in Fig. 16, the cross-sectional area $A$ of the fin is $bL$ and the circumference $C$ is $2L$, when $b$ is small compared with $L$. The value $m$ therefore is derived by introducing the above values into Eq. (46):

$$m = \sqrt{\frac{2h}{kb}} \tag{56}$$

The heat loss of the fin is given by Eq. (54) or (55).

It is of primary interest to know the conditions for which the finned surface has advantages over the plane wall. The answer to this question is somewhat different, depending on whether the price, the weight, or the space needed is of primary importance. First, we shall answer the question, under what circumstances can the heat flow through a wall be increased at all by fins. Obviously, fins are advantageous for the case where the heat flow through a fin increases with increased fin height. If the heat flow decreases with increasing fin height, it is advantageous to make the fins as low as possible or, finally, to omit them. The limit of the conditions, for which fins are advantageous, is given therefore by the equation

$$\frac{dQ_1}{dl} = 0 \tag{57}$$

This equation gives a result only when Eq. (55) for $Q_1$ is used. As the factors $k$, $A$, $m$, and $\vartheta_1$ must be regarded as constant for the problem under consideration, it suffices to differentiate the fraction only in Eq. (55). The resulting expression becomes zero when its numerator is zero or its denominator infinite. The last possibility results in a trivial statement only, for when $k = 0$, Eq. (57) is fulfilled. We, therefore, consider only the numerator. Differentiating Eq. (55) gives for the numerator

$$\left(1 + \frac{h}{k}\frac{1}{m}\tanh ml\right) m \frac{1}{\cosh^2 ml} - \left(\frac{h}{k}\frac{1}{m} + \tanh ml\right)\frac{h/k}{\cosh^2 ml} = 0 \qquad (58)$$

This equation may be simplified to the expression

$$m - \frac{h^2}{k^2}\frac{1}{m} = 0$$

Introducing Eq. (56) gives

$$\frac{2k}{hb} = 1 \qquad (59)$$

The equation may be written in the form

$$\frac{1}{h} = \frac{b/2}{k}$$

The left-hand expression is the film heat-transfer resistance; the right-hand expression is the thermal-conduction resistance of a plane wall of thickness equal to one-half the fin thickness. When both resistances have the same magnitude, the limit is reached at which fins are useless. We must bear in mind, of course, that real conditions in short fins differ from those assumed in the calculations. The heat-flow lines and the isotherms in such an actual fin must have the shape sketched in Fig. 17. For the above calculations, it was assumed that the temperature varies only in the direction of the height, and is therefore constant on normals to the height. The numerical value of Eq. (59) is influenced by this. We may be sure, however, that it is advantageous to use finned surfaces, as soon as the condition

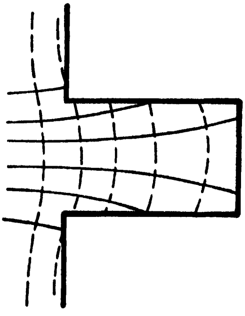

FIG. 17. Heat flow in a short rectangular fin.

$$\frac{2k}{hb} > 5 \qquad (60)$$

is fulfilled.

**Example 1.** It is to be determined when iron fins of 0.12-in. thickness on a heating surface are advantageous. The thermal conductivity of iron is found in the Appendix. We take the mean value, $k = 33$ Btu/(hr)(ft)(F). If the heat is transferred to air, the heat-transfer coefficient is 2 to 20 Btu/(hr)(ft$^2$)(F) (Table 1). We insert the higher value and find

$$\frac{2k}{hb} = 330$$

For heat transfer to air (or other gases), fins are advantageous, therefore. If the heat is transferred to water, the heat-transfer coefficients lie between the limits 100 and 1000 Btu/(hr)(ft$^2$)(F). If we take again the higher value, the characteristic becomes

$$\frac{2k}{hb} = 6.6$$

As this value is very low, fins bring practically no increase in heat transfer. The effectiveness of fins for liquids can be increased by using thinner fins of a metal with better thermal conductivity. But practically, the thickness cannot be reduced appreciably below 0.12 in., and the conductivity of copper, the best conduction metal, is only 5 times that of iron; therefore fins bring no great improvement to heat transfer to liquids.

When fins are advantageous, the heat transfer is increased by placing them as near each other as possible. But there is a limit for the distance between two fins, for the heat-transfer coefficients decrease when the boundary layers which occur on the surfaces of the fins mutually influence each other. The distance between two fins must not be much smaller, therefore, than twice the boundary-layer thickness. The thickness of boundary layers will be calculated later. Air flowing along a plate 1 ft long with 50 fps velocity creates a boundary layer, which is approximately 0.1 in. thick. The low velocities which occur in free convection, for instance on a radiator, result in bigger boundary layers about 0.5 in. thick.

For the design of cooling devices on vehicles, especially for airplanes, the problem of exchanging the greatest amount of heat with the least amount of weight of the heat exchanger is of primary importance. This question will now be answered for finned surfaces. The weight of one fin (Fig. 16) is

$$W = \gamma Lbl = \gamma LA_1 \qquad (61)$$

when $\gamma$ is the specific weight of the material for the fin, and $A_1$ is the area of the fin cross section normal to $L$. The length $L$ has a given value, whereas the two dimensions $b$ and $l$ are to be changed so as to give maximum heat flow for a given area $A_1$. In Eq. (54) we insert $m = \sqrt{2h/kb}$ and $A = bL$. (Note the difference between $A$ and $A_1$. $A$ is measured normal to the heat flow, $A_1$ in the plane of the drawing, Fig. 17.) If we express the height $l$ of the fin by the area $A_1/(l = A_1/b)$ we get

$$Q_1 = L\sqrt{2hkb}\,\vartheta_1 \tanh\left(\sqrt{\frac{2h}{kb}}\frac{A_1}{b}\right) \tag{62}$$

This becomes a maximum for $dQ_1/db = 0$. By differentiating Eq. (62) and making the differential quotient equal zero, we get

$$\frac{1}{2\sqrt{b}} \tanh\left(\sqrt{\frac{2h}{kb}}\frac{A_1}{b}\right) - \sqrt{b}\sqrt{\frac{2h}{k}}A_1\frac{3}{2b^2\sqrt{b}}\frac{1}{\cosh^2\left(\sqrt{\frac{2h}{kb}}\frac{A_1}{b}\right)} = 0 \tag{63}$$

Introducing the abbreviation

$$\sqrt{\frac{2h}{kb}}\frac{A_1}{b} = u \tag{64}$$

gives

$$\tanh u = \frac{3u}{\cosh^2 u} \tag{65}$$

This equation must be solved numerically or graphically, for example, by plotting both sides against $u$ and determining the point where the two curves intersect. Thus, the value $u = 1.419$, can be obtained. The maximum heat flow through a fin of given weight is obtained, therefore, when the equation

$$l\sqrt{\frac{2h}{kb}} = 1.419$$

is fulfilled. It can be written in the form

$$\frac{l}{b/2} = 1.419\sqrt{\frac{2k}{hb}} \tag{66}$$

Here it can be seen that the ratio of the height to half the fin thickness depends on the same characteristic value found in

Eq. (59). The temperature excess of the end of the fin over the surrounding gas is

$$\vartheta_2 = \frac{\vartheta_1}{\cosh u} = 0.457\vartheta_1 \tag{67}$$

This allows us to test whether or not the optimum height of the fin is obtained by measuring the temperatures $\vartheta_1$ and $\vartheta_2$.

When the heating surface has no fins, the area equal to the fin base transmits the heat flow $Q^1 = hbL\vartheta_1$. The ratio of the heat flow through the fins to the heat flow $Q^1$ without fin is therefore for the best fin according to Eq. (62)

$$\frac{Q_1}{Q^1} = \sqrt{\frac{2k}{hb}}\tanh u = 0.889\sqrt{\frac{2k}{hb}}$$

This equation determines how much the heat flow through the wall can be increased by the addition of fins.

**Example 2.** For an iron fin 0.12 in. thick, the characteristic value $2k/hb$ was determined on p. 32. Introducing it into Eq. (66), the optimum ratio $l/(b/2)$ becomes 25.8 for the heat transfer to air, and 3.64 for the heat transfer to water. An aluminum fin 0.04-in. thick, with a thermal conductivity value of $k = 120$, has an optimum ratio $h/(b/2) = 85.1$ for air, and 12.0 for water. It can be seen that the fin must be thicker when the ratio of the film resistance to the conduction resistance becomes smaller. Iron fins for heat transfer to water are of little use.

The iron fins of air-cooled cylinder barrels for reciprocating aeroengines are approximately 0.04 in. thick and 0.8 in. high with 0.16-in. spacing. The cylinder head is mostly equipped with aluminum fins about 0.06 in. thick and 1.4 in. high with 0.2-in. spacing. These dimensions are very close to the optimum values according to Eq. (66). The radiators of liquid-cooled aeroengines also have very thin fins (approximately 0.004 to 0.008 in. thick, 0.2 in. high). Stationary heat-transfer equipment has fins which are generally thicker than the optimum value, as the saving of weight is not so important here. Finned tubes of economizers for steam boilers have fins 0.16 to 0.25 in. thick, 0.6 to 1 in. high, with 0.6 to 0.8 in. spacing; finned tubes for warm-water heating have fins 0.04 to 0.1 in. thick, 1 to 1.6 in. high, 0.4 to 1-in. spacing.

In determining the optimum fin, there arises the question as to whether weight may or may not be gained by using other shapes for the fin cross section than the rectangular, as has been considered until now. The calculation for other forms is much more troublesome. Therefore, the results only are given here.[1] The ratio of the height $l$ to the thickness $b$ at the base for a optimum triangular fin (Fig. 18) is

$$\frac{l}{b/2} = 1.309\sqrt{\frac{2k}{hb}} \tag{68}$$

The temperature excess on the peak of the fin is

$$\vartheta_2 = 0.277\vartheta_1 \tag{69}$$

The ratio of the thickness $b$ of the triangular fin to the thickness of the rectangular fin with equal heat flow is 1.31; the ratio of the cross-sectional areas is 1/1.44. Therefore, using the triangular fin, 44 per cent of material can be saved.

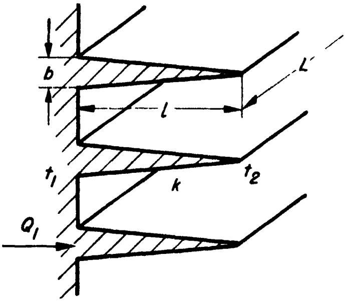

FIG. 18. Triangular fins.

Now it is of interest to determine what is the optimum shape of a fin having the smallest weight for a given heat flow. It is evident that in such a fin every part should be utilized to the same degree, or that the specific rate of heat flow should be constant throughout the fin. The proof of this fact was presented by E. Schmidt.[2] The heat-flow lines in such a fin must have the shape indicated in Fig. 19. They are equally spaced straight lines parallel to the fin axis. With a constant specific rate of heat flow the temperature decreases linearly along any flow line from the value $t_1$ at the root of the fin. We shall try to approach the value $t_g$ of the surrounding gas on the fin edge. The temperatures within the fin are indicated in the upper part of Fig. 19. At the distance $x$ from the edge the temperature is $t$. Because of the linearity of the temperature field the difference between the temperature $t$ and the gas temperature $t_g$ may be expressed as

---

[1] E. Schmidt, *Z. Ver. deut. Ing.*, **70**, 885 (1926). Calculations were made for needles on a heating surface, by R. Focke, *Forsch. Gebiete Ingenieurw.*, **13**: 34–42 (1942). Experimental investigation on different fin arrangements, by R. H. Norris and W. A. Spofford, High Performance Fins for Heat Transfer, *Trans. ASME*, **64**, 489–496 (1942).

[2] E. Schmidt, *Z. Ver. deut. Ing.*, **70**, 885 (1926).

$$t - t_g = \frac{x}{l}(t_1 - t_g)$$

The constant rate of heat flow in the direction of the fin axis may be $q$. Now consider a surface element of the fin at the distance $x$. It may be inclined toward the fin axis by the angle $\alpha$. The specific rate of heat flow through this element is $q \sin \alpha$, and since the heat flowing through this surface element has to be transferred to the surrounding gas, the equation

$$q \sin \alpha = h(t - t_g) = h\frac{x}{l}(t_1 - t_g)$$

is valid. This equation determines the angle $\alpha$ of the surface element as a function of the distance $x$:

$$\sin \alpha = \frac{h(t_1 - t_g)}{ql}\,x$$

The fraction on the right-hand side of the equation has a constant value. The contour of the fin defined in this way is a circle, for a circle is described by the equation $\sin \alpha = x/r$ (Fig. 19), which corresponds exactly to the above equation. The radius $r$ of the circle has the value $\frac{ql}{h(t_1 - t_g)}$. The fact that the contour lines of the fin with minimum weight are circles was first pointed out by F. Weinig. It is not necessary to give the fin an infinitely thin edge as shown in Fig. 19. Any part out of the circle can be used to build up a contour for a fin with constant heat-flow density. This is shown by the dashed line in Fig. 19. The difference in weight between a fin of circular shape and one of triangular shape is very small. As the triangular shape is easier to manufacture, it may practically be regarded as the best form.

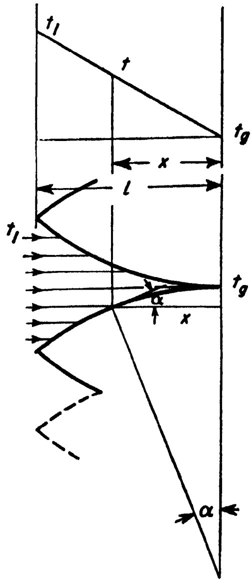

FIG. 19. Fin with smallest weight.

The cross-sectional area $A_1$ necessary for a certain heat flow in the rectangular fin is derived from Eq. (62) by introducing

Eq. (64) and solving for $A_1$:

$$A_1 = \left(\frac{Q_1}{\vartheta_1}\right)^3 \frac{1}{L^3} \frac{u}{\tanh^3 u} \frac{1}{\sqrt{16h^4k^2}} = \frac{2.109}{4L^3h^2k} \left(\frac{Q_1}{\vartheta_1}\right)^3 \qquad (70)$$

This equation shows that it is advantageous to make the fins as small as possible. For, to double the heat flow, the area of one fin must be increased eightfold, whereas it is sufficient to use two fins of the original size.

Equation (70) also allows comparison of different materials for fins. Accordingly, the cross-sectional area $A_1$ is inversely proportional to the thermal conductivity $k$. The weight, therefore, is proportional to $\gamma/k$. In Table 5, the quotient of the specific weight $\gamma$ to the thermal conductivity $k$ is listed for different materials. It is to be seen that by the use of aluminum 50 per cent of the weight can be saved as compared with the use of copper. Iron fins have a tenfold weight, and alloyed iron fins a fiftyfold weight. It is of no use, therefore, to make the fins for air-cooled cylinders of aeroengines of copper instead of aluminum, whereas the change from iron to aluminum promises great advantages.

TABLE 5. EFFICIENCY VALUES FOR FINS

| Material | Heat conductivity $k$, Btu/(hr)(ft)(F) | Specific weight $\gamma$, lb/ft$^3$ | $\gamma/k$, $\frac{\text{(hr)(lb)(F)}}{\text{Btu/(ft}^2)}$ | $\frac{\gamma/k}{(\gamma/k)_{\text{Al}}}$ |
|---|---|---|---|---|
| Copper | 220 | 560 | 2.55 | 1.96 |
| Aluminum, pure | 130 | 170 | 1.30 | 1 |
| Aluminum alloy | 90 | 166 | 1.85 | 1.42 |
| Magnesium, pure | 100 | 110 | 1.31 | 1.01 |
| Steel | 32 | 490 | 15.3 | 11.8 |
| Steel, stainless | 8 | 490 | 61.2 | 47.1 |

## 9. The wall with heat sources

Our previous considerations must be extended, when in the body in which the heat flows, heat is generated in any manner, or if, as we call it, *heat sources* prevail in the body. This is explicitly the case in an electric conductor in which, due to the resistance, electric energy is transformed into heat. The mathematical calculations of the temperatures which originate by this generation of heat are of interest for electric machines and apparatus. The greatest difficulty in the design and construction of fast-running motors and generators is diversion of the heat generated by the electrical losses. Even the construction business has to deal with similar occurrences. For instance, special means must be applied on thick concrete walls in order to prevent production of inadmissibly high temperatures by the generation of heat during the setting of the concrete. For this reason, cooling tubes had to be installed in various dams made of concrete. The flow losses in gases and liquids are also transformed into heat. The temperature increases thus caused reach rather high values in gases flowing with high velocities. A projectile with 2,000 fps muzzle velocity reaches a temperature of up to 250° F from the friction of the air. Considerable temperature differences also occur in the oil films of fast-running bearings from the intrinsic frictional heat. We shall discuss the latter occurrences in a subsequent section. In this section, we shall treat only the heat flow in solid bodies, and especially the case which can be handled conveniently by simple mathematical calculations, *i.e.*, the plane wall. We consider an infinitely thin layer of thickness $dx$, which is cut out from the wall by two parallel planes (Fig. 20). Uniformly distributed heat sources exist in the wall, and thus a heat quantity $r$ per unit of space and time is generated. Hence $r$ is independent of $x$. On each surface, the wall may be bounded by a gas with the temperature $t_g$. The film heat-transfer coefficient for each surface is $h$. The temperature of the wall at the point $x$ is $t$, and the excess temperature above the gas temperature is $\vartheta$. The heat flow per unit area through the plane at point $x$ is given by the equation

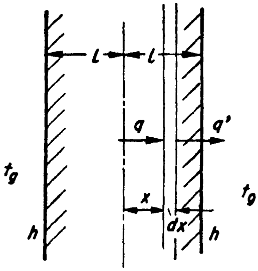

FIG. 20. Wall with heat sources.

$$q = -k\frac{dt}{dx} = -k\frac{d\vartheta}{dx} \tag{71}$$

At point $(x + dx)$ it has the value

$$q' = q + \frac{dq}{dx}dx = -k\frac{d\vartheta}{dx} - k\frac{d^2\vartheta}{dx^2}dx \tag{72}$$

The difference $(q' - q)$ must in the steady state be equal to the heat quantity, which is generated in the wall layer of thickness $dx$:

$$q' - q = r\,dx \tag{73}$$

From the relations (71) to (73) we obtain the differential equation

$$r = -k\frac{d^2\vartheta}{dx^2} \tag{74}$$

By double integration its solution

$$\vartheta = -\frac{r}{2k}x^2 + C_1x + C_2 \tag{75}$$

is obtained. The boundary conditions for the determination of the constants $C_1$ and $C_2$ are the following. Because of the symmetry of the problem, the highest temperature must occur in the center of the plate ($x = 0$), and hence the temperature curve must have a horizontal tangent at this point. On the plate surface ($x = l$), the heat transported to the surface by conduction must be transmitted to the gas. The boundary conditions are then

$$\left(\frac{d\vartheta}{dx}\right)_{x=0} = 0 \tag{76}$$

$$-k\left(\frac{d\vartheta}{dx}\right)_{x=l} = h\vartheta_{x=l} \tag{77}$$

If we define the constants with these aids, we obtain for the excess temperature in the plate the equation

$$\vartheta = \frac{r}{2k}(l^2 - x^2) + \frac{rl}{h} \tag{78}$$

Hence, the isotherms in a plate with uniform heat generation are parabolas, as shown in Fig. 21. The maximum excess temperature is obtained from Eq. (78) when $x = 0$, thus

$$\vartheta_0 = \frac{r}{2k}l^2 + \frac{rl}{h} \tag{79}$$

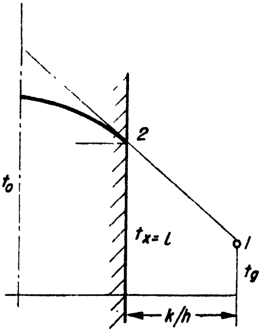

FIG. 21. Temperature profile in a wall with heat sources.

The temperature gradient on the surface can be easily found by the method given in Fig. 21. We plot the distance $k/h$ from the surface, add the temperature $t_g$ as ordinate, and connect point 1, which is obtained in this manner, with point 2 as defined by the surface temperature. The direction of the straight line connecting both points yields the temperature gradient on the wall. We realize this immediately if we solve Eq. (77) for $d\vartheta/dx$:

$$-\left(\frac{d\vartheta}{dx}\right)_{x=l} = \frac{\vartheta_{x=l}}{k/h} \tag{80}$$

**Example.** A cylindrical transformer coil made of insulated copper wire has an inside diameter of 6.6 in. = 0.55 ft and an outside diameter of 9.6 in. = 0.8 ft. The fraction $\varphi = 0.6$ of the total cross section of the coil is copper and the rest insulation. The density of the current in the conductors is $j = 1{,}300$ amp/in.$^2$; the specific resistance of copper is $\rho = 9.5 \times 10^{-6}$ (ohms)(in.$^2$)/(ft). Whence the generation of heat per unit of space in the coil is $r = \varphi j^2 \rho = 0.6 \times 1.69 \times 10^6$ amp$^2$/in.$^4$ $\times$ 9.5 $\times$ $10^{-6}$ ohms in.$^2$/ft $\times$ 144 in.$^2$/ft$^2$ $\times$ 3.412 Btu/watt-hr = 4730 Btu/(hr)(ft$^3$). The heat-transfer coefficient on both surfaces of the coil, which are cooled by air at 70 F, is $h = 4$ Btu/(hr)(ft$^2$)(F); the thermal conductivity of the coil is $k = 0.2$ Btu/(hr)(ft)(F) (mica, glue). If we consider the coil in a first approximation as a plane wall with the thickness $2l = 1.5$ in. = 0.125 ft, we obtain the highest temperature prevailing in it, according to Eq. (79),

$$\vartheta_0 = \frac{4730 \times 0.0039}{2 \times 0.2} + \frac{4730 \times 0.0625}{4} = 120.1 \text{ F}$$

Thus the temperature $t_0$ at the center of the spool is 120.1 + 70 = 190 F. Accurate calculation of the thermal field in the coil when considered as a hollow cylinder yields the value 191 F. Consequently, it can be seen that the calculation as for a plane wall yields useful results even on rather thick-walled coils.

## 10. The general heat-conduction equation

We shall now include unsteady heat-flow processes in our considerations. For the time we shall use the symbol $\tau$. At first we shall derive the equation for heat conduction in its most general form for a system of rectangular coordinates. We consider, in the body, a small parallelepiped with the dimensions $dx$, $dy$, and $dz$ (Fig. 22). According to Eq. (30) the heat

$$dQ_x = -k \frac{\partial t}{\partial x} dy\, dz \tag{81}$$

enters through the area 1 this parallelepiped. With progressing $dx$ this heat flow has generally changed so that the heat flow

$$dQ'_x = dQ_x + \frac{\partial(dQ_x)}{\partial x}\,dx = -k\left(\frac{\partial t}{\partial x} + \frac{\partial^2 t}{\partial x^2}\,dx\right)dy\,dz \tag{82}$$

leaves the parallelepiped through the area 2. The excess heat flow through area 2 over the heat flow through area 1 is

$$dQ'_x - dQ_x = -k\,\frac{\partial^2 t}{\partial x^2}\,dx\,dy\,dz \tag{83}$$

In the same manner, the excess of the heat flow leaving the element through area 4 over the heat flow entering the parallelepiped through area 3 is

$$dQ'_y - dQ_y = -k\,\frac{\partial^2 t}{\partial y^2}\,dx\,dy\,dz \tag{84}$$

and the surplus of the heat flow through area 6 as compared to that through area 5 is

$$dQ'_z - dQ_z = -k\,\frac{\partial^2 t}{\partial z^2}\,dx\,dy\,dz \tag{85}$$

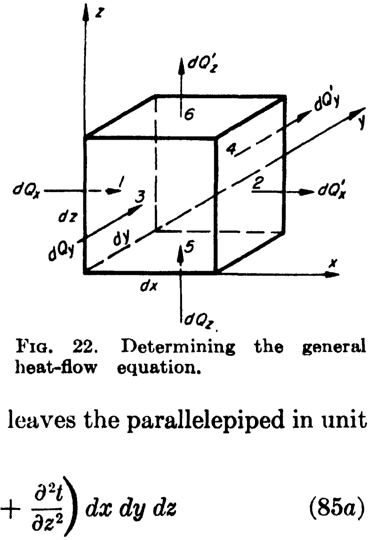

FIG. 22. Determining the general heat-flow equation.

The sum of the heat flow given by Eqs. (83), (84), and (85) specifies the heat quantity which leaves the parallelepiped in unit time:

$$-k\left(\frac{\partial^2 t}{\partial x^2} + \frac{\partial^2 t}{\partial y^2} + \frac{\partial^2 t}{\partial z^2}\right)dx\,dy\,dz \tag{85a}$$

If per unit of space and time, the heat quantity $r$ is generated, the heat generation in the parallelepiped considered is

$$r\,dx\,dy\,dz \tag{86}$$

The difference between the heat generated in the parallelepiped and the heat leaving the parallelepiped by conduction is used for the purpose of heating up the parallelepiped. The temperature of the parallelepiped is $t$, hence its temperature change per unit of time is $\partial t/\partial\tau$. If we denote the specific weight of the parallelepiped by $\gamma$ and its specific heat per unit of weight by $c$, then the heat quantity necessary to increase the temperature is given by

$$c\gamma \frac{\partial t}{\partial \tau} dx\, dy\, dz \tag{87}$$

According to the discussion above, this heat must be equal to the difference of the generated heat [Eq. (86)] and the heat losses [Eq. (85*a*)]. Thus we obtain the differential equation

$$c\gamma \frac{\partial t}{\partial \tau} dx\, dy\, dz = r\, dx\, dy\, dz + k\left(\frac{\partial^2 t}{\partial x^2} + \frac{\partial^2 t}{\partial y^2} + \frac{\partial^2 t}{\partial z^2}\right) dx\, dy\, dz \tag{88}$$

If we divide the equation by $\gamma c$ and introduce the abbreviation $k/c\gamma = \alpha$ we obtain the general Fourier heat-conduction equation

$$\frac{\partial t}{\partial \tau} = \alpha \left(\frac{\partial^2 t}{\partial x^2} + \frac{\partial^2 t}{\partial y^2} + \frac{\partial^2 t}{\partial z^2}\right) + \frac{r}{c\gamma} \qquad 89)$$

The value

$$\alpha = \frac{k}{c\gamma} \tag{90}$$

is called the thermal diffusivity. It is a property of the material and is compiled for a series of solids, liquids, and gases in the Appendix of this book. If the heat generation is $r = 0$, the thermal diffusivity represents the only property value which enters the heat-conduction equation. How fast temperature equalization takes place in a body without internal heat generation depends therefore only on the value of the thermal diffusivity. From the tables in the Appendix it can be seen that of the solids, the metals have the highest thermal diffusivity. Liquids have thermal diffusivities of approximately the same order of magnitude as nonmetals. The thermal diffusivities for gases, however, lie in the order of magnitude of those for the metals. In a stagnant gas, the temperature differences equalize about as fast as in metal. On the other hand, more time is required in a stagnant liquid for temperature equalization, namely, time of the same order of magnitude as in nonmetals.

All special cases of heat conduction can be derived from the general heat-conduction equation. For example, the stationary heat flow through a plane wall without heat sources, which is given by Eq. (1), can be obtained in the following manner. In the plane wall, the temperature depends only on the direction perpendicular to the wall surface. If we arrange the $x$ axis of our coordinate system in this direction, the derivatives with respect to $y$ and $z$ in Eq. (89) become zero. For a steady-state process, the derivative with respect to time must also become zero and, because of the absence of heat sources, $r$ is also zero. Therefore from Eq. (89) only the following expression remains:

$$\frac{\partial^2 t}{\partial x^2} = 0 \tag{91}$$

By double integration we obtain from this the temperature field

$$t = C_1 x + C_2 \tag{92}$$

and if we define both surface temperatures of the wall, $t_{w1}$ and $t_{w2}$, as boundary conditions for the determination of both constants, Eq. (92) becomes

$$t = (t_{w2} - t_{w1}) \frac{x}{b} + t_{w1} \tag{93}$$

We find that the linear temperature gradient shown in Fig. 1 actually exists. The temperature gradient $dt/dx$ in the wall is equal to

$$\frac{dt}{dx} = \frac{t_{w2} - t_{w1}}{b} \tag{94}$$

and from this results the specific heat flow

$$q = -k \frac{dt}{dx} = \frac{k}{b} (t_{w1} - t_{w2}) \tag{95}$$

in accordance with Eq. (2).

## 11. Unsteady heat flow

The exact solution of the heat-conduction equation (89) presents considerable mathematical difficulties. Fourier occupied himself with solving this equation and thereby developed the method of the Fourier series.[1] However, in most cases a quicker solution can be obtained by an approximate graphical process, which was developed by E. Schmidt.[2] We shall study this process only for a plane wall. In the wall the heat-conduction equation changes into the following form in the absence of heat sources:

---

[1] Fourier, J. B., "Théorie analitique de la chaleur, oeuvres de Fourier," Gauthier-Villars & Cie, Paris, 1822; English translation by Freeman, Cambridge, 1878.

[2] E. Schmidt in "Beitrage zur technischen Mechanik and technischen Physik" (Foeppl-Festschrift), Springer-Verlag, Berlin, 1924; see also E. Schmidt, "Einführung in die technische Thermodynamik," p. 262, Springer-Verlag, Berlin, 1936.

$$\frac{\partial t}{\partial \tau} = a \frac{\partial^2 t}{\partial x^2} \tag{96}$$

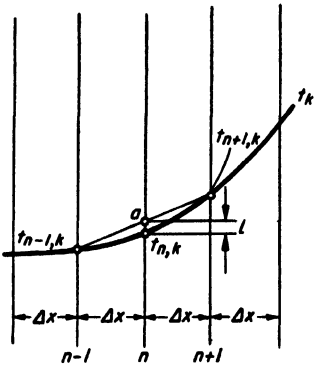

FIG. 23. Unsteady heat flow in a plane wall determined by a Schmidt plot.

This equation can be changed into an equation of finite differences by splitting the time into finite intervals $\Delta\tau$, and by splitting the plate thickness into intervals $\Delta x$ and considering the temperature in these intervals (Fig. 23). Equation (96), as a difference equation, is written

$$\frac{\Delta_\tau t}{\Delta\tau} = a \frac{\Delta_x{}^2 t}{\Delta x^2} \tag{97}$$

The indices indicate that the time $\tau$ or the location $x$ is variable with the differential formation $\Delta t$. The length intervals and the time intervals may be numbered continuously. Thus the number $n$ (Fig. 23) may refer to any arbitrary place in the plate, and the number $k$ may indicate any arbitrary moment in the time scale. Hence, we can write the value $\Delta_\tau t$ in the form

$$\Delta_\tau t = t_{n,k+1} - t_{n,k} \tag{98}$$

and also the value

$$\Delta_x t = t_{n+1,k} - t_{n,k}$$

The expression $\Delta_x{}^2 t$ is the difference of two successive differences; hence we obtain

$$\begin{aligned} \Delta_x{}^2 t &= (t_{n+1,k} - t_{n,k}) - (t_{n,k} - t_{n-1,k}) \\ &= t_{n+1,k} - 2t_{n,k} + t_{n-1,k} \end{aligned} \tag{99}$$

Therewith, the differential equation (97) is changed into

$$t_{n,k+1} - t_{n,k} = a \frac{\Delta\tau}{\Delta x^2} (t_{n+1,k} - 2t_{n,k} + t_{n-1,k}) \tag{100}$$

From this, the temperature throughout the wall at the time $(k + 1)$ can be computed if the temperatures in the wall are known at the time $k$. By continued application of the equation, the development of the temperature field with time can gradually be determined from a known initial temperature distribution. In lieu of the calculations, the graphical solution illustrated in Fig. 23 can be used. The temperature field $t_k$ for the time $k$ is plotted in this figure. Now we connect the temperature points, which are two $x$ intervals apart, by a straight line; for example, in Fig. 23 the point $t_{n-1,k}$ on the vertical line $(n - 1)$ with the point $t_{n+1,k}$ on the ordinate $(n + 1)$. In this manner we arrive at the point of intersection $a$. The distance designated $l$ has the value

$$l = \frac{t_{n-1,k} + t_{n+1,k}}{2} - t_{n,k} = \frac{1}{2}(t_{n+1,k} - 2t_{n,k} + t_{n-1,k}) \qquad (101)$$

This agrees closely with the temperature difference defined by Eq. (100), the only difference being that in place of the factor ½ in Eq. (101), there occurs the expression $\alpha(\Delta\tau/\Delta x^2)$ in Eq. (100). However, since there is still at our free disposal the time interval $\Delta\tau$, it can always be arranged with a freely chosen interval $\Delta x$ so that the condition $\alpha(\Delta\tau/\Delta x^2) = ½$ is fulfilled. By the procedure shown in Fig. 23 we have therefore gained in point $a$ a point of the temperature field for the time $(k + 1)$, which is given by the value

$$\Delta\tau = \frac{\Delta x^2}{2\alpha} \qquad (102)$$

later than the time $k$. In the same manner, by plotting additional straight lines (Fig. 23), other points of the temperature field for the time $(k + 1)$ can be obtained, and thus is determined the entire temperature field solely by the use of a ruler. In order to use this graphical solution, the temperature field in the wall must be known for a specific moment. If, in addition, the change of the surface temperature with time is known, the temperature field in the wall can be plotted as shown in Fig. 24. Here the temperature $t_0$ for the time $\tau = 0$ and the temperatures of the surface (point 0, 1, 2, etc.) for successive time intervals $\Delta\tau$ are given. Fre-

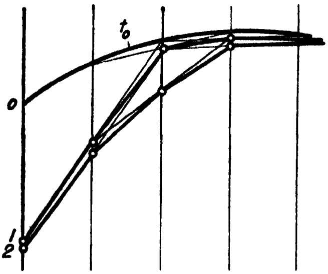

**FIG. 24. Unsteady heat flow in a plane wall determined by a Schmidt plot.**

quently, however, only the temperature $t_0$ of the medium outside the wall and the heat-transfer coefficient on the surface of the wall is known. Hence, subdivision into layers is more suitably accomplished in the way shown in Fig. 25. In this case, the gradient of the temperature-distribution curve on the surface for each instant is defined by the surface condition

$$-k\frac{dt}{dx} = h(t - t_0) \qquad (103)$$

Graphically this condition means that the tangent to the temperature curve at the surface must pass through a reference point whose distance from the wall is $k/h$ and whose ordinate is the surrounding temperature $t_0$. This relationship has already been pointed out, in Fig. 21. It can be used here in the following manner. We extend the given temperature distribution 1, 2, 3 at the beginning of the equalization process (Fig. 25) through the straight line ($r - a$) past the surface of the wall and now start our design connecting point 0 with 2, 1 with 3, etc., by straight lines. Thus is obtained a new temperature line 1′, 2′, 3′. This line can be extended again by connection with the guide point $r$, and it yields in this manner the point 0′. In this manner the design is repeated, etc. If during the course of time the surrounding temperature $t_0$ or the heat-transfer coefficient changes, it can be easily compensated by a displacement of the guide point $r$ in vertical or horizontal direction, respectively. This is an advantage of the graphical procedure as compared to a mathe-

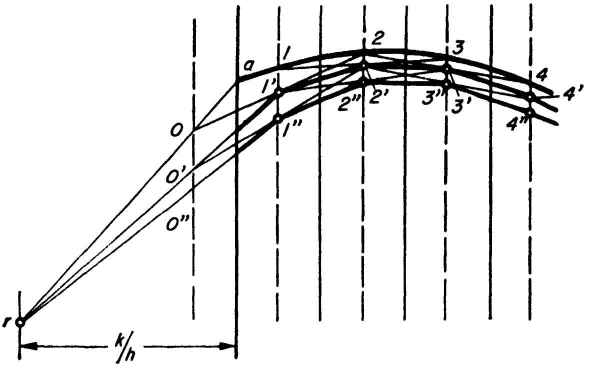

FIG. 25. Unsteady heat flow in a plane wall including film heat transfer determined by a Schmidt plot.

matical treatment of the differential equation, where a variable heat-transfer coefficient leads to considerable mathematical difficulties. Lately this method has been extended[1] by A. Nessi and L. Nisolle to other body forms, *e.g.*, the cylinder or the sphere.

**Example 1.** A living room with brick walls, which has initially an outside temperature of 30 F, is heated by some unit. It is to be determined how long it takes to establish a steady-state temperature distribution in the walls and in the room. The final temperature in the room is to be 70 F. The heat-transfer coefficient on the inside of the wall is $h_i = 1.2$ Btu/(hr)(ft$^2$)(F), the heat-transfer coefficient on the outside $h_a = 3.0$ Btu/(hr)(ft$^2$)(F), the thermal conductivity of the wall, $k = 0.25$ Btu/(hr)(ft)(F), the thermal diffusivity $\alpha = 0.012$ ft$^2$/hr, and the thickness of the wall is 1.3 ft. The steady-state temperature in the wall is given by a straight line connecting the two points $a$ and $b$, which are separated from the two wall surfaces by $k/h_i$ and $k/h_a$, respectively, and have respective temperatures 30 F and 70 F. If we assume the rate of heat transfer to the inside of the wall to be constant, all temperature gradients in the wall during the heating process must have the same inclination to the inner surface. To start now with the graphical method, the wall is divided into six layers, each with the thickness $\Delta x = 0.217$ ft. Then the time interval is given by

$$\Delta\tau = \frac{\Delta x^2}{2\alpha} = \frac{0.217^2}{2 \times 0.012} = 1.97 \text{ hr}$$

The construction of the temperature curves can be easily followed in Fig. 26. It can be seen that more than 80 hr or 4 days are needed before steady-state conditions are reached. After the time 9.85 hr the length interval was made $2\Delta x$; accordingly the time interval now becomes $4 \times 1.97 = 7.89$ hr.

Exact solutions of the differential equation (89) without heat sources are known for two cases. First is for the equalization process where the body had initially a constant temperature and whereupon the surrounding temperature suddenly is changed to a different value which is thereafter kept constant. The second process is a quasi-stationary process. The body is in a surrounding whose temperature executes periodic oscillations. The calculations for both cases are discussed in detail in the textbook of

---

[1] E. Schmidt, *Forsch. Gebiete Ingenieurw.*, **13**, 166–185 (1942). Some complementary information is given by H. Pfriem, *Z. Ver. deut. Ing.*, **86**, 703–709 (1942), and *Kältetechnik*, **45**, 33–38 (1943).

H. S. Carslaw and T. C. Jaeger.[1] Diagrams of the solutions for various body forms can be found in the book of McAdams.[2]

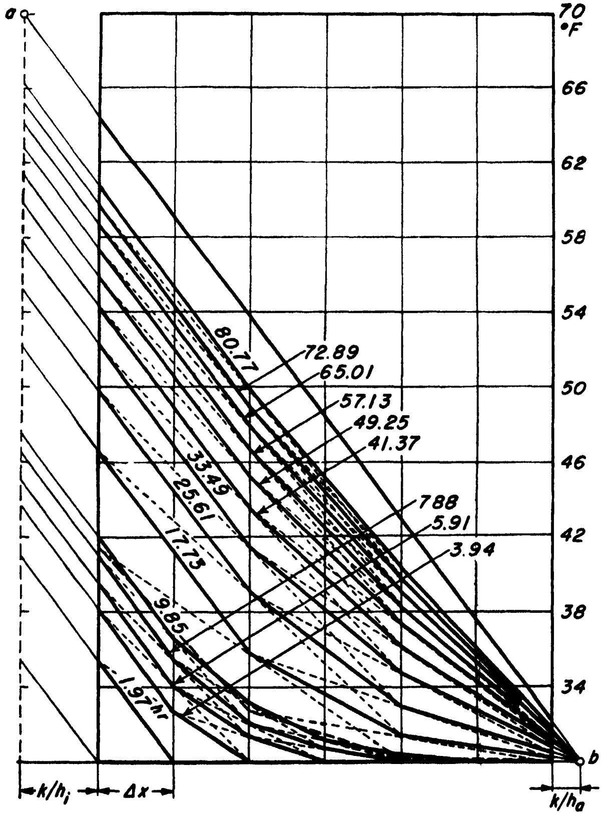

Fig. 26. Unsteady heat flow into a brick wall.

Figure 27 shows a compilation for bodies of various forms, which at first have a uniform temperature $t_0$ and whose surfaces are suddenly cooled to a temperature $t = 0$.[3]

The ratio of the highest temperature $t$ within the body during the cooling process to its temperature $t_0$ at the time $\tau = 0$ is plotted against the dimensionless characteristic group $\alpha\tau/X^2$ in this diagram. This dimensionless group is sometimes called Fourier number. The length $X$ indicates half the thickness of the body, which on the cylinder and on the sphere therefore means the radius. The surrounding temperature is set equal to zero. The heat-transfer coefficient $h$ is taken as infinitely large, so that the surface of the body immediately assumes the surrounding temperature 0 F at the beginning of the process, at the time $\tau = 0$. We can see from the diagram that the plate cools most slowly and the sphere most rapidly. The time required for other bodies lies in between the two. If a heat-transfer coefficient of finite value exists, the cooling process is slowed. This is illustrated in Fig. 28 for the plane plate, which is cooled on both sides. The ratio $t/t_0$ of the temperature in the center plane to the initial temperature depends only on the two characteristic dimensionless groups $\alpha\tau/X^2$ and value $hX/k$. The first has already been employed in Fig. 27. The line $hX/k = \infty$ agrees with the corresponding line in Fig. 27. If the thermal conductivity is high as compared to the heat-transfer coefficient, in other words, if the characteristic value $hX/k$ (sometimes called Biot number) is small, the temperature differences which occur in the body during the cooling process are very low and can be disregarded. Thus, we obtain for the distribution of the excess temperature $t$ the simple relation

---

[1] H. S. Carslaw and J. C. Jaeger, "Conduction of Heat in Solids," Oxford University Press, New York, 1947.

[2] W. H. McAdams, "Heat Transmission," 2d ed., McGraw-Hill Book Company, Inc., New York, 1942.

[3] H. Groeber and S. Erk, "Die Grundgesetze der Wärmeübertragung," Springer-Verlag, Berlin, 1933.

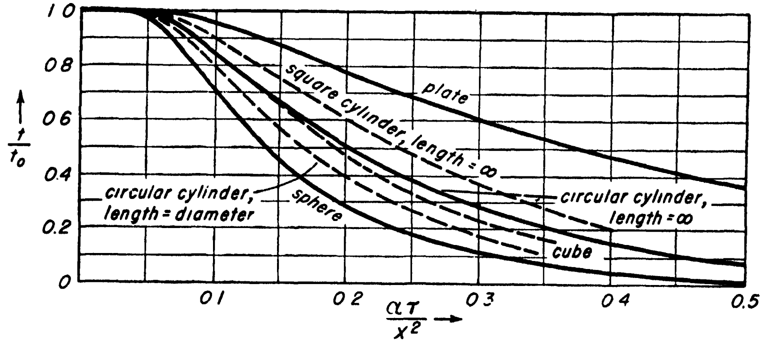

FIG. 27. Temperature at the axis of different shapes during the process of cooling. (*From H. Groeber and S. Erk, "Die Grundgesetze der Wärmeübertragung," p. 59, Fig. 28, Springer-Verlag, Berlin,* 1933.)

$$\frac{t}{t_0} = e^{-(h/Xc\gamma)\tau} \tag{104}$$

or with the characteristic values which were employed in Fig. 28,

$$\frac{t}{t_0} = e^{-(\alpha\tau/X^2)(hX/k)} \tag{104a}$$

This relation is given in Fig. 28 by the line with the parameter $hX/k = 0$. The temperature distribution during the cooling of a cylinder or a sphere with radius $X$, for small values of the characteristic value $hX/k$, is given by Eq. (104) or (104$a$) if the exponent is multiplied by 2 and 3, respectively.

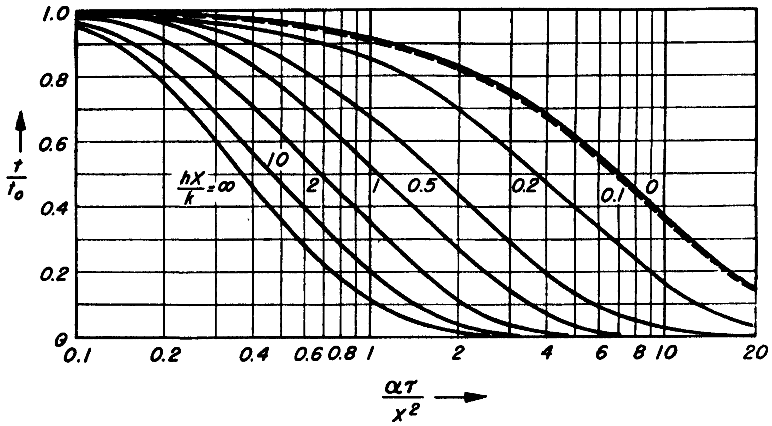

FIG. 28. Temperature in the center plane of a wall cooled on both sides during the process of cooling. (*According to H. Groeber.*)

**Example 2.** If it is intended to measure an unsteady temperature with a thermometer, it is very important that one understand how fast the thermometer follows this process. The *half-value time* is the time within which the initial difference between the true temperature and the indicated temperature of the thermometer is reduced to half after a sudden change of the true temperature. This *half-value time* is to be determined for a mercury thermometer which is installed in an air stream. The mercury bulb may have a cylindrical shape with a 0.12-in. = 0.01-ft radius. The thermal conductivity of the mercury according to the Appendix is $k = 5$ Btu/(hr)(ft)(F), its thermal diffusivity is $\alpha = 0.178$ ft²/hr. The thermal resistance of the thin glass wall is disregarded. The heat-transfer coefficient in the air stream is

$$h = 10 \text{ Btu/(hr)(ft}^2\text{)(F)}$$

Hence the characteristic value is $hX/k = (10 \times 0.01)/5 = 0.02$. A comparison with the values in Fig. 28 shows that it is permissible to apply Eq. (104*a*) (with the factor 2 in the exponent) to the existing case. The temperature ratio $t/t_0$ becomes 0.5 in Eq. (104) when the exponent has the numerical value 0.693. Thus is obtained the equation for the determination of the half-value time $\tau_H$, $2(\alpha\tau_H/X^2)(hX/k) = 0.693$. The characteristic value $\alpha\tau_H/X^2$ thus becomes

$$\frac{\alpha\tau_H}{X^2} = \frac{0.693}{2 \times 0.02} = 17.3$$

and the *half-value time*,

$$\tau_H = \frac{(1 \times 10^{-4} \times 17.3)}{0.178} \text{ hr} = 0.0098 \times 3{,}600 \text{ sec} = 35 \text{ sec}$$

Only for unsteady temperature changes, which are slower (with a sine-shaped temperature oscillation the period duration must be about tenfold), may we expect that the thermometer records the temperature trend accurately.[1]

The solution of the heat-conduction equation for the quasi-stationary case, where the surrounding temperature changes periodically with the time, shows that the fluctuations of the surrounding temperature penetrate only to a certain depth inside the body. The temperature distribution in an infinitely thick wall is shown in Fig. 29 according to Groeber and Erk. It is assumed that the surface temperature changes according to the equation

$$t_0 = t_{0M} \sin\left(2\frac{\pi}{\tau_0}\tau\right) \tag{105}$$

This is sine-shaped with a frequency of $1/\tau_0$. The solution for the trend of the temperature $t$ can be presented in the form

$$\frac{t}{t_{0M}} = f\left(\frac{\tau}{\tau_0}, \frac{x}{2\sqrt{\pi\alpha\tau_0}}\right) \tag{106}$$

Consequently, it depends only on the ratio of the time $\tau$ to the period $\tau_0$ of the temperature oscillation of the surface, and on the characteristic value $x/(2\sqrt{\pi\alpha\tau_0})$ in which $x$ is the distance from the surface and $\alpha$ is the thermal diffusivity. The temperature distribution for several time increments is given in Fig. 29. From this we learn that the temperature oscillation in the wall becomes increasingly smaller, the higher the value $x/(2\sqrt{\pi a \tau_0})$, and that it also lags in time behind the temperature oscillation of the surface. The depth of penetration of the temperature oscillation is smaller the smaller the time $\tau_0$; hence, the greater the oscillation frequency on the surface. The quantity of heat which is absorbed and given off per unit area by the wall during such an oscillation is determined by the equation

---

[1] F. Lieneweg, *Wiss. Veröffentl. Siemens-Werken*, **16**, 112–126 (1937); **17**, 19–32 (1937); **19**, 73–87 (1940); also a brief report on the subject in *Z. Ver. deut. Ing.*, **85**, 272–273 (1941).

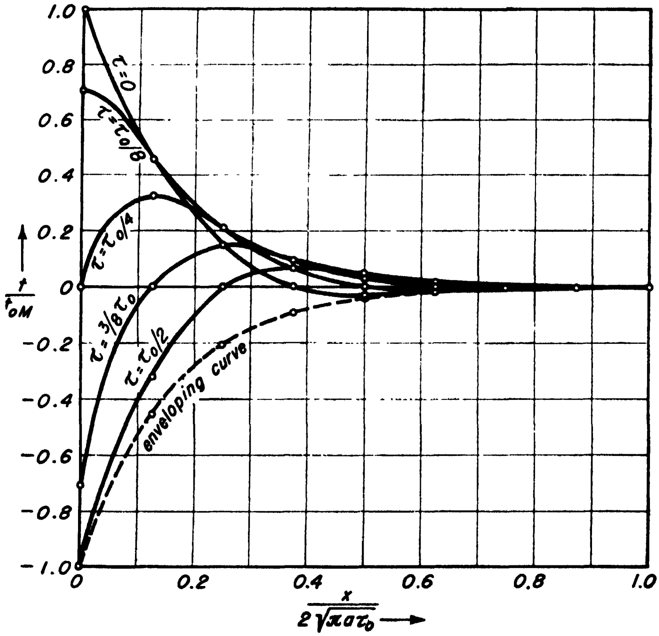

FIG. 29. Penetration of a temperature oscillation into an infinitely thick wall. (*From H. Groeber and S. Erk, "Die Grundgesetze der Wärmeübertragung," p. 75, Fig.* 36, *Springer-Verlag, Berlin,* 1933.)

$$q = c\gamma \int_0^\infty 2t_M\,dx$$

in which $t_M$ signifies the enveloping curve of the temperature curves in Fig. 29. The expression is given by an area which lies between the two enveloping curves in Fig. 29, if we multiply such an area by the specific heat $c$, the specific weight $\gamma$ of the wall, the temperature amplitude $t_{0M}$, and by $2\sqrt{\pi a \tau_0}$. This area has the value $(1/\sqrt{2\pi})$ and thus there is obtained for the quantity of heat which is stored up in the wall during an oscillatory period the equation

$$q = 0.8\sqrt{\pi k c \gamma \tau_0}\, t_{0M} \tag{107}$$

Such temperature oscillations determine, for instance, the wall losses in steam engines, in which at the time when the cylinder is filled with high-temperature steam, heat is transmitted to the wall. This heat, however, is returned to the steam when it is cooled by expansion. Also, the knowledge of temperature oscillations in walls is of importance for determination of thermal stresses which occur in cylinders and pistons of combustion engines.

**Example 3.** It is to be determined to what depth the daily and yearly temperature fluctuations penetrate the ground. From the Appendix can be obtained the thermal diffusivity of clayey soil, 0.039 ft²/hr, and the thermal diffusivity of sandstone, 0.041 to 0.049 ft²/hr. Calculations are performed with the lower value 0.039. We infer from Fig. 29 that the oscillations have practically died off when $x/(2\sqrt{\pi\alpha\tau_0}) = 0.8$. For the daily fluctuations $\tau_0 = 24$ hr. Thus is obtained

$$x = 1.6\sqrt{\pi 0.039 \times 24}\text{ ft} = 2.73\text{ ft}$$

With the yearly fluctuation, the depth of penetration is the $\sqrt{365}$-fold, hence 52.2 ft.

It can also be calculated to what depth the temperature oscillations penetrate into the cylinder wall of a piston engine, which operates at 2,000 rpm. The duration of an oscillation is

$$\tau_0 = \frac{1}{60 \times 2{,}000} = \frac{1}{12 \times 10^4}\text{ hr}$$

the thermal diffusivity of iron is $\alpha = 0.64$ ft²/hr. Thus is obtained the depth of penetration,

$$x = 1.6\sqrt{\frac{\pi \times 0.64}{12 \times 10^4}} = 6.54 \times 10^{-3}\text{ ft}$$

The fluctuation penetrates only to a depth of 0.08 in. into the cylinder wall. Due to the finite surface heat-transfer coefficient, the fluctuation of the surface temperature is also much lower than the fluctuation of the gas temperature. According to tests of A. Meier[1] with an Otto engine with $n = 2{,}000$ rpm the fluctuation of the surface temperature is approximately 20 F.

---

[1] A. Meier, *Forsch. Gebiete Ingenieurw.*, **10**, 41–54 (1939).

## 12. The calculation of the regenerator

Transient heat-conduction processes also occur in regenerator heating processes. A regenerator is understood to be a heat exchanger through which flows alternately warm and cold gas, normally in counterflow, and wherein a mass of high heat capacity absorbs and rejects the transferred heat periodically. Regenerators with brick walls as heat accumulators are frequently used in the steel industry (air heaters for blast furnaces). In the case of steam boilers also, regenerators made of metal have found a definite place as well as in low-temperature operations for separating gases. A very elegant method for calculating heat exchangers, which will be discussed here, was given by H. Hausen.[1] In such a heat exchanger through which there flow alternately hot and cold gases in opposite direction, the temperatures of the gases as well as of the heat-accumulating walls change not only with respect to location but also with time. The variation of temperatures with time in a cross section within the regenerator is given in Fig. 30*a*. Figure 30*b* shows the temperature distribution in the wall for various elapsed times after switching from the heating to the cooling period. Apart from the regenerator ends, the temperature $t_{g1}$ of the hot gas rises almost linearly with time, and the temperature $t_{g2}$ decreases practically linearly with time. The mean wall temperature $t_m$ changes linearly with time. The surface temperature $t_0$ of the wall changes rapidly immediately after switching, and approaches soon thereafter a linear course.

For the quantity of heat $Q_P$,[2] which is transferred to the regenerator wall by the hot gas during the time $\tau_H$ of the heating period, the equation

$$Q_P = h_H A(t_{g1} - t_0)\tau_H$$

can be written. There $h_H$ is the film heat-transfer coefficient of the gas to the wall; $\tau_H$ is the time of the heating cycle; and $t_{g1}$ and $t_0$ are the mean values of the temperatures with respect to time. These mean values of the temperatures agree practically with the instantaneous values in the middle of the heating period.

---

[1] H. Hausen, *Arch. Eisenhüttenw.*, **12**, 473–480 (1938–1939).

[2] It may be emphasized that $Q_P$ is not the heat flow per unit time, but the heat transferred in the heating (and in the cooling) period.

The same quantity of heat is transferred from the wall to the cold gas during the cold period of duration $\tau_c$. With the film heat-transfer coefficient $h_c$ existing in the period $\tau_c$ and the corresponding temperatures $(t'_0 - t_{g2})$,

$$Q_P = h_c A(t'_0 - t_{g2})\tau_c$$

In these equations $A$ is the surface of the heat-accumulating walls which is in contact with the gases. Now the surface temperature is to be eliminated from the equations in the same manner as was done with the mathematical computations of the steady-state heat transfer. For this it is necessary to compute the temperature difference $\Delta t_0 = t_0 - t'_0$, which according to Fig. 30$a$ is composed of the two components $(t_0 - t_m)$ and $(t_m - t'_0)$. The latter value is plotted in Fig. 30$b$. If the heat-accumulating brick walls are assumed plane, the temperature distribution in them can be found by Eq. (96). If the temperature distribution is linear with respect to time as is shown in Fig. 30$a$, then $\partial t/\partial \tau$ = constant. Thus $\alpha(\partial^2 t/\partial x^2)$ = constant, and the double integration leads to the parabolas plotted in Fig. 30$b$. A different temperature distribution occurs only immediately after switching, since at this moment the temperature change with respect to time is also different. The slope of the parabolic temperature profile at the surface of the wall can be determined

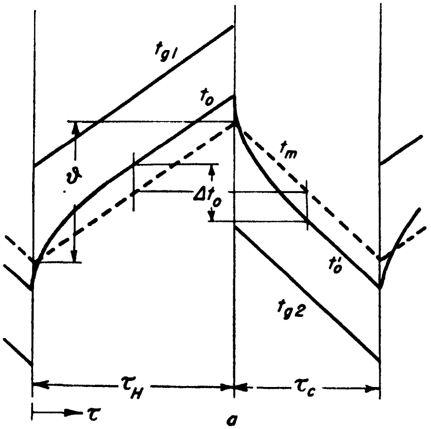

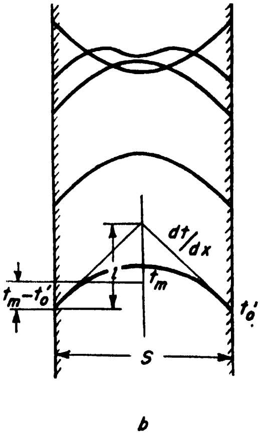

FIG. 30a. Time-temperature fluctuation of the walls and gases in a regenerator.
FIG. 30b. Temperature profiles in the wall of a regenerator at different instants.
[*From H. Hausen, Arch. Eisenhüttenw.*, **12**, 473–480 (1938).]

from the fact that the quantity of heat which passes from the surface to the gas per unit of time must equal the heat flowing by conduction from the inside of the wall to the surface, or

$$\frac{Q_P}{\tau_c} = -kA\left(\frac{\partial t}{\partial x}\right)_0$$

The distance $l$ in Fig. 30*b* is, $l = (s/2)(\partial t/\partial x)_0 = (Q_P/A)(s/2k\tau_c)$, the height of the parabola is half this value, and the distance $(t_m - t_0')$ is two-thirds the height of the parabola. Therefore,

$$t_m - t_0' = \frac{Q_P}{A}\frac{s}{6k\tau_c}$$

In the same manner for the heating period

$$t_0 - t_m = \frac{Q_P}{A}\frac{s}{6k\tau_H}$$

and consequently for the temperature difference

$$t_0 - t_0' = \frac{Q_P}{A}\left(\frac{1}{\tau_H} + \frac{1}{\tau_c}\right)\frac{s}{6k}$$

If the first two equations of the paragraph are solved for the temperature,

$$t_{g1} - t_0 = \frac{Q_P}{A}\frac{1}{h_H\tau_H}$$

$$t_0' - t_{g2} = \frac{Q_P}{A}\frac{1}{h_c\tau_c}$$

and by adding the last three equations,

$$t_{g1} - t_{g2} = \frac{Q_P}{A}\left[\frac{1}{h_H\tau_H} + \frac{1}{h_c\tau_c} + \left(\frac{1}{\tau_H} + \frac{1}{\tau_c}\right)\frac{s}{6k}\right]$$

Hence, the result is

$$\mathbf{Q}_P = \frac{1}{\dfrac{1}{\mathbf{h}_H\tau_H} + \dfrac{1}{\mathbf{h}_c\tau_c} + \left(\dfrac{1}{\tau_H} + \dfrac{1}{\tau_c}\right)\dfrac{\mathbf{s}}{\mathbf{6k}}}\mathbf{A}(\mathbf{t}_{g1} - \mathbf{t}_{g2}) \qquad (108)$$

With this equation the heat $Q_P$ which is transferred from the hot to the cold gas during a full period of the duration $(\tau_H + \tau_c)$ can be computed if the mean values of the gas temperatures with respect to times $t_{g1}$ and $t_{g2}$ are known. The equation was deduced only for a cross section in the heat exchanger. If it is desired to compute the heat delivery of the total regenerator, then there must be introduced for the temperature difference $(t_{g1} - t_{g2})$ the logarithmic mean temperature difference according to Eq. (24), which is obtained from the intake and outlet temperatures of the gases. Eq. (108) shows a great similarity to Eq. (11) for steady-state heat passage through a plane wall. The fraction in Eq. (108) corresponds to the over-all heat-transfer coefficient in the latter case.

If the heating period is equal to the cooling period $\tau_H = \tau_c = \tau$ then $Q$, the heat exchanged per unit of time, is given as

$$Q = \frac{Q_P}{2\tau} = \frac{1}{\frac{1}{h_H} + \frac{1}{h_c} + \frac{s}{3k}} \frac{A}{2} (t_{g1} - t_{g2})$$

If this relation is compared with Eq. (11), it must be borne in mind that in the recuperator only one surface of the wall, but here both surfaces have to be employed for $A$. The heat delivery of both heat exchangers becomes equal when the wall thickness of the stationary heat exchanger, which is also called recuperator, amounts to one-third the wall thickness of the regenerator. The difference is accounted for by the fact that with the recuperator the total heat quantity flows through the wall, while with the regenerator the heat flows into the wall through both surfaces during the heating period and during the cold period leaves the wall in the same way it entered. Hence it is not necessary that the heat flow through the entire wall in the case of the regenerator.

The exchange of heat may be reduced by a layer of dust. If a layer of dust of thickness $s_0$ and thermal conductivity $k_0$ is placed on each surface of the wall, Eq. (108) becomes

$$Q_P = \frac{1}{\frac{1}{h_H\tau_H} + \frac{1}{h_c\tau_c} + \left(\frac{1}{\tau_H} + \frac{1}{\tau_c}\right)\left(\frac{s}{6k} + \frac{s_0}{k_0}\right)} A(t_{g1} - t_{g2})$$

The temperature change $\vartheta$ of the wall during a hot or cold period is obtained from the equation

$$Q_P = c\gamma s \frac{A}{2} \vartheta$$

in which $c$ is the specific heat and $\gamma$ the specific weight of the wall.

In the preceding calculations the processes immediately after switching and at the regenerator entrance and exit of the flow passageways were simplified. Considerable inaccuracies in the results occur by this simplification only in rare cases. H. Hausen[1] has also examined these processes and has published diagrams from which such influences can be seen. According to Hausen's diagram the term $\frac{s}{6k}\left(\frac{1}{\tau_H} + \frac{1}{\tau_c}\right)$ in Eq. (108) must be reduced by 10 per cent if $\frac{s^2}{2\alpha}\left(\frac{1}{\tau_H} + \frac{1}{\tau_c}\right) = 3$ ($\alpha$ = thermal diffusivity of the wall). For values lower than 3 the correction is less.

The influences of the regenerator entrance and exit are determined by two characteristic values, $\frac{\kappa}{c\gamma s}$ and $\frac{\kappa A}{(G_H c_H \tau_H + G_c c_c \tau_c)}$, where $\kappa$ is the fraction in Eq. (108), that is, the value corresponding to the over-all heat-transfer coefficient. $G_H$ and $G_c$ are the weight rates of the hot and cold gas, and $c_H$ and $c_c$ are their respective specific heats. The exchange of heat according to Eq. (108) is correctly determined within 10 per cent as long as $\frac{\kappa}{c\gamma s} < 0.3$ at $\frac{\kappa A}{(G_H c_H \tau_H + G_c c_c \tau_c)} \approx 0$ or $\frac{\kappa}{c\gamma s} < 7$ at $\frac{\kappa A}{(G_H c_H \tau_H + G_c c_c \tau_c)} \approx 50$. The actual value $Q_P$ is somewhat less than the computed value. The recuperators which are most frequently used fulfill the above conditions.

---

[1] H. Hausen, *Z. Ver. deut. Ing., Beilage Verfahrenstechnik*, No. 2, 1942, pp. 31–43.

# CHAPTER 3

# HEAT TRANSFER BY CONVECTION

## 13. The various types of heat transfer

In this paragraph there is discussed heat transfer between a gas or a liquid and a limiting wall. In the interior of the liquid the heat exchange takes place essentially in such a manner that the heat given off by the wall is carried along by the flowing liquid. This form of heat transfer is called heat transfer by convection. The flow of the liquid or gas can be forced from outside sources, *e.g.*, by means of a blower; or it can be caused by the temperature differences which develop as a result of heating. An example of the second type of heat transfer is the heat which a stove gives off to the air in a heated room. The heat exchange between a wall and a gas or fluid when the flow is caused by external forces is termed *heat transfer by forced convection.* The heat exchange between a gas or liquid set in motion by temperature differences only and a wall is called *heat transfer by free convection.* In both cases the resistance to heat transfer is usually concentrated, as mentioned in Sec. 2, in a thin layer immediately adjacent to the wall surface. The heat transfer is essentially a problem of heat conduction within this boundary layer. Hence, the heat-transfer coefficient is determined essentially by the thickness of this boundary layer, and it, in turn, depends on the type of fluid flow along the surface. For forced convection we can deduce from the differential equations which control the fluid-flow and heat-flow process the fact that neither the velocity field nor the development of the boundary layer is influenced by the heat transfer as long as the fluid property values which enter into the flow equations are independent of the temperature. The development of the boundary layer is then a pure fluid-mechanics problem. As can be seen in the property-value tables in the Appendix, all property values are more or less dependent on the temperature. In most cases, however, the temperature dependency is not so great that it would decisively effect the fluid-flow process as long as the temperature differences are not too great. Hence the temperature dependency of the property values is usually disregarded when computing heat transfer. This will be done in the following discussions of heat transfer. Only in certain cases, *e.g.*, with lubrication, does the temperature dependency of the viscosity become so great that the velocity field is fundamentally changed by the temperature differences. The relationships describing the heat-transfer process, however, become then so involved that they have not been clarified fully at the present time. Density is also included as a property value in these calculations. For liquids, density can forthwith be considered as constant in value. The pressure dependency of density is very noticeable, however, for gases as soon as the velocities exceed a certain limit. For air, at normal temperatures, this limit is approximately 300 fps. More generally, for any arbitrary gas it can be fixed at approximately one-third the sonic velocity. For the greatest part in technical applications the velocities that occur lie below this limit. Hence, density can be considered constant for gases also, so that no specific differences between liquids and gases exist. The following formulas developed for heat-transfer coefficients are therefore equally applicable for liquids as for gases. Heat transfer for gases at high velocities, of the order of magnitude of sonic velocity, is discussed in a special section.

In free convection, the flow is generated by the temperature differences only. Consequently, from the outset the flow and heat-exchange processes are intimately connected.

It is to be noted that nearly all relationships known today for heat transfer presuppose that the temperature of solid bodies which absorb or give off heat is the same over the whole surface.

The present work deals almost exclusively with the clarification of heat transfer for steady-state processes. With an unsteady process (transient and periodic) as compared to the steady-state processes, the given relationships change as soon as the temperatures in the boundary layer lag noticeably due to heat accumulation (approximately as in Fig. 29). This is the case only for very rapid changes because the boundary-layer thicknesses are generally small. Heat transfer in the cylinders of diesel engines for ships can be computed with steady-state heat-transfer coefficients.[1]

---

[1] H. Pfriem, Unsteady Heat Transfer in Gases, Especially in Piston Engines, *VDI-Forschungsheft* 413, 1942.

Since heat transfer, as discussed previously, is determined by hydrodynamic processes, familiarity with these processes is absolutely necessary for an understanding of heat-transfer phenomena. Therefore, the most important factors of the flow theory will be repeated in the following section.

## BASIC CONCEPTIONS OF THE FLOW THEORY

### 14. Boundary layer and turbulence

Primarily, there are two conceptions of the flow theory, which are essential for understanding heat transfer; namely, the conception of the boundary layer and the conception of turbulence. Even though liquids and gases have a measurable viscosity which in flow problems causes frictional forces on solid surfaces, it is still possible in many cases to approximate the actual conditions by the hypothesis of a frictionless liquid. In it, two types of forces occur, namely, forces of inertia and forces of pressure. The balance of both forces, along each streamline, is given by the Bernoulli equation (D. Bernoulli 1700–1782)

$$p + \gamma \frac{V^2}{2g} = \text{const} \tag{108a}$$

in which $p$ signifies the fluid pressure, $\gamma$ the specific weight, $g$ the acceleration of gravity, and $V$ the flow velocity. In addition to the forces above, other forces exist in real liquids and gases, which are caused by viscosity. These forces manifest themselves as shearing stresses between the individual streamlines, where they are flowing with different velocities. In a flow according to Fig. 31, in which the velocity $u$ is directed parallel to the wall $ab$ and velocity differences occur in the $y$ direction normally to the wall, a shearing stress $\tau$ occurs due to the viscosity in an arbitrary plane, 1-1, which is parallel to the wall. The value of the stress is given by Newton's equation

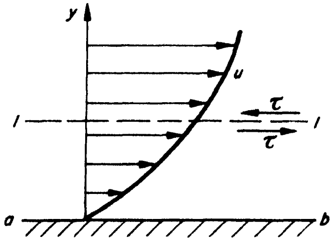

FIG. 31. Shearing stress in a viscous fluid.

$$\tau = \mu \frac{du}{dy} \tag{109}$$

The shearing stress is therefore proportional to the velocity gradient normal to the direction of flow. The proportionality factor $\mu$ is a property value and is called the *dynamic viscosity.* Its dimension is obtained from the equation of definition (109) as pound-seconds per square foot. Besides the dynamic viscosity, the kinematic viscosity is frequently applied. Kinematic viscosity $\nu$ is related to dynamic viscosity by the relation

$$\nu = \frac{\mu}{\rho} = \frac{g\mu}{\gamma} \tag{110}$$

where $\rho$ signifies the density. The dimension of the kinematic viscosity is square feet per second. In the tables of property values in the Appendix some viscosities are shown. Since the dynamic viscosity in some handbooks is given in the absolute system, namely, in poises [1 poise = 1 g/(sec)(cm)], errors occur frequently in its application to the engineering measuring system. These errors can be avoided if the calculations are made with the kinematic viscosity which has the same dimensions in both measuring systems. For this reason the kinematic viscosity is recorded in the tables in the Appendix.

In liquids as well as in gases the dynamic viscosity $\mu$ depends primarily upon the temperature, and only slightly upon the pressure. Only in the vicinity of the critical point does there occur a strong pressure dependency. Figure 139 shows these relationships for water and steam. All other liquids behave principally in the same manner. According to Eq. (110) the kinematic viscosity $\nu$ in liquids is also practically independent of pressure because of their low compressibility. In gases, according to the equation of state, it is inversely proportional to the pressure. The numerical value of dynamic viscosity is considerably higher for liquids than for gases. For kinematic viscosity this relationship is often reversed. For example, the value for water at room temperature is approximately one-tenth the value for air at room temperature.

Since the numerical values of the viscosity are comparatively low, higher shearing stresses in a flow, according to Eq. (109), occur only where high velocity gradients, *du/dy*, exist. These high gradients are always found on solid walls within a flow field. If the velocity field is tested with a fine pitot tube in the immediate vicinity of such a wall, a velocity profile is obtained as in

Fig. 32. The velocity begins with the value zero at the wall and increases within a thin layer of the thickness $\delta$ to the value of the undisturbed stream which occurs at some distance from the body. This knowledge, which is essential for the flow theory and for the heat-transfer theory, is the contribution of Ludwig Prandtl (1904). The term *boundary layer for the thin layer with steep velocity increase* was also conceived by Prandtl. Outside the boundary layer, the velocity gradient normal to the direction of flow is so low that the viscosity effects may be disregarded. Hence it can be assumed that each flow can be divided into two regions; namely, the boundary layers to which the viscosity effect is confined, and the main flow outside the boundary layer which can be considered frictionless and in which region for this reason the Bernoulli equation applies for each streamline. The fact that the boundary layers are the cause of all flow separations and in this manner bring about a change in the main flow will be discussed in the following section.

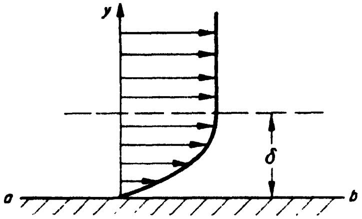

FIG. 32. Boundary layer on a solid surface.

In 1883, Osborne Reynolds proved for the first time that two basically different forms of flow exist, namely, a *laminar* and a *turbulent* flow. In laminar flow the individual streamlines run in an orderly manner side by side, while in turbulent flow the streamlines are interwoven with each other in an irregular manner. In the latter case, the individual fluid particles execute fluctuating motions around some mean flow path in an irregular manner. In daily life for example, one can observe both flow processes in the smoke which rises from a cigarette. The smoke, as can be seen in Fig. 33, rises first in the form of a straight thread. After a certain distance, however, it becomes wavy and curly and the smoke thread vanishes quickly by mixing with the air. The first part represents the laminar form of flow and the second part the turbulent form of flow. Turbulence can be generated in an air stream by holding a wire grid in the flow. In every wind tunnel there is a certain turbulence, which is induced in the air stream by the blower and the guide vanes. Heat exchange by convection is promoted by the fluctuating motions in turbulent flow. Consequently, heat transfer in turbulent flow is considerably higher than in laminar flow. The flow can also be turbulent within the boundary layer. This type of turbulence is of considerable interest when considering the heat-exchange process. On a flat plate which is parallel to the flow, a boundary layer is formed as illustrated in Fig. 34. Its thickness increases toward the rear, being zero at the plate leading edge. At a certain critical distance $x_c$ from the leading edge, the flow within the boundary layer, which is at first laminar, changes into turbulent motion. If the velocity $u_s$ is increased, the critical length $x_c$ becomes continuously less in such a manner that the product $u_s x_c$ remains unchanged. If finally the tests are made with gases or liquids with various viscosities, it is found that the change from laminar to turbulent flow takes place at a definite value of the dimensionless term $(u_s x_c/\nu)$. This fact was first discovered by Reynolds. In his honor the dimensionless term, which is obtained by multiplication of a velocity with a length and by division with a kinematic viscosity, was named the Reynolds number or Reynolds modulus *Re*. The value of the Reynolds number at which the flow changes into the turbulent form is called the critical Reynolds number, $Re_c$. A more intensive investigation reveals that the

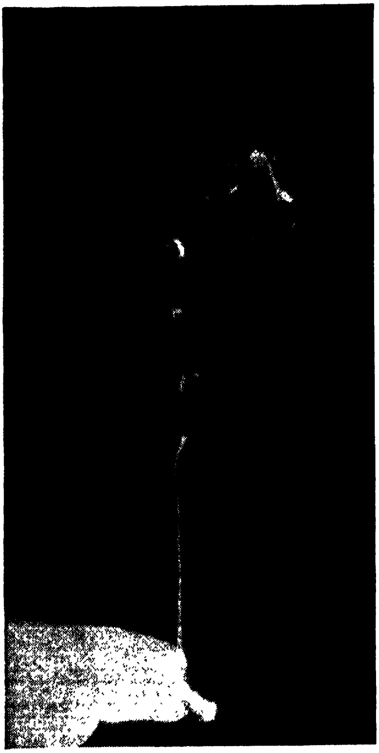

**Fig. 33. Laminar and turbulent flow of cigarette smoke.**

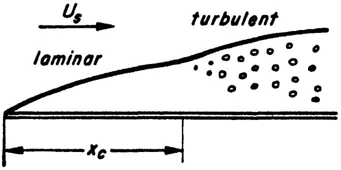

**Fig. 34. Laminar and turbulent boundary layer on a plate.**

critical Reynolds number, at which the change takes place, can be influenced by outer circumstances. If the approaching flow has already been disturbed, *e.g.*, by a turbulence grid or by a special shape of the leading edge of the plate,[1] or if the surface of the plate is rough, the change is attained at a lower critical Reynolds number. If these disturbances are prevented, it is possible to obtain a higher critical Reynolds number. Up to the present time, the change from laminar to turbulent flow has been observed in the range of $Re_c$ between 80,000 and 5,000,000. It is assumed that the lower limit can be forced down still further by very strong disturbances. Likewise, the upper boundary can be increased still further by carefully eliminating all disturbances. Under industrial conditions we can always expect a turbulent boundary layer for critical Reynolds numbers over 500,000.

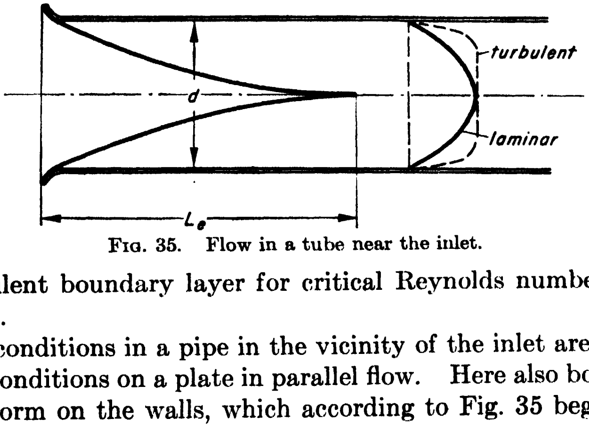

FIG. 35. Flow in a tube near the inlet.

The conditions in a pipe in the vicinity of the inlet are similar to the conditions on a plate in parallel flow. Here also boundary layers form on the walls, which according to Fig. 35 begin with the thickness zero at the pipe inlet and increase continuously toward the rear. It is assumed that by taking a suitable shape for the inlet, the flow into the pipe is smooth and without separation. At a certain distance $L_e$ from the inlet the boundary layers become so thick that they make contact with each other. The velocity profile downstream from this point (Fig. 35) has the form of either a parabola or an arched curve, depending on whether the boundary layers are still laminar or already turbulent. Further downstream the velocity profile does not change its shape. This downstream part of the flow is called *developed flow.* The entrance length $L_e$ divided by the diameter $d$ of the tube is a function of the Reynolds number. In the developed-flow region, the flow is turbulent if the Reynolds number exceeds a critical value. If the Reynolds number is defined by the mean velocity $u_m$ over the cross section and the tube diameter $d$, the critical value for undisturbed inflow is $Re_c = u_m d/\nu = 2{,}300$. By carefully avoiding all disturbances, a critical Reynolds number of 500,000 was reached. Under conditions as they prevail in industrial applications flow in tubes certainly is turbulent when the Reynolds number exceeds the value 3,000.

---

[1] Even a round leading edge may cause turbulence for thicker plates.

## 15. The momentum equation of the boundary layer

For the following calculations of heat transfer it is necessary first to calculate the boundary layer, especially its thickness. For laminar boundary layers on bodies of various shapes this problem was solved by integration of the boundary layer equations derived by L. Prandtl in 1904. The computations, however, are difficult and lengthy. Therefore there will be used here an approximate method originated by T. von Kármán.[1] This method is much simpler, and has an advantage in that it can be applied to cases for which an exact solution is impossible. In all cases where the approximate method was applied with physical logic it gave very satisfactory results. It starts from the law of momentum, which may be formulated for a steady flow in the following way:

*Imagine in the flow field a certain region enclosed by a stationary control surface of arbitrary form. The fluid particles in flowing through this region generally change their momentum*

$$\textit{Momentum} = \textit{mass} \times \textit{velocity}$$

*The increase of momentum per unit of time of all particles passing this region may be expressed also as the difference between the momentum leaving the region per unit time and the momentum flowing into it through the enveloping surface. This change in momentum is equivalent to inertia forces and must be in equilibrium with the external forces acting on the surface or within it.*

This law may now be applied to two-dimensional flow along a plane wall (Fig. 36). Use is made of a system of coordinates whose $x$ axis is parallel to the wall and whose $y$ axis is normal to it. The velocities $u$ have essentially a direction parallel to the wall. Only small velocities $v$ normal to the wall will occur. The law of momentum is used for the $x$ direction. The control surface is built by two planes 1-2 and 3-4, spaced apart from each other by the small distance $dx$, by a plane parallel to the wall at a distance $l$, and by the wall. The distance $l$ may be greater than the boundary-layer thickness $\delta$. The velocity profile in the plane 1-2 has the sketched shape. At a distance $y$ from the wall the velocity is $u$. The outside flow velocity $u_s$ is reached at the distance $\delta$ from the wall, therefore within the length $l$. The control surfaces which are parallel to the plane of the paper are a unit distance apart. Through a strip with the height $dy$ at a distance $y$ the mass flow per unit time is $\rho u\, dy$. Its momentum in the $x$ direction is obtained by multiplying it by the velocity component $u$. The momentum flow therefore is $\rho u^2\, dy$. The momentum flow through the whole plane 1-2 is

---

[1] T. von Kármán, *Z. angew. Math. Mech.*, **1**, 235 (1921).

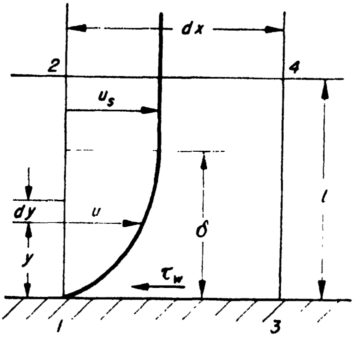

FIG. 36. Calculation of the flow boundary layer.

$$\rho \int_0^l u^2\, dy$$

Progressing in the $x$ direction this momentum flow changes by

$$\rho \frac{d}{dx}\left(\int_0^l u^2\, dy\right) dx = \rho\, dx \frac{d}{dx} \int_0^l u^2\, dy$$

Through the wall 1-3 there is no flow. Through the plane 2-4, however, a flow occurs, the amount of which may be calculated in the following way. The mass flow through plane 1-2 per unit time is $\rho \int_0^l u\, dy$. In progressing by the distance $dx$ this flow changes by $\rho\, dx \frac{d}{dx} \int_0^l u\, dy$. This is the difference between the flow through the planes 3-4 and 1-2, and it must have entered the cube through plane 2-4. The velocity component in the $x$ direction in this plane is $u_s$. Therefore the $x$ momentum flow through plane 2-4 is

$$\rho u_s\, dx \frac{d}{dx} \int_0^l u\, dy$$

The whole increase in momentum within the cube is therefore

$$-\rho u_s\, dx \frac{d}{dx} \int_0^l u\, dy + \rho\, dx \frac{d}{dx} \int_0^l u^2\, dy$$
$$= -\rho\, dx \frac{d}{dx} \int_0^l (u_s - u) u\, dy + \rho\, dx \frac{du_s}{dx} \int_0^l u\, dy$$

The following external forces act on the surface of the parallelepiped in the $x$ direction: a shearing stress $\tau_w$ along the wall, and the pressures $p$ and $p + (dp/dx)\, dx$ on the planes 1-2 and 3-4. In the plane 2-4 no shearing stresses occur, since the plane is beyond the boundary layer. By equating these forces with the increase of momentum,

$$\rho \frac{d}{dx} \int_0^l (u_s - u) u\, dy - \rho \frac{du_s}{dx} \int_0^l u\, dy = \tau_w + l \frac{dp}{dx} \qquad (111)$$

This is the *momentum equation of the boundary layer.* Since the thickness of this layer is very small, Eq. (111) can be used also for curved walls as long as the curvature is not very sharp. The coordinate $x$ must then be measured along the surface of the wall, the coordinate $y$ normal to it. The velocity $u_s$ outside the boundary layer or the pressure along the wall must be known either by calculation or by measurement, if Eq. (111) is to be solved. Both values are connected by the Bernoulli equation (108*a*). Equation (111) can be solved according to von Kármán's suggestion, when the approximate shape of the velocity profile is known. By evaluation of the integral in Eq. (111) the boundary-layer thickness and the friction coefficient are found. The result naturally becomes the more accurate the better the shape of the velocity profile as introduced into the calculation, but it has been stated that rough assumptions also give quite accurate results.

## 16. The plane plate in longitudinal flow

Equation (111) is to be used to calculate the boundary-layer thickness along a plane wall. It has been mentioned that on the surface next to the leading edge a laminar boundary layer develops (Fig. 34). The velocity $u_s$ outside the boundary layer may be constant along the plate. The Bernoulli equation states that pressure is constant. The last term on both sides of Eq. (111) therefore vanishes. The velocity profile in a laminar boundary layer was found by measurements to be similar to a parabola (Fig. 37). It is, however, more suitable to use a cubic parabola,

$$u = ay + cy^3 \tag{112}$$

instead of the ordinary one for the following reason. In the immediate proximity of the wall, the velocities must be very small; therefore no inertia forces but only friction forces act on a fluid particle in this region. The equilibrium condition for such a particle demands, therefore, that the shearing stresses be constant in the $y$ direction in the immediate neighborhood of the plate. This means, according to Eq. (109), that the velocity gradient $du/dy$ is constant or $d^2u/dy^2$ is zero:

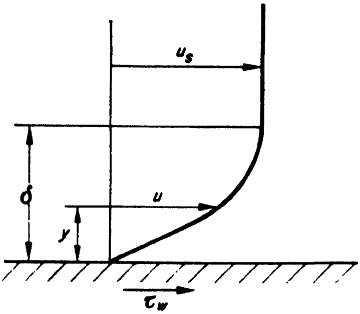

Fig. 37. Laminar boundary layer on a flat plate.

$$\left(\frac{d^2u}{dy^2}\right)_w = 0 \tag{113}$$

This condition is fulfilled by Eq. (112). The selected velocity profile must have the value zero at the wall ($y = 0$), and must pass over to the constant velocity $u_s$ outside the boundary layer without discontinuity. This gives the following equations, by which the constants $a$ and $c$ in Eq. (112) can be determined:

$$\text{For } y = 0,\ u = 0$$

$$\text{For } y = \delta,\ u = u_s \text{ and } \frac{du}{dy} = 0$$

This gives

$$a = \frac{3}{2}\frac{u_s}{\delta} \qquad c = -\frac{1}{2}\left(\frac{u_s}{\delta^3}\right)$$

and for the velocity profile

$$\frac{u}{u_s} = \frac{3}{2}\frac{y}{\delta} - \frac{1}{2}\left(\frac{y}{\delta}\right)^3 \tag{112a}$$

With this equation the integral in Eq. (111) becomes

$$I = \rho \int_0^l (u_s - u)u\,dy$$

$$= \rho u_s^2 \int_0^\delta \left[\frac{3}{2}\frac{y}{\delta} - \frac{1}{2}\left(\frac{y}{\delta}\right)^3\right]\left[1 - \frac{3}{2}\frac{y}{\delta} + \frac{1}{2}\left(\frac{y}{\delta}\right)^3\right] dy$$

The upper limit in the integral had to be changed to $\delta$, since for a condition $y > \delta$, the velocity $u = u_s$, and therefore the integrand is zero. If the multiplication of the two terms in the brackets is completed and the integration accomplished for every summand, the integral gives

$$I = {}^{39}\!/_{280}\,\rho u_s^2 \delta$$

The velocity gradient at the wall gives Eq. (112*a*),

$$\left(\frac{\partial u}{\partial y}\right)_w = \frac{3}{2}\frac{u_s}{\delta}$$

Therefore the shearing stress at the wall is

$$\tau_w = \mu \left(\frac{\partial u}{\partial y}\right)_w = \frac{3}{2}\mu\frac{u_s}{\delta}$$

By introducing this expression and the value $I$ in the equation of momentum, Eq. (111), the following differential equation results:

$$\frac{39}{280}\rho u_s^2 \frac{d\delta}{dx} = \frac{3}{2}\mu\frac{u_s}{\delta}$$

and by separating the variables,

$$\delta\,d\delta = \frac{140}{13}\frac{\nu}{u_s}dx \tag{114}$$

Integrating gives

$$\delta = 4.64\sqrt{\frac{\nu x}{u_s}} \tag{114a}$$

The integration constant is accounted for, when $x$ is measured from the leading edge, as then for $x = 0$ the thickness $\delta$ must also be 0. Equation (114*a*) shows that $\delta$ increases with the square root of the distance $x$. It is practicable to write the equation in dimensionless form as

$$\frac{\delta}{x} = \frac{4.64}{\sqrt{u_s x/\nu}}$$

The expression under the radical is the Reynolds number formed with the distance $x$. It may be denoted as $Re_x$. Therefore

$$\frac{\delta}{x} = \frac{4.64}{\sqrt{Re_x}} \tag{115}$$

The boundary-layer thickness $\delta$ is the distance from the wall where the velocity as approximated by Eq. (112*a*) reaches the value of the outside flow velocity. It is clear that the so defined boundary-layer thickness is somewhat arbitrary. The exact calculation of laminar boundary layers gives velocity profiles which reach the outside velocity only asymptotically. For such profiles there exists no finite value $\delta$ corresponding to the one above. Other definitions for the boundary-layer thickness were used, *e.g.*, the wall distance where the velocity is 0.99 of the outside flow velocity. Presently, however, the value called *displacement thickness* is almost generally accepted. It is obtained by a procedure shown in Fig. 38. The area above the velocity profile is transformed into a rectangle *abcd* with equal area. The width of this rectangle $\delta\star$ is the displacement thickness. Mathematically it is obtained from the equation

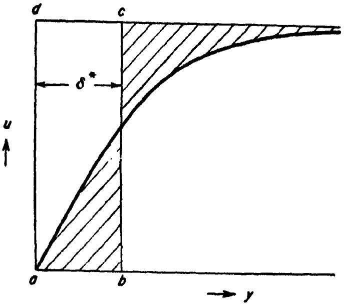

FIG. 38. Displacement thickness of the boundary layer.

$$\delta\star = \int_0^\infty \left(1 - \frac{u}{u_s}\right) dy \tag{115a}$$

The name comes from the fact that in a frictionless fluid flow without boundary layers the walls would have to be displaced in outward direction by the amount $\delta\star$ to keep the flow field unchanged as compared with the real flow with boundary layers. For the velocity profile given by Eq. (112*a*) the above integral gives

$$\delta\star = 0.375\delta \sim \frac{\delta}{3}$$

The shearing stress at the wall follows as

$$\tau_w = \frac{0.323\rho u_s^2}{\sqrt{Re_x}} \tag{116}$$

Instead of this value, the friction coefficient $f_p$ is generally used. This is the resistance force of the plate divided by the area of the surface and the dynamic pressure in the flow. There must be discerned two values: the local coefficient $f_p$ and the average coefficient $f_{pm}$. The first is defined by the equation

$$\tau_w \, dx = f_p \, dx \, \rho \frac{u_s^2}{2}$$

Therefore

$$f_p = \frac{2\tau_w}{\rho u_s^2}$$

The second is given by

$$\int_0^x \tau_w \, dx = f_{pm} x \rho \frac{u_s^2}{2}$$

$$f_{pm} = \frac{2}{x\rho u_s^2} \int_0^x \tau_w \, dx = \frac{1}{x} \int_0^x f_p \, dx$$

The result is

$$\mathbf{f}_{pm} = \frac{\mathbf{1.292}}{\sqrt{\mathbf{Re}_x}}$$

**By exact calculation the same formula has the numerator 1.327, which is 3 per cent greater. The formula is also in good agreement with the results of experiments.**

✓**Example.** The thickness of the boundary layer which builds up on a plate 4 in. distant from the leading edge is to be determined for longitudinal air flow. The velocity is 33 fps, the temperature of the air 60 F, and the pressure atmospheric. The Reynolds number is

$$Re_x = \frac{u_s x}{\nu} = \frac{33 \text{ (fps)} \times 4/12 \text{ (ft)}}{16 \times 10^{-5} \text{ (ft}^2\text{/sec)}} = 69{,}000$$

The kinematic viscosity was taken from the Appendix. The ratio of the boundary-layer thickness to the distance from the leading edge is

$$\frac{\delta}{x} = \frac{4.64}{\sqrt{69{,}000}} = 0.0177$$

The boundary layer is therefore 0.071 in. thick at the 4-in. distance. The displacement thickness is $\delta^\star = 0.0266$ in. It can be seen that for usual velocities and distances the boundary layers build up to about 0.1-in. thickness.

In the *turbulent boundary layer* the shape of the velocity profile is much more curved than in the laminar layer. The measured velocity profile agrees satisfactorily with the equation given by Prandtl:

$$u = u_s \left(\frac{y}{\delta}\right)^{1/7} \tag{117}$$

The equation cannot hold true, however, in the immediate proximity of the wall. This can be shown if the shearing stress at the wall is calculated. The velocity gradient is

$$\frac{du}{dy} = \frac{1}{7}\frac{u_s}{\delta^{1/7} y^{6/7}}$$

and at the wall ($y = 0$) it is infinite. This would give an infinite value of the shearing stress, which is physically impossible. In reality, the turbulence always dies down in the neighborhood of the wall. The real conditions may be simplified, according to Prandtl, by the conception that between the turbulent boundary layer and the wall there exists a laminar sublayer within which the velocity increases linearly with the distance $y$. Outside this sublayer Eq. (117) holds true. The approximated velocities at the border between both layers join each other at a small angle as is shown in Fig. 39. The shearing stress at the wall must be determined by measurement. For not too large Reynolds numbers and smooth surfaces, the equation of Blasius

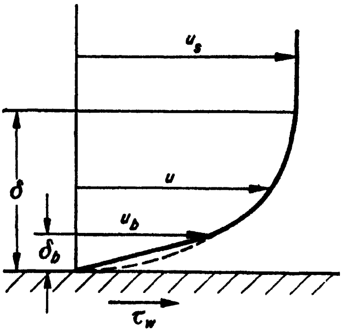

FIG. 39. Laminar sublayer within a turbulent boundary layer.

$$\tau_w = 0.0228\rho u_s^2 \left(\frac{\nu}{u_s\delta}\right)^{1/4} \tag{118}$$

holds true. The equation was determined by experiments on the flow through tubes. It was confirmed from experiments by Schultz-Grunow[1] up to a Reynolds number $10^7$ for flat plates. For higher Reynolds numbers a very complicated equation exists. Such high Reynolds numbers seldom occur in heat-transfer calculations.

With Eq. (117), the momentum integral in Eq. (111) becomes

$$I = \rho \int_0^l u(u_s - u)\,dy = \rho u_s^2 \int_0^\delta \left(\frac{y}{\delta}\right)^{1/7} \left[1 - \left(\frac{y}{\delta}\right)^{1/7}\right] dy = \frac{7}{72}\,\rho u_s^2 \delta$$

Here again the upper limit of the integral must be changed to $\delta$ since Eq. (117) holds true only for $y < \delta$. For $y > \delta$, $u = u_s$; therefore the integrand equals zero.

Introducing the integral $I$ and Eq. (118) into the equation of momentum gives the differential equation

$$\frac{7}{72}\,\rho u_s^2 \frac{d\delta}{dx} = 0.0228 \rho u_s^2 \left(\frac{\nu}{u_s \delta}\right)^{1/4}$$

By separation of the variables there arises

$$\delta^{1/4}\,d\delta = 0.235 \left(\frac{\nu}{u_s}\right)^{1/4} dx$$

and by integration

$$\delta = 0.376 \left(\frac{\nu}{u_s}\right)^{1/5} x^{4/5} \tag{119}$$

According to Fig. 34 the turbulent boundary layer begins at the critical distance $x_c$ from the leading edge. It has there already a certain thickness as it originates from the laminar layer. According to L. Prandtl[2] the calculation agrees satisfactorily with measurements, if the thickness of the boundary layer is determined as if it began at the leading edge with the thickness zero. Newer measurements indicate that this is not quite correct, we will however maintain this simple assumption. The length $x$ in Eq. (119) is then the distance from the leading edge. In dimensionless form the equation is written

---

[1] F. Schultz-Grunow, A New Resistance Law for Smooth Plates, *Luftfahrt-Forsch.*, **17**, 239–246 (1940).

[2] L. Prandtl, Ergebnisse der aerodynamischen Versuchsanstalt Göttingen, **3**, p. 4 (1927).

$$\frac{\delta}{x} = \frac{0.376}{\left(\frac{u_s x}{\nu}\right)^{1/5}} = \frac{0.376}{(Re_x)^{1/5}} \tag{120}$$

On the right side again the Reynolds number calculated with the distance $x$ appears. The displacement thickness of the turbulent profile according to Eq. (117) is $\delta^\star = \delta/8$. If the laminar and the turbulent boundary layers are calculated for the critical distance $x_c$, it can be seen that the turbulent layer is the thicker. In reality an instantaneous increase in boundary-layer thickness is not possible. The transition from the laminar to the turbulent boundary layer takes place in a transition zone as is indicated in Fig. 40.

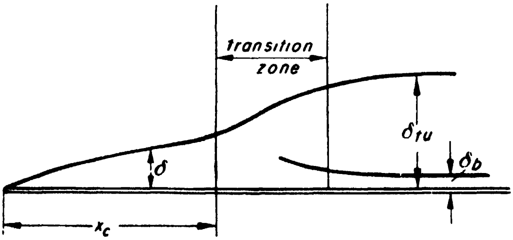

FIG. 40. Laminar and turbulent boundary layers on a flat plate.

The transition from laminar to turbulent flow within the boundary layer starts with oscillations of comparatively long wave lengths. They are basically of the same nature as the waves which can be clearly observed in the thermal free-convection boundary layer on a vertical plate in Fig. 95. It was shown mathematically by W. Tollmien[1] and H. Schlichting[2] that the boundary-layer flow becomes unstable for such oscillations with a certain wave length as soon as the boundary-layer thickness reaches a certain value. This means that such oscillations always present from time to time because of small outer disturbances in the flow are not damped but increase in amplitude as they travel downstream. On their way they become irregular in shape and transform into vortices which finally dissolve into the more small-scaled turbulence. It is easily understood that the flow in

[1] W. Tollmien, *Nachr. Ges. Wiss. Göttingen, Math. physik. Klasse,* 1929, p. 21.

[2] H. Schlichting, *Nachr. Ges. Wiss. Göttingen, Math. physik. Klasse,* 1933, p. 181; 1935, p. 48.

the transition zone where this process takes place is subject to irregular fluctuations with time. This region is extremely difficult to study and our knowledge on this phase is therefore very limited. The calculations given in this section deal with the zone of fully established turbulence.

For the following heat-transfer calculations the thickness $\delta_b$ of the laminar sublayer is needed. To determine this we must first calculate the velocity $u_b$ at the border between the turbulent layer and the laminar sublayer. The linear velocity increase in the sublayer is derived from the shearing stress on the wall,

$$\tau_w = \mu \frac{du}{dy} = \mu \frac{u}{y}$$

Introducing the expression for $\tau_w$ gives

$$u = 0.0228\rho \frac{u_s^2}{\mu} \left(\frac{\nu}{u_s\delta}\right)^{1/4} y$$

Solving this equation for $y$ and taking into account that for $y = \delta_b$, $u = u_b$ the sublayer thickness is obtained as

$$\frac{\delta_b}{\delta} = \frac{u_b}{u_s} \frac{1}{0.0228} \left(\frac{\nu}{u_s\delta}\right)^{3/4}$$

On the other hand at this place Eq. (117) and therefore

$$\frac{\delta_b}{\delta} = \left(\frac{u_b}{u_s}\right)^7$$

also hold true. Equating both expressions gives

$$\frac{u_b}{u_s} = 1.869 \left(\frac{u_s\delta}{\nu}\right)^{-1/8} = \frac{1.869}{(Re_\delta)^{1/8}} \tag{121}$$

The Reynolds number is calculated here with the boundary-layer thickness. By Eq. (119) the distance $x$ can be introduced

$$\frac{u_b}{u_s} = 2.11 \left(\frac{\nu}{u_s x}\right)^{0.1} = \frac{2.11}{(Re_x)^{0.1}} \tag{122}$$

The sublayer thickness is then

$$\frac{\delta_b}{\delta} = \left(\frac{u_b}{u_s}\right)^7 = \frac{191}{Re_x^{0.7}} \tag{123}$$

The shearing stress at the wall is given by

$$\tau_w = \mu \frac{u_b}{\delta_b}$$

$$\tau_w = \frac{0.0296}{(Re_x)^{0.2}} \rho u_s^2$$

The resistance force of the plate can be calculated from the shearing stresses on the first part with the laminar boundary layer and the second part with the turbulent boundary layer.

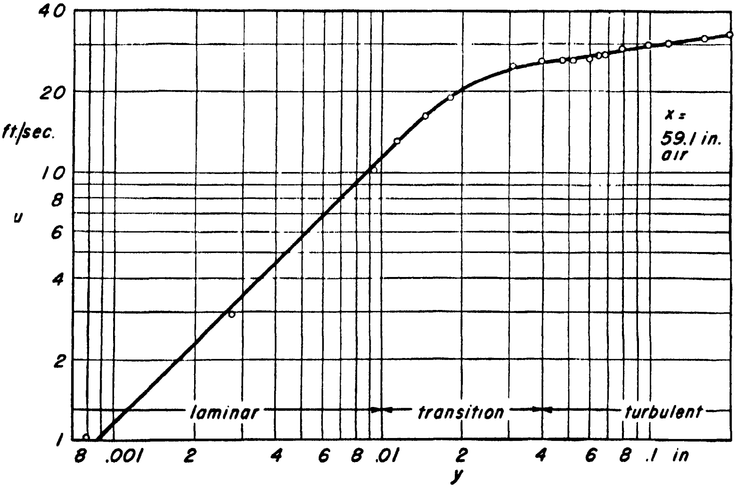

Fig. 41. Velocity profile in the turbulent boundary layer on a flat plate as measured by van der Hegge-Zynen. ("*Measurements of the Velocity Distribution in the Boundary Layer along a Plane Surface,*" *I. Waltmann, Delft,* 1924.)

For a critical Reynolds number of 485,000 this calculation gives

$$f_{pm} = \frac{0.074}{(Re_x)^{1/5}} - \frac{1,700}{Re_x}$$

There corresponds to a critical Reynolds number of 85,000

$$f_{pm} = \frac{0.074}{(Re_x)^{1/5}} - \frac{300}{Re_x}$$

Figure 41 shows the velocity field in the turbulent boundary layer as measured by van der Hegge-Zynen.[1] Here also, instead of a sharp boundary a transition curve arises in which the turbulence dies down. Figure 42 shows a comparison of the above two formulas for the friction coefficient with experimental results.

---

[1] B. G. van der Hegge-Zynen, "Measurements of the Velocity Distribution in the Boundary Layer along a Plane Surface," I. Waltmann, Delft, 1924.

**Example.** The thickness is to be calculated of the turbulent boundary layer which builds up in a 12-in. distance from the leading edge of a plane plate in an air stream flowing with 33 fps velocity, at 60 F, and 14.2 lb/in.$^2$ pressure. The Reynolds number is

$$Re_x = \frac{33 \times 1}{16 \times 10^{-5}} = 200,000$$

Equation (120) gives the ratio of the boundary-layer thickness to the distance from the leading edge: $\delta/x = 0.0333$. The boundary-layer thickness itself is 0.4 in. and the displacement thickness is 0.05 in. The ratio of the laminar sublayer to the turbulent layer is, according to Eq. (123), $\delta_b/\delta = 0.036$. The sublayer thickness is 0.014 in. Because of this small thickness, the shearing stress at the wall for turbulent flow depends much on the roughness of the wall, whereas in laminar flow the roughness has only a small influence. This may be explained by the fact that the shearing stresses and the resistance of the wall increase when the roughnesses are not filled out by the laminar sublayer. Exact measurements show that an increase in resistance arises as soon as the height of the roughnesses is greater than approximately one-third the thickness of the sublayer. For the example calculated above, a plate with roughnesses smaller than 0.004 in. can be called hydraulically smooth. The laminar sublayer thickness decreases with the velocity $u_\infty$, whereas it depends very little on the distance $x$. For high velocities the plate must be especially carefully finished, if an increase of the resistance by roughness is to be avoided. Equation (118) holds true

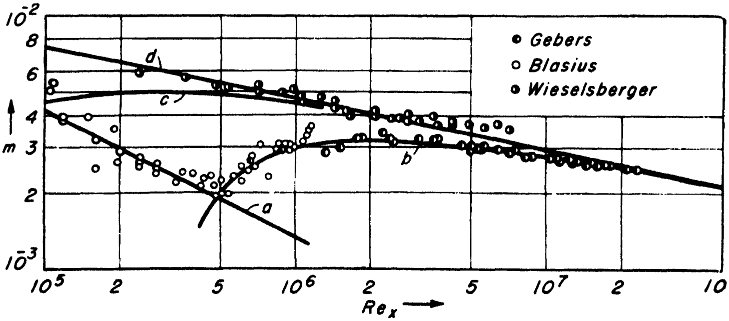

(a) $f_{pm} = 1.327/\sqrt{Re_x}$; (b) $f_{pm} = 0.074/\sqrt[5]{Re_x} - 1700/Re_x$; (c) $f_{pm} = 0.074/\sqrt[5]{Re_x} - 300/Re_x$; (d) $f_{pm} = 0.074/\sqrt[5]{Re_x}$.

FIG. 42. Friction coefficient for laminar and turbulent boundary-layer flow on a flat plate. (*From L. Prandtl, Erg. aerodyn. Versuchsanst. Göttingen,* **3,** 1.)

only for the smooth plate. The laws for a rough plate are much more complicated.[1]

## 17. The flow in a tube

The flow through a pipe near the entrance can also be calculated with the momentum equation (111). For a tube with circular cross section this calculation was made by L. Schiller.[2] He approximated the velocity profile by a curve built up by two parabolas and a straight line. The vertices of the parbolas lie on the border of the boundary layer, as shown in Fig. 43. The velocity in the core of the flow outside the boundary layer increases with increasing distance from the entrance, since through any cross section the same amount of fluid flows and the boundary-layer thickness increases. The pressure therefore decreases according to the Bernoulli equation, which is valid for the core. After the inflow region ends (at $L_e$), the velocity profile is a parabola. The difference in pressures in the cross section where the flow is already fully developed and a place outside the tube can be calculated according to L. Schiller by adding to the pressure loss which the flow would have if it were fully developed in the whole tube length

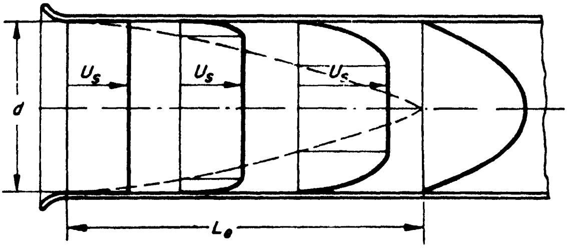

FIG. 43. Development of the laminar velocity profile in the intake region of a tube.

$$\Delta p = 2.16\gamma \frac{u_m^2}{2g} \tag{124}$$

The results of this calculation agree very well with test results. The ratio of the entrance length $L_e$ to the tube diameter $d$ depends on the Reynolds number:

---

[1] W. H. McAdams, "Heat Transmission," 2d ed., McGraw-Hill Book Company, Inc., New York, 1942.

[2] L. Schiller, Strömung in Rohren in Wien-Harms, *Handbuch exp. Physik*, Vol. IV/4, p. 48, Akademische Verlagsgesellschaft, Leipzig, 1931.

$$\frac{L_e}{\mathbf{d}} = 0.0288\,\frac{u_m d}{\nu} = \mathbf{0.0288Re}_d \qquad (125)$$

The Reynolds number is calculated with the mean velocity in a cross section and the tube diameter $d$. This is the way the Reynolds number is usually calculated in technical literature. It must be kept in mind that a sharp limit for the entrance-flow region does not exist in reality. The flow approaches the fully developed condition asymptotically. Therefore, for distances greater than the entrance length given by Eq. (125), small deviations from the developed condition can still be measured.

If the Reynolds number exceeds the critical value, the boundary layer changes somewhere in the entrance-flow region into turbulent flow. The transition place moves toward the entrance when the Reynolds number increases. Since the turbulent boundary layer increases its thickness faster than the laminar layer [Eq. (120)], the entrance length $L_e$ decreases in this range. For a Reynolds number $Re_d = 3{,}000$ the whole entrance flow is laminar. The entrance length $L_e$ is, according to Eq. (125), approximately $100d$. When the Reynolds number increases over this value the entrance length first decreases to about $40d$ and then increases again.

The velocity profile in the fully developed turbulent flow is well represented by Eq. (117) up to $Re = 100{,}000$, if the boundary-layer thickness is replaced by the radius $r$. This corresponds to the concept that the two boundary layers have touched each other in the tube axis. The velocity $u_s$ is now the velocity in the axis. Also Eq. (118) for the shearing stress on the wall holds true, as does Eq. (121) for the velocity at the border between the turbulent flow and the laminar sublayer. This sublayer builds up here in the same way as on the plate. If in these equations the radius $r$ is replaced by the diameter $d$, and the velocity $u_s$ by the mean velocity $u_m$ [$u_m = 0.82u_s$ is found by integration of Eq. (117)], the following equations arise which will be used later:

$$\tau_w = 0.0396\rho u_m^2 \left(\frac{\nu}{u_m d}\right)^{1/4} = \frac{0.0396}{(Re_d)^{1/4}}\,\rho u_m^2 \qquad (126)$$

$$\frac{u_b}{u_m} = 2.43\left(\frac{\nu}{u_m d}\right)^{1/8} = \frac{2.43}{(Re_d)^{1/8}} \qquad (127)$$

$$\frac{\delta_b}{d} = 250\left(\frac{\nu}{u_m d}\right)^{7/8} = \frac{250}{(Re_d)^{7/8}} \qquad (128)$$

In reality here as on the plate, a transition zone exists between the laminar sublayer and the turbulent flow. Equations taking into account this transition zone are shown in Fig. 45. Instead of the shearing stress the friction coefficient $f$ is generally used as defined by the equation

$$\Delta p = f \frac{L}{d} \gamma \frac{u_m^2}{2g} \qquad (129)$$

where $\Delta p$ is the pressure drop along the tube length $L$. In a piece of the tube as shown in Fig. 44 equilibrium exists between the pressures in the cross sections 1-1 and 2-2 and the shearing stresses on the wall of the tube of length $L$ in steady flow according to the momentum law. This gives

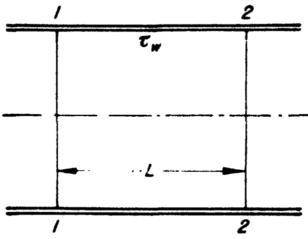

FIG. 44. Using the momentum law for fully developed flow in a tube.

$$\Delta p \frac{d^2\pi}{4} = \tau_w \, d\pi L \qquad (130)$$

With Eqs. (126), (129), and (130) the friction coefficient can be calculated from the shearing stress:

$$\mathbf{f} = \frac{8\tau_w}{\rho \mathbf{u}_m^2} = \frac{\mathbf{0.316}}{(\mathbf{Re}_d)^{1/4}} \qquad (131)$$

This expression is usually called the Blasius law. Temperature differences exist where the flow is connected with heat transfer. Then the property values are introduced at the temperature $(t_w + t_m)/2$ (where $t_w$ = wall temperature; $t_m$ = mean temperature in flow) according to McAdams,[1] or the friction coefficient calculated with the property values at the temperature $t_m$ is multiplied by $(\mu_m/\mu_w)^{0.14}$ where $\mu_m$ = viscosity at $t_m$; $\mu_w$ = viscosity at $t_w$ according to Sieder and Tate.[1] Experiments of Rohonczy[2] with water agreed best with Eq. (131) when the property values were introduced at the wall temperature $t_w$.

For Reynolds numbers greater than $10^5$, Eq. (131) must be replaced by the general resistance law developed by L. Prandtl,

---

[1] W. H. McAdams, *op. cit.*

[2] G. Rohonczy, *Schweiz. Arch. angew. Wiss. u. Tech.*, **5**, 121–140, 167–175, 239–275, 349–366 (1939).

T. von Kármán, and coworkers:[1]

$$\frac{1}{\sqrt{f}} = 2.0 \log \left[(Re_d)\sqrt{f}\right] - 0.8 \qquad (132)$$

This law is more complicated than Eq. (131) since the friction coefficient appears on both sides.

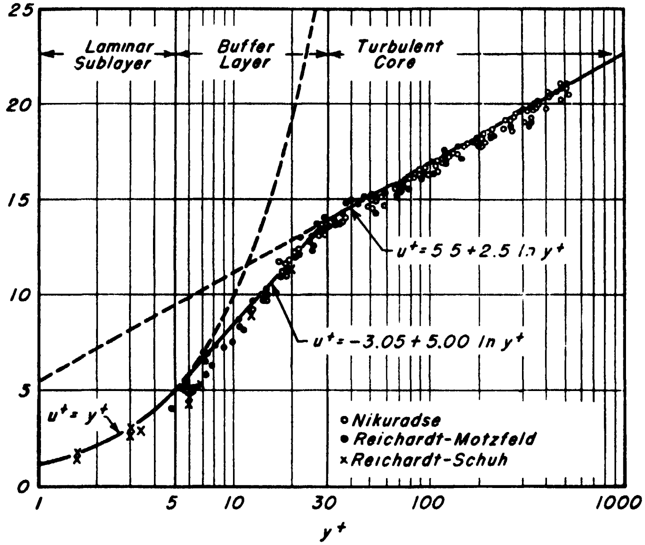

FIG. 45. Universal velocity profile. [*From R. C. Martinelli, Trans. ASME,* **69**, 947–959 (1947).]

Recently it became customary to present the turbulent velocity profile in a logarithmic plot as shown in Fig. 45.[2] The velocities are made dimensionless by the value $\sqrt{\tau_w/\rho}$ which has the dimension of a velocity and is called *shearing-stress velocity*: $u^+ = u/\sqrt{\tau_w/\rho}$. They are plotted in this way on the ordinate. The distance from the tube wall is transformed into a Reynolds number by multiplying it by the shearing-stress velocity and dividing it by the kinematic viscosity: $y^+ = y\,\frac{\sqrt{\tau_w/\rho}}{\nu}$. In this way of plotting, the velocity profile becomes independent of the

---

[1] L. Prandtl, "Führer durch die Strömungslehre," Friedrich Vieweg und Sohn, Brunswick, 1942.

[2] Taken from R. C. Martinelli, Heat Transfer to Molten Metals, *Trans. ASME*, **69**, 947–959 (1947).

Reynolds number $Re_d$. It is therefore called *universal velocity profile*. Measurements by Nikuradse, Reichardt, and coworkers are shown in Fig. 45. In the logarithmic plot the linear relationship between the velocity and the wall distance expected in the laminar sublayer is represented by the curve on the left-hand side of the figure. It can be seen that the measured values follow this curve up to approximately $y^+ = 5$. The straight line on the right-hand side gives the velocities in the turbulent core. The figure shows that between both regions a buffer layer exists, within which the turbulence gradually dies down in the direction toward the wall. T. von Kármán[1] proposed another straight line shown in the figure as approximation for the velocities in this range and fixed the limits of the buffer layer at $y_1^+ = 5$ and $y_2^+ = 30$. The equation for this line as well as the equations for the laminar sublayer and the turbulent zone are inserted in Fig. 45.

For rough tubes similar equations hold true in which the degree of the roughnesses enters as a new parameter.

## 18. Cylinder in crossflow

The boundary layer has a great influence on the flow around a cylinder. Fig. 46 shows a photograph of such a flow. It can be seen that the flow separates on both sides from the cylinder surface and builds up a dead water filled with vortices. If the pressure distribution along the surface is calculated for a frictionless flow without separation, the dash-dotted line in Fig. 47 results. The pressure decreases first from the stagnation point ($\alpha = 0$) and reaches its minimum value at $\alpha = 90$ deg. On the rearward side it increases again and attains for $\alpha = 180$ deg the same value as at the forward stagnation point. In a fluid with friction, a boundary layer builds up along the surface. The fluid particles outside the boundary layer are able to move against the pressure increase on the back side of the cylinder by changing their kinetic energy into pressure energy. The fluid particles in the boundary layer do not possess this kinetic energy. They can therefore move only a certain distance into the region of increasing pressure, until their velocity is consumed. Then they reverse their flow direction. In this way the flow separates from the surface. By this separation the pressure distribution along the

---

[1] T. von Kármán, *Trans. ASME*, **61**, 705–710 (1939).

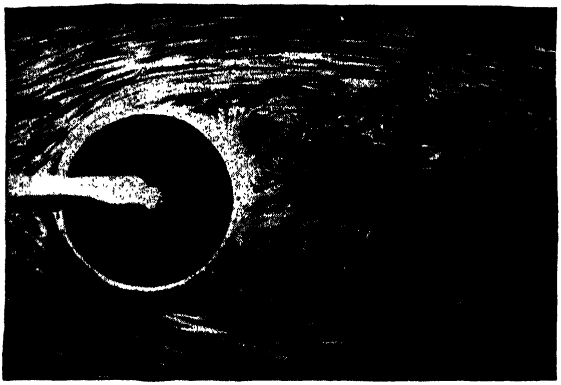

FIG. 46. Flow around a cylinder. (*Photograph by H. L. Rubach, Mitt. Forschungsarb.* 185, 1916.)

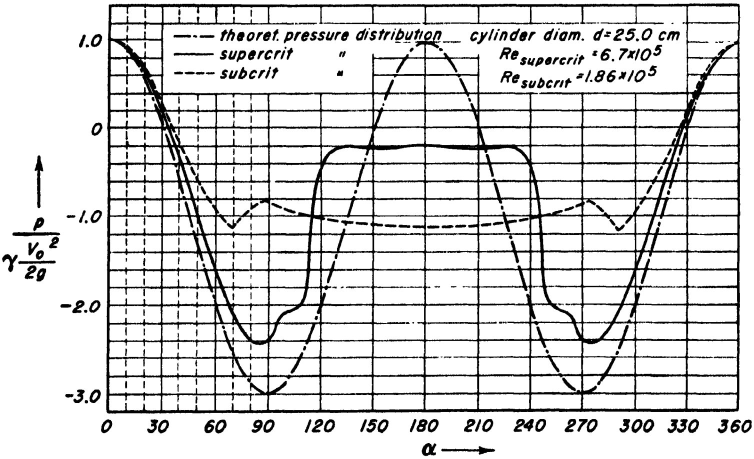

FIG. 47. Pressure distribution around the circumference of a circular cylinder. $p$, local pressure; $\gamma \frac{V_0^2}{2g}$, free-steam impact pressure; $\alpha$, angle measured from stagnation point. (*From L. Flachsbart, Handb. Exp. Physik, Vol.* IV, *Part* 2, *p.* 316, *Fig.* 37.)

back side of the cylinder is changed also. How far the fluid particles penetrate the region of increasing pressure depends on their kinetic energy. This is greater in the turbulent boundary layer (Fig. 39) than in the laminar boundary layer. The turbulent boundary layer separates at approximately $\alpha = 110$ deg, and the laminar boundary layer at $\alpha = 70$ deg. The corresponding pressure distributions are shown in Fig. 47. The pressures on the rear side are smaller than on the front. This gives a force in fluid direction, which is called *form resistance.* To it is added a frictional resistance originated by the shearing stresses along the cylinder walls. Both parts are included in the drag coefficient $f_c$ defined by the equation

$$D = f_c L\,d\gamma \frac{u_0^2}{2g} \tag{133}$$

in which $d$ is the diameter, $L$ the length, $D$ the drag of the cylinder, $\gamma$ the specific weight, and $u_0$ the onstream velocity, and $Ld$ is the cross section normal to the air flow. Figure 48 shows the drag coefficient $f_c$ for various Reynolds numbers. The

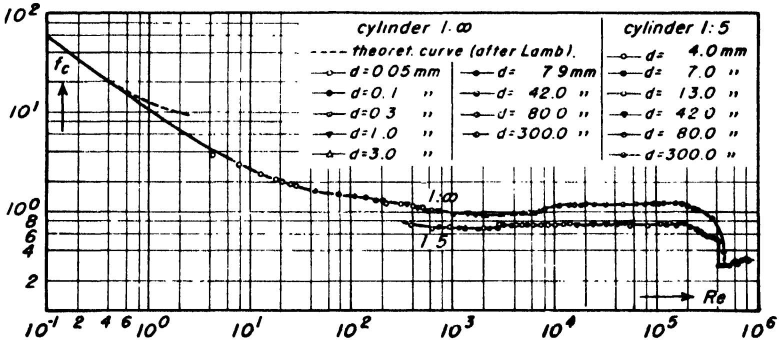

FIG. 48. Drag coefficient of a circular cylinder in a flow normal to its axis. (*From C. Wieselsberger, Ergeb. aerodyn. Versuchsanstalt Göttingen,* **2**, 24.)

Reynolds number is calculated with the onstream velocity $u_0$ and the diameter $d$. At very small velocities no separation occurs and the drag is built up only by the shearing stresses. From $Re \approx 1$ a dead water builds up behind the cylinder. With further increasing Reynolds numbers the dead water becomes greater. From $Re \approx 100$ vortices separate alternately from the left and right sides (Kármán's vortex wake) and are carried away by the flow in a regular pattern. The sudden decrease in drag at $Re \approx 4 \times 10^5$ is originated by the fact that the boundary layer before the separation point has become turbulent. At $Re > 4 \times 10^5$ no vortex wake forms but only small irregular vortices in the dead water. The drag of the cylinder at small velocities is mostly frictional resistance and at $Re > 1{,}000$ mostly form resistance. All of these flow forms influence the heat transfer.

## FORCED CONVECTION IN LAMINAR FLOW

### 19. The heat-flow equation

When a body submerged in a flow is heated or cooled, a temperature field builds up in the surrounding medium. This field comprises only a region within a small distance from the body surface as long as very small velocities and the wake within which the heat is carried away are excluded. This region along the body is called the *thermal boundary layer.* Within this layer the temperature changes from the value $t_w$ on the surface of the body to the value $t_s$ in the undisturbed flow. The temperature profile in the proximity of the wall is shown in Fig. 49. At the distance $\delta_t$ from the wall, the same temperature $t_s$ is measured in the flowing fluid as in the case when the body is neither heated nor cooled. The length $\delta_t$ is the thickness of the thermal boundary layer. Figure 49 shows also the velocity profile and the hydrodynamic boundary layer with the thickness $\delta$. Both boundary layers have generally different thicknesses. For the determination of the thermal boundary layer and the heat transfer a *heat-flow equation of the thermal boundary* layer can be used. It is derived from a heat balance of a volume element on the surface, built up by two planes 1-2 and 3-4 in Fig. 50, each separated from the other by the length $dx$, and by a plane 2-4 parallel to the wall at the distance $l$. The length $l$ is assumed greater than both boundary-layer thicknesses $\delta$ and $\delta_t$. The calculation may be again confined to two-dimensional problems. In Fig. 50 the volume element has unit length normal to the plane of the paper. Through the plane 1-2 a quantity of heat, which is determined by

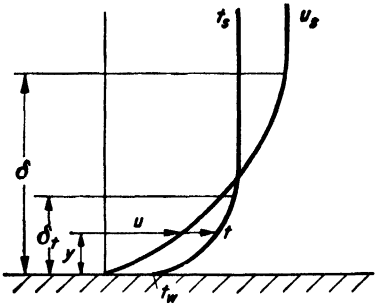

FIG. 49. Temperature and velocity profiles on a wall.

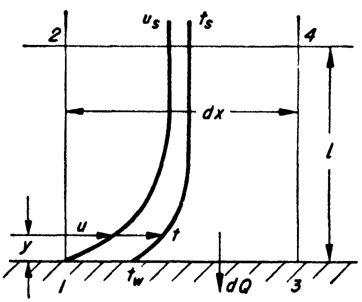

FIG. 50. Deriving the heat-flow equation for the boundary layer.

the following integral, is transported per unit time:

$$\gamma c_p \int_0^l tu \, dy$$

where $c_p$ is the specific heat at constant pressure per unit weight.[1] This heat flow changes with the length $dx$ by

$$\gamma c_p \, dx \frac{d}{dx} \int_0^l tu \, dy$$

The heat flow leaving the volume element through plane 3-4 is greater by this amount than the heat flow entering the element through plane 1-2. Through the plane 2-4 there flows the fluid weight $\gamma \, dx \frac{d}{dx} \int_0^l u \, dy$ as was derived in the preceding chapter. This transports an amount of heat given by $\gamma c_p t_s \, dx \frac{d}{dx} \int_0^l u \, dy$ into the volume element. Through the plane 1-3 a certain amount of heat flows from the volume element to the wall or in the opposite direction. Since the fluid particles adjacent to the wall have the velocity zero, this heat must be transferred by conduction through this fluid layer. Therefore Eq. (30) holds true. With the nomenclature used here it is

$$dQ = -k \, dx \left(\frac{dt}{dy}\right)_w$$

where $k$ is the thermal conductivity of the fluid or gas. The sum of the heat carried into the volume element by convection with the flow and the heat lost from the element by conduction to the wall must be zero for steady state:

$$\gamma c_p \frac{d}{dx} \int_0^l t_s u \, dy - \gamma c_p \frac{d}{dx} \int_0^l tu \, dy - k \left(\frac{dt}{dy}\right)_w = 0 \quad (134)$$

Introducing the thermal diffusivity of the fluid $\alpha = k/\gamma c_p$ gives

$$\frac{d}{dx} \int_0^l (t_s - t)u \, dy = \alpha \left(\frac{dt}{dy}\right)_w \quad (135)$$

✓

---

[1] It will be explained on page 150 that the specific heat at constant pressure is to be used.

This is the *heat-flow equation of the boundary layer*, by which the heat transfer can be calculated.[1] The property values used in Eq. (135) are tabulated in the Appendix. The specific heat $c_p$ and the thermal conductivity $k$ as well as the viscosity $\mu$ depend upon pressure only in the proximity of the critical point. Figures 141 and 142 show this for water vapor. The specific heat at the critical point theoretically approaches infinity. This is indicated by the very steep increase of $c_p$ in Fig. 138 near the critical point. The specific weight $\gamma$ for fluids depends very little on the pressure. For gases it can be calculated from the equation of state. In the proximity of the critical point the dependency on the pressure is more complicated. As an example Fig. 136 shows this relationship for water and steam. The thermal diffusivity $\alpha$ and the kinematic viscosity $\nu$ for fluids depend only in a very small degree on the pressure outside the critical pressure range. For gases both values are inversely proportional to the pressure.

## 20. The plane plate in longitudinal flow

The heat transfer from a plane wall with a constant temperature $t_w$ in a flow of constant velocity may be calculated. The first part of the plate with the length $x_0$ may not be heated and has the same temperature as the fluid, as shown in Fig. 51.[2] The hydrodynamic boundary layer begins at the edge of the unheated plate, and the thermal boundary layer at the edge of the heated part. Both increase their thicknesses $\delta$ and $\delta_t$ in the direction of flow. Just as for the determination of the hydrodynamic boundary layer in the preceding chapter, for the determination of the thermal boundary layer a suitable statement must be made as

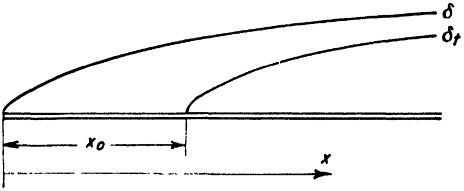

FIG. 51. Flow boundary layer and thermal boundary layer on a flat plate.

---

[1] G. Kroujiline [*Tech. Phys. U.S.S.R.* **3**, 183, 311 (1936)] was apparently the first to use Eq. (135) for heat-transfer calculations.

[2] Heat transfer on a plate with a surface temperature varying along its length was investigated in the paper by R. Chapman and M. W. Rubesin in *J. Aeronaut. Sci.*, **16**, 547–565 (1949).

to the shape of the temperature profile in the boundary layer. As for the velocity profile, the curvature of the temperature profile on the wall must also be zero. Since the fluid layers adjacent to the wall are at rest, the heat flow from the wall must be transferred by conduction through these layers. Therefore

$$Q = -kA\,\frac{dt}{dy}$$

The thermal conductivity $k$ and the area $A$ through which the heat flow passes are constant. Therefore $(dt/dy)_w$ = constant and $(d^2t/dy^2) = 0$. Hence a cubic parabola is a suitable assumption for the temperature profile. If the temperature difference $\vartheta = t - t_w$ is introduced, all conditions for the temperature profile are the same as for the velocity profile. Therefore the expression for the temperature profile becomes

$$\frac{\vartheta}{\Theta} = \frac{3}{2}\frac{y}{\delta_t} - \frac{1}{2}\left(\frac{y}{\delta_t}\right)^3$$

with

$$\vartheta = t - t_w \qquad \Theta = t_s - t_w$$

Now the integral in the heat-flow equation can be calculated:

$$\int_0^l (t_s - t)u\,dy = \int_0^l (\Theta - \vartheta)u\,dy$$

$$= \Theta u_s \int_0^{\delta_t}\left[1 - \frac{3}{2}\frac{y}{\delta_t} + \frac{1}{2}\left(\frac{y}{\delta_t}\right)^3\right]\left[\frac{3}{2}\frac{y}{\delta} - \frac{1}{2}\left(\frac{y}{\delta}\right)^3\right]dy$$

It may be presumed that the thermal boundary layer is smaller than the hydrodynamic boundary layer. Then the second integral must be extended only to $y = \delta_t$ since for $y > \delta_t$, $\vartheta = \Theta$ and therefore the integrand is zero. By introducing the ratio $\zeta = \delta_t/\delta$ of the thermal to the hydrodynamic boundary layer and evaluating the integral there follows

$$\int_0^l (\Theta - \vartheta)u\,dy = \Theta u_s \delta\left(\tfrac{3}{20}\zeta^2 - \tfrac{3}{280}\zeta^4\right)$$

As we assumed $\delta_t$ to be smaller than $\delta$, and therefore $\zeta < 1$ the second term in the right-hand expression is small compared with the first and may be neglected. According to Fig. 51 the ratio $\zeta$ is a function of $x$.

If the above integral is introduced into Eq. (135) there is obtained

$$\frac{3}{20}\,\Theta u_s \frac{d}{dx}(\zeta^2\delta) = \frac{3}{2}\,\alpha\frac{\Theta}{\zeta\delta}$$

or

$$\frac{1}{10}\,u_s\left(\zeta^3\delta\frac{d\delta}{dx} + 2\zeta^2\delta^2\frac{d\zeta}{dx}\right) = \alpha$$

introducing Eq. (114) for $\delta\, d\delta/dx$, and (114$a$) for $\delta^2$ gives

$$\frac{14}{13}\,\frac{\nu}{\alpha}\left(\zeta^3 + 4x\zeta^2\frac{d\zeta}{dx}\right) = 1$$

The ratio $\nu/\alpha$ in the equation is a dimensionless value very common in heat-transfer calculations. It is called the Prandtl number or Prandtl modulus and is written as $Pr$.

$$\mathbf{Pr} = \frac{\nu}{\alpha} = \frac{\mathbf{g}\mathbf{c}_p\mu}{\mathbf{k}} \tag{136}$$

The Prandtl number is composed of property values and is therefore itself a property value. It has the advantage that it is dimensionless. The tables in the Appendix give this value for liquids and gases. The Prandtl number for liquids and gases depends on the temperature. Only near the critical point does a marked dependency also on the pressure occur. The variation with temperature is small for gases.

Putting $14/13 \approx 1$ in the above equation gives

$$\zeta^3 + \frac{4}{3}\,x\,\frac{d(\zeta^3)}{dx} = \frac{1}{Pr}$$

or with substitution $\zeta^3 = y$,

$$y + \frac{4}{3}\,x\,\frac{dy}{dx} = \frac{1}{Pr}$$

A particular integral is $y = 1/Pr$. The general solution of the homogeneous equation can be found by trying the expression $y = x^n$; $n$ becomes $-3/4$. Therefore the complete solution of the above equation is

$$y = \frac{1}{Pr} + Cx^{-3/4}$$

From the boundary condition: for $x = x_0$, $\zeta = 0$ or $y = 0$ there follows

$$\zeta = \frac{1}{\sqrt[3]{Pr}} \sqrt[3]{1 - \left(\frac{x_0}{x}\right)^{3/4}} \tag{137}$$

If the plate is heated over the whole length ($x_0 = 0$)

$$\zeta = \frac{1}{\sqrt[3]{Pr}} \tag{137a}$$

Viscous oils have a Prandtl number $Pr = 1{,}000$ or more. For these fluids the thickness of the thermal boundary layer is only one-tenth the thickness of the hydrodynamic boundary layer. Gases have Prandtl numbers smaller than 1. For these, $\zeta$ is greater than 1 and therefore the proposition in the preceding calculation does not hold true. Since the smallest value for gases is $Pr = 0.6$ and therefore $\zeta = 1.18$, the error introduced by this is very small. The only materials with a very small Prandtl number are fluid mercury and molten metals. For these the result (137*a*) is not valid.

The heat flow from or to the plate per unit area is given by

$$q = -k\left(\frac{d\vartheta}{dy}\right)_w$$

On the other hand a heat-transfer coefficient $h$ can be introduced:

$$q = h(t_s - t_w) = h\Theta$$

Equating both equations gives (if the minus sign is neglected)

$$h = -\frac{k}{\Theta}\left(\frac{d\vartheta}{dy}\right)_w = \frac{3}{2}\frac{k}{\delta_t} = \frac{3}{2}\frac{k}{\zeta\delta} \tag{137b}$$

The heat-transfer coefficient is therefore inversely proportional to the thermal boundary-layer thickness. With the ratio $\zeta$ and Eq. (114*a*),

$$h = 0.323k \frac{\sqrt[3]{Pr}}{\sqrt[3]{1 - \left(\frac{x_0}{x}\right)^{3/4}}} \sqrt{\frac{u_s}{\nu x}} \tag{138}$$

and for the plate heated over its entire length

$$h = 0.323k \sqrt[3]{Pr} \sqrt{\frac{u_s}{\nu x}} \tag{138a}$$

As shown in Fig. 52, the heat-transfer coefficient begins with an infinite value at the leading edge of the plate and decreases with increasing $x$. It is advantageous to write Eq. (138) in dimensionless form, or

$$\frac{hx}{k} = 0.323\sqrt[3]{Pr}\sqrt{\frac{u_s x}{\nu}}\frac{1}{\sqrt[3]{1-\left(\frac{x_0}{x}\right)^{3/4}}}$$

On the right there appears again the Reynolds number calculated with the free-stream velocity $u_s$ and the length $x$. The dimensionless expression on the left side is called *Nusselt number* or Nusselt modulus and is indicated as $Nu$. $Nu_x$ is written to indicate that the Nusselt number is calculated with the length $x$.

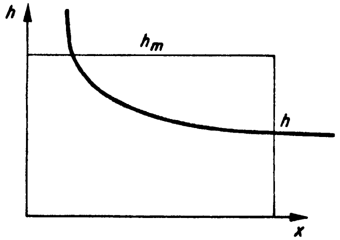

FIG. 52. Local film heat-transfer coefficient on a flat plate as a function of the distance from the leading edge.

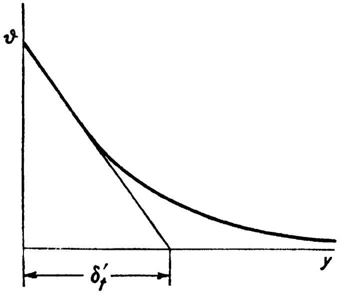

FIG. 53. Determination of the Nusselt number.

$$Nu_x = \frac{hx}{k} \tag{139}$$

With this notation it can be written

$$Nu_x = 0.323\sqrt[3]{Pr}\sqrt{Re_x}\frac{1}{\sqrt[3]{1-\left(\frac{x_0}{x}\right)^{3/4}}} \tag{140}$$

For the plate heated over its entire length the heat transfer coefficient was calculated by an exact solution of the differential equations of the boundary layer. This calculation resulted in the eq. (138*a*) with the numerical value 0.332 instead of 0.323. The Nusselt number then is

$$\mathbf{Nu_x = 0.332\sqrt[3]{Pr}\sqrt{Re_x}} \tag{140a}$$

The Nusselt number can be expressed as the ratio of two lengths.

In Sec. 2 there was introduced a boundary-layer thickness $\delta_t'$ (Fig. 3) which really is the length of the subtangent to the temperature profile within the boundary layer at the wall. Figure 53 shows this in detail. For the temperature profile represented by the cubic parabola the relationship $\delta_t' = \frac{2}{3}\delta_t$ holds. The film heat-transfer coefficient is, according to Sec. 3,

$$h = \frac{k}{\delta_t'}$$

and therefore the Nusselt number

$$Nu_x = \frac{hx}{k} = \frac{x}{\delta_t'}$$

is the ratio of the length $x$ to the thermal boundary-layer thickness $\delta_t'$. Since the boundary-layer thickness is always small as compared with the length $x$, the Nusselt number will be large. The thermal boundary-layer thickness decreases with increasing Reynolds and Prandtl numbers. Both values therefore increase the Nusselt number. For calculations on industrial heat exchangers not the local but the average value of the heat-transfer coefficient is important. For the plate heated over its entire length this value is

$$\mathbf{h}_m = \frac{1}{\mathbf{x}}\int_0^x \mathbf{h}\,d\mathbf{x} = \frac{\mathbf{C}}{\mathbf{x}}\int_0^x \frac{d\mathbf{x}}{\sqrt{\mathbf{x}}} = \frac{\mathbf{C}}{\mathbf{x}}\,2\sqrt{\mathbf{x}} = 2\,\frac{\mathbf{C}}{\sqrt{\mathbf{x}}} = 2\mathbf{h} \qquad (141)$$

In $C$ are combined all values which do not depend on $x$. The average value of the heat-transfer coefficient is therefore twice the local value at the end of the plate. If the property values in the equation depend on temperature then they must be introduced at a mean temperature. Most of the experiments on heat transfer on a flat plate were done in an air flow. For gases the temperature dependancy of the property values is not great. Therefore the reference temperature for the property values to be used in the heat-transfer calculations can be determined only from experiments with very great temperature differences between wall and air flow. Few such experiments are known.[1] Knowledge of the reference temperature can be derived however from calculations by L. Crocco[1] and others on the heat transfer to a plate at high subsonic and supersonic velocities. This problem which is dealt with in more detail in Sec. 29 involves always great temperature differences and therefore the calculations take into account the variation of the property values. M. W. Rubesin[2] and H. A. Johnson have studied the information on the reference temperature that can be obtained from the results of these calculations. They find that the calculations presented here with the assumption that the property values are independent of temperature give the same results as the calculations by Crocco which take into account the variation of the property values when the property values are introduced at a reference temperature $t^\star$ determined by the equation

---

[1] A paper was published recently by W. H. Lowdermilk and M. D. Grele, *NACA, TM* E8L03; or Heat Transfer and Fluid Mechanics Institute, 1949, Berkeley, Calif., published by ASME.

$$t^\star - t_s = 0.58(t_w - t_s)$$

This equation which holds for air ($Pr = 0.71$) gives practically the same reference temperature as Eq. (159) derived for turbulent flow. Exact measurements on this type of heat transfer were made by Jakob and Dow. They summarize in their paper also all previous experiments.[3]

**Example.** The heat-transfer coefficient is to be calculated for a plate in an air stream for a distance of 4 in. from the leading edge. The plate is heated over its entire length; the air velocity $u_s = 33$ fps, its temperature $t_s = 125$ F, the surface temperature of the plate $t_w = 255$ F.

The kinematic viscosity of air at 200 F and ambient pressure is $25.5 \times 10^{-5}$ ft²/sec (Appendix). Therefore the Reynolds number is $Re_x = 43{,}000$. The Prandtl number is found in the Appendix to be 0.682. Eq. (140*a*) gives $Nu_x = 0.331 \times \sqrt[3]{0.682} \times \sqrt{43{,}000} = 60.4$. The local heat-transfer coefficient at a distance 4 in. from leading edge is, from Eq. (139), $h = (k/x)60.4$. The thermal conductivity $k$ for air at 200 F is $k = 0.0186$ Btu/(hr)(ft)(F). Therefore

$$h = \frac{0.0186 \times 12}{4} \times 60.4 = 3.37 \frac{\text{Btu}}{(\text{hr})(\text{ft}^2)(\text{F})}$$

---

[1] L. Crocco, *NACA, TM* 690, 1932; also *Rend. mat. univ. Roma V*, **2**, 138 (1941).

[2] Paper presented at the Institute on Heat Transfer and Fluid Mechanics in Los Angeles, Calif., June, 1948. *Trans. ASME*, **71**, 183–188 (1949).

[3] M. Jakob and W. M. Dow, Heat Transfer from a Cylindrical Surface to Air in Parallel Flow with or without Unheated Starting Sections, *Trans. ASME*, **68**, 124–134 (1946).

The average value at the 4-in. station is $h_m = 6.74$ Btu/(hr)(ft²)(F). The heat flow from a plate $b = 1$ ft wide is

$$Q = hbx(t_w - t_s) = 6.74 \times \frac{4}{12} \times (255 - 125) = 292 \text{ Btu/hr}$$

## 21. Cylindrical bodies in flow normal to their axes

In Sec. 18 it was mentioned that on the forward side of a body in flow a boundary layer builds up. This boundary layer is always laminar near the stagnation point. If the body is heated a thermal boundary layer exists in the same way. In the immediate proximity of the stagnation point the velocity outside the boundary layer always increases linearly with the distance from the stagnation point as measured along the body surface. This is expressed by the equation $u_s = Cx$. The heat transfer in this region on cylindrical bodies in a flow normal to their axes was calculated by Squire[1] by an exact solution of the differential equations, when the temperature of the body is constant along its surface. This calculation gives the heat-transfer coefficient

$$h = Bk\sqrt{\frac{u_s}{\nu x}} = Bk\sqrt{\frac{C}{\nu}} \tag{142}$$

The heat-transfer coefficient is therefore independent of the distance from the stagnation point in its neighborhood. The dimensionless value $B$ is given in Table 6 for some Prandtl numbers.

TABLE 6. CONSTANT $B$ FOR CALCULATION OF HEAT TRANSFER AT THE STAGNATION POINT BY EQ. (142)*

| *Pr* | 0.7 | 0.8 | 1.0 | 5 | 10 |
|---|---|---|---|---|---|
| *B* | 0.496 | 0.523 | 0.570 | 1.043 | 1.344 |

* E. Eckert, *VDI-Forschungsheft*, **416**, 1942.

Equation (142) as written in dimensionless form is

$$Nu_x = hx/k = B\sqrt{u_s x/\nu}$$

On the right-hand side the Reynolds number again appears.

The velocity $u_s$ outside the boundary layer around a cylinder with circular cross section is for potential flow $u_s = 2u_0 \sin(2x/d)$, where $u_0$ is the onstream velocity, $x$ the distance along the surface from the stagnation point, and $d$ the diameter of the cylinder. In the neighborhood of the stagnation point the sine can be replaced by the angle. This gives $u_s = 4u_0(x/d)$ and

---

[1] S. Goldstein, "Modern Developments in Fluid Dynamics," Vol. 2, Oxford University Press, New York, 1938.

$$h = 2Bk\sqrt{\frac{u_0}{\nu d}}$$

or in dimensionless form,

$$Nu_d = \frac{hd}{k} = 2B\sqrt{\frac{u_0 d}{\nu}} = 2B\sqrt{Re_d} \qquad (143)$$

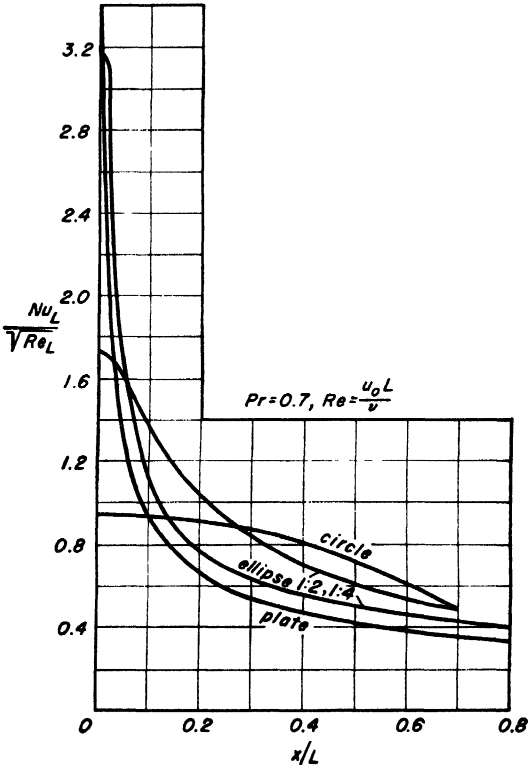

**Fig. 54.** Local laminar film heat-transfer coefficients along the circumference of cylinders with circular and elliptical cross section and along a flat plate. (*From E. Eckert, VDI-Forschungsheft*, **416**, 1942.)

The local heat-transfer coefficients along the surface of a cylindrical body at a greater distance from the stagnation point can also be calculated with Eq. (135). Methods for such calculations were developed by Kroujiline, Frössling, and Eckert.[1] In the paper by E. Eckert they are all described. Figure 54 shows the heat-transfer coefficients along the circumference of cylinders with circular and elliptical cross sections and for the flat plate. The distance $x$ from the stagnation point is divided by the greatest diameter of the cylinder (its depth $L$). In all laminar boundary layers the Nusselt number increases with the square root of the Reynolds number. Therefore the values $Nu/\sqrt{Re}$ are plotted in Fig. 54 against the ratio $x/L$. It can be seen that the distribution of the heat transfer becomes more and more

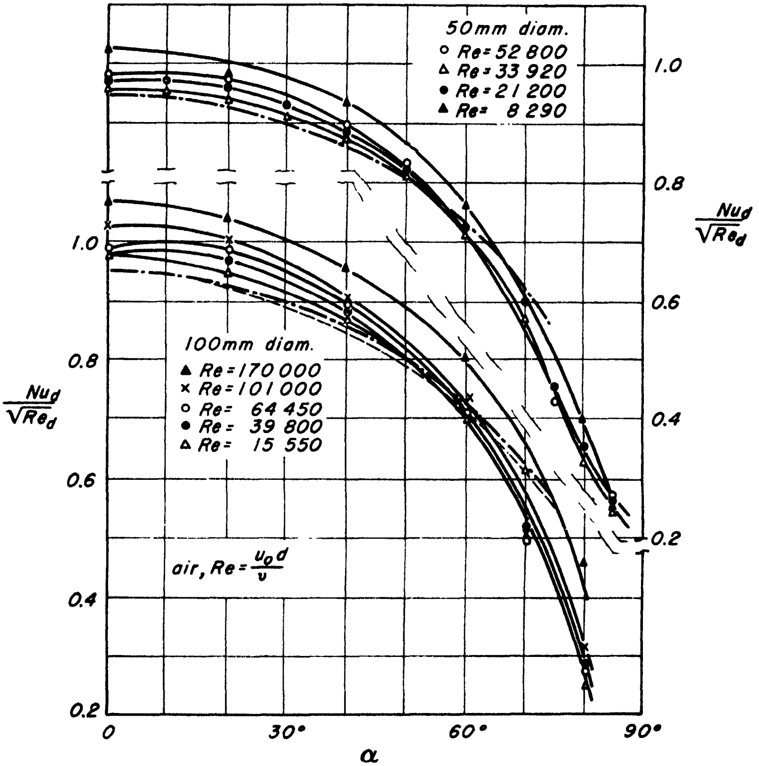

FIG. 55. Comparison between calculated and measured film heat-transfer coefficients on circular cylinders. (*Measured values according to E. Schmidt and K. Wenner, from E. Eckert, VDI-Forschungsheft,* **416**, 1942. *Dashed line calculated from Kroujiline, dash-dotted line calculated from E. Eckert.*)

---

[1] E. Eckert, Die Berechnung der Wärmeüberganges in der laminaren Grenzschicht umströmter Koerper, *VDI-Forschungsheft,* **416,** 1942.

similar to the plate the more slender the cross section of the cylinder. The smaller the radius of curvature on the stagnation point, the greater the heat-transfer coefficient at this place. A comparison between calculated values and results of experiments by E. Schmidt and K. Wenner[1] is shown in Fig. 55. The calculation gives the heat-transfer coefficients only for the laminar boundary layer. The distance of the place of transition to the turbulent boundary layer from the stagnation point is determined for the plane plate to be at a Reynolds number 80,000 to 500,000. For a flow with pressure decrease along the surface, the transition takes place at a greater Reynolds number; for a flow with pressure increase at a smaller Reynolds number. Experiments on an inclined flat plate interesting in this connection were made by R. M. Drake.[2]

## 22. Flow through a tube

If the wall of a tube through which a liquid or gas flows is heated or cooled, a thermal boundary layer builds up along the walls. The boundary layers meet in the axis at a certain distance from the starting cross section (Fig. 43). At this cross section the inflow region ends. First, the heat transfer in the region of fully developed thermal conditions may be calculated. As for the plate, the temperature profile in the tube is assumed as a cubic parabola. Again there can be derived a condition for the curvature of the temperature profile at the wall. The heat flow through the layer immediately adjacent to the wall must be constant as this layer has a negligibly small velocity and therefore no heat is carried away by convection. The heat flows through this layer only by conduction. For a cylindrical area of length $L$ and radius $\rho$ (Fig. 56) the equation

$$Q = -k 2\pi\rho L \frac{dt}{dy}$$

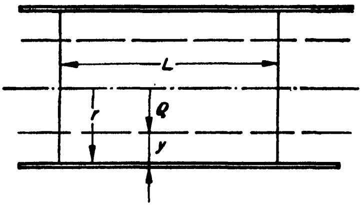

FIG. 56. Determination of the temperature profile in a tube with laminar flow distant from the inlet.

---

[1] E. Schmidt and K. Wenner, *Forsch. Gebiete Ingenieurw.*, **12**, 65–73 (1941).

[2] R. M. Drake, *J. Applied Mechanics*, **16**, 1–8 (1949).

holds, where $y$ is again the distance from the wall and $r$ the radius of the tube. Introducing $\rho = r - y$ into the above equation, solving for the temperature gradient, and differentiating for $y$ gives

$$\frac{d^2t}{dy^2} = -\frac{1}{(r-y)^2}\frac{Q}{2\pi Lk} = \frac{1}{r-y}\frac{dt}{dy}$$

at the wall ($y = 0$) therefore,

$$\left(\frac{d^2t}{dy^2}\right)_w = \frac{1}{r}\left(\frac{dt}{dy}\right)_w \tag{144}$$

The rate of change of the temperature gradient is not zero here but is connected by the above relationship with the temperature gradient. The reason is that the cross section through which the heat flows decreases with increasing distance from the wall whereas it remains constant on the flat plate. To fulfill the above condition we must write for the temperature difference between the wall and the free stream,

$$\vartheta = ay + by^2 + cy^3$$

By differentiation and introduction into Eq. (144) there is obtained

$$b = \frac{a}{2r}$$

The temperature difference between the tube axis and the wall may be $\Theta$. The temperature gradient must be zero in this place:

$$\text{For } y = r,\ \vartheta = \Theta,\ \frac{d\vartheta}{dy} = 0$$

This gives

$$\frac{\vartheta}{\Theta} = \frac{6}{5}\frac{y}{r} + \frac{3}{5}\left(\frac{y}{r}\right)^2 - \frac{4}{5}\left(\frac{y}{r}\right)^3 \tag{145}$$

The heat flow per unit area at the wall is

$$q = -k\left(\frac{d\vartheta}{dy}\right)_w = \frac{6}{5}k\frac{\Theta}{r} \tag{145a}$$

The heat-transfer coefficient for the flow in a tube is commonly calculated with the difference between the average temperature of the fluid and the wall temperature. The average temperature most commonly used is one which would result if the fluid were mixed after the cross section considered. This value is called the bulk temperature $t_B$. It is defined by the equation

$$t_B = \frac{\int tu\,dA}{\int u\,dA} = \frac{\int_0^r tu\rho\,d\rho}{\int_0^r u\rho\,d\rho} \qquad (146)$$

Introducing the temperature profile, Eq. (145), and the velocity profile,

$$\frac{u}{u_s} = 2\frac{y}{r} - \left(\frac{y}{r}\right)^2$$

where $u_s$ = velocity in the axis, we obtain for the difference between the bulk temperature and the wall temperature,

$$\vartheta_B = 0.583\Theta$$

The heat-transfer coefficient is defined by

$$q = h(t_B - t_w) = h\vartheta_B$$

With Eq. (145*a*) there results

$$h = k\frac{6}{5}\frac{1}{r}\frac{\Theta}{\vartheta_B} = 4.12\frac{k}{d}$$

where $d$ is the diameter of the tube. In dimensionless form

$$Nu_d = \frac{hd}{k} = 4.12$$

The heat-transfer coefficient was calculated exactly by Graetz[1] and Nusselt.[2] They found

$$\mathbf{Nu_d = 3.65} \qquad (147)$$

The result of the approximate solution is greater by 13 per cent. The temperature profile agrees quite well with the exact calculation (Fig. 57). The heat transfer in a slit built by two plane walls at a distance $b$ from each other was calculated by L. Ehret and H. Hahnemann.[3] They found

$$Nu_b = \frac{hb}{k} = 3.75$$

---

[1] L. Graetz, *Ann. Physik*, **18**, 79–94 (1889); **25**, 337–357 (1895).

[2] W. Nusselt, *Z. Ver. deut. Ing.*, **54**, 1154–1158 (1910).

[3] L. Ehret and H. Hahnemann, *Wärme- u. Kältetech.*, **44**, 167 (1942).

Existing experiments on heat transfer in laminar flow are not very well suited for comparison with the above equations for three reasons. First, experiments were conducted principally with viscous liquids, because in heat exchangers laminar flow is usually encountered with such fluids. Liquids with high viscosities (oils) have a peculiarity in that their viscosity changes greatly with temperature. The assumption of constant property values in the above calculations is therefore fulfilled only to a small degree in these experiments. The velocity profile, which is a parabola in isothermal flow, changes as a consequence of the variable viscosity. Velocity profiles according to Keevil and McAdams[1] are reproduced in Fig. 58. If heat flows from the tube walls to the liquid, the velocity profile (curve $b$) is flatter than a parabola (curve $a$) because the fluid layers in the neighborhood of the wall are warmer and consequently the viscosity is smaller

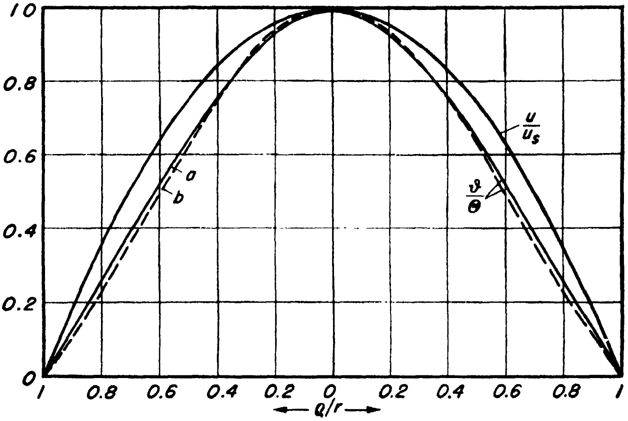

FIG. 57. Laminar velocity and temperature profiles in a tube at a great distance from the entrance. ($a$) Approximate solution by E. Eckert; ($b$) exact solution by L. Graetz and W. Nusselt.

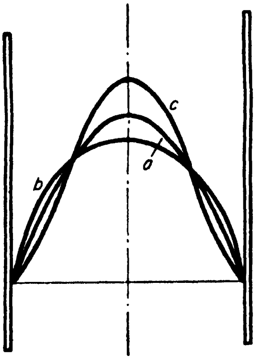

FIG. 58. Distortion of the velocity profile in a heated or cooled tube when the viscosity of the fluid depends on temperature.

---

[1] C. S. Keevil and W. M. McAdams, *Chem. Met. Eng.*, **36,** 464 (1929).

than in the fluid core. For heat flow from the liquid to the wall, the fluid in the core is warmer and therefore less viscous than the layer near the wall; thus, the velocity profile has the form of curve *c*. Because of this change in the shape of the velocity profile, both the temperature profile and the heat transfer are influenced. The heat-transfer coefficient now depends on the direction of the heat flow, and on its amount. A calculation of heat transfer in viscous liquids was made by K. Yamagata.[1] Second, there is difficulty in comparing the calculated and measured values because frequently, for the low velocities necessary for laminar flow, eddy currents by free convection change the flow pattern. A combination of forced and free convection results, which combination can be expressed only by complicated laws.[2] Third, the tube length necessary for completion of hydrodynamically and thermally fully developed flow becomes so great for oils that in heat exchangers there usually is no fully developed flow. Thus, the experiments are concerned with the exploration of the intake region.

It is necessary to distinguish two different modes of heat transfer in the intake region. If the tube is heated over its entire length beginning at the intake cross section, the thermal and the hydrodynamic boundary layers develop simultaneously. A thorough investigation of this case apparently does not exist. As long as the boundary layers are small compared with the tube diameter, the formulas for a plane plate may be applied. On the other hand the tube may be heated only beginning at a cross section where the velocity profile is already fully developed. This case was calculated in 1889 by Graetz and later on by Nusselt (1910). From the results of these calculations Figs. 59 and 60 are reproduced here. Figure 59 shows the temperature profile and Fig. 60 the Nusselt number. Both depend only on the value $(1/Re\,Pr)(L/d)$. The temperature profile, which has a rectangular shape in the section where the heat transfer starts, changes in the direction of flow by the boundary layers forming along the walls. The temperature profile is fully developed as soon as the boundary layers meet at the tube axis. From here on the temperature profile does not change its shape; it only decreases gradually in the direction of flow. In Fig. 60, the Nusselt number is formed with the local film heat-transfer coefficient along the tube length for the dashed curve. It can be seen how the Nusselt number starts with an infinite value at the beginning of the heated length and decreases in flow direction to the value 3.65, which is reached asymptotically. Practically, this value is reached at $(1/Re\,Pr)(L/d) = 0.05$. The tube length in which the temperature profile is not developed can therefore be calculated from the equation

---

[1] K. Yamagata, A Contribution to the Theory of Nonisothermal Laminar Flow of Fluids inside a Straight Tube of Circular Cross Section, *Mem. Faculty Eng. Kyushu Imp. Univ.*, **8**, 365–445 (1940).

[2] A. P. Colburn, *Trans. Am. Inst. Chem. Engrs.*, **29**, 166 (1933).

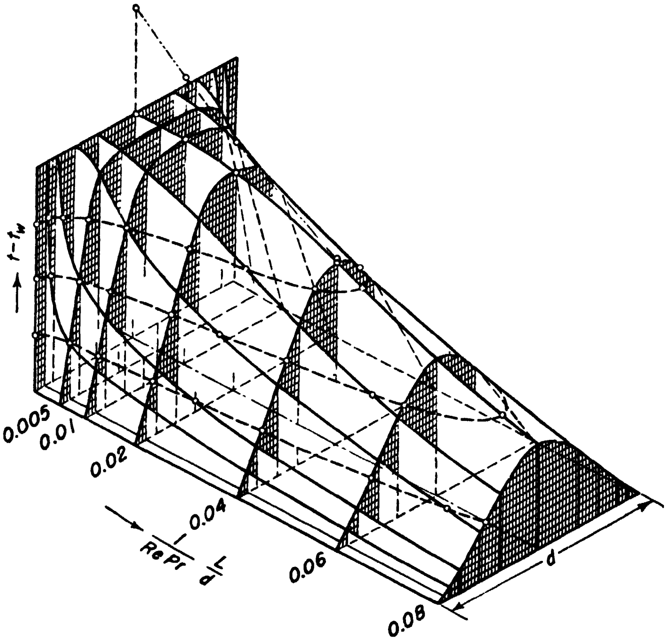

FIG. 59. Temperature profile in laminar flow through the entrance region of a tube. (*From L. Prandtl, "Stroemungslehre," 3d ed., p. 377, Fig. 305, Friedrich Vieweg & Sohn, Brunswick,* 1949.)

$$\frac{L_e}{d} = 0.05 Re\,Pr$$

The solid line in Fig. 60 gives the average film heat-transfer coefficient. According to calculations made by H. Hahnemann and L. Ehret, the tube length within which the temperature and velocity profiles change shapes when they start at the same cross section (heat transfer on the entire tube length) can also be calculated with the same equation. As viscous fluids have Prandtl numbers equal to 100 or more, the thermal intake length $L_e$ becomes 100 times as long as the hydrodynamic intake length. In Fig. 61 the Nusselt number resulting from the calculations of Graetz and Nusselt is compared with formulas derived by Kraussold[1] and by Sieder and Tate[2] from their experiments. Notwithstanding the fact that the experiments were carried out principally with oil, the agreement with the calculated results is fairly reasonable. Some results of experiments with gases by Nusselt[3] are inserted and shown by points. New experiments by J. Boehm[4] give similar results. The logarithmic mean temperature difference is to be used in connection with the average Nusselt numbers in

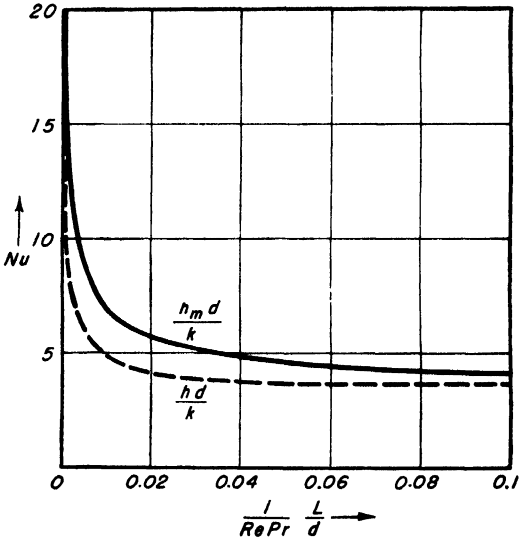

FIG. 60. Local and average film heat-transfer coefficient in laminar flow through the entrance region of a tube. (*According to W. Nusselt, from H. Hausen, Z. Ver. deut. Ing., Beiheft Verfahrenstechnik*, No. 4, 1943, *pp.* 91–98.)

---

[1] H. Kraussold, *VDI-Forschungsheft* **351**, 1931.

[2] E. N. Sieder and G. E. Tate, *Ind. Eng. Chem.*, **28**, 1429–1435 (1936).

[3] H. Nusselt, "Habilitationsschrift," Dresden, 1909.

[4] J. Boehm, *Wärme*, **66**, 143–152 (1943).

Figs. 60 and 61. H. Hausen[1] developed a formula which represents the results of Graetz and Nusselt very well:

$$\mathrm{Nu}_m = 3.65 + \frac{0.0668(d/L)\mathrm{Re\,Pr}}{1 + 0.04[(d/L)\mathrm{Re\,Pr}]^{2/3}} \tag{147}$$

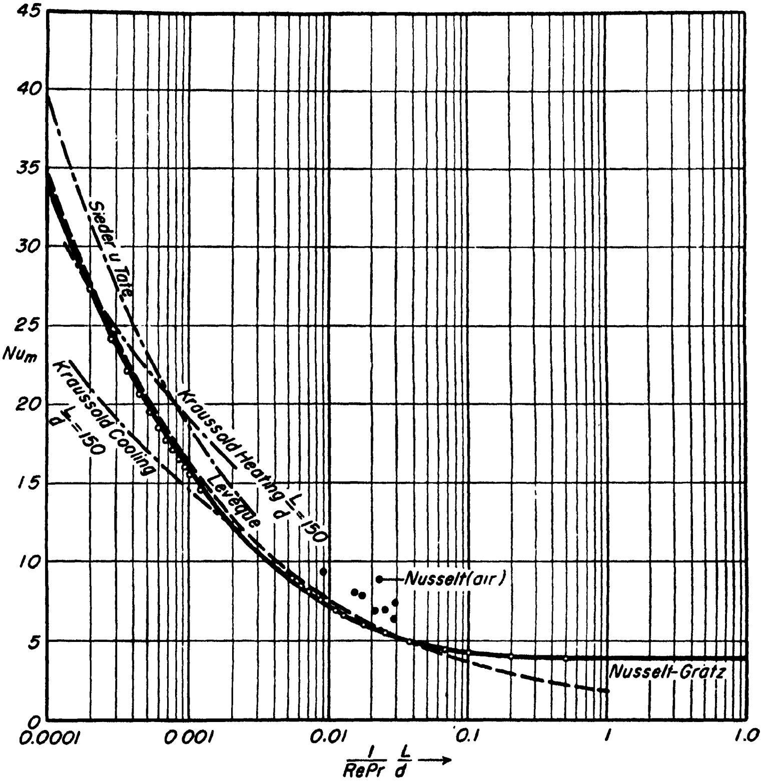

FIG. 61. Comparison of measured and calculated average film heat-transfer coefficients in laminar flow through the entrance region of a tube. (*From H. Hausen, Z. Ver. deut. Ing., Beiheft Verfahrenstechnik, No. 4, 1943, pp. 91–98.*)

For greater temperature differences, the influence of the variable viscosity can be taken into account by multiplying the right-hand side of the above equation by the ratio $(\mu_B/\mu_w)^{0.14}$, if $\mu_B$ is the viscosity at the fluid bulk temperature and $\mu_w$ the viscosity at wall temperature.

---

[1] H. Hausen, *Z. Ver. deut. Ing., Beiheft Verfahrenstechnik,* No. 4, 1943, pp. 91–98.

## FORCED CONVECTION IN TURBULENT FLOW

### 23. Exchange of momentum and heat

In turbulent flow there always exists a laminar sublayer in the immediate neighborhood of solid surfaces. This was already described in Sec. 16. A heat flow from the surface into the fluid must penetrate this sublayer before it can be transported by the turbulent mixing. This interaction *between the laminar sublayer* and the turbulent flow determines the laws of heat transfer. To this date no one has succeeded in predicting from calculations the heat transfer in turbulent flows. On the other hand it is possible in a way as shown by Reynolds, Prandtl, Taylor, von Kármán, and others to derive formulas for heat transfer from hydrodynamic measurements and to gain a good insight into the mechanism of turbulent heat exchange in this way. Only the fluid layers in the proximity of a wall influence the heat transfer essentially. The velocities in these layers are practically parallel to the wall. The heat flow is normal to the wall. Therefore, in the following the laws of heat transfer in a flow parallel to the wall (the $x$ direction) are investigated. The velocity may change materially only in the $y$ direction and the heat may flow in the $y$ direction. Therefore the temperature changes materially only in the $y$ direction. In any arbitrary plane parallel to the wall, *i.e.*, parallel to the $x$ axis, within the laminar sublayer there exists a shearing stress

$$\tau = \mu \frac{du}{dy}$$

The heat flow per unit area of the plane is, according to Eq. (31),

$$q = -k \frac{dt}{dy}$$

Now let us consider the same plane in turbulent flow. By the turbulent mixing motions fluid particles are continuously carried through this plane. This is presented in Fig. 62 simplified in such a way that the fluid weight $w'$ penetrating the plane $aa$ per unit time and unit area in an upward direction comes from the plane 1-1, where the velocity is $u$, and the temperature is $t$, and is transported to the plane 2-2. In steady flow the same amount $w'$ must be transported from plane 2-2 where the velocity is $u'$, and the temperature is $t'$, to the plane 1-1. The fluid flowing upward transports an amount of heat equal to $w'c_pt$, and the fluid flowing downward carries the heat $w'c_pt'$. If the temperature $t$ is greater than $t'$, as a result of the mixing movements a heat flow

$$q_t = w'c_p(t - t') \tag{148}$$

is transported per unit area. The fluid particles also carry with them their kinetic energy. If the velocity $u$ is greater than $u'$, the fluid above the plane *aa* is accelerated by the particles moving upward, whereas the fluid below the plane is decelerated. By such a turbulent exchange the difference in the velocities $u$ and $u'$ is therefore decreased. The turbulent mixing acts in the same way as a shearing stress in plane *aa*. According to the law of momentum as formulated in Sec. 15, the virtual turbulent shearing stress equals the increase or decrease of momentum generated by the action of the fluid mass $w'/g$ exchanged per unit time. Therefore the equation

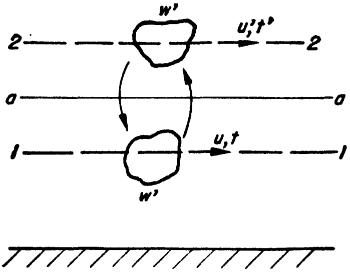

FIG. 62. Simplified picture of turbulent exchange.

$$\tau_t = \frac{w'}{g}(u - u') \tag{148a}$$

holds for the turbulent shearing stress $\tau_t$. If the unknown value $w'$ is eliminated from Eqs. (148) and (148*a*), the following relation between heat flow and shearing stress in turbulent flow is obtained:

$$q_t = \tau_t g c_p \frac{t - t'}{u - u'} \tag{149}$$

This relation was first derived by Reynolds in 1874 and is therefore called Reynolds analogy. If a corresponding relation is constructed for a plane in the laminar sublayer by dividing the two equations at the beginning of this section, there follows, neglecting the minus signs,

$$q = \tau \frac{k}{\mu} \frac{dt}{du} \tag{150}$$

For the ratio of the heat flow to the shearing stress the same law holds true in turbulent or laminar flow, when

$$\frac{k}{\mu} = gc_p \qquad (151)$$

or

$$\frac{gc_p\mu}{k} = \frac{\nu}{\alpha} = Pr = 1 \qquad (151)$$

In a fluid or gas with a Prandtl number equal to 1, the heat transfer in laminar and turbulent flow are connected in the same way with the shearing stress. Therefore it is possible to locate one of the planes in Fig. 62 in the laminar, the other in the turbulent layer. It is useful to locate one plane in the wall ($t = t_w$, $u = 0$), the other may be located in the border between the boundary layer and the main flow ($t = t_s$, $u = u_s$).

For fully developed flow in a tube, the mean velocity $u_m$ and the mean temperature $t_m$ may be used. This gives for the tube,

$$q_w = \tau_w g c_p \frac{t_m - t_w}{u_m}$$

By multiplying both sides of this equation by the tube wall surface $A$, there is obtained

$$Q_w = R\frac{gc_p}{u_m}(t_m - t_w) \qquad (152)$$

where $R$ is the resistance ($R = \tau_w A$). This simple relation between the heat flow $Q_w$ and the resistance $R$ holds true only for a medium with $Pr = 1$. Inasmuch as all gases have Prandtl numbers which deviate only little from 1, Eq. (152) is very useful to get a first approximation for the heat transfer where the resistance is known. The resistance can be replaced by the power which is necessary to drive the gas through the tube. The resistance of a tube with a pressure loss $\Delta p$ is $R = \Delta p\ (d^2\pi/4)$, and the volume flowing per unit time through the tube is $V = u_m(d^2\pi/4)$; therefore the power necessary for the flow is

$$W = V\,\Delta p = Ru_m$$

The ratio of the heat flow to the power necessary is therefore

$$\frac{Q}{W} = \frac{gc_p}{u_m^2}(t_m - t_w) \qquad (153)$$

This important relationship shows that the power necessary for a certain heat transfer becomes smaller when the velocity $u_m$ is decreased. This fact is utilized in coolers or heat exchangers for airplanes by surrounding the cooler by a duct. The air stream is thus decelerated before it flows through the cooler, and afterward the pressure increase gained by deceleration is utilized to accelerate the air again. Such a ducted cooler is schematically sketched in Fig. 63. By this ducting, which is today in general use in airplanes, but which is useful as well for fast locomotives and motorcars, the power necessary to drag the cooler through the air can be decreased very much. Something must be paid, however, for this gain, for the lower the velocity of the air through the cooler, the greater the surface area necessary for a given heat flow. The same balancing between the amount of surface on one hand and the power necessary on the other hand is necessary in the design of a steam boiler. If it is desired to decrease the weight and dimensions of such a boiler by increasing the gas velocity, use must be made of a cheap source of energy which drives the gases through the boiler. This problem was solved in the Velox boiler by using a gas turbine to drive the blower for the combustion air.

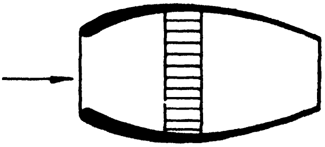

FIG. 63. Ducted cooler for aircraft.

**Example.** Through a tube of 0.8 in. diameter and 3 ft long there flows air with 100 fps velocity. The air intake temperature is 68 F; its pressure is 14.2 lb/in.² The pressure loss in the tube is 3.2 in. water column = 0.114 lbs/in.² How much heat is transferred from the tube wall to the air when the wall is heated to a temperature $t_w$ = 200 F?

For a first approximation Eq. (152) may be used, although air has a Prandtl number equal to 0.72. The resistance of the tube is

$$R = \Delta p \frac{d^2\pi}{4} = 0.114 \frac{\text{lb}}{\text{in.}^2} \times \frac{0.64 \times \pi}{4} \text{ in.}^2 = 0.0574 \text{ lb}$$

The heat transfer to the air is

$$Q = 0.0574 \frac{32.2 \times 0.24}{100} (t_w - t_m) \frac{\text{Btu}}{(\text{sec})(\text{F})}.$$

$$= 0.00443 \times 3600 (t_w - t_m) \frac{\text{Btu}}{(\text{hr})(\text{F})} = 15.9 (t_w - t_m) \qquad \text{Btu/(hr)(F)}$$

The tube-wall temperature is $t = 200$ F. The mean temperature of the air $t_m$ is not yet known. The heat $Q$ taken up by the air may be written as $Q = \gamma c_p u_m (d^2\pi/4)(t_e - t_i)$ if $\gamma$ is the specific weight of the air ($\gamma = 0.0750$ lb/ft$^3$ for 68 F and 14.2 lb/in.$^2$); $t_i$ is the intake temperature into the tube, and $t_e$ is the bulk exit temperature from the tube. Inserting the numerical values into this equation gives

$$Q = 0.075 \times 0.24 \times 100 \times \frac{0.64\pi}{144 \times 4} (t_e - t_i) \frac{\text{Btu}}{(\text{sec})(\text{F})}$$
$$= 0.00626\ (t_e - t_i) \frac{\text{Btu}}{(\text{sec})(\text{F})}$$

The mean temperature difference $\Delta t_m = t_w - t_m$ is, according to Sec. 3, $\Delta t_m = a\ (\Delta t_i + \Delta t_e)/2$. The wall temperature here is constant. Therefore $\Delta t_m = t_w - t_m = a[t_w - (t_i + t_e)/2]$. By equating the two equations for $a$ there is obtained

$$0.00443b \left(t_w - \frac{t_i + t_e}{2}\right) = 0.00626(t_e - t_i)$$

The factor $a$ cannot be determined from Table 2, as the ratio $\Delta t_i/\Delta t_e$ is unknown; therefore, estimate $a = 1$. Now the equation gives $t_e = 137$ F. To establish $a$ use the ratio

$$\frac{\Delta t_i}{\Delta t_e} = \frac{200 - 68}{200 - 137} = 2.1$$

Therefore $a = 0.96$ from Table 2. As the whole calculation gives only a first approximation it is not necessary to repeat it with the new value for $a$. The heat flow is $Q = 0.00626 \times (137 - 68)3{,}600 = 1550$ Btu/hr. An exact calculation with the formulas in the next paragraph gives a heat flow greater by 15 per cent.

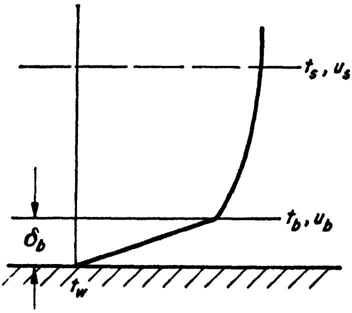

FIG. 64. Turbulent temperature and velocity profile with laminar sublayer.

For a medium whose Prandtl number deviates greatly from 1, the heat resistance of the laminar sublayer and the turbulent flow must be calculated separately. Let the temperature of the wall be $t_w$ (Fig. 64), the temperature in the border between laminar sublayer and turbulent boundary layer be $t_b$, and the temperature in the stream outside the boundary layer be $t_s$. The corresponding velocities are $u_w = 0$, $u_b$, and $u_s$.

The temperature distribution in the laminar sublayer may be assumed as linear since the thickness $\delta_b$ of this layer is very small. Therefore the specific heat flow through this layer is

$$q_w = \frac{k}{\delta_b}(t_b - t_w)$$

because heat flows there only by conduction. The law for the shearing stress at the wall is

$$\tau_w = \mu \frac{u_b}{\delta_b}$$

If the sublayer thickness is eliminated from both equations there is obtained

$$q_w = \tau_w \frac{k}{\mu}\frac{1}{u_b}(t_b - t_w) \tag{154}$$

The heat flow in the turbulent boundary layer is given by Eq. (149). The two planes for which the temperatures and velocities will be inserted into this equation may be located in the border between the laminar sublayer and turbulent layer and between the turbulent layer and the outside flow. As the sublayer is very thin it can be assumed the heat flow and the shearing stress have the same values at the border between the laminar and the turbulent layer as at the wall. Therefore Eq. (149) may be written

$$q_w = \tau_w g c_p \frac{t_s - t_b}{u_s - u_b} \tag{154a}$$

The film heat-transfer coefficient $h$ at the wall is defined by the equation

$$q_w = h(t_s - t_w) \tag{154b}$$

If Eqs. (154), (154*a*), and (154*b*) are solved for the temperature differences, and the first and second are subtracted from the third we get

$$\frac{1}{h} = \frac{1}{\tau_w g c_p}(u_s - u_b) + \frac{\mu u_b}{\tau_w k} = \frac{u_s}{\tau_w g c_p}\left(1 - \frac{u_b}{u_s} + \frac{\mu g c_p}{k}\frac{u_b}{u_s}\right)$$

$$= \frac{u_s}{\tau_w g c_p}\left[1 + \frac{u_b}{u_s}(Pr - 1)\right]$$

The heat-transfer coefficient is

$$h = \frac{\tau_w g c_p / u_s}{1 + (u_b/u_s)(Pr - 1)} \tag{155}$$

This equation was derived by L. Prandtl (1910 and 1928) and G. I. Taylor (1916).[1]

## 24. Flow in a tube

In fully developed flow the boundary layers have met at the axis of a tube. For the velocity $u_s$ and temperature $t_s$, the values at the axis must therefore be used. It is usual however to establish the heat transfer with the bulk temperature $t_B$ and to use the mean velocity $u_m$ in Eq. (155). This is not quite correct, but the resultant error is small. If the shearing stress is taken from Eq. (126) and the velocity ratio from Eq. (127), the above equation becomes

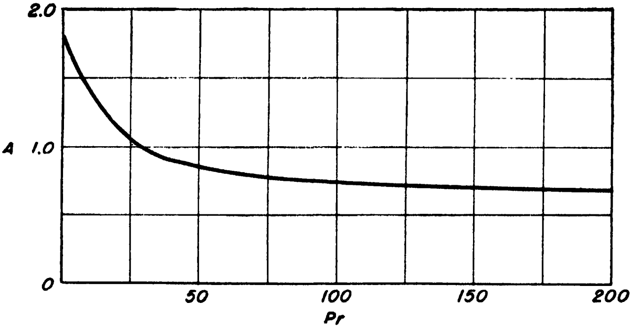

FIG. 65. Factor $A$ in Eqs. (156) and (160). [*From W. Buehne, Wärme*, **61**, 162 (1938).]

$$\frac{h}{\gamma c_p u_m} = \frac{0.0396 \left(\frac{u_m d}{\nu}\right)^{-1/4}}{1 + A \left(\frac{u_m d}{\nu}\right)^{-1/8} (Pr - 1)} \tag{156}$$

The constant $A$ has the value 2.43. A comparison with experimental results on viscous fluids shows, however, that this value is too great, and furthermore that $A$ is a function of the Prandtl number. In Fig. 65 this function is given according to W. Bühne.[2] Equations for this function were derived by ten Bosch,[3] Hoffman,[4] and others. The expression on the left-hand side of

---

[1] L. Prandtl, *Z. Physik*, **11**, 1072 (1910); **29**, 487 (1928). G. I. Taylor, *Rept. Mem. Brit. Aeronaut. Comm.*, No. 272, 1916, p. 423.

[2] W. Bühne, *Wärme*, **61**, 162 (1938).

[3] M. ten Bosch, "Die Wärmeübertragung," Berlin, 1936.

[4] E. Hoffman, *Z. ges. Kälte-Ind.*, **44**, 99–107 (1937).

Eq. (156) is equivalent to the following product of dimensionless values: $Nu_d/(Re_d\,Pr)$. It is sometimes called Stanton number and denoted by *St*. The final formula for heat transfer in a tube with turbulent flow is therefore

$$\mathbf{St} = \frac{\mathbf{Nu}_d}{\mathbf{Re}_d\,\mathbf{Pr}} = \frac{0.0396(\mathbf{Re}_d)^{-1/4}}{1 + A(\mathbf{Re}_d)^{-1/8}\,(\mathbf{Pr} - 1)} \tag{157}$$

The value $A$ can be taken from Fig. 65. E. Hoffman gives the formula $A = 1.5Pr^{-1/6}$.

The shape of the velocity profile for different Prandtl numbers can also be derived from the above equations. By equating (154) and (154*a*), the ratio of the temperature drop in the laminar sublayer to the temperature drop in the turbulent zone becomes

$$\frac{t_b - t_w}{t_s - t_b} = \frac{\mu g c_p}{k}\,\frac{u_b}{u_s - u_l} = Pr\,\frac{u_b}{u_s - u_b}$$

For a medium with $Pr = 1$ the ratio of the temperature differences equals the ratio of the corresponding velocity differences. Both profiles are similar. For two Prandtl numbers greater than 1 the temperature profiles are shown in Fig. 66. For large Prandtl numbers the temperature drop in the laminar sublayer is the essential one. Only for very small Prandtl numbers (*e.g.*, mercury or molten metals with Prandtl numbers in the neighborhood of 0.01) is the drop in the turbulent zone the greater.

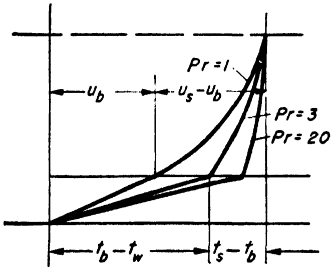

FIG. 66. Turbulent temperature profiles for various Prandtl numbers.

The temperature profiles for low Prandtl numbers, when determined in the same way as the profiles in Fig. 66, would look S-shaped, with a very small temperature rise in the laminar sublayer and most of the temperature difference concentrated in the turbulent core. This behavior is determined by a very low heat resistance in the laminar sublayer as compared with the turbulent zone. This of course does not correspond to reality. In any turbulent flow, the turbulent heat exchange is superimposed on a heat flow by conduction. For Prandtl numbers near 1 or greater than 1 the heat conduction is small compared with the turbulent exchange, and was neglected in the previous calculations accordingly. At low Prandtl numbers, however, it is of equal or greater importance, and in the limiting case the turbulent exchange can be neglected and the heat conduction is the dominating factor. The calculations in Sec. 22 should therefore present a reasonable approximation for the heat transfer in a turbulent flow within a tube at very low Prandtl numbers. The only way in which the turbulence makes itself felt in heat transfer is in changing the velocity profile from the parabolic to a fuller shape, but this influences the temperature profile only in a minor degree.

A thorough investigation on heat transfer to liquids at small Prandtl numbers was published by R. C. Martinelli.[1] This problem became interesting recently in connection with atomic power plants, where molten metals seem to fulfill the demand for a medium that transfers heat very readily.

The combination of the values $Nu$, $Re$, and $Pr$ on the left-hand side of Eq. (157) is especially useful for heat-transfer calculations. The heat flow to the wall of a tube of length $L$ is

$$Q = h\, d\pi\, L(t_B - t_w)$$

The heat flow may also be expressed by the cooling of the liquid from the intake temperature $t_i$ to the exit temperature $t_e$:

$$Q = \gamma c_p u_m \frac{d^2\pi}{4} (t_i - t_e)$$

Both equations give

$$\frac{h}{\gamma c_p u_m} = \frac{Nu}{Re\, Pr} = \frac{d}{4L} \frac{t_i - t_e}{t_B - t_w} \tag{158}$$

From this equation the temperature $t_e$ with which the liquid leaves the tube can be calculated without using any property values, as soon as the tube dimensions, the intake temperature $t_i$, and the wall temperature $t_w$ are given and the value $Nu/(Re\, Pr)$ is known. For the bulk temperature $t_B$, the logarithmic mean of intake and exit temperature differences must be used.

For the derivation of Eq. (155) the property values were considered as constant. E. Hoffman[2] investigated the influence of the variability of the property values on the heat transfer. He found that Eq. (157) holds true when the property values are inserted at the reference temperature

---

[1] R. C. Martinelli, *Trans. ASME*, **69**, 947–959 (1947).

[2] E. Hoffmann, *Z. Ver. deut. Ing.*, **82**, 741–782 (1938).

$$t^\star = t_B - \frac{0.1Pr + 40}{Pr + 72}(t_B - t_w) \tag{159}$$

For gases (Prandtl number near 1) this equation gives approximately the arithmetic mean between liquid and wall temperature as $t^\star$. The greater the Prandtl number, the more $t^\star$ approaches the mean liquid temperature $t_B$. The temperature $t_b$ between laminary sublayer and turbulent zone (Fig. 66) has the same trend.

Besides the theoretically founded Eq. (157) empirical formulas are often used. Dittus and Boelter's[1] equations are well known; for example,

$$Nu = 0.0243(Re)^{0.8}(Pr)^{0.4}$$

for heat flow from the wall to the liquid and

$$Nu = 0.0265(Re)^{0.8}(Pr)^{0.3}$$

for heat flow from the liquid to the wall.

Use of two different expressions for heating and cooling[2] is somewhat unsatisfactory. The equations up till now are good for fully developed turbulent flow. In the intake region there may be expected greater heat-transfer coefficients. H. Hausen[3] gave an expression

$$Nu_m = 0.116[(Re)^{2/3} - 125](Pr)^{1/3}\left[1 + \left(\frac{d}{L}\right)^{2/3}\right]\left(\frac{\mu_B}{\mu_w}\right)^{0.14}$$

where $\mu_B$ is the viscosity at bulk liquid temperature and $\mu_w$ the viscosity at tube-wall temperature. Apart from these the property values are to be inserted at $t_B$. This formula takes into account the conditions in the intake region. It also satisfactorily reproduces the values in the transition zone $Re = 2{,}300$ to 6,000. Figure 67 shows the transition region according to a summary of available test results by Sieder and Tate.[4]

The heat transfer in a curved tube with the radius of curvature $R$ can be found by multiplying the values of the straight tube by $(1 + 1.77d/R)$.

---

[1] F. W. Dittus and L. M. K. Boelter, *Univ. Calif. Pub. Eng.*, **2**, 443 (1930).

[2] E. Eckert, *Z. Ver. deut. Ing.*, **80**, 137–138 (1936).

[3] H. Hausen, *Z. Ver. deut. Ing.*, *Beiheft Verfahrenstechnik*, No. 4, 1943, pp. 91–98.

[4] E. N. Sieder and G. E. Tate, *Ind. Eng. Chem.*, **28**, 1429–1435 (1936).

With Eq. (157) and those just stated the heat transfer in a tube with noncircular cross section can also be calculated. Instead of the diameter $d$, the hydraulic diameter $d_h = 4A/C$ (where $A$ is the cross-sectional area and $C$ is the wetted perimeter) must be inserted. The whole perimeter must be used also in the case when only part is heated or cooled.[1] Only in calculating the heat flow with Eq. (8) is the heated area to be used.

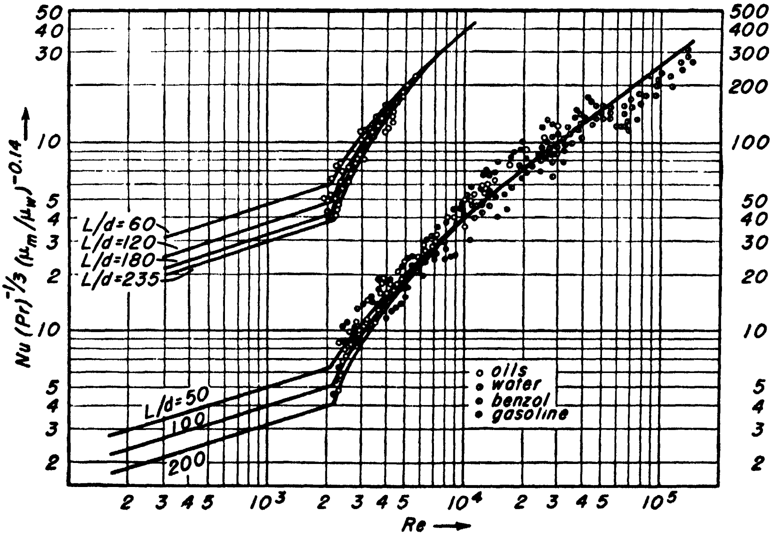

FIG. 67. Film heat-transfer coefficients in a tube within the transition zone from laminar to turbulent flow. [*According to E. N. Sieder and G. E. Tate, Ind. Eng. Chem.*, **28**, 1429–1435 (1936).]

**Example.** The radiator of a motorcar is constructed of finned tubes. The tubes are 0.24 in. in diameter and 24 in. long. Cooling water flows through them with a 3-fps velocity and 140 F temperature. The film heat-transfer coefficient on the tube wall is to be calculated. The kinematic viscosity of water at 140 F can be found in the Appendix as $\nu = 0.514 \times 10^{-5}$ ft²/sec and the Prandtl number $Pr = 3.02$. The Reynolds number is $Re = \dfrac{3 \times 0.24/12}{0.514 \times 10^{-5}} = 11{,}600$. The flow therefore is turbulent. The intake length for turbulent flow is $L_e/d = 40$. Here the ratio of the tube length to the diameter is 100. Therefore the greater part of the flow is fully developed, and calculations can be made with Eq. (157). From Fig. 65 the value $A$ is found to be 1.5. With it $\frac{Nu}{Re\,Pr} = \frac{0.0396/11{,}600^{1/4}}{1 + 1.5 \times 2.02/11{,}600^{1/8}} = 0.00194$. The Nusselt number is $Nu = 0.00194 \times 11{,}600 \times 3.02 = 68$, and the heat-transfer coefficient, with $k = 0.376$ Btu/(ft)(hr)(F), is

---

[1] M. ten Bosch, *op. cit.*

$$h = Nu\,\frac{k}{d} = 68\,\frac{0.376}{0.24/12} = 1275 \text{ Btu/(hr)(ft}^2\text{)(F)}$$

Within the first half of the tube length the heat-transfer coefficient drops to this value. The heating of the water may be calculated immediately from $Nu/(Re\,Pr)$. We get

$$\frac{t_e - t_i}{t_B - t_W} = \frac{4L}{d}\,0.00194 = 0.776$$

### 25. The plate in longitudinal flow

In order to calculate the heat transfer from a plane plate with Eq. (155), the value $u_s$ must be inserted for the free-stream velocity, and $t_s$ accordingly for the temperature in the free stream. Introducing the shearing stress from Eq. (118), and the velocity ratio from Eq. (122) gives

$$\mathrm{St} = \frac{\mathrm{Nu}_x}{\mathrm{Re}_x\,\mathrm{Pr}} = \frac{0.0296(\mathrm{Re})^{-1/5}}{1 + 0.87\mathrm{A}(\mathrm{Re})^{-1/10}(\mathrm{Pr} - 1)} \tag{160}$$

The value $A$ may be taken from Fig. 65 or from the equation $A = 1.5Pr^{-1/6}$. The factor 0.87 arises by the change from the average velocity used for the tube to the velocity $u_s$ used here, which corresponds to the velocity in the tube axis. Equation (160) gives the local heat-transfer coefficient. It was pointed out in Sec. 13 that a laminar boundary layer exists in the neighborhood of the leading edge. Only where the Reynolds number as constructed with the distance from the leading edge has reached the critical value (approximately $5 \times 10^5$) does the flow in the boundary layer become turbulent. Now Eq. (160) gives the heat-transfer coefficient in the turbulent zone, whereas for the laminar part Eq. (140) is to be used.[1] For gases the above equation can be simplified since the range of Prandtl numbers is small in this case and the denominator can be regarded as constant. By integrating this simplified equation over the plate length the average heat-transfer coefficient is obtained. Assuming the boundary layer to be turbulent over the whole length the Nusselt number built with the average heat-transfer coefficient is[1]

---

[1] M. Jakob and W. M. Dow, *Trans. ASME,* **68,** 124–134 (1946).

$$\overline{Nu}_x = 0.037(Re_x)^{0.8}(Pr)^{1/3}$$

In reality probably a certain part of the boundary layer near the leading edge is always laminar. Integration must then be carried out in two steps, over the laminar part and over the turbulent part separately. Assuming that the heat-transfer coefficients in the turbulent zone are the same as if the turbulent boundary layer started right on the leading edge, and carrying out the integration gives

$$\overline{Nu}_x = 0.037(Pr)^{1/3}[(Re_x)^{0.8} - 23{,}100]$$

for $Re_{cr} = 5 \times 10^5$ and

$$\overline{Nu}_x = 0.037(Pr)^{1/3}[(Re_x)^{0.8} - 4{,}200]$$

for $Re_{cr} = 10^5$.

The Stanton number in Eq. (160) can be interpreted as the ratio of two lengths for boundary-layer flow. For this purpose we use the fact that all the heat $Q$ transferred from a hot plate to the flow past its surface within the length $x$ (Fig. 68) must in steady state be carried with the flow through the plane I-I. In mathematical form this gives

$$Q = \gamma c_p \int_0^\infty u(t - t_s)\, dy$$

The integration has to be carried out practically only within the thermal boundary layer. On the other hand the heat flow $Q$ can be expressed by a heat-transfer coefficient averaged over the length $x$:

$$Q = \bar{h}x(t_w - t_s)$$

From both equations the average Stanton number can be determined:

$$\overline{St} = \frac{\bar{h}}{\gamma c_p u_s} = \frac{1}{x}\int_0^{\delta_t} \frac{u(t - t_s)}{u_s(t_w - t_s)}\, dy$$

The integral has the dimension of a length and can be regarded as a kind of boundary-layer thickness. Since it characterizes the heat carried by convection within the boundary layer we shall call it *convection thickness* ($\delta_c$). It corresponds closely to a value called *impulse thickness* of the boundary layer which is used in hydrodynamics. The diagram on the lower side of Fig. 68 shows the determination of the convection thickness. Multiplying for all values $y$ the ordinates of the nondimensional velocity profile $u/u_s$ by the nondimensional temperature profile $(t - t_s)/(t_w - t_s)$ leads to curve $a$, the area under which is the above integral. It can be transformed into a rectangle with unit height and the length $\delta_c$. It is easily understood that the convection thickness is smaller than the thermal boundary-layer thickness $\delta_t$ (page 92) and also smaller than the *displacement thickness* as defined on page 71. Since the boundary-layer thickness is always small as compared with the length $x$, it can be seen that the Stanton number is always a small value.

---

[1] H. A. Johnson and M. W. Rubesin, *Trans. ASME*, **71**, 447–456 (1949).

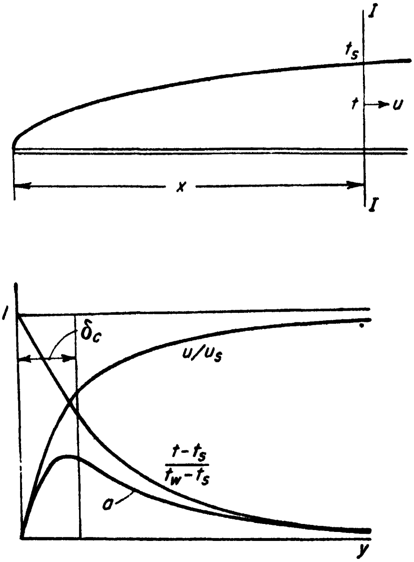

FIG. 68. Determination of the convection thickness of the thermal boundary layer.

**Example.** A flat plate heated to 176 F is cooled by an air stream at 68 F, 14.2 lb/in.$^2$ and a velocity $u_s$ = 30 fps. The local heat-transfer coefficient at a distance $x$ = 12 in. is to be calculated.

According to page 115 the property values for gases are to be inserted at the arithmetic mean between wall and gas temperature. This gives $t^\star = 122$ F. From the Appendix we get, $\nu = 19.89 \times 10^{-5}$ ft²/sec, $k = 0.0160$ Btu/(hr)(ft)(F), $Pr = 0.701$,

$$Re = \frac{u_s x}{\nu} = \frac{30 \times 12/12}{19.89 \times 10^{-5}} = 151{,}000$$

At this Reynolds number the boundary layer may be laminar or turbulent. If it is turbulent, there is obtained from Eq. (160),

$$St = \frac{Nu_x}{Re_x Pr} = \frac{0.0296(151{,}000)^{-1/5}}{1 - 0.87 \times 1.75(151{,}000)^{-1/10} \times 0.299} = 0.00312$$

It is questionable as to which length must be inserted as $x$, since the boundary layer is laminar in the vicinity of the leading edge. Following the suggestion of Prandtl (page 74) the distance from the leading edge was used as $x$. The Nusselt number becomes

$$Nu = 0.00312 \times 0.701 \times 151{,}000 = 330$$

and the heat-transfer coefficient

$$h = Nu \frac{k}{x} = 330 \frac{0.0160}{1} = 5.28 \text{ Btu/(hr)(ft}^2\text{)(F)}$$

If the flow is laminar at the distance $x = 12$ in., there is obtained from Eq. (140*a*),

$$Nu = 0.331 \sqrt[3]{Pr}\sqrt{Re} = 0.331 \times \sqrt[3]{0.70} \times \sqrt{151{,}000} = 115$$

and the heat-transfer coefficient

$$h = 115 \times 0.0160 = 1.85 \text{ Btu/(hr)(ft}^2\text{)(F)}$$

Therefore, the heat transfer increases very much when the boundary layer becomes turbulent.

## 26. Recent improvements in the theory of turbulent heat transfer

In the last sections the velocity ratio $u_b/u_s$ in the fundamental Eq. (155) had to be determined empirically from heat-transfer experiments. In recent years T. von Kármán[1] succeeded in refining the theory of turbulent heat exchange in such a way that good agreement with experimental results is obtained without introduction of any correction factors. His calculations were extended and compared with experimental results by Boelter, Martinelli, and Jonassen.[1]

---

[1] T. von Kármán, *Trans. ASME*, **61**, 705–710 (1939).

Prandtl and Taylor idealized the turbulent flow near a wall by assuming a laminar sublayer and a turbulent layer separated by a sharp border line. It is known that in reality the turbulence gradually decreases in the neighborhood of a wall. Figure 41 revealed that the flow field is better subdivided into three regions, the laminar sublayer, the buffer layer, and the turbulent layer.

For the laminar sublayer the equations on page 106 hold true. They can be written in the form

$$\tau_l = \nu\rho \frac{du}{dy}$$

$$q_l = \frac{\nu}{Pr} \gamma c_p \frac{dt}{dy} \tag{161}$$

The corresponding equations for the turbulent zone will be somewhat transformed by introducing the concept of the eddy diffusivity. In analogy to the above equation for the laminar sublayer we write for the turbulent shearing stress

$$\tau_t = \epsilon\rho \frac{du}{dy} \tag{162}$$

The eddy diffusivity $\epsilon$ has the same dimension as kinematic viscosity. It is however not a constant but a function of the wall distance, Reynolds number, and other variables, and must be determined separately. According to Eq. (148*a*) in which the difference $(u - u')$ may be replaced by an infinitesimally small difference $du$, the eddy diffusivity is $\epsilon = (w'/\gamma)\,dy$. The Reynolds analogy demands that the specific turbulent heat flow follow the equation

$$q_t = \epsilon\gamma c_p \frac{dt}{dy} \tag{162a}$$

with the same value $\epsilon$ as in the equation for the turbulent shearing stress. We can prove this by dividing one above equation by the other. This results in $q_t/\tau_t = gc_p(dt/du)$, an expression identical with Eq. (149).

---

[1] L. M. K. Boelter, R. C. Martinelli, and F. Jonassen, *Trans. ASME*, **63**, 447–455 (1941).

In any turbulent flow turbulent shearing stress and turbulent heat flow are present, together with the laminar shearing stress and heat flow represented by Eqs. (161), but in the turbulent layer the eddy diffusivity is ordinarily so much bigger than the kinematic viscosity and the thermal diffusivity that the molecular exchange given by Eq. (161) can be neglected as compared to the molar exchange of Eqs. (162). In the buffer layer, however, all these are of the same order of magnitude. It is assumed generally that there is no mutual interaction and that we can write therefore for this layer

$$\tau_b = (\nu + \epsilon)\rho \frac{du}{dy}$$

$$q_b = \left(\frac{\nu}{Pr} + \epsilon\right)\gamma c_p \frac{dt}{dy} \tag{162b}$$

We shall now calculate the drop in temperature in the buffer layer with the help of these equations. The second equation gives

$$\Delta t_b = \frac{q_b}{\gamma c_p} \int_{y_1}^{y_2} \frac{dy}{(\nu/Pr) + \epsilon}$$

The eddy diffusivity is determined from the first equation

$$\epsilon = \frac{\tau_b}{\rho}\frac{dy}{du} - \nu$$

The laminar sublayer and the buffer layer are very thin compared with the tube radius; therefore, the shearing stress and the specific heat flow can change by only a small amount within these layers. It was therefore assumed constant throughout the layer. Accordingly we replace the values $\tau_b$ and $q_b$ by $\tau_w$ and $q_w$. In addition we introduce the dimensionless values $y^+$ and $u^+$. From the equations which define these values (page 82) it follows that

$$\frac{\rho}{\tau_w}\frac{du}{dy} = \frac{1}{\nu}\frac{du^+}{dy^+}$$

Kármán's equation for the velocity in the buffer layer

$$u^+ = 5[1 + \ln(y^+/5)]$$

gives $du^+/dy^+ = 5/y^+$. Therefore

$$\epsilon = \nu\frac{y^+}{5} - \nu$$

and

$$\Delta t_b = \frac{q_w}{\gamma c_p \nu} \int_{y_1}^{y_2} \frac{dy}{\frac{1}{Pr} + \frac{y^+}{5} - 1} = \frac{q_w}{\gamma c_p} \sqrt{\frac{\rho}{\tau_w}} \int_{5}^{30} \frac{dy^+}{\frac{1}{Pr} + \frac{y^+}{5} - 1}$$

Integrated

$$\Delta t_b = \frac{q_w}{\gamma c_p} \sqrt{\frac{\rho}{\tau_w}}\, 5 \ln(5\,Pr + 1)$$

The linear temperature drop in the laminar sublayer is represented by

$$\Delta t_l = \frac{q_w}{k} y_1 = \frac{q_w}{\gamma c_p} \frac{Pr}{\nu} y_1$$

Introducing the dimensionless value $y^+ (y_1^+ = 5)$ gives

$$\Delta t_l = \frac{q_w}{\gamma c_p} \sqrt{\frac{\rho}{\tau_w}}\, Pr\, y_1^+ = \frac{q_w}{\gamma c_p} \sqrt{\frac{\rho}{\tau_w}}\, 5Pr$$

Within the turbulent layer the Reynolds' analogy is applied [Eq. (154*a*)]:

$$\Delta t_t = \frac{q_w}{\gamma c_p} \frac{\rho}{\tau_w} (u_s - u_b)$$

Introducing again the dimensionless value $u_b^+$ gives

$$\Delta t_t = \frac{q_w}{\gamma c_p} \sqrt{\frac{\rho}{\tau_w}} \left[ \frac{u_s}{\sqrt{\tau_w/\rho}} - u_b^+ \right]$$

The border of the turbulent zone, where the velocity is $u_b$, is fixed by the wall distance $y_2^+ = 30$. Therefore with Kármán's equation $u_b^+ = 5(1 + \ln y^+/5)$ and $y^+ = 30$,

$$\Delta t_t = \frac{q_w}{\gamma c_p} \sqrt{\frac{\rho}{\tau_w}} \left[ \frac{u_s}{\sqrt{\tau_w/\rho}} - 5(1 + \ln 6) \right]$$

By summing up all the individual temperature drops, the whole temperature difference between the tube wall and the end of the turbulent zone (the tube axis) is found:

$$t_w - t_s = \frac{q_w}{\gamma c_p} \sqrt{\frac{\rho}{\tau_w}} \left[ \frac{u_s}{\sqrt{\tau_w/\rho}} + 5(Pr - 1) + 5 \ln \frac{5Pr + 1}{6} \right]$$

The dimensionless heat-transfer coefficient is

$$St = \frac{Nu}{Re\,Pr} = \frac{q_w}{\gamma c_p u_s (t_w - t_s)}$$
$$= \frac{\tau_w/\rho u_s^2}{1 + \sqrt{\dfrac{\tau_w}{\rho u_s^2}}\left[5(Pr - 1) + 5 \ln \dfrac{5\,Pr + 1}{6}\right]}$$

This equation supersedes Eq. (155) derived by Prandtl and Taylor. It is valid for the flat plate as well as for the tube.

To adapt it to the *flat plate* one can introduce the equation $\tau_w/\rho u_s^2 = f_P/2$ from page 72. This gives

$$St = \frac{Nu}{Re\,Pr} = \frac{f_P/2}{1 + \sqrt{\dfrac{f_P}{2}}\left[5(Pr - 1) + 5 \ln \dfrac{5\,Pr + 1}{6}\right]}$$

For a smooth wall $f_P/2 = 0.0296/(Re_x)^{0.2}$. In adapting it to the *tube* one must keep in mind that the heat-transfer coefficient is usually built with the bulk temperature $t_B$ of the flowing substance, whereas in the above equation the temperature $t_s$ of the tube axis appears. The equations for the shearing stress at the tube wall also contain the average velocity $u_m$ and not the velocity $u_s$ in the tube axis as used here. Denoting the ratio of the two velocities $\varphi_m = u_m/u_s$ and the temperature ratio

$$\vartheta' = \frac{t_w - t_B}{t_w - t_s}$$

and using the expression $\tau_w/\rho u_m^2 = f/8$ (page 81) we get for the *tube*

$$St = \frac{Nu}{Re\,Pr} = \frac{(\varphi_m/\vartheta')f/8}{1 + \varphi_m\sqrt{\dfrac{f}{8}}\left[5(Pr - 1) + 5 \ln \dfrac{5\,Pr + 1}{6}\right]}$$

The velocity ratio can be derived from Eq. (117) of the turbulent velocity profile $\varphi_m = 0.82$. In reality, it changes a bit with Reynolds number. For the friction coefficient $f$ Eq. (131) or (132) is to be used.

Boelter, Martinelli, and Jonassen avoided introduction of the velocity ratio $\varphi_m$ for the tube by writing the temperature drop in the turbulent region in a different way. By repeating the deduction given here for the buffer layer but putting $\nu = 0$ and using the equation $u^+ = 5.5 + 2.5 \ln y^+$ for the turbulent zone we get

$$\Delta t_t = 2.5 \frac{q_w}{\gamma c_p} \sqrt{\frac{\rho}{\tau_w}} \int_{y_2^+}^{r^+} \frac{dy^+}{y^+} = 2.5 \frac{q_w}{\gamma c_p} \sqrt{\frac{\rho}{\tau_w}} \ln \frac{r^+}{30}$$

$$= 2.5 \frac{q_w}{\gamma c_p} \sqrt{\frac{\rho}{\tau_w}} \ln \frac{r u_m}{30 \nu} \sqrt{\frac{f}{8}} = 2.5 \frac{q_w}{\gamma c_p} \sqrt{\frac{\rho}{\tau_w}} \ln \frac{Re_d}{60} \sqrt{\frac{f}{8}}$$

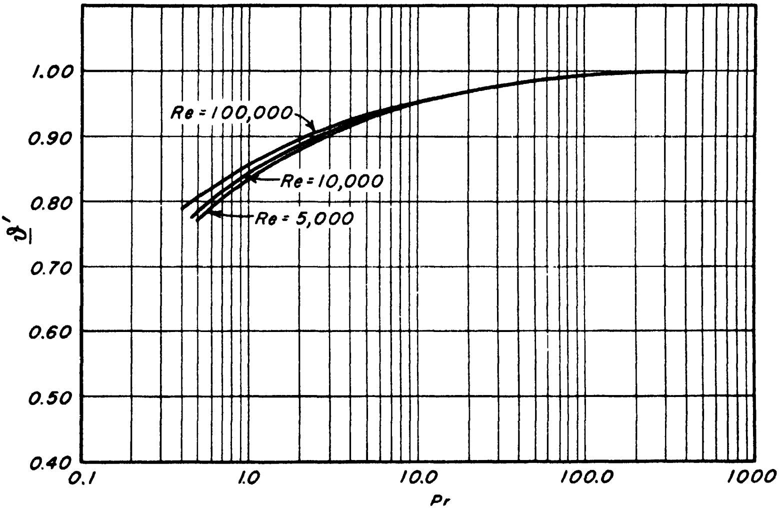

FIG. 69. Temperature ratio $\vartheta'$ for turbulent heat transfer in a tube. [*From L. M. K. Boelter, R. C. Martinelli, and F. Jonassen, Trans. ASME,* **63**, 447–455 (1941).]

and for the dimensionless heat-transfer coefficient,

$$St = \frac{Nu}{Re\,Pr} = \frac{(1/\vartheta')\sqrt{f/8}}{5\left[Pr + \ln(1 + 5Pr) + \frac{1}{2}\ln \frac{Re_d}{60}\sqrt{\frac{f}{8}}\right]}$$

Figure 69 shows the temperature ratio $\vartheta'$ which is necessary for the evaluation of the equations for the tube.

Boelter, Martinelli, and Jonassen compared the heat-transfer coefficients calculated by the last equation with measured values and found a very good agreement. Figure 70 illustrates this. To take into account the variable property values they introduced a thickness $y_1^+$ for the laminar sublayer depending on the ratio of the viscosity at wall temperature to the viscosity at bulk-fluid

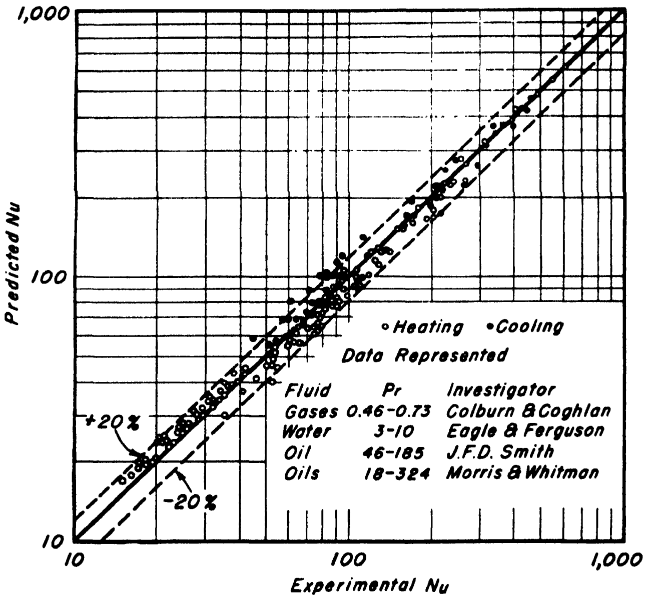

FIG. 70. Comparison between calculated and measured film heat-transfer coefficients for turbulent flow in a tube. (*From L. M. K. Boelter, R. C. Martinelli, and F. Jonassen, Trans. ASME*, **63**, 1941, *pp.* 447–455.)

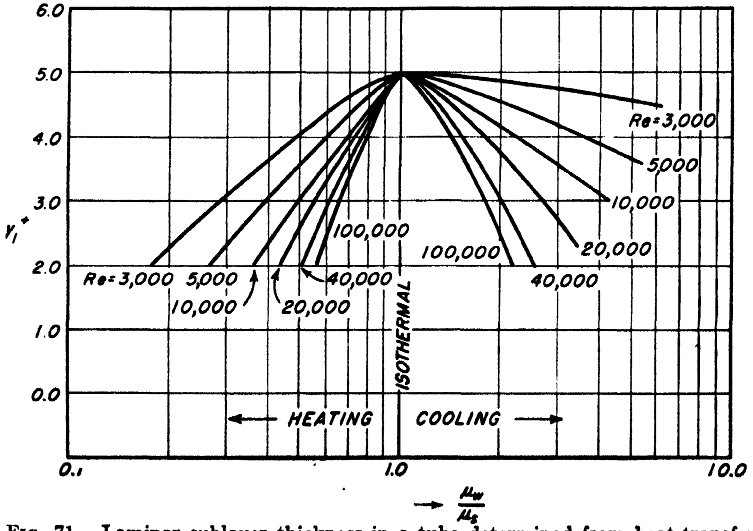

**FIG. 71. Laminar sublayer thickness in a tube determined from heat-transfer data, by L. M. K. Boelter, R. C. Martinelli, and F. Jonassen (*Trans. ASME*, 63, 1941, pp. 447–455).**

temperature. This sublayer thickness was determined from heat-transfer experiments and is shown in Fig. 71. The property values in the equation itself are introduced at bulk temperature.

A thorough theoretical investigation of turbulent heat transfer from a flat plate and in a tube was made by H. Reichardt.[1] He inquired first whether the Reynolds' analogy is really true or not, and found from measured temperature and velocity profiles that the ratio of the eddy diffusivity for momentum transfer to the eddy diffusivity for heat transfer is not 1, but has some value between 1.4 and 1.5. His evaluation of heat-transfer measurements, however, gave for the same ratio the value 1.1. It is known that in wakes behind bodies in flow this value is 2. Further experiments to answer this question are of much interest.

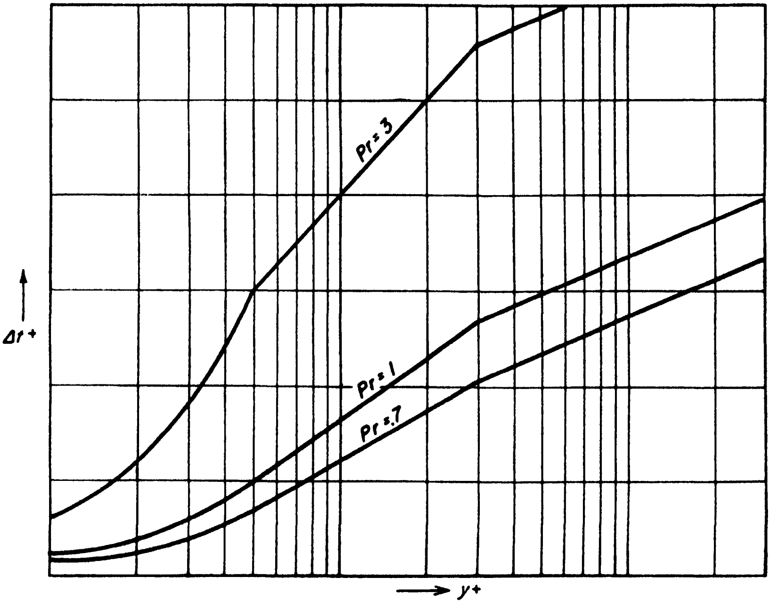

FIG. 72. Universal temperature profiles for turbulent heat transfer in a tube.

The formulas in this paragraph can be used also to calculate the heat transfer on rough surfaces when the friction coefficient of these surfaces is introduced.[2] An extension of the derivation is necessary for substances with very low Prandtl numbers, *e.g.*, molten metals and liquid mercury. In these substances the molecular exchange of momentum and heat cannot be neglected in the turbulent zone as compared with the turbulent exchange. Such an extension was made by R. C. Martinelli.[1]

---

[1] H. Reichardt, *Z. angew. Math. Mech.*, **20**, 297–328 (1940).

[2] R. C. Martinelli, *Trans. ASME*, **68**, 947–959 (1947).

By using especially adapted coordinates there can be constructed temperature profiles which do not depend on the Reynolds number and which can therefore be called *universal temperature profiles* in analogy to the universal velocity profile. In the formulas for the temperature drop in the different layers there appeared the factor $q_w/\sqrt{\tau_w/\rho}\ \gamma c_p$ which has the dimension of a temperature. By dividing the difference in temperature between an arbitrary point within the boundary layer and the wall $(t - t_w)$ by the above factor, a dimensionless $\Delta t^+$ is built which serves as ordinate for the universal temperature profile. The abscissa is the same $(y^+)$ as in Fig. 45. Figure 72 shows these temperature profiles for different Prandtl numbers. The profile for $Pr = 1$ is identical with the universal velocity profile when the eddy diffusivity of momentum and heat are equal. The plotting of measured temperature profiles in this form is useful in checking the assumptions of the theory presented in this paragraph.

## 27. Dimensional analysis of heat transfer

The different types of heat transfer reviewed up to this point could be calculated. For other types, however, calculation is hopeless at the present time. This is true for all bodies which create wakes in the flow. As an example the circular tube in Fig. 46 can be mentioned. For such a tube the only possibility that remains is to derive heat-transfer data from experiments and to generalize the results by dimensional analysis. This theory teaches that all physical processes depend on certain dimensionless values, and shows how to find these values. The application of this theory to heat transfer enabled Nusselt[2] to coordinate systematically earlier experimental results for the first time and to plan new experiments systematically.

When the hydrodynamic boundary layer on the flat plate was calculated it was found that the result could be presented as function of the Reynolds number alone. This was true for the boundary-layer thickness [Eq. (115), (120), and (123)], as well as for the friction coefficient. The thermal boundary layer and the heat-transfer coefficient in dimensionless form could be presented as functions of two dimensionless values, the Reynolds number and the Prandtl number. We shall now try to answer the question whether it is possible to obtain these results from the differential equations without solving them. For this purpose it is necessary to write these equations in dimensionless form. Start with the momentum equation (111). For the flat plate, the pressure gradient $dp/dx$ is zero. Considering this and introducing the shearing stress $\tau_w$ from Eq. (109), there is obtained

---

[1] R. C. Martinelli, *Trans. ASME*, **69**, 947–959 (1947).

[2] W. Nusselt, *Gesundh. Ing.*, **38**, 477–490 (1915).

$$\rho \frac{d}{dx} \int_0^l (u_s - u)\, u\, dy = \mu \left(\frac{du}{dy}\right)_w$$

Now make the velocity $u$ dimensionless by dividing it by the known free-stream velocity $u_s$. The dimensionless velocity is denoted by $u' = u/u_s$. In the same way a length can be selected to make the other lengths dimensionless with it. By selecting the distance $x$ from the leading edge, we get $y' = y/x$ and $dy' = dy/x$. In the same way $dx' = dx/x$ and $l' = l/x$.

Introducing these into the above equation gives

$$\rho u_s^2 \frac{d}{dx'} \int_0^{l'} (1 - u')u'\, dy' = \frac{\mu u_s}{x} \left(\frac{du'}{dy'}\right)_w$$

In this equation only the property values and the reference values $x$ and $u_s$ have dimensions. If both sides are divided by $\rho u_s^2$ the equation must become dimensionless, for then the left-hand side has only dimensionless values. On the right-hand side there appears the value $\nu/u_s x$, which is the reciprocal value of the Reynolds number $Re_x$. The momentum equation in dimensionless form is

$$\frac{d}{dx'} \int_0^{l'} (1 - u')u'\, dy' = \frac{1}{Re_x} \left(\frac{du'}{dy'}\right)_w \qquad (163)$$

It differs from the original equation in that in place of the property values there now appears the dimensionless Reynolds number. The solution of the equation must present the unknown dimensionless velocity $u'$ as a function of the dimensionless coordinate $y'$ and of the Reynolds number

$$u' = f(y', Re) \qquad (163a)$$

The value of $y'$ at which $u = u_s$, where therefore $u' = 1$ is called the dimensionless boundary-layer thickness $\delta'$. For this value an equation

$$\delta' = \frac{\delta}{x} = f(Re) \tag{164}$$

must exist. As the shearing stress on the wall is calculated from the velocity profile [Eq. (163*a*)], it is clear that the coefficient of friction is also a function of the Reynolds number. It can be seen that it is actually possible to predict the form of the results of the calculations from the differential equation.

Now we shall apply these same reflections to the heat-flow equation (135). Beside the values already used in the momentum equation there must be defined a dimensionless temperature difference $\vartheta'$ by dividing the temperature difference $\vartheta = (t_s - t)$ by the difference $\Theta = (t_s - t_w)$ between free-stream temperature and wall temperature, $\vartheta' = \vartheta/\Theta$. Introducing it into Eq. (135) there is obtained

$$u_s \frac{d}{dx'} \int_0^l (1 - \vartheta')u'\,dy' = \frac{\alpha}{x}\left(\frac{d\vartheta'}{dy'}\right)_w$$

By dividing by $u_s$ the equation becomes dimensionless. On the right-hand side there appears $\alpha/u_s x$. Its reciprocal value differs from the Reynolds number in such a way that the thermal diffusivity $\alpha$ takes the place of the kinematic viscosity $\nu$. The dimensionless value $u_s x/\alpha$ is called the Peclet number and is denoted by *Pe*.

$$Pe_x = \frac{u_s x}{\alpha} \tag{165}$$

The solution of the dimensionless equation

$$\frac{d}{dx'} \int_0^{l'} (1 - \vartheta')u'\,dy' = \frac{1}{Pe_x}\left(\frac{d\vartheta'}{dy'}\right)_w \tag{166}$$

must give the temperature profile in the form

$$\vartheta' = f(u', y', Pe_x)$$

The dimensionless velocity may be introduced from Eq. (163*a*):

$$\vartheta' = f(y', Re_x, Pe_x)$$

In this form the equation is impracticable for numerical calculations because in both values $Re$ and $Pe$ there appear the velocity $u_s$ and the distance $x$. Therefore it is better to build a new dimensionless value by dividing $Pe$ by $Re$. This gives

$$\frac{Pe}{Re} = \frac{\nu}{\alpha} = Pr$$

The ratio is therefore the Prandtl number, which is known already. Now we may write

$$\vartheta' = f(y', Re_x, Pr) \tag{167}$$

for if $\vartheta'$ is a function of the Reynolds number and Peclet number it must also be a function of the Prandtl number, the ratio of the two preceding ones. The heat-transfer coefficient according to Eq. (137*b*) is

$$h\Theta = k\left(\frac{d\vartheta}{dy}\right)_w$$

In dimensionless form this becomes

$$\frac{hx}{k} = \left(\frac{d\vartheta'}{dy'}\right)_w$$

On the left-hand side appears the Nusselt number, $Nu_x$. The dimensionless temperature is, according to Eq. (167), a function of the dimensionless distance from the wall $y'$ and of the Reynolds and Prandtl numbers. The same must be true for the derivative $d\vartheta'/dy'$ and its value at the wall (for $y' = 0$) must be a function of $Re_x$ and $Pr$. Therefore

$$Nu_x = f(Re_x, Pr) \tag{167a}$$

For the heat transfer of a flat plate with a laminar boundary layer there was given in Eq. (140*a*)

$$Nu_x = 0.331\,\sqrt[3]{Pr}\,\sqrt{Re_x}$$

Introducing the Peclet number by the relation $Pr = Pe_x/Re_x$ there is obtained

$$Nu_x = 0.331\,\sqrt[3]{Pe_x}\,\sqrt[6]{Re_x}$$

In this example it can be seen that the Prandtl number can be replaced by the Peclet number, and conversely.

The reflections up to now were made only on a special example, the flat plate. Since the momentum equation (111) and the heat-flow equation (135) are generally applicable for boundary layers, the results must also be generally presentable as functions of the above dimensionless numbers. The general momentum equation (111) has a summand with the pressure gradient, which vanishes for the flat plate. It will be shown later that this summand does not influence the above results. The special form of the functions in (163) and (167) depends on the shape of the body whose surface transfers heat and on the velocity variation along the surface and outside the boundary layer. These factors fix the boundary conditions of the differential equations (111) and (135). They also must be presented in dimensionless form by dividing all lengths by a reference dimension of the body, and all velocities by a reference velocity $u_0$. If the differential equations can be solved for one pair of the boundary conditions, the solutions are also known for a whole group of cases, namely, for all bodies which arise from the original one by virtue of increasing or decreasing the scale, because all these bodies are similar dimensionally. On the other hand the reference velocity $u_0$ may be varied freely, for the boundary condition requires only that the dimensionless ratio $u_s/u_0$ have a certain value. The dimensionless velocity field $u'$ depends only upon the Reynolds number for all these cases, and the dimensionless temperature field $\vartheta'$ depends upon both Reynolds number and Prandtl number. In other words, all the dimensioned velocity fields $u$ and the temperature fields $\vartheta$ of the above cases may be brought into congruence if they are divided by the reference velocity $u_0$ or by the reference temperature difference $\Theta_0$, respectively, and if they are plotted on the dimensionless coordinates $x'$ and $y'$, as long as the Reynolds number and the Prandtl number each has a constant value.

All bodies arising from the original one by changing the scale are called *geometrically similar* bodies. In the same way fields of physical quantities such as the velocity and temperature field are called *physically similar* if they can be made congruent by dividing the quantities by a reference quantity of the same dimension and plotting them over the dimensionless coordinates.

Now the result of the above considerations can be formulated in the following way:

*The velocity fields of geometrically similar bodies are physically similar if the velocities on the borders of the field are similar and the Reynolds number has a constant value. The temperature fields of the same bodies are similar if the additional conditions are fulfilled that the temperatures on the borders of the field are similar and the Prandtl number has a constant value.*

As a last step these considerations must be extended to cases where no boundary layers arise, for instance in the case of wakes behind blunt bodies. For this purpose it must be remembered that the momentum equation (111) of the boundary layer is the expression for the equilibrium of all forces acting on a fluid particle in the boundary layer. If, in the same way, the equilibrium conditions are formulated for a fluid element in a flow of a fluid with friction forces the Navier-Stokes differential equations[1] (Navier 1882, Stokes 1845) are obtained. The derivation of these equations is a very long process. It is not necessary, however, to have the exact form of these equations for our considerations, but only their principal structure.

Assuming a mass particle with the shape of a small parallelepiped (dimensions $dx$, $dy$, $dz$) moving in the $x$ direction with a variable velocity $u$. On the particle there acts an inertia force $\rho(du/dt)\,dx\,dy\,dz$, with $t$ being denoted as the time for a moment. If the flow is steady, then the velocity of the particle changes only by the fact that the particle is carried to another place. Therefore $du/dt = \partial u/\partial x \quad dx/dt = u\,\partial u/\partial x$. The interia force is $\rho u(\partial u/\partial x)\,dx\,dy\,dz$. Friction forces arise by the action of shearing stresses on the surface of the particle. On one surface $dx\,dz$ (Fig. 22) the shearing stress $\tau$ acts in the $x$ direction. On the other surface $dx\,dz$ the shearing stress is $\tau + (\partial\tau/\partial y)\,dy$. As a result of these stresses there is acting on the particle a friction force $(\partial\tau/\partial y)\,dx\,dy\,dz$. With Newton's formula (109), this gives $\mu(\partial^2u/\partial y^2)\,dx\,dy\,dz$. A friction force in the $x$ direction arises also from shearing stresses on the two surfaces $dy\,dx$. This force is $\mu(\partial^2u/\partial z^2)\,dx\,dy\,dz$. Only the pressures acting on the surfaces $dy\,dz$ give a force in the $x$ direction. This force is $-(\partial p/\partial x)\,dx\,dy\,dz$. As an equilibrium expression of the inertia, friction and pressure forces there is obtained

---

[1] For example, W. F. Durand, "Aerodynamic Theory," Vol. 3, Springer-Verlag, Berlin, 1935.

$$\rho u \frac{\partial u}{\partial x} + \cdots = \mu \frac{\partial^2 u}{\partial y^2} + \mu \frac{\partial^2 u}{\partial z^2} + \cdots - \frac{\partial p}{\partial x} \qquad (168)$$

In reality the variations of the velocity component $u$ in the $y$ and $z$ directions also cause inertia and friction forces in the $x$ direction. These have, however, the same character as the corresponding expressions in the above equation and are therefore only indicated by the dots.

To make the equation dimensionless it is treated in the same way as before, that is, all velocities $u$, $v$, $w$ are divided by a reference velocity $V_0(u' = u/V_0,\ v' = v/V_0,\ w' = w/V_0)$ and all coordinates by a reference length $l$ $(x' = x/l,\ y' = y/l,\ z' = z/l)$. The pressure $p$ can be made dimensionless with the dynamic pressure $\rho(V_0^2/2)$ of the reference velocity, or $p' = p\Big/\left(\rho\frac{V_0^2}{2}\right)$

Equation (168) changes to the following form:

$$\rho\frac{V_0^2}{l}\left(u'\frac{\partial u'}{\partial x'} + \cdots\right) = \mu\frac{V_0}{l^2}\left(\frac{\partial^2 u'}{\partial y'^2} + \cdots\right) - \rho\frac{V_0^2}{l}\frac{1}{2}\frac{\partial p'}{\partial x'} \qquad (169)$$

To make this expression dimensionless it is divided by $\rho(V_0^2/l)$ and thus

$$u'\frac{\partial u'}{\partial x} + \cdots = \frac{1}{Re}\left(\frac{\partial^2 u'}{\partial y'^2} + \cdots\right) - \frac{1}{2}\frac{\partial p'}{\partial x'} \qquad (169a)$$

Two other equations of the same form are obtained for the equilibrium of the forces in the $y$ and $z$ directions. A fourth equation can be written by the consideration that in steady flow as much fluid leaves the volume element as enters it. In the same way as the heat-flow equation was obtained in Sec. 10, the continuity equation can be written

$$\frac{\partial u}{\partial x} + \frac{\partial v}{\partial y} + \frac{\partial w}{\partial z} = 0$$

or in dimensionless form

$$\frac{\partial u'}{\partial x'} + \frac{\partial v'}{\partial y'} + \frac{\partial w'}{\partial z'} = 0 \qquad (170)$$

From the three Eqs. (169*a*) and Eq. (170), the velocity components $u'$, $v'$, $w'$, and the pressure $p'$ can be calculated and the solutions can be presented as functions of the dimensionless coordinates $x'$, $y'$, $z'$ and the Reynolds number $V_0 l/\nu$.

The dimensioned factors in Eq. (169) are inertia and friction forces per unit volume built up with the reference values of velocity and length. The Reynolds number therefore is the ratio of these two forces. A large Reynolds number indicates that the inertia forces predominate, a small Reynolds number indicates predomination of the friction forces.

The heat-flow equation in the boundary layer expresses the equilibrium between the convection heat carried with the flow into a small volume element within the boundary layer and the heat leaving the element by conduction. To get the heat-flow equation for a volume element in any general position within a viscous fluid use is made of Eq. (89). This equation also holds true in a liquid if the volume element moves with the flow and always consists of the same mass particles. In a steady flow the temperature of this element changes only by the change in the position of the element

$$\frac{d\vartheta}{dt} = \frac{\partial\vartheta}{\partial x}\frac{dx}{dt} + \frac{\partial\vartheta}{\partial y}\frac{\partial y}{dt} + \frac{\partial\vartheta}{\partial z}\frac{dz}{dt} = u\frac{\partial\vartheta}{\partial x} + v\frac{\partial\vartheta}{\partial y} + w\frac{\partial\vartheta}{\partial z}$$

where $t$ = time.

By introducing this expression, Eq. (89) becomes

$$\gamma c_p u \frac{\partial\vartheta}{\partial x} + \cdots = k\frac{\partial^2\vartheta}{\partial x^2} + \cdots \qquad (171)$$

The specific-heat value used here must be that for constant pressure.[1] In reality heat sources are always present in a flowing liquid, inasmuch as the energy losses from the friction forces are converted into heat. For velocities which are not too high, the temperature increase produced by these sources is so small that it can be neglected. At high velocities, however, the heating effect by friction is very marked. This effect will be discussed in a later section. In Eq. (171) only one representative of any type of summand is written. In order to characterize the two expressions on the left- and right-hand sides as convective and conductive heat flow, respectively, the property values are not united to the thermal diffusivity as in Eq. (89). Since in the equation only temperature differentials occur, $\vartheta$ can be considered a temperature difference with respect to any arbitrary temperature. To make Eq. (171) dimensionless, we introduce in addition to the same dimensionless values as in Eq. (170) the dimensionless temperature difference $\vartheta' = \vartheta/\Theta$ ($\Theta$ is a reference temperature difference). Therefore

---

[1] This will be explained in Sec. 29.

$$\gamma c_p \frac{u_0\Theta}{l} u' \frac{d\vartheta'}{dx'} + \cdots = k \frac{\Theta}{l^2} \frac{\partial^2\vartheta'}{\partial y'^2} + \cdots$$

and in dimensionless form

$$u' \frac{d\vartheta'}{dx'} + \cdots = \frac{1}{Pe}\left(\frac{\partial^2\vartheta'}{\partial y'^2} + \cdots\right) \tag{172}$$

The solution of Eq. (172) must present the dimensionless temperature such that

$$\vartheta' = f(u', v', w', x', y', z', Pe)$$

or by introducing the velocities as functions of the coordinates and the Reynolds number, and using *Pr* instead of *Pe*,

$$\vartheta' = f(x', y', z', Re, Pr)$$

The heat transfer at a certain place on a body surface can be derived from this equation as

$$\mathbf{Nu} = \mathbf{f(Re, Pr)} \tag{173}$$

All temperature fields and heat-transfer coefficients in forced convection can therefore be presented in dimensionless form as a function of the Reynolds and Prandtl numbers.

To determine the dimensionless groups for heat transfer by free convection there must be included in the previous equations those movements which are generated by temperature differences. If the specific weight $\gamma$ changes with temperature, buoyant forces arise which must be included in Eq. (169). The buoyant force acting on the element $dx\,dy\,dz$ has the value $(\gamma - \gamma_0)\,dx\,dy\,dz$, where $\gamma_0$ denotes the specific weight of the fluid at some reference point. The expansion coefficient $\beta$ which represents the relative change in volume per degree temperature increase $\beta = (1/v)(\partial v/\partial T)_p$ may be introduced. If an average value $\beta_m$ is constructed with the temperature difference $\vartheta$ from a reference temperature and with the specific weight $\gamma_0$, $\left(\beta_m = \frac{1}{\vartheta}\frac{v - v_0}{v}\right)$, the buoyant force is given as

$$(\gamma - \gamma_0)\,dx\,dy\,dz = \gamma_0\left(\frac{\gamma}{\gamma_0} - 1\right)dx\,dy\,dz$$
$$= \gamma_0\left(\frac{v_0}{v} - 1\right)dx\,dy\,dz = \gamma_0\beta_m\vartheta\,dx\,dy\,dz$$

For gases $1/v = p/RT$ and $(dv/dT)_p = R/p$. Therefore $\beta = 1/T$, and $\beta_m$ has the same value. Equation (169) presents the forces per unit volume. Therefore to it must be added the summand $\gamma_0\beta_m\vartheta$, or $\gamma_0\beta_m\Theta\vartheta'$. To make Eq. (169) dimensionless it was divided by $\rho(u_0^2/l)$. The buoyancy summand in the expanded Eq. (169*a*) is therefore $(\gamma_0\beta_m\Theta l/\rho u_0^2)\vartheta'$. The dimensionless temperature $\vartheta'$ as a solution of Eq. (169*a*) is a function of the dimensionless factor $\gamma_0\beta_m\Theta l/\rho u_0^2$ in addition to those previously mentioned. For small temperature differences it becomes $\gamma\beta_m\Theta l/\rho u_0^2 = g\beta_m\Theta l/u_0^2$. This characteristic value has the disadvantage that it contains the temperature difference $\Theta$ and the velocity $u_0$ as well. To eliminate one of them it is necessary to construct a new characteristic value by multiplying the above by the square of the Reynolds number. The characteristic number arising in this way is called the Grashof number or Grashof modulus and is indicated by *Gr*:

$$Gr = \frac{g\beta_m\Theta l}{u_0^2}\,\frac{u_0^2 l^2}{\nu^2} = \frac{g\beta_m\Theta l^3}{\nu^2} \tag{174}$$

This characteristic number must be added to those previously derived, where the buoyant forces noticeably affect the flow. The heat transfer may then be expressed by an equation of the form

$$Nu = f(Re, Pr, Gr) \tag{175}$$

The expansion coefficient necessary for the calculation of the Grashof number is contained in the Appendix. It depends essentially only on the temperature for liquids and gases except in the proximity of the critical point, where a marked dependency upon pressure arises. At the critical point the expansion coefficient theoretically becomes infinite. Figure 137 shows the coefficient of expansion for water over the whole range of state. Within a liquid near its critical point the temperature differences are equalized very rapidly because the great expansion coefficient evokes great buoyancy forces.

If flow in a liquid or gas is caused only by the temperature differences, there is no reference velocity available which can enter the problem as a boundary condition. Therefore no Reynolds number can be computed. For *free convection* an equation of the form

$$\mathbf{Nu} = \mathbf{f}(\mathbf{Gr}, \mathbf{Pr}) \tag{176}$$

exists. In one of the following sections such an equation will be derived by solving the boundary-layer equations. If the temperature differences are very small the arising velocities are small. Then in the expanded equations of momentum (168) the inertia forces may be neglected. Dimensional analysis of this equation shows that the heat transfer then depends only on the product *Gr Pr*.

Nusselt extended the dimensional investigation in that he assumed the property values hitherto considered constant as dependent upon the temperature. If the property values follow the laws $\nu = \nu_0(T/T_0)^{b_1}$, $\alpha = \alpha_0(T/T_0)^{b_2}$, he finds that the heat transfer may be presented in the form

$$Nu = f\left(Re, Pr, Gr, \frac{T_w}{T_0}\right) \tag{177}$$

where $T_w$ is the absolute temperature of the wall, $T_0$ an absolute reference temperature in the flowing medium (gas or liquid). For gases, the above equations approximate the real temperature dependency of the property values fairly well. For liquids the expressions can always be used for a certain temperature range whereby the zero point for the temperatures can be fixed arbitrarily. In Eq. (177) there then appear the differences with respect to this zero point instead of the absolute temperatures.

At high velocities, the heat generated by internal friction in the flowing medium must be considered in the heat-flow equation. This causes the Mach number *Ma*, *i.e.*, the ratio of the reference velocity to the sound velocity, to appear in the result:

$$Nu = f\left(Re, Pr, Ma, \frac{T_w}{T_0}\right) \tag{178}$$

The Grashof number disappears as at high velocities the buoyancy effects can be neglected.

No evidence as to the form of the function $f$ in the previous equations can be gained by dimensional analysis. This must be obtained by experimentation or calculation. Nevertheless the advantage of knowing upon what values the result depends before starting the experiments is very great and cannot be overestimated. For example, if it is desired to investigate the heat transfer on a circular tube and if it is known from dimensional analysis that it depends only on the Reynolds number, it is sufficient to use only one tube diameter and to vary the free-stream velocity. The results of these experiments allow the calculation of heat transfer for tubes of any diameter, since the Reynolds number shows that heat transfer depends only on the product of the diameter times velocity. Yet another generalization is possible. After finishing the experiments with only one gas or liquid, the heat transfer is known not only for this particular gas but for all media with the same Prandtl number.

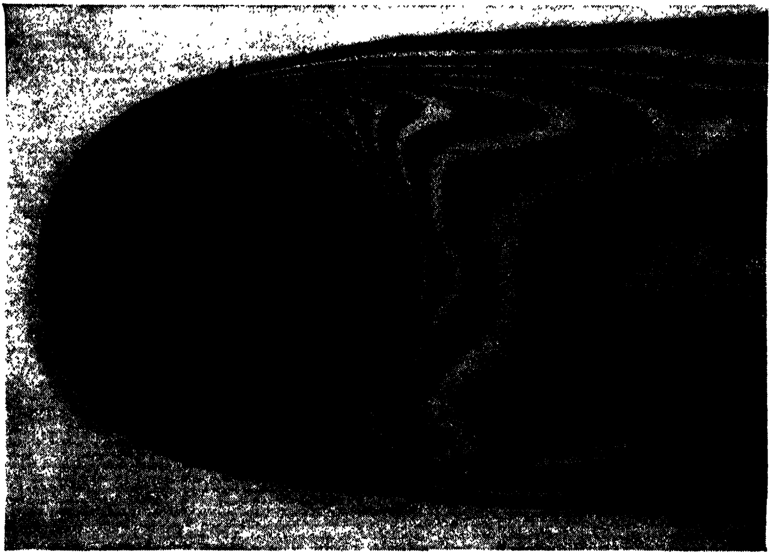

FIG. 73. Isotherms around a cylinder cooled by a fluid flowing normal to its axis as revealed by an interference photograph. $Re = 1{,}260$. (*Photograph by E. Eckert and E. Soehngen.*)

Nusselt proposed to evaluate experiments in such a way that for the function $f$ a product of exponentials is used, for instance,

$$Nu = K(Re)^m(Pr)^n \tag{179}$$

Equations of such a form were very widely used. Lately it has become clear, however, that equations of another type are more suitable for presenting test results over a wider range. Equation (157) and the equations in Sec. 26 are examples.

## 28. Tubes and tube bundles in crossflow

Among the differently shaped bodies from whose surface there is flow separation, circular tubes are those of the greatest engineering importance; therefore, a great number of experimental investigations of heat transfer from tubes are known. The flow around a circular tube was discussed in Sec. 18.

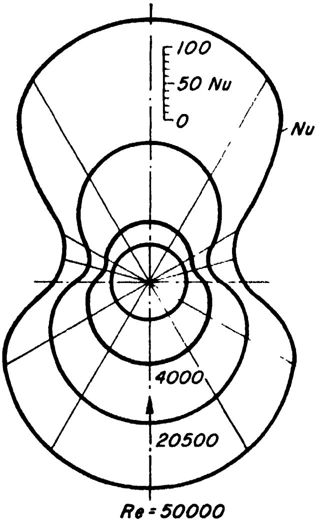

FIG. 74. Local film heat-transfer coefficients around a cylinder in a flow normal to its axis. (*According to W. Lorisch from M. ten Bosch, "Die Wärmeübertragung," 3d ed., Springer-Verlag, Berlin,* 1936.)

The temperature field around a heated cylinder is revealed by the interference photograph in Fig. 73. The dark lines around the shadow of the cylinder are lines of constant temperature. This figure thus shows the thermal boundary layer on the front half of the cylinder. A kind of boundary layer exists also along the back half. Within it the temperature drops from the surface value to the temperature within the wake. The flow shown in this photograph has a small Reynolds number. At higher Reynolds numbers the boundary layers are thinner and the temperatures in the wake more fluctuating and irregular.

The distribution of the heat-transfer coefficient around the tube surface is shown in Figs. 74 and 75. Heat transfer on the front side of the tubes was discussed in Sec. 21 and is shown by Fig. 55. The heat transfer on the back side occurs in the wake. Our knowledge of this kind of heat transfer is very limited. At low Reynolds numbers, the heat transfer on the front side is much greater than that on the back side. With increasing Reynolds number the heat flow from the back side increases comparatively, and for Re = 50,000 it is as high as on the front side. The reason for this fact is that the vortices, while separating alternately from the right and left flank of the cylinder, wash the surface of the rear half of the cylinder with an intensity that increases with the Reynolds number. If the boundary layer changes to turbulent flow before it separates from the surface, the distribution of the heat-transfer coefficient along the surface changes.

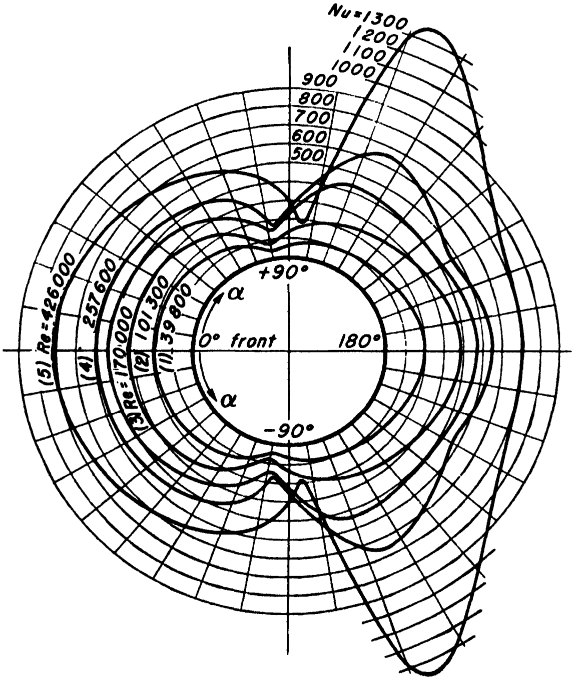

**Fig. 75.** Local film heat-transfer coefficients around a cylinder in a flow normal to its axis. [*From E. Schmidt and K. Wenner, Forsch. Gebiete Ingenieurw.*, **12,** 65–73 (1933).]

This is the case when the Reynolds number exceeds the value $Re_d = 4 \times 10^5$. Figure 75 shows that for a high Reynolds number the heat-transfer coefficient increases very much at an angle of 100 deg. This indicates the transition in the flow within the boundary layer. It was seen also on the plate in longitudinal flow, that the heat transfer increases appreciably at the place where the laminar boundary layer changes to a turbulent one. The place on the cylinder surface where the flow separates probably lies in the neighborhood of the second minimum for the heat-transfer coefficient.

For calculations on heat exchangers the interest is mostly in the total heat flow from, or to, a tube or, what is equivalent, the average heat-transfer coefficient around the circumference. R. Hilpert[1] made accurate measurements of this average value on an air flow. Figure 76 shows the result. The Nusselt and the Reynolds numbers are calculated with the tube diameter as the reference length and with the onflow velocity as the reference velocity. From Fig. 76 it can be seen that in various ranges of the Reynolds number, the Nusselt number can be presented in the form

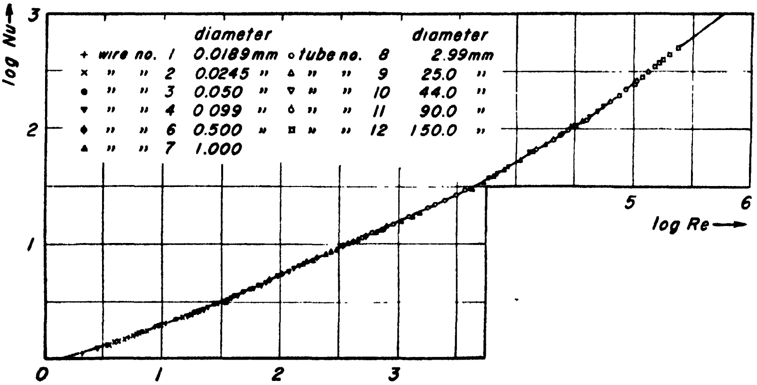

FIG. 76. Average film heat-transfer coefficient on a cylinder in a flow normal to its axis. $Pr = 0.72$. [*From R. Hilpert, Forsch. Gebiete Ingenieurw.*, **4**, 215 (1933).]

$$Nu = C(Re)^m \tag{180}$$

With the property values introduced at the arithmetic mean temperature. The numerical values for the constant $C$ and the

TABLE 7. COEFFICIENTS FOR CALCULATION OF HEAT TRANSFER ON A CIRCULAR CYLINDER TO AIR FLOW NORMAL TO ITS AXIS, BY EQ. (180)*

| $Re$ | $C$ | $m$ |
|---|---|---|
| 0.4–4 | 0.891 | 0.330 |
| 4–40 | 0.821 | 0.385 |
| 40–4,000 | 0.615 | 0.466 |
| 4,000–40,000 | 0.174 | 0.618 |
| 40,000–400,000 | 0.0239 | 0.805 |

* R. Hilpert, *Forsch. Gebiete Ingenieurw.*, **4**, 215 (1933).

---

[1] R. Hilpert, *Forsch. Gebiete Ingenieurw.*, **4**, 215 (1933).

exponent $m$ are tabulated in Table 7. Hilpert also made experiments with temperatures of the cylinder surface ranging from 200 to 1800 F whereas the air had a 68 F temperature. He found that the dimensionless heat-transfer coefficient could be expressed by the equation

$$Nu = C_1(Re)^m \left(\frac{T_w}{T_0}\right)^{\frac{m}{4}} \tag{181}$$

where $T_w$ is the absolute surface temperature, and $T_0$ is the absolute air temperature in the onstream. The temperature dependency of Eq. (181) is very small. For $t_a = 68$ F and $t_w = 1800$ F the heat-transfer coefficient is only 6 per cent greater than for the values $t_a = 68$ F and $t_w = 200$ F. The values of the constant $C$ in Eq. (180) hold true exactly at

$$t_w = 200 \text{ F}$$

Heat transfer from the front side of the tube can be calculated with the heat-flow equation of the boundary layer. Figure 55 shows the comparison between the calculated and the measured values. The ratio of heat flow to loss of momentum (friction loss) in the boundary layer on the front side of the tube corresponds approximately to Eq. (152), although in the accelerated flow along the surface the assumptions necessary for this equation are not strictly fulfilled. For small Reynolds numbers the whole resistance of the tube is essentially friction resistance. Equation (152) then gives the ratio of the total heat flow $Q$ to the total resistance $R$. For Reynolds numbers higher than 1,000, a wake arises in the flow and the form resistance caused by this wake exceeds the friction loss, as was mentioned in Sec. 18. The heat transfer on the rear half of the tube, however, is only approximately as great as on the front half. By that it can be understood that bodies which cause wakes in a flow are inferior to those bodies which do not with respect to the ratio of the heat flow to the resistance. For a quantitative comparison the dimensionless value $\Omega = \frac{W}{Q}\frac{gc_p(t_m - t_w)}{u_m^2}$ is very suitable (see page 108). For boundary-layer flow of a fluid with $Pr = 1$ this value is 1 according to Eq. (153). For a tube in cross flow at Reynolds numbers from 2,000 to 40,000 the value of $\Omega$ is 10 to 40. With respect to heat transfer *per unit area,* surfaces in the range of wakes are approximately as effective as in the range of boundary layers (Figs. 74 and 75). In this respect a tube with streamline-shaped cross section has no advantages over a tube with circular cross section.

By experiments with different liquids (water, oils) the dependency of the heat transfer on the Prandtl number was determined. The relation

$$\mathbf{Nu} = \mathbf{K}(\mathbf{Re})^{m}(\mathbf{Pr})^{0.31} \tag{182}$$

gives this connection. With the values in Table 7, the heat transfer in any liquid can be calculated by multiplying the constant $C$ by the factor $1.11 \times Pr^{0.31}$. In Table 8 the constants $C$ and the exponents $m$ of Eq. (180) are presented for cylinders with different cross sections, according to R. Hilpert. The dimensionless values are built using the diameter of a circular tube with equal surface.

TABLE 8. COEFFICIENTS FOR CALCULATION OF HEAT TRANSFER FROM CYLINDERS WITH DIFFERENT CROSS SECTIONS TO AN AIR FLOW NORMAL TO THEIR AXES BY EQ. (180)*

| Cross section | *Re* | *C* | *m* |
|---|---|---|---|
| → □ | 5,000–100,000 | 0.0921 | 0.675 |
| → ◇ | 5,000–100,000 | 0.222 | 0.588 |
| → ⬡ | 5,000–100,000 | 0.138 | 0.638 |
| → ⎔ | 5,000– 19,500 | 0.144 | 0.638 |
|  | 19,500–100,000 | 0.0347 | 0.782 |

* R. Hilpert, *Forsch. Gebiete Ingenieurw.*, **4**, 215 (1933).

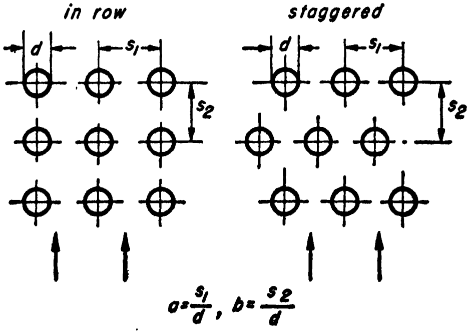

FIG. 77. Tube bundles with tubes in line and staggered

Heat transfer of tube bundles with the flow normal to the tube axis depends on the configuration of the tubes. The available test results were summarized by E. D. Grimison.[1] There are two possibilities: to arrange the tubes either in lines or staggered in flow direction (Fig. 77). The heat-transfer coefficients can be presented again in the form of Eq. (180). As a reference velocity, the average velocity in the narrowest cross section between the tubes is used. The values of the constant $C$ and the exponent $m$ are tabulated in Table 9. For ratios $a = s_1/d$ and $b = s_2/d$ greater than the values in the table, the equation

TABLE 9. COEFFICIENTS FOR CALCULATION OF HEAT TRANSFER FROM A TUBE BUNDLE TO AN AIR FLOW NORMAL TO ITS AXIS BY EQ. (180)*
$Re = 2{,}000$–$40{,}000$  $a = s_1/d$  $b = s_2/d$ (Fig. 67)

| $b$ \ $a$ | 1.25 | | 1.5 | | 2 | | 3 | |
|---|---|---|---|---|---|---|---|---|
| | $C$ | $m$ | $C$ | $m$ | $C$ | $m$ | $C$ | $m$ |
| | Tubes in lines | | | | | | | |
| 1.25 | 0.348 | 0.592 | 0.275 | 0.608 | 0.100 | 0.704 | 0.0633 | 0.752 |
| 1.5 | 0.367 | 0.586 | 0.250 | 0.620 | 0.101 | 0.702 | 0.0678 | 0.744 |
| 2 | 0.418 | 0.570 | 0.299 | 0.602 | 0.229 | 0.632 | 0.198 | 0.648 |
| 3 | 0.290 | 0.601 | 0.357 | 0.584 | 0.374 | 0.581 | 0.286 | 0.608 |
| | Staggered tubes | | | | | | | |
| 0.6 | | | | | | | 0.213 | 0.636 |
| 0.9 | | | | | 0.446 | 0.571 | 0.401 | 0.581 |
| 1 | | | 0.497 | 0.558 | | | | |
| 1.125 | | | | | 0.478 | 0.565 | 0.518 | 0.560 |
| 1.25 | 0.518 | 0.556 | 0.505 | 0.554 | 0.519 | 0.556 | 0.522 | 0.562 |
| 1.5 | 0.451 | 0.568 | 0.460 | 0.562 | 0.452 | 0.568 | 0.488 | 0.568 |
| 2 | 0.404 | 0.572 | 0.416 | 0.568 | 0.482 | 0.556 | 0.449 | 0.570 |
| 3 | 0.310 | 0.592 | 0.356 | 0.580 | 0.440 | 0.562 | 0.421 | 0.574 |

* E. Grimison, *Trans. ASME*, **59**, 583–594 (1937).

$$Nu = 0.297(Re)^{0.602} \tag{183}$$

given by R. Benke can be used. This equation and Table 9 are for heat transfer in air. For other liquids, the constants are to be determined in the same way as for single tubes. The property values must be introduced at the temperature given by Eq. (159). The formulas hold true for tube banks with 10 and more rows. For a smaller number of rows the average heat-transfer coefficient of the bundle is smaller; as an example, for four rows the heat-transfer coefficient is smaller by 12 per cent. The first row has approximately the same heat transfer as a single tube.

---

[1] E. D. Grimison, *Trans. ASME*, **59**, 583–594 (1937).

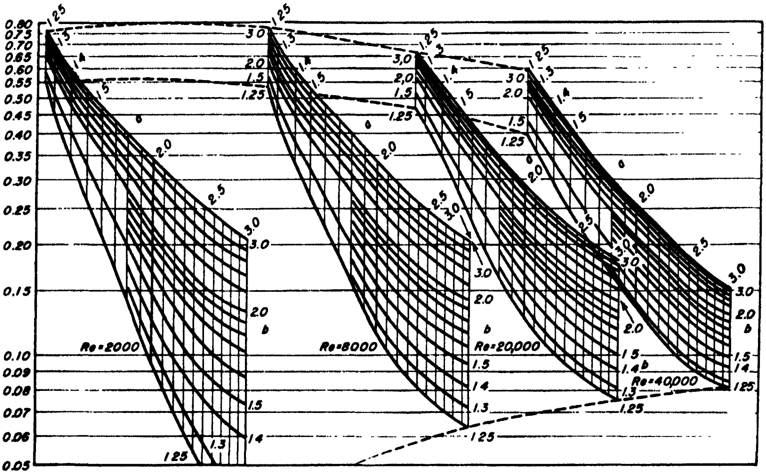

Fig. 78. Resistance coefficient for tube bundles—tubes in line. [*According to E. D. Grimison, Trans. ASME,* **59**, 583–594 (1937).]

The pressure loss $\Delta p$ in the flow through the bank is given by the equation

$$\Delta p = nf\gamma \frac{u^2}{2g} \tag{184}$$

in which $n$ is the number of rows in flow direction, $\gamma$ the specific weight of the air, and $u$ the average velocity between the tubes. The resistance coefficient $f$ can be taken from Figs. 78 and 79, according to Grimison. The property values must be again introduced at the temperature given by Eq. (159). The values in Figs. 78 and 79 hold true for 10 and more rows. Banks with a smaller number of rows have greater resistance coefficients. For example, a bank with four rows has a value greater by 8 per cent. For rough surfaces the heat transfer and the resistance are enlarged. With very rough surfaces increases up to 20 per cent were measured.

Tube bundles with flow in the direction of the tube axes can be calculated with Eq. (157). The hydraulic diameter which must be introduced here is

$$d_h = d\left(\frac{4ab}{\pi} - 1\right)$$

If different configurations of tube banks are to be compared with respect to the power necessary to effectuate the air flows through the tube banks, the dimensionless value $\Omega$ can be used as a basis for coolers on vehicles (airplanes, motorcars, locomotives, etc.). For such coolers a small frontal area is most important as the drag of the cooler is determined primarily by this area.

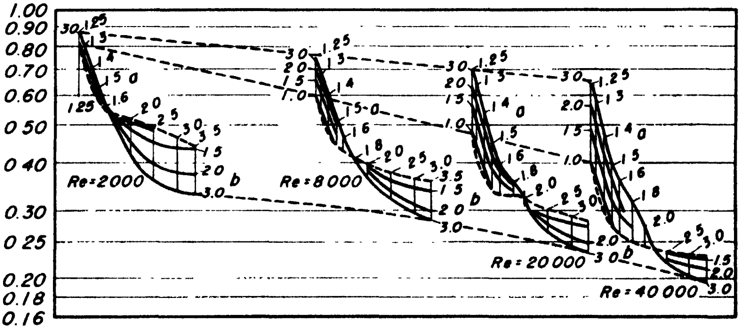

FIG. 79. Resistance coefficient for tube bundles—tubes staggered. [*According to E. D. Grimison, Trans. ASME*, **59**, 583–594 (1937).]

If such coolers with different configuration of the tubes are to have the same frontal area, the velocity $u_m$ between the tubes in the value $\Omega = \frac{W}{Q}\frac{gc_p(t_m - t_w)}{u_m^2}$ is fixed. Besides, a certain heat flow $Q$ is to be transferred at a given temperature difference $(t_m - t_w)$. Therefore, the power necessary per unit heat flow is proportional to the value $\Omega$. For banks of circular tubes in a gas flow normal to the tube axes this value lies between 1.5 and 10. Smaller tube spacings result in smaller values. Tubes in a gas flow parallel to their axes and tubes with streamlined cross section in crossflow have a value $\Omega \approx 1$. They are therefore better for such coolers.

For heat exchangers in stationary plants the magnitude of the heating surface is most important since the weight and price primarily depend upon it. Now the question is which configuration of the tubes transfers a certain heat flow with a given pressure loss and with the smallest heating surface. In this problem each configuration demands a different velocity depending on the heat-transfer coefficient. A calculation shows that tubes in crossflow are better than in flow parallel to the axis. The latter have a pressure loss three to 15 times greater when the heating surface area is the same. By spacing a given number of tubes closer together in the rows, thus decreasing the number of tube rows required, a given quantity of heat can be transferred with a reduction in the over-all pressure loss through the tube bundle. Therefore, it is advantageous to make the distance of the tubes in such a heat exchanger as small as the manufacturing and maintenance allow. There is almost no difference in pressure loss whether the arrangement of the tubes is in line or staggered. Only at small Reynolds numbers are staggered tubes somewhat better.

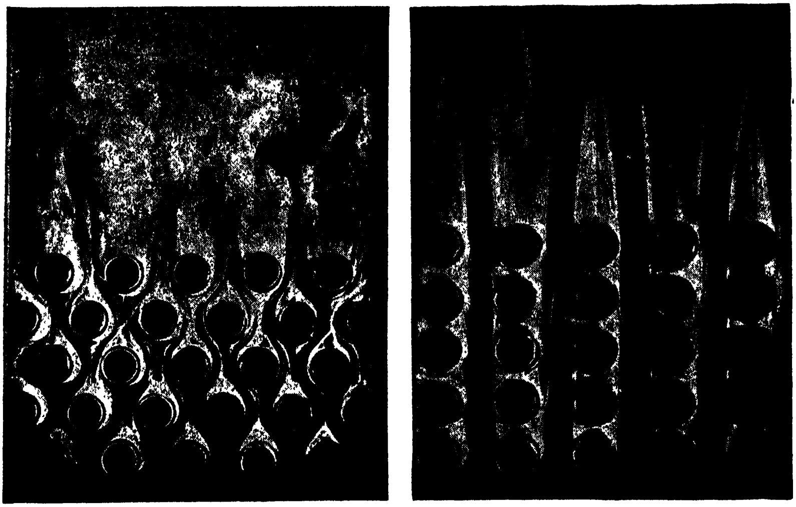

FIG. 80. FIG. 81.

FIGS. 80 and 81. Visualization of the flow through tube banks. [*According to H. Thoma, photograph from W. Lorisch, Mitt. Forschungsarb.* 322 (1929).]

Figures 80 and 81 show photographs of the flow through two tube banks; they were made according to a proposal of H. Thoma.[1] The porous surfaces of the tubes were wetted with hydrochloric acid and ammonia vapor was mixed with the air. Where this vapor mixes with the acid vapor, a white fog of sal ammoniac arises. In this way the boundary layers and the wakes can be seen in the photos. These are also the regions within which the air stream is cooled or heated from the tubes.

---

[1] H. Thoma, "Hochleistungskessel," Springer-Verlag, Berlin, 1921; also W. Lorisch, *Mitt. Forschungsarb.* 322 (1929).

**Example.** A bank of 4 rows (in line) in a steam boiler is traversed by combustion gases with a temperature of 1100 F and a 24-fps velocity. The steam pressure is 1,420 lb/in.$^2$ The tubes have a diameter of 2.4 in. and are arranged on the corners of squares with sides of length 4.8 in. The heat-transfer coefficient and the pressure loss are to be calculated.

The saturation temperature of water vapor at 1,420 lb/in.$^2$ is 588 F. Because of the large heat-transfer coefficient on the water side and the high thermal conductivity of the tube wall, the temperature on the outer surface of the tube is only slightly greater than the steam temperature. It may be assumed to be 600 F. The gas property values must be introduced at the temperature given by Eq. (159); therefore at

$$\frac{600 + 1{,}100}{2} = 850 \text{ F}$$

Since the property values of combustion gases deviate very little from the values for air, the calculations will be made with the latter. From the Appendix:

$$\nu = 79.6 \times 10^{-5} \text{ ft}^2/\text{sec} \qquad k = 0.0338 \text{ Btu/(hr)(ft)(F)}$$

This gives $Re = 24 \times (2.4/12)/79.6 \times 10^{-5} = 6{,}030$. The ratios $a$ and $b$ are $a = b = 2$. Therefore from Table 9, $C = 0.229$, $m = 0.632$, and Eq. (180) gives $Nu = 0.229 \times 6{,}030^{0.632} = 56.6$. The heat-transfer coefficient becomes

$$h = \frac{k}{d} Nu = \frac{0.0338 \times 12}{2.4} 56.6 = 9.58 \text{ Btu/(hr)(ft}^2\text{)(F)}$$

This value holds true for 10 and more tube rows. For four rows the heat-transfer coefficient is smaller by 12 per cent. Therefore

$$h = 8.55 \text{ Btu/(hr)(ft}^2\text{)(F)}$$

The pressure loss follows Eq. (184). The specific weight is best introduced at the gas temperature: $\gamma = 0.0244$ lb/ft$^3$. The resistance coefficient is from Fig. 78, $f = 0.225$. Therefore

$$\Delta p = 4 \times 0.225 \times 0.0244 \frac{24^2}{2 \times 32.2} = 0.196 \text{ lb/ft}^2$$

## 29. Heat transfer in gases at high velocities[1]

As soon as the velocities of a gas become comparable with the velocity of sound, the equations in the previous chapter are not immediately applicable for calculating heat transfer. The conditions in the flowing gas change so much that the property values can in no way be considered constant. This causes a new dimensionless value to appear in the dimensionless equations describing the flow and heat transfer, *i.e.*, the Mach number

$$Ma = \frac{V_0}{V_s}$$

the ratio of a reference velocity $V_0$ to the sound velocity $V_s$ in the gas at a reference point. The Mach number influences the flow pattern considerably as soon as it reaches values of 0.6 to 0.7. We must then expect that heat transfer is changed too.

There is yet another fact that influences the heat transfer. In the boundary layers the velocities are decreased by shearing stresses, that is, by inner frictional forces. The lost kinetic energy is transformed into heat and this *heat of dissipation* influences the temperature field in the boundary layer and therefore the heat transfer at high velocities, whereas this effect can be neglected at small velocities. Because of this skin friction, the temperature of a body in a high-velocity gas stream becomes higher than the gas temperature. Before discussing these things in detail we must premise some basic considerations.

The state in a gas stream is fixed by the velocity and by two state functions. The easiest to measure are the pressure and the temperature. It is useful to distinguish two states. The first is given by the pressure and temperature, which are measured with instruments moving along with the flowing gas. We call this state the *static state*, fixed by the static pressure $p_{st}$ and the static temperature $t_{st}$. The static pressure can be measured by a small hole in a wall parallel to the flow direction. The measurement of the static temperature is much more difficult. Up until now no simple instrument for measuring this value is known.

---

[1] A summarizing report on this subject was presented by H. A. Johnson and M. W. Rubesin in *Trans. ASME*, **71**, 447–456 (1949). As an introduction to the general laws of high-velocity flow see, for example, H. W. Liepmann and A. E. Puckett, "Introduction to Aerodynamics of a Compressible Fluid," John Wiley & Sons, Inc., New York, 1948.

The second state in a gas stream is the one which arises by isentropically decreasing the velocity to zero. We call this state the *total state.* It is fixed by the total pressure $p_T$ and the total temperature $t_T$. The total pressure is indicated by a pitot tube at subsonic velocities. At supersonic velocities the pitot tube indicates a lower pressure since a shock wave arises before the instrument, and the transformation of the kinetic energy to pressure in this shock wave is not isentropic. It is, however, easy to calculate the total pressure if the static pressure and the pressure indicated by the pitot tube are measured. The connection between the velocity $V$, the total pressure $p_T$, the absolute total temperature $T_T$, and the static pressure $p_{st}$ is given by the formula by D. S. Venant and Wantzel:[1]

$$V = 2g \frac{\kappa}{\kappa - 1} RT_T \left[ 1 - \left( \frac{p_{st}}{p_T} \right)^{\frac{\kappa - 1}{\kappa}} \right]$$

where $\kappa$ is the ratio of the specific heat at constant pressure and constant volume, and $R$ is the gas constant. The difference between total pressure and static pressure is called *dynamic pressure difference*

$$\Delta p_{dy} = p_T - p_{st}$$

Analogously, the difference between total temperature and static temperature may be called *dynamic temperature difference,* $\vartheta_{dy} = t_T - t_{st}$.

The connection between velocity, total temperature, and static temperature is represented by the first law of thermodynamics. If $i_T$ is the enthalpy in the total state and $i_{st}$ the enthalpy in static state, the first law of thermodynamics for a steady gas flow without addition or subtraction of heat and external work gives

$$i_T = i_{st} + \frac{V^2}{2g} \tag{185}$$

By expressing the enthalpy by the specific heat $c_p$ and the temperature we get

$$\vartheta_{dy} = t_T - t_{st} = \frac{V^2}{2gc_p} \tag{185a}$$

---

[1] D. S. Venant and Wantzel, *Journal de l'école polytechnique,* **116,** (1839).

For air the specific heat is

$$c_p = 0.24 \text{ Btu/(lb)(F)} = 187 \text{ ft-lb/(lb)(F)}$$

and the dynamic temperature increase in degrees F becomes

$$\vartheta_{dy} = \frac{V^2}{12{,}000}$$

if the velocity $V$ is introduced in feet per second. As Eq. (185) is derived from the first law of thermodynamics, it holds true not only for isentropic changes of the velocity but always when the velocity is diminished to zero without addition or subtraction of heat and without external work. In the boundary layers on surfaces the velocity is diminished by friction forces and its kinetic energy is transformed to heat. This process is connected, however, with exchange of heat and work between the different gas layers even when the solid surface does not exchange heat with the gas. Therefore the temperature of the gas layer immediately on the surface whose velocity is zero may be greater or smaller than the total temperature in the gas stream. The wall assumes the same temperature if it is not heated or cooled either by radiation or by heat flow through the surface into the interior of the wall. We call this temperature which an unheated wall in a gas stream assumes the *adiabatic wall temperature* $t_{ad}$ and denote the difference between this temperature and the static temperature $t_{st}$ in the gas stream by $\vartheta_{ad}$. This temperature difference follows the law

$$\vartheta_{ad} = \sigma \frac{V^2}{2gc_p} \tag{186}$$

The factor $\sigma$ was calculated by E. Pohlhausen[1] for a plate in longitudinal laminar flow with subsonic velocities. His results can be expressed by the equation $\sigma = \sqrt{Pr}$ for Prandtl numbers smaller than 10. L. Crocco[2] extended the calculation to high Mach numbers and found that the equation holds true also for supersonic velocities. For air with $Pr = 0.72$ the equation gives $\sigma = 0.84$. E. Eckert and W. Weise[3] measured the value $\sigma$ for

[1] E. Pohlhausen, *Z. angew. Math. Mech.* **1,** 115–121 (1921).

[2] L. Crocco, *Publ. dell instituto per le applicat on del calcolo consigtio maisonale delle richerche,* No. 120, Roma, 1942.

[3] E. Eckert and W. Weise, *Forsch. Gebiete Ingenieurw.,* **13,** 246–254 (1942).

subsonic velocities and flow along a cylinder (Fig. 82). For laminar boundary layers the calculated value $\sigma = 0.84$ was confirmed. In the turbulent boundary layer the $\sigma$ value increases with the Reynolds number up to approximately 0.90. These values were confirmed also by experiments at supersonic velocities. For other bodies however the results of experiments do not yet agree so well. At the stagnation point, the total temperature is reached as long as temperature equalization within the body by conduction is negligible. Approximately the same values can be expected in a tube as on the plate.

For temperature measurements in high-velocity gas streams two instruments proved suitable, the cylinder thermometer[1] (Fig. 83) and the diffuser thermometer[2] (Fig. 84). The cylinder thermometer measures the surface temperature on a cylinder in longitudinal flow. Since the boundary-layer thickness is small compared with the cylinder diameter the $\sigma$ values for the flat plate (Fig. 82) can be used and the static temperature calculated from Eq. (186) when the velocity is known. The diffuser thermometer (Fig. 84) measures the total temperature. The gas enters the diffuser through the opening $b$ and is decelerated in the tube $a$. The temperature of the gas is measured by the thermocouple $d$. Afterwards the gas escapes by the small holes $c$. If the holes were not present, the gas in the interior would cool off and would indicate an erroneous temperature. The static temperature can be calculated with Eq. (185$a$) where the

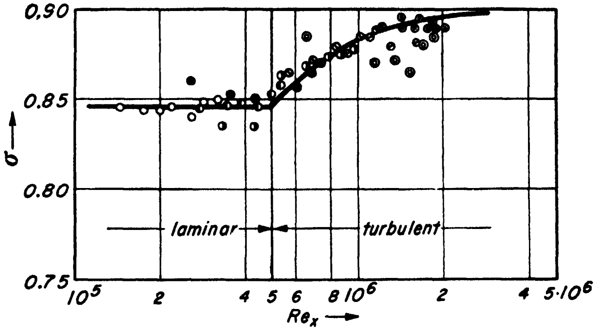

FIG. 82. Recovery factor $\sigma$ for flow along a cylinder. [*According to E. Eckert and W. Weise, Forsch. Gebiete Ingenieurw.*, **13**, 246–254 (1942).]

---

[1] E. Eckert, *Z. Ver. deut. Ing.*, **84**, 813–817 (1940).

[2] A. Franz, *Jahrb.* 1938 *deut. Luftfahrt-Forsch.*, **II**, pp. 215–218.

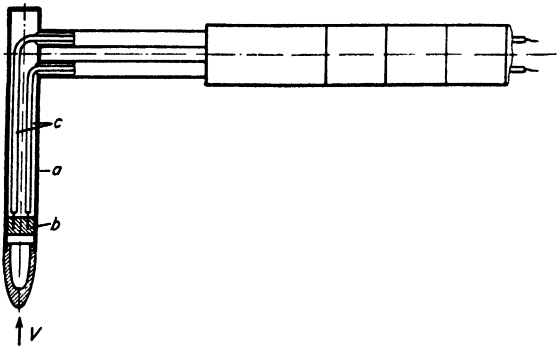

FIG. 83. Cylinder thermometer. [*From E. Eckert, Z. Ver. deut. Ing.*, **84,** 813 817 (1940).]

(*a*) Thin-walled tube; (*b*) copper bar; (*c*) thermocouples.

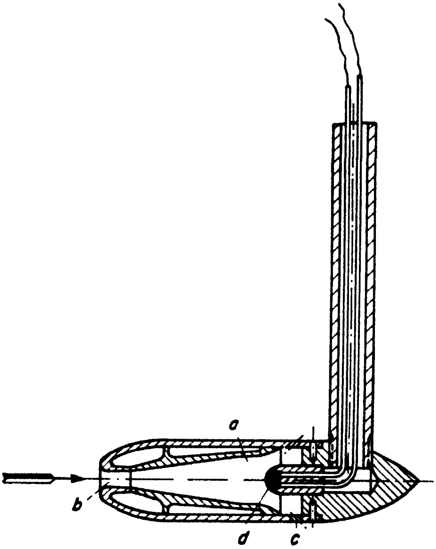

FIG. 84. Diffuser thermometer. (*From A. Franz, Jahrb.* 1938 *deut. Luftfahrt-Forsch. II, pp.* 215–218.)

velocity in the gas stream is known. Both thermometers have their field of application. The advantage of the diffuser thermometer is that it measures immediately the total temperature. On the other hand the cylinder thermometer can be made in very small dimensions and follows changes in gas temperature very rapidly.

As soon as the surface temperature of a body deviates from its adiabatic wall temperature, heat transfer arises between the body and the flowing gas. The temperature profiles in the boundary layer for heat transfer to and from the wall are shown in Fig. 85. The horizontal tangent of curve *a* on the wall shows that no heat exchange occurs between the gas and the wall. The static temperature, which has the value $t_s$ in the outside flow, rises within the boundary layer and on this curve reaches the adiabatic wall temperature $t_{ad}$ at the wall. As soon as the wall temperature is lower heat flows from the gas into the wall. This holds for the temperature profiles below curve *a* in Fig. 85. At wall temperatures higher than the adiabatic, the heat flows in the opposite direction from the wall to the gas. The heat flow *q* per unit surface area must be calculated with the equation

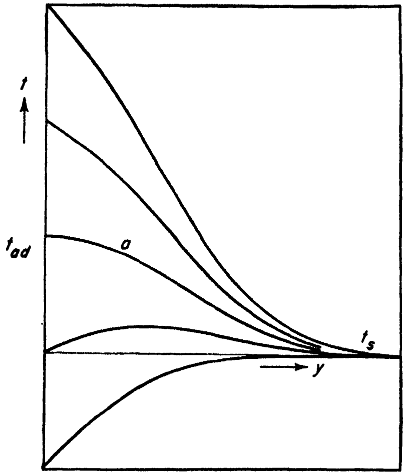

FIG. 85. Temperature profiles in the laminar boundary layer of a heated or cooled plate in a high-velocity gas stream.

$$\mathbf{q} = \mathbf{h}(\mathbf{t}_w - \mathbf{t}_{ad}) \qquad (187)$$

that is, with the difference between the real surface temperature and that temperature which the surface would assume in the gas stream without heat transfer. For the plane plate in longitudinal flow with laminar boundary layer, E. Eckert and O. Drewitz[1] showed that the heat-transfer coefficient $h$ for subsonic velocities is independent of the Mach number and can be calculated with the equation presented in Sec. 20 for low velocities. Also, for supersonic velocities and turbulent flow the influence of the Mach number is small. Figure 86 shows a comparison between the values calculated with the formulas for low velocities and the results of experiments on a flying V-2 rocket by Fischer and Norris.[1] The measurements were made on different places of the conical head of the missile. The different symbols distinguish these places. The lower line represents the heat-transfer values as expected from the formulas for low velocities with laminar boundary layer. On the cone they are greater by the factor $\sqrt{3}$ than on the plane plate because the surface increases in downstream direction and the boundary layer therefore does not grow so fast. The higher line holds for heat transfer with turbulent boundary layer as calculated with the formulas for small velocities [considering Eq. (187)]. It can be seen that the measured points follow the laminar line for small Reynolds numbers and with increasing Reynolds number change over to the turbulent line. The transition depends obviously on some characteristic value other than the Reynolds number. Johnson and Rubesin[2] showed by an analysis of values calculated by dif-

---

[1] E. Eckert and O. Drewitz, *Forsch. Gebiete Ingenieurw.*, **11**, 116–124 (1940).

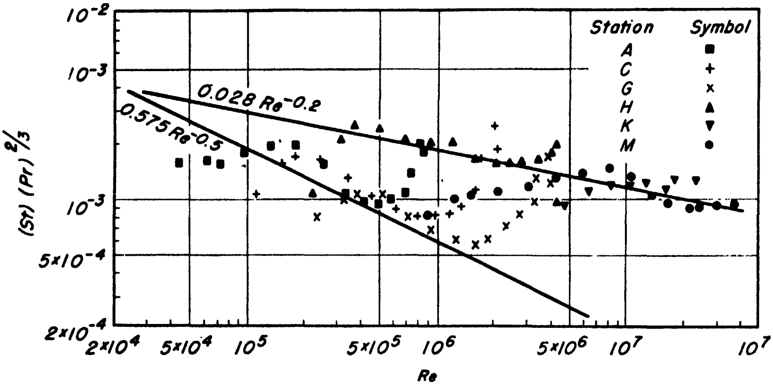

FIG. 86. Comparison between calculated and measured film heat-transfer coefficients for high-velocity flow. [*From W. Fischer and R. H. Norris, Trans. ASME*, **71**, 457–469 (1949).]

---

[1] W. W. Fischer and R. H. Norris, *Trans. ASME*, **71**, 457–469 (1949).

[2] See page 94.

ferent authors for laminar boundary-layer flow on a flat plate that the reference temperature $t^\star$ for the property values in the heat-transfer equations is given by

$$t^\star - t_s = 0.58(t_w - t_s) + 0.17(t_{ad} - t_s)$$

This reference temperature was used in the preparation of Fig. 86. For streamlined bodies the heat-transfer coefficient calculated with the formulas for low velocities can be used in the same way as for the plate for subsonic and supersonic velocities. The need to explore the field of heat transfer at high velocities is of a comparatively recent origin. In the Velox steam boiler the heating surface was considerably decreased, by using gas velocities of some hundred feet per second. The development of the gas turbine brought up cooling problems for the turbine blades and for other parts washed with fast-flowing gases. Modern airplanes approaching or exceeding the speed of sound are heated by the aerodynamic heating effect to such a degree that cooling has to be provided for the cabin and sometimes for the structural parts. The cooling of rockets and missiles becomes critical at low altitudes. At very high altitudes where the density of the air is exceedingly small the heat transfer from the heated boundary layer to the rocket wall is decreased because of this fact and is partially compensated for by radiation of heat to the universe. An example in the next chapter will deal with these conditions.

A problem very similar to those mentioned in the above paragraph is the cooling of the oil film in bearings running at high velocity.

**Example.** A plate $x = 4$ in. long is suspended in an air flow with $u_s = 400$ mph $= 586$ fps. The temperature of the plate is $t_w = 196$ F, the air temperature $t_s = 79$ F, its pressure 14.2 lb/in.$^2$ The heat transfer from the plate to the air is to be calculated.

First we must determine the adiabatic wall temperature of the plate in the air stream. The Reynolds number is

$$Re = \frac{u_s x}{\nu} = \frac{586 \times (4/12)}{21.2 \times 10^{-5}} = 9.22 \times 10^5$$

From Fig. 82 take $\sigma = 0.88$. Equation (186) gives

$$t_{ad} = 79 + 0.88 \times \frac{586^2}{12{,}000} = 79 + 25.2 = 104.2 \text{ F}$$

This is the temperature the plate assumes if it is not heated. The heat-transfer coefficient can be calculated with Eq. (160). The local value is $h = 71.6$ Btu/(hr)(ft$^2$)(F). The average value is

$$\bar{h} = 1.25h = 89.5 \text{ Btu/(hr)(ft}^2\text{)(F)}$$

The heat flow per unit area is, by Eq. (187),

$$q = 89.5(196 - 104.2) = 8200 \text{ Btu/ft}^2$$

The values assumed for this calculation correspond approximately to those of a fast airplane flying near the ground. The cabin of such an airplane assumes without cooling a temperature of approximately 104.2 F when the air temperature is 79 F.

## FREE CONVECTION

### 30. Vertical plate and horizontal tube

Free-convection flow which is caused by temperature differences only in a gas or liquid also builds boundary layers on the surfaces of solid bodies. Because of the low velocities encountered, the thicknesses of these boundary layers are greater than those in the examples treated up to now. ✓The boundary-layer equations for momentum and heat flow can be used again to calculate the heat transfer in free convection. In this chapter there may be solved the simplest problem, namely, that of the vertical plate.[1] If such a plate is heated, the gas or liquid in its immediate neighborhood experiences an increase in its temperature by heat transfer from the plate and begins to flow in an upward direction. In this way a boundary layer arises with the thickness zero at the lower edge and with an increasing thickness in the upward direction. The distance along the surface from the lower edge may be called $x$, the distance from the plate surface $y$. Within the boundary layer, the temperature decreases from the value on the plate surface to the uniform value which the gas or liquid has outside the heated region. The temperature of the plate may be constant over the whole surface and steady. The difference between this value and the temperature outside the boundary layer is designated as $\Theta$. The difference between the

[1] **An analogous calculation for gases was made by Squire in S. Goldstein, "Modern Developments in Fluid Dynamics," Oxford University Press, New York, 1938.**

temperature at any point within the boundary layer and the temperature outside it may be $\vartheta$. The temperature field in the neighborhood of the plate must have the shape sketched in Fig. 87. In the figure, $\delta$ is the boundary-layer thickness. The velocity $u$ must be zero on the plate surface and outside the boundary layer. Therefore, the velocity field must have the shape sketched in Fig. 87. To solve the boundary-layer equation the temperature profile is approximated by a parabola

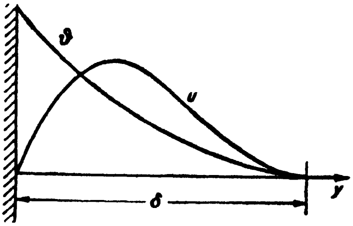

FIG. 87. Temperature and velocity profile in free-convection flow on a vertical wall.

$$\vartheta = \Theta\left(1 - \frac{y}{\delta}\right)^2 \tag{188}$$

This equation already fulfills the boundary conditions $\vartheta = \Theta$ for $y = 0$ and $\vartheta = 0$ for $y = \delta$. A velocity profile similar to the one shown in Fig. 87 is represented by the equation

$$u = u_1 \frac{y}{\delta}\left(1 - \frac{y}{\delta}\right)^2 \tag{188a}$$

The maximum value of the velocity $u$ arises, according to this equation, at the distance $y = \delta/3$ from the wall. Its value is $u_{max} = (4/27)u_1$. The boundary-layer thickness is assumed to be the same for the temperature and the velocity. This assumption has its justification in that the results of the calculation performed with it agree quite well with experimental results.[1] On the other hand it is to be expected from what we learned about the boundary layers for laminar forced convection that at high Prandtl numbers the velocity boundary layer is thicker than the temperature boundary layer. Probably the inner part of the velocity profile from the value zero at the wall to the maximum changes little with the Prandtl number in its relation to the temperature profile, since the driving force for the flow lies in the temperature differences and only the outer part of the velocity profile from the maximum on becomes thicker for viscous fluids (high Prandtl numbers).

---

[1] Y. S. Touloukian, G. A. Hawkins, and M. Jacob, *Trans. ASME*, **70**, 13 (1948).

The momentum equation (111) must be expanded by a summand which expresses the buoyancy force. This force is $\gamma\beta\vartheta$ per unit volume of a small particle (see page 137). There acts on a volume element of height $dx$ and length $l$ (greater than the boundary-layer thickness, Fig. 50) the force $dx\,\gamma\beta \int_0^l \vartheta\, dy$. If this summand is added to Eq. (111) and it is considered that at the small velocities connected with free convection, the pressure may be assumed as constant and that the velocity $u$ outside the boundary layer is here zero, there is obtained

$$\frac{d}{dx}\int_0^l u^2\,dy = g\beta\int_0^l \vartheta\,dy - \nu\left(\frac{du}{dy}\right)_w \tag{189}$$

The heat-flow equation (135) remains in its old form

$$\frac{d}{dx}\int_0^l u\vartheta\,dy = -\alpha\left(\frac{d\vartheta}{dy}\right)_w \tag{189a}$$

The temperatures are replaced here by the temperature difference $\vartheta$. The integrals in Eqs. (189) and (189a) may be solved by introducing the temperature and velocity profiles (188) and (188a).

$$\int_0^l u^2\,dy = \frac{u_1{}^2\delta}{105} \qquad \int_0^l \vartheta\,dy = \frac{\Theta\delta}{3} \qquad \int_0^l \vartheta u\,dy = \frac{1}{30}u_1\Theta\delta$$

Now the boundary-layer equations assume the form

$$\frac{1}{105}\frac{d}{dx}(u_1{}^2\delta) = \frac{1}{3}g\beta\Theta\delta - \nu\frac{u_1}{\delta}$$

$$\frac{1}{30}\Theta\frac{d}{dx}(u_1\delta) = 2\alpha\frac{\Theta}{\delta}$$

To solve these equations let us try $u_1$ and $\delta$ as exponential functions of $x$:

$$u_1 = C_1x^m \qquad \delta = C_2x^n$$

Introducing these expressions we get

$$\frac{2m+n}{105}C_1{}^2C_2x^{2m+n-1} = g\beta\Theta\frac{C_2}{3}x^n - \frac{C_1}{C_2}\nu x^{m-n}$$

$$\frac{m+n}{30}C_1C_2x^{m+n-1} = \frac{2\alpha}{C_2}x^{-n}$$

Since these equations must be valid for any value $x$, the exponents must have the same value for every summand:

$$2m + n - 1 = n = m - n$$
$$m + n - 1 = -n$$

This gives

$$m = \tfrac{1}{2} \qquad \text{and} \qquad n = \tfrac{1}{4}$$

Introducing these values into the above equation gives

$$\frac{C_1{}^2C_2}{84} = g\beta\Theta\frac{C_2}{3} - \frac{C_1}{C_2}\nu$$
$$\frac{C_1C_2}{40} = \frac{2\alpha}{C_2}$$

or

$$C_1 = 5.17\nu\left(\frac{20}{21} + \frac{\nu}{\alpha}\right)^{-\frac{1}{2}}\left(\frac{g\beta\Theta}{\nu^2}\right)^{\frac{1}{2}}$$
$$C_2 = 3.93\left(\frac{20}{21} + \frac{\nu}{\alpha}\right)^{\frac{1}{4}}\left(\frac{g\beta\Theta}{\nu^2}\right)^{-\frac{1}{4}}\left(\frac{\nu}{\alpha}\right)^{-\frac{1}{2}}$$

Now the maximum velocity within the boundary layer is

$$u_{max} = \frac{4}{27}u_1 = 0.766\nu\left(0.952 + \frac{\nu}{\alpha}\right)^{-\frac{1}{2}}\left(\frac{g\beta\Theta}{\nu^2}\right)^{\frac{1}{2}}x^{\frac{1}{2}} \qquad (189b)$$

and the boundary-layer thickness

$$\delta = 3.93\left(\frac{\nu}{\alpha}\right)^{-\frac{1}{2}}\left(0.952 + \frac{\nu}{\alpha}\right)^{\frac{1}{4}}\left(\frac{g\beta\Theta}{\nu^2}\right)^{-\frac{1}{4}}x^{\frac{1}{4}} \qquad (190)$$

Again it is useful to make the boundary-layer thickness dimensionless by dividing it by the distance $x$ from the lower edge of the plate. In this equation there appears the Grashof number $Gr_x = g\beta\Theta x^3/\nu^2$ built up with the temperature difference between the plate and gas or liquid and the distance $x$, [(Eq. (174)], and the Prandtl number, $Pr = \nu/\alpha$:

$$\frac{\delta}{x} = 3.93Pr^{-\frac{1}{2}}(0.952 + Pr)^{\frac{1}{4}}(Gr_x)^{-\frac{1}{4}} \qquad (191)$$

The specific heat flow from the plate surface is represented by the equation

$$q = -k\left(\frac{d\vartheta}{dy}\right)_0$$

From Eq. (188) if the minus sign is neglected there is obtained

$$q = \frac{2k\Theta}{\delta}$$

On the other hand for the specific heat flow there is the equation by which the film heat-transfer coefficient is defined:

$$q = h\Theta$$

Therefore

$$h = \frac{2k}{\delta} \tag{192}$$

and in dimensionless form

$$\frac{hx}{k} = Nu_x = 2\frac{x}{\delta}$$

By introducing the boundary-layer thickness there is obtained

$$\mathbf{Nu}_x = \mathbf{0.508Pr}^{1/2}(\mathbf{0.952} + \mathbf{Pr})^{-1/4}(\mathbf{Gr}_x)^{1/4} \tag{193}$$

The local film heat-transfer coefficient decreases according to Eqs. (190) and (192) with increasing distance $x$. It is inversely proportional to the fourth root of $x$. By integration over the distance the average heat-transfer coefficient is found:

$$\bar{h} = \tfrac{4}{3}h$$

This means that the average heat-transfer coefficient of a vertical plate with a height $x$ is $\tfrac{4}{3}$ the local value at the point $x$. For ideal gases the relationship $\beta = 1/T$ holds true (page 137). As long as the temperature differences are small there can be written $\beta = 1/T_0$, where $T_0$ is the absolute temperature in the gas outside the boundary layer. For air with a Prandtl number $Pr = 0.714$,

$$Nu = 0.378(Gr_x)^{1/4} \tag{194}$$

For this medium the heat transfer was calculated exactly by E. Pohlhausen in collaboration with E. Schmidt and W. Beckmann.[1] This resulted in a numerical value of 0.360 instead of 0.378 as in Eq. (194). The approximate treatment agrees therefore quite well with the much longer exact calculation. A comparison between the values calculated here and those measured and calculated by E. Schmidt and W. Beckmann[1] is presented in Figs. 88 and 89. In the calculations, the property values were introduced

---

[1] E. Schmidt and W. Beckmann, *Tech. Mech. u. Thermodynam.*, **1**, 1–24 (1930).

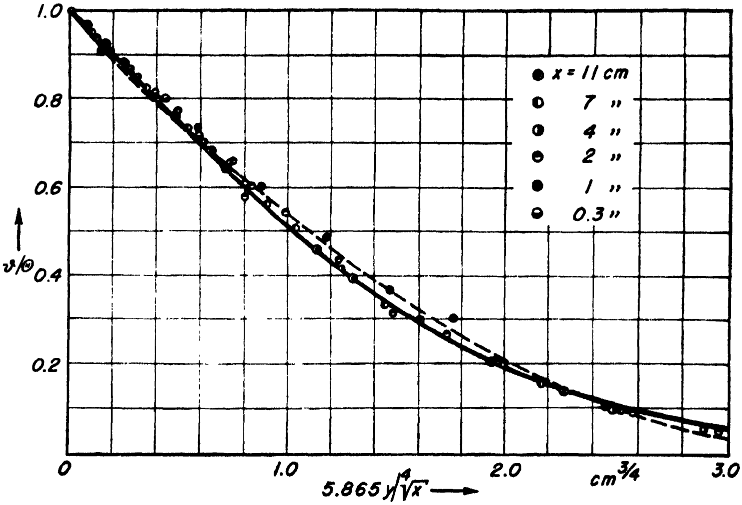

FIG. 88. Comparison between the measured and calculated temperature profile in free-convection flow on a vertical plate. (*Measured values according to E. Schmidt and W. Beckmann, solid-line exact solution by E. Schmidt and E. Pohlhausen, dashed-line approximate solution according to Squire.*)

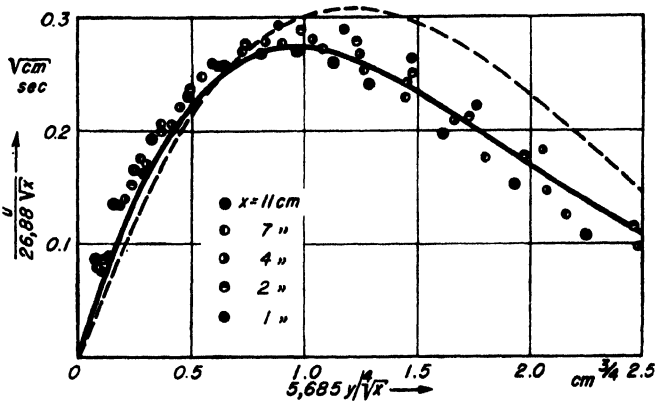

FIG. 89. Comparison between the measured and calculated velocity profile in free-convection flow on a vertical plate. (*Measured values according to E. Schmidt and W. Beckmann, solid-line exact solution by E. Schmidt and E. Pohlhausen, dashed-line approximate solution according to Squire.*)

at the plate temperature. A. Saunders[1] made experiments with air, water, and mercury. These measurements also prove Eq. (193). The agreement with this equation is slightly better than with the formula $Nu = C(Pr\,Gr)^{1/4}$, which is mostly used and which was derived by a generalization of the experiments with air on the assumption that the velocities are so small that the inertia forces may be neglected (page 138).

Beside the vertical wall the horizontal tube is important for industrial applications. The boundary-layer equations were solved for this problem by R. Hermann.[2] The solutions agree well with the experimental results found by K. Jodlbauer.[3] The result can be summarized in the following way: the average film heat-transfer coefficient on a circular tube with the diameter $d$ has the same value as the average film heat-transfer coefficient on a vertical wall with the height $2.5d$ (see Fig. 90).

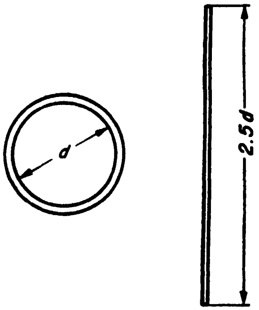

FIG. 90. Horizontal tube and vertical plate with equal average film heat-transfer coefficient in free convection.

For thin wires, the assumption that the boundary-layer thickness is small compared with the diameter does not hold true. The boundary-layer calculations of R. Hermann are based on this assumption, however. To take into account this fact we will follow an idea first developed by Langmuir[4] and taken up by Rice.[5] We idealize the boundary layer as a stationary cylindrical air layer around the wire through which the heat given off by the wire must flow by conduction. Equations (34) and (35), therefore, determine this heat flow, with $r_i$ equal to the radius of the wire (in this paragraph the diameter $d = 2r_i$ is used), $t_{wi}$ the wire temperature, and $t_{wa}$ the outside air temperature. On the other hand the definition equation

$$Q = \bar{h}2\pi r_i l(t_{wi} - t_{wa})$$

holds. Equating this expression with Eq. (34) gives

---

[1] A. Saunders, *Proc. Roy. Soc.* (*London*), **A172**, No. 948, 55–71 (1939).

[2] R. Hermann, *Z. angew. Math. Mech.*, **13**, 433 (1933).

[3] K. Jodlbauer, *Forsch. Gebiete Ingenieurw.*, **4**, 157 (1933).

[4] I. Langmuir, *Phys. Rev.*, **34**, 401 (1912).

[5] C. W. Rice, *Trans. AIEE*, **42**, 653 (1923).

$$\bar{h} = k_m \frac{r_m}{r_i} \frac{1}{r_a - r_i}$$

Considering Eq. (35) leads to

$$\overline{Nu}_d = \frac{\bar{h}d}{k_m} = 2\frac{r_m}{r_a - r_i} = \frac{2}{\ln (r_a/r_i)} = \frac{2}{\ln (1 + 2b/d)}$$

where $b = r_a - r_i$ is the thickness of the idealized boundary layer. This thickness is so determined that for a boundary layer whose thickness is small as compared with the wire diameter the equation transforms into an expression derived from Eq. (194). By changing to the average film heat-transfer coefficient and introducing the diameter ($d = 2.5x$) we get

$$\overline{Nu}_d = 0.400(Gr_d)^{1/4}$$

For small values of $b/d$ the denominator $\ln (1 + 2b/d)$ transforms to $2b/d$ and therefore $\overline{Nu}_d$ into $d/b$. Therefore $d/b = 0.400(Gr_d)^{1/4}$ and introducing this into the above equation gives

$$\overline{Nu}_d = \frac{2}{\ln \left(1 + \dfrac{2}{0.400(Gr_d)^{1/4}}\right)}$$

This equation gives excellent agreement with experimental results.

The dimensions of the boundary layer and the temperature field can be readily observed in schlieren or interference photographs. A schlieren method which can be realized by very simple means was described by E. Schmidt.[1] An example of this method is shown in the photograph (Fig. 91), demonstrating free convection on a horizontal cylinder. A light source arranged at a great distance from the heated cylinder so that its light rays are parallel to the cylinder axis produces on a screen, without other means, the picture shown in Fig. 91. A light ray in passing through a field with a density gradient normal to its direction is bent through a certain angle. Therefore, the light rays which traverse the heated boundary layer are deflected away from the cylinder, and the dark zone surrounding the contour in Fig. 91 indicates the boundary layer. It was shown by E. Schmidt that the distance of the heart-shaped bright line from the cylinder contour is proportional to the heat-transfer coefficient. The principle of an interferometer according to Zehnder-Mach[1] is shown in Fig. 92. Light from a monochromatic source *A* is made parallel by a condensing lens *B*. It then falls on a plane glass plate *c* whose surface is coated in such a way that half the light is reflected, the other half transmitted. The reflected part strikes the mirror *D*, is reflected by it and falls on the glass plate *F*, which is coated in the same way as plate *C*. That part of the light which is trans-

---

[1] E. Schmidt, *Forsch. Gebiete Ingenieurw.*, **3**, 181–189 (1932).

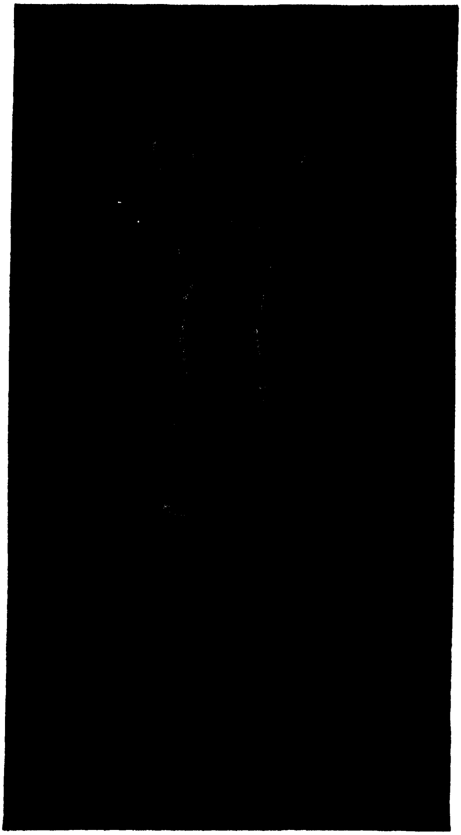

FIG. 91. Visualization of the boundary layer and film heat-transfer coefficient around a horizontal tube in free-convection flow by a schlieren photograph. [*From E. Schmidt, Forsch. Gebiete Ingenieurw.*, **3**, 81–89 (1932).]

---

[1] H. Schardin, *Z. Instrumentenk.*, **53**, 396–403, 424–436 (1933).

mitted through this plate is united with the second light beam which is transmitted through plate $C$ and reflected by mirror $E$ and plate $F$. If the four plates $C$, $D$, $E$, $F$ are exactly parallel to each other all light rays in the two beams have the same path length. On a screen $G$ there can then be observed a dark or a bright field depending on whether the path lengths of the two beams vary by half a wave length or an odd multiple of it thus extinguishing each other, or by a full wave length or a multiple thus augmenting each other.

If a heated body, *e.g.*, a cylinder $H$, is placed in one of the light beams, the temperature and therefore the density of the air are changed in the neighborhood of the body. Since the wave length of light varies with density, there are now rays in the two beams which differ by one or more full wave lengths and others which differ by an odd number of half wave lengths. As a consequence of this there can now be observed on the screen $G$ a field of dark and bright bands around the shadow of cylinder $H$. The sharpness of this shadow can be improved if a lens is placed between

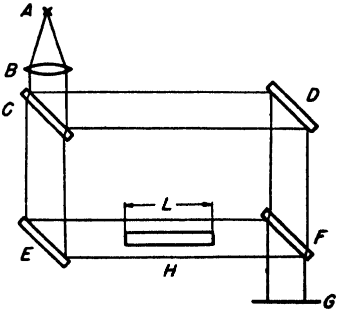

**FIG. 92.** Principle sketch of an interferometer according to Zehnder-Mach.

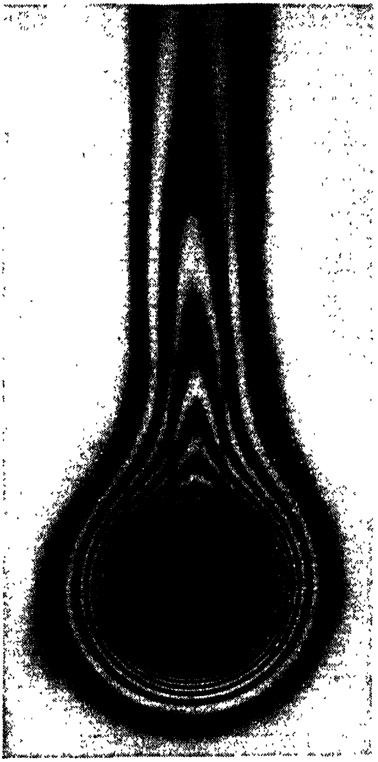

**FIG. 93.** Isotherms around a horizontal tube in free-convection flow as revealed by an interference photograph. (*Photograph by E. Eckert and E. Soehngen.*)

plate *F* and the screen, which depicts the central plane of the cylinder on the plane in which the screen *G* is located. Figures 93 and 94 show photographs made in this way. Figure 93 represents the free convection around a horizontal tube and Fig. 94 free convection along a vertical plane. The dark interference bands are lines of constant air density, and as the pressure can be assumed constant these lines are isotherms. The temperature difference between any two successive bands can be easily calculated from the length of the cylinder or plate in light-ray direction and the data of the interferometer. From the photograph the temperature gradient in the air along the surface and therefore the heat-transfer coefficient can be determined. As the boundary-layer thickness is also seen this method is very useful for investigating heat-transfer problems. The interferometer

FIG. 94. Isotherms around a vertical plate in free-convection flow as revealed by an interference photograph. (*Photograph by E. Eckert and E. Soehngen.*)

was first described by Zehnder and Mach. It was used for aerodynamic studies by T. Zobel.[1] Studies in heat transfer were made by R. B. Kennard[2] and E. Eckert and E. Soehngen.[3]

In the examples considered so far the boundary layers were always laminar. The boundary layers which arise by free convection also change to turbulent flow when they have reached a certain thickness. In air the change occurs at a critical Grashof number around $Gr = 10^9$. This corresponds to a Reynolds number, $Re_{cr} = u_{max}\delta/\nu = 550$. The transition therefore takes place at a lower Reynolds number in free convection than in forced convection. Figure 95 is an interference photograph of a heated vertical plate of sufficient length to produce a turbulent boundary layer (3 ft). The interference lines represent again isotherms, the figures indicate the distance from the lower plate end in inches. It can be seen that the flow is smooth and laminar near the lower end. At some distance, however, waves of long wave lengths start, since the boundary-layer flow becomes unstable against transverse oscillations at a certain boundary-layer thickness. These waves increase their amplitude in the downstream direction, become irregular, roll up into vortices, and break up into a coarse turbulence. The region shown in the photograph comprises only the first part of the transition zone to turbulent flow. It gives a very clear impression of the beginning of turbulence. It can be shown experimentally that even strong disturbances do not influence the laminar flow near the lower plate end but start waves at some distance from it. The fluctuations are felt through the whole boundary layer up to the plate surface and cause the heat transfer to fluctuate periodically with time.[4]

The heat transfer in turbulent free-convection flow is, according to A. Saunders,[5] represented by the equation derived from experiments:

$$Nu_x = C(Pr\,Gr)^{1/3} \tag{195}$$

---

[1] T. Zobel, *Z. Ver. deut. Ing.*, **81**, 503 (1937).

[2] R. B. Kennard, *Bur. Standards J. Research*, **8**, 787 (1932).

[3] E. Eckert and E. Soehngen, *USAF Tech. Rept.* 5747, 1949, Wright Patterson Air Force Base, Dayton, Ohio.

[4] E. Eckert, Heat Transfer and Fluid Mechanics Institute, Berkeley, Calif., 1949, published by ASME.

[5] A. Saunders, *Proc. Roy. Soc.* (*London*), **A157**, 278–291 (1936).

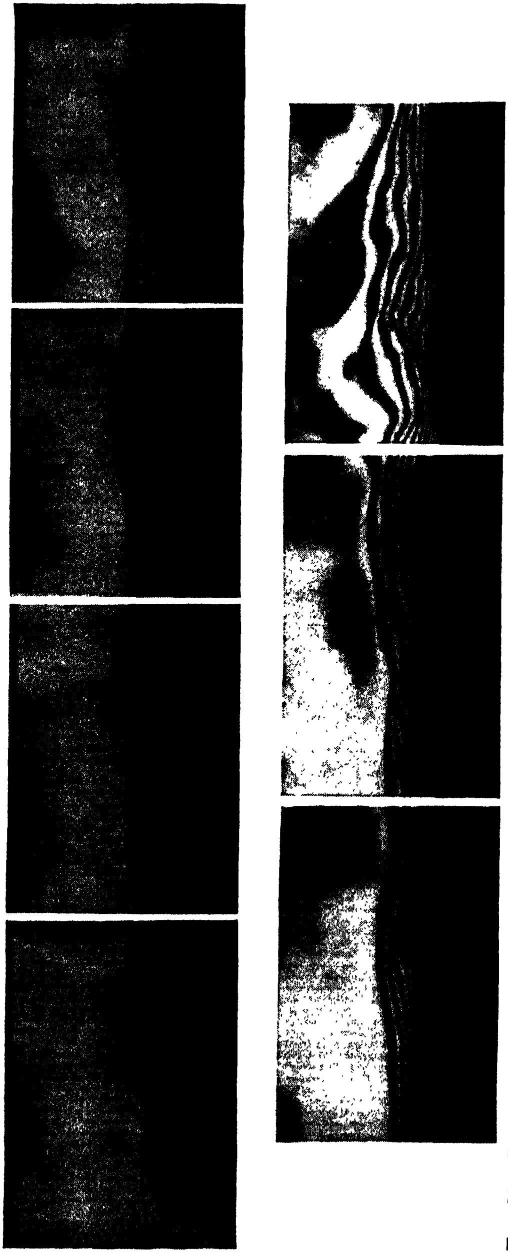

FIG. 95. Laminar and turbulent free-convection flow on a vertical plate revealed by interference photographs. Numbers give distance from the lower plate end in inches. (*Photograph by E. Eckert and E. Soehngen.*)

The constant $C$ has the value 0.10 for air and 0.17 for water. In industrial heat exchangers utilizing free convection, the boundary layers are usually laminar.

**Example.** A vertical wall is heated from one side by steam to a temperature of 200 F. On the other side is air at 14.5 lb/in.² pressure and 68 F temperature. The local heat-transfer coefficient for free convection at a distance of 8 in. from the lower edge is to be calculated.

The experiments of E. Schmidt and W. Beckmann[1] showed that the property values are introduced most advantageously at the surface temperature. From the Appendix:

$$\nu = 25.1 \times 10^{-5} \text{ ft}^2\text{/sec}, \; k = 0.0186 \text{ Btu/(hr)(ft)(F)}, \; Pr = 0.690$$

The expansion coefficient is $\beta = 1/T_0 = 1/528$ 1/deg R). Therefore

$$Gr = \frac{g\beta\Theta x^3}{\nu^2} = \frac{32.2 \times 132 \times (8/12)^3}{528 \times 25.1^2 \times 10^{-10}} = 37.8 \times 10^6$$

The boundary layer therefore is laminar. Equation (191) gives

$$\frac{\delta}{x} = 3.93 \frac{1}{0.690^{1/2}} (0.952 + 0.690)^{1/4} \times 37.8^{-1/4} \times 10^{-6/4} = 0.0682$$

The boundary-layer thickness is $\delta = 0.545$ in. The film heat-transfer coefficient is, according to Eq. (192),

$$h = 2\frac{k}{\delta} = 2\,\frac{0.0186 \times 12}{0.545} = 0.82 \qquad \text{Btu/(hr)(ft}^2\text{)(F)}$$

The average heat-transfer coefficient over the length of 8 in. is

$$h_m = \tfrac{4}{3}h = 1.09 \text{ Btu/(hr)(ft}^2\text{)(F)}$$

The average heat-transfer coefficient on a horizontal tube with a diameter $d = 8/2.5 = 3.2$ in. has the same value. The maximum velocity within the boundary layer at a distance 8 in. from the bottom edge can be derived from Eq. (189*b*). By introducing the Grashof number, this equation becomes

$$u_{max} = 0.766\,\frac{\nu}{x}\,(0.952 + Pr)^{-1/2}(Gr)^{1/2}$$

$$= 0.766\,\frac{25.1 \times 10^{-5}}{8/12}\,(0.952 + 0.690)^{-1/2} \times 37.8^{1/2} \times 10^{6/2} = 1.38 \text{ ft/sec}$$

As a consequence of the low velocity, small additional air velocities increase the heat transfer considerably. This fact must be kept in mind when considering industrial applications.

---

[1] E. Schmidt and W. Beckmann, *Tech. Mech. u. Thermodynam.*, **1,** 1–24 (1930).

## CONDENSATION AND EVAPORATION

### 31. Condensation

If vapor is contained in a vessel whose walls have a temperature lower than the saturation temperature, the vapor condenses on the wall. The heat liberated by this process must be led away through the walls. The heat transfer connected with this process was calculated in 1916 by W. Nusselt[1] by his liquid-film theory. Nusselt starts with the conception that the condensed liquid forms a continuous film on the wall and that the heat flow is determined by the thermal resistance of this film. Again, the simplest case will be calculated, the condensation on a vertical wall at a constant temperature $t_w$. The condensed liquid builds up a film which flows by gravity downward and is continuously renewed by newly condensing vapor. The film has zero thickness at the upper edge of the wall and the thickness increases in a downward direction as is indicated in Fig. 96. At a distance $x$ from the upper edge the film thickness may be $\delta$. The velocity profile within the film can be assumed as a parabola:

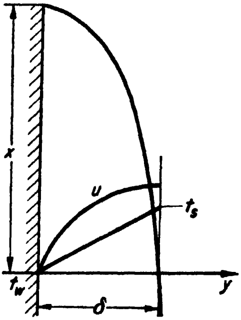

FIG. 96. Condensate-film thickness, velocity, and temperature profile for film condensation on a vertical wall.

$$u = U\left(2\frac{y}{\delta} - \frac{y^2}{\delta^2}\right) \tag{196}$$

In this equation, $y$ is the distance from the wall and $U$ is the downward velocity of the liquid at the border adjacent to the vapor. Nusselt showed that the parabola exactly represents the real velocity profile. As the heat of condensation flows normal to the velocities in the film the temperature profile must be essentially linear, with a temperature $t_w$ at the wall and the saturation temperature $t_s$ at the border of the film adjacent to the vapor. It is surprising perhaps that the temperature field has here another shape than in the boundary layer of a liquid or gas (Sec. 20 or 30). This is explained by the fact that the entire amount of heat flow to the wall originates in the boundary layer in the previously investigated problems, whereas here all the heat is generated at the outer border of the liquid film by condensation of the vapor.

---

[1] W. Nusselt, *Z. Ver. deut. Ing.*, **60**, 541 (1916).

The heat flow through an element of the film with the height $dx$ and unit dimension in the horizontal direction along the wall is therefore

$$dQ = \frac{k}{\delta}\, dx(t_s - t_w) \tag{197}$$

Again a film heat-transfer coefficient $h$ is defined by the equation

$$dQ = h\, dx(t_s - t_w)$$

and therefore

$$h = \frac{k}{\delta} \tag{198}$$

The velocity with which the liquid film flows down the plate can be calculated from the equilibrium condition for the element of film under consideration. The weight of this film element must be counteracted by the shearing stress $\tau_w$ at the wall:

$$\gamma\delta\, dx = \tau_w\, dx$$

Acceleration and pressure forces are neglected as small. By introducing Newton's law (109) for the shearing stress and solving the above equation for the velocity gradient at the wall there is obtained

$$\left(\frac{du}{dy}\right)_w = \frac{2U}{\delta} = \frac{\gamma\delta}{\mu}$$

and therefore

$$U = \frac{\gamma}{2\mu}\,\delta^2$$

Equation (196) therefore changes to

$$u = \frac{\gamma}{2\mu}\,\delta^2\left(2\frac{y}{\delta} - \frac{y^2}{\delta^2}\right)$$

The average velocity $u_m$ at the cross section $x$ is two-thirds the maximum value since the velocity profile is a parabola:

$$u_m = \frac{\gamma}{3\mu}\,\delta^2 \tag{199}$$

The weight of liquid flowing through the cross section $x$ is

$$G = \gamma u_m \delta = \frac{\gamma^2}{3\mu} \delta^3$$

Through the cross section at a distance $dx$ in the downward direction the weight flow is greater by the amount

$$dG = \frac{\gamma^2}{\mu} \delta^2 \, d\delta \tag{200}$$

This amount must be generated by condensation of vapor. With the equation $dQ = r\,dG$, in which $r$ is the heat of condensation per pound of liquid, there is obtained from Eq. (197),

$$dG = \frac{k}{r\delta} dx(t_s - t_w) \tag{201}$$

and by equating (200) and (201) the formula

$$\delta^3 \frac{d\delta}{dx} = \frac{\mu k}{r\gamma^2} (t_s - t_w)$$

is obtained. Integration gives

$$\frac{\delta^4}{4} = \frac{\mu k}{r\gamma^2} (t_s - t_w) x$$

If the dynamic viscosity $\mu$ is replaced by the kinematic viscosity $\nu$ there is obtained for the thickness of the liquid film

$$\delta = \sqrt[4]{\frac{4\nu k(t_s - t_w)x}{g\gamma r}} \tag{202}$$

and for the film heat-transfer coefficient,

$$h = \frac{k}{\delta} = \sqrt[4]{\frac{k^3 g r \gamma}{4\nu(t_s - t_w)x}} \tag{203}$$

In dimensionless form it may be written

$$\mathrm{Nu}_x = \frac{\mathbf{hx}}{\mathbf{k}} = \frac{\mathbf{x}}{\delta} = \sqrt[4]{\frac{\mathbf{g}\gamma\mathbf{r}\mathbf{x}^3}{4\nu\mathbf{k}(\mathbf{t}_s - \mathbf{t}_w)}} \tag{204}$$

Equation (203) gives the local heat-transfer coefficient at a distance $x$ from the upper edge of the plate. The average value along the distance is found by integration:

$$\bar{\mathbf{h}} = \tfrac{4}{3}\mathbf{h} \tag{205}$$

According to Eq. (204), the Nusselt number depends on the dimensionless value on the right-hand side of the equation. No name or symbol has been given to this value. The property values of the condensate must be introduced into the equation.

The liquid film changes to turbulent flow when its thickness exceeds a certain value. Heat transfer through the turbulent film can be calculated in the same way as for turbulent flow of liquids or gases along a plate. Such a calculation was done by U. Grigull.[1] The result shows that in the turbulent film, the Nusselt number is a function of the dimensionless value in Eq. (204) and of the Prandtl number of the condensate. The equation for heat transfer in a turbulent film is rather complex. It is therefore better to take the heat-transfer coefficient from Fig. 97. In this figure the Reynolds number of the film is plotted over the dimensionless value $\frac{k\gamma^{2/3}(t_s - t_w)x}{1.082rg^{1/3}\mu^{5/3}}$ with the Prandtl number as a parameter. The Reynolds number is built with the film thickness $\delta$ and the average velocity in the film $u_m$:

$$Re_\delta = \frac{u_m\delta}{\nu} \tag{206}$$

From this, the average heat-transfer coefficient can be calculated by the fact that the heat flowing to the wall over the height $x$ originates from the heat of condensation of the condensate passing through a cross section of the film at the point $x$:

$$\bar{h}x(t_s - t_w) = \gamma u_m \delta r$$

Therefore

$$Re_\delta = \frac{u_m\delta}{\nu} = \frac{\bar{h}x(t_s - t_w)}{gr\mu} \tag{207}$$

The Reynolds number calculated from Eq. (204), for laminar flow is

$$Re_\delta = \left(\frac{k\gamma^{2/3}x(t_s - t_w)}{1.082rg^{1/3}\mu^{5/3}}\right)^{3/4} \tag{208}$$

This equation is represented in Fig. 97 by the dashed line. For turbulent flow, two bundles of lines are inserted in Fig. 97. One is calculated with a critical Reynolds number $Re_{cr} = 400$, the other with $Re_{cr} = 300$. The great number of inserted points

---

[1] U. Grigull, *Forsch. Gebiete Ingenieurw.*, **13**, 49–57 (1942).

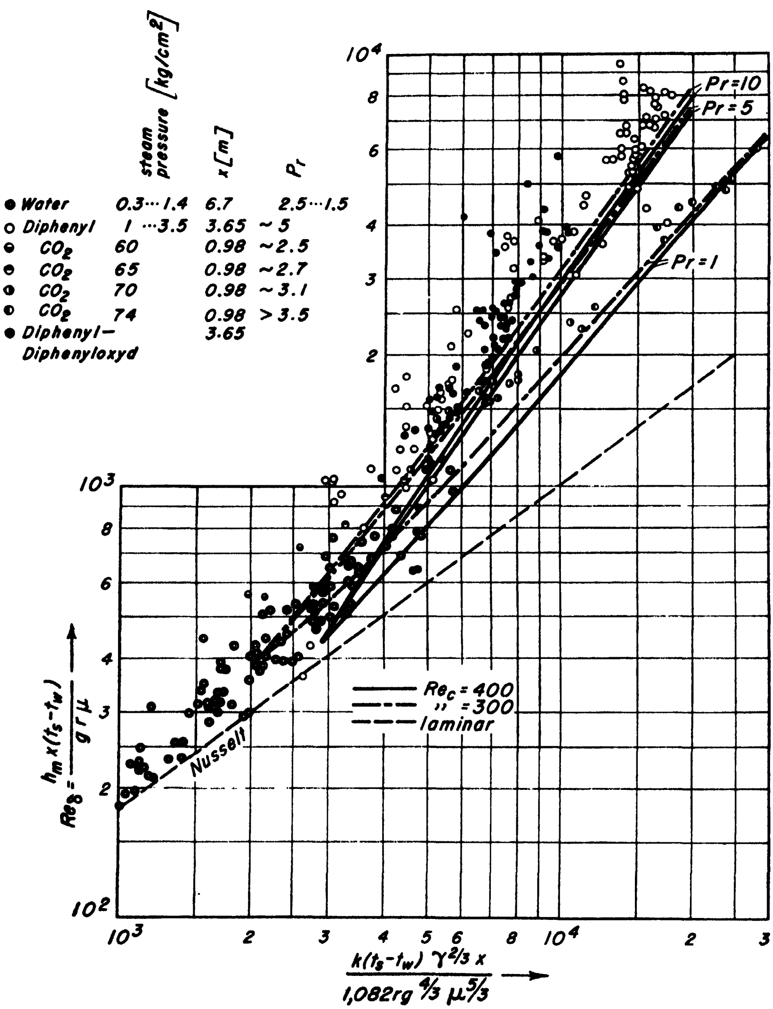

FIG. 97. Film condensation with laminar and turbulent film. [*From U. Grigull, Forsch. Gebiete Ingenieurw.*, **13**, 49–57 (1942).]

representing experimental results indicate that $Re_{cr} = 300$ conforms better with reality. In the laminar region, Nusselt's theory is proved by the experiments.

Nusselt also calculated the heat transfer by condensation on a horizontal circular tube. The result can be expressed simply so that the average film heat-transfer coefficient on a tube with diameter $d$ has the same magnitude as the average film heat-transfer coefficient on a vertical wall with the height $x = 2.5d$. If more tubes are arranged one above the other, the condensate from the highest tube flows to the next underlying, etc. (Fig. 98). By this action the heat transfer of every successive tube is diminished. Nusselt's calculations showed that the heat flow of the second tube is only 60 per cent of the first. This decrease in the heat flow can be greatly diminished by an arrangement proposed by Ginabat (Fig. 99).

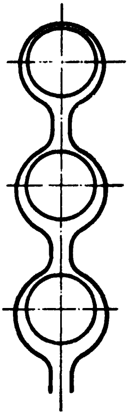

FIG. 98. Film condensation on three tubes above each other.

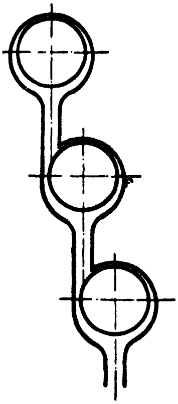

FIG. 99. Film condensation on a tube arrangement used in the Ginabat condenser.

Most experiments confirmed Nusselt's liquid-film theory. Sometimes, however, much higher values were measured. E. Schmidt, W. Schurig, and W. Sellschopp[1] showed that this is because the vapor sometimes condenses not as a connecting film but in the form of small droplets which increase in size with time until they are so heavy that they run down the wall. In so doing they sweep their paths free of droplets. On these places the formation of new tiny droplets begins immediately. Figure 100 shows a photograph of this type of condensation. It can be easily understood that heat transfer for this type of condensation is much greater than for filmwise condensation. A great number of American experiments were conducted which analyze the conditions under which the condensation will be filmwise or dropwise. Pure vapor on clean surfaces condenses always as a film. Impurities in the vapor or on the wall, especially of fatty acids, lead to condensation in the form of droplets. The formation of droplets is easier on rough surfaces than on smooth ones. On steel or aluminum tubes under ordinary conditions one must always expect filmwise condensation. Since it is difficult to predict with certainty the formation of dropwise condensation, it is recommended that calculations always be made with the equation for film condensation.

---

[1] E. Schmidt, W. Schurig, and W. Sellschopp, *Tech. Mech. u. Thermodynam.*, **1**, 53 (1930).

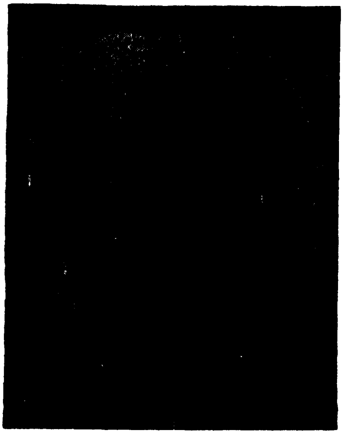

FIG. 100. Dropwise condensation. [*Photograph by E. Schmidt, W. Schurig, and W. Sellschopp, Tech. Mech. u. Thermodynam,* **1**, 53 (1930).]

Superheated vapor has practically the same film heat-transfer coefficients as saturated vapor. If a noncondensing gas is present together with the vapor, an additional resistance to the heat flow arises by concentration of the gas near the liquid-film surface. The heat transfer is thus much decreased. This problem is discussed in the last paragraphs dealing with mass transfer.

**Example.** Saturated water vapor condenses as film on a vertical wall. The film heat-transfer coefficient at a distance of 3 in. from the upper edge is to be calculated. The steam pressure is 1.43 lb/in.$^2$; the corresponding saturation temperature $t_s$ = 114 F. The wall temperature is $t_w$ = 105 F.

From steam tables take the heat of evaporation, $r$ = 1029 Btu/lb, and the specific weight $\gamma$ = 62 lb/ft$^3$. The property values $k$ and $\nu$ can be found in the Appendix:

$$\nu = 0.654 \times 10^{-5} \text{ ft}^2/\text{sec}$$

$k$ = 0.367 Btu/(hr)(ft)(F). The dimensionless value in Eq. (204) is

$$\frac{g\gamma r x^3}{\quad} = \frac{32.2 \times 62 \times 1029 \times 3^3 \times 3600}{\quad} = 1.34 \times 10^{12}$$

and the Nusselt number is $Nu = \sqrt[4]{1.34 \times 10^{12}} \quad 1.08 \times 10^3$. The local film heat-transfer coefficient is

$$h = \frac{0.367 \times 12}{3} \times 1.08 \times 10^3 = 1580\,\text{Btu/(hr)(ft}^2\text{)(F)}$$

and the average value along the height of 3 in. is

$$\bar{h} = (4/3)\times 1580 = 2110\ \text{Btu/(hr)(ft}^2\text{)(F)}$$

The average film heat-transfer coefficient on a horizontal tube with a diameter $d = 3/2.5 = 1.2$ in. has the same magnitude. It can be seen that the heat-transfer coefficients connected with condensation are very great.

## 32. Evaporation

Among all the different kinds of heat transfer the one concerned with the evaporation of a boiling liquid is least explored. A general treatment by calculation is therefore not possible now and one can rely only upon the numerous experiments. Since the evaporation process is rather complex and the relative importance of the different physical laws connected with it is not known, it is neither possible to generalize the results of experiments on certain liquids by dimensional analysis nor to transfer these results to other liquids in this way. The basic work on this kind of heat transfer was done by M. Jakob and his coworkers.

Most of the experiments were done on horizontal heating surfaces at ambient pressure and 210 F temperature. Figure 101 shows the temperature field measured in boiling water above a horizontal electrically heated plate.[1] It can be seen that in a thin boundary layer on the surface a steep temperature gradient arises. Outside this boundary layer the temperature in the boiling water is practically constant, but higher by 0.7 F than in the steam above the water surface. The explanation for this fact is that the pressure in the steam bubbles generated in the water is higher than in the liquid, since the surface tension in the surface of the bubbles tends to reduce the size of the bubbles and must be counteracted by a higher pressure inside the bubble. For this higher pressure there must occur a higher evaporation temperature. The pressure difference between the bubble interior and the surrounding liquid is the greater, the smaller the size of the bubble. Therefore, bubbles can originate in a liquid only where starting places in the form of small gas bubbles or roughness of the walls are present. The evaporation can therefore be influenced by the quality of the surfaces and the purity of the liquid and surfaces. Generally the bubbles originate on the heated surfaces. They continue to grow, however, during their ascent through the liquid. The termal resistance in the evaporation process is concentrated essentially in the boundary layer at the heated surface. The generation and growth of the bubbles is of secondary importance to the magnitude of the heat flow from the heated surface. The thickness of the boundary layer and therefore the film heat-transfer coefficient are determined by the natural convection currents arising within the liquid at small heat-flow values. In the range of heat flow $q$ up to 3700 Btu/(hr)(ft$^2$), the film heat-transfer coefficient can be represented by the equation[1]

---

[1] M. Jakob and W. Fritz, *Forsch. Gebiete Ingenieurw.*, **2**, 435 (1931).

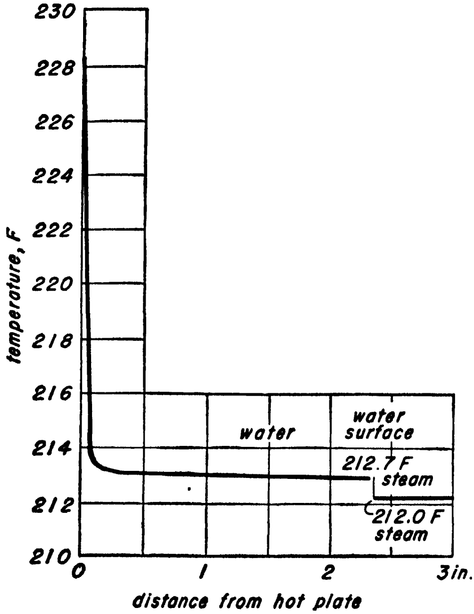

FIG. 101. Temperature profile in boiling water above a horizontal heating plate. (*According to M. Jakob and W. Fritz, from M. ten Bosch, "Die Wärmeübertragung," 3d ed., Springer-Verlag, Berlin,* 1936.)

$$h = Cq^{0.26} \tag{209}$$

---

[1] W. Fritz, *Z. Ver. deut. Ing., Beiheft Verfahrenstechnik,* No. 5, 1937, pp. 149–155.

For an evaporation temperature of 210 F, the constant $C$ has the value $274 \frac{1}{\mathrm{F}}$. The film heat-transfer coefficient in this equation is formed with the difference between the temperatures of the heated surface and the temperatures within the liquid outside the boundary layer. It can be shown that Eq. (209) can be transformed into a dimensionless expression of the form

$$Nu = Cf(Gr\,Pr)$$

and that the results of experiments with different liquids lead to the same dimensionless equation. By this fact, the assumption that the heat transfer is determined by the free-convection currents within the liquid is proved.

Of greater industrial importance is the heat transfer at higher specific heat flow. In this range, the boundary-layer thickness is determined by the stirring action of the steam bubbles.

Measured film heat-transfer coefficients are shown in Fig. 102. Figure 102*a* gives the variation of $h$ with the temperature difference $\Delta t$ between the heating surface and the boiling liquid for water boiling under 1 atm pressure. The range of heat flow under the stirring action of the bubbles is indicated by the steeper increase of $h$ with $\Delta t$. The film heat-transfer coefficient reaches a maximum and decreases thereafter. In the region behind the maximum the heat-transferring surface is covered by a steam film and the higher heat resistance of this film is the reason for the lower $h$ values. The phenomenon that a vapor film separates heating surface and liquid was described by Leidenfrost in 1756. The influence of pressure or boiling temperature on the film heat-transfer coefficient is shown in Fig. 102*b*. The two sets of experimental results at low and higher temperature difference do not agree well. They show, however, that the $h$ value increases with increasing boiling temperature (pressure). No great differences exist between the film heat-transfer coefficient on horizontal plates (curve $A$ in Fig. 102*a*) or on horizontal tubes (curves $B$ and $C$). Neither has the number, diameter, and arrangement of tubes or the horizontal or vertical position of the heating surface in an evaporator an appreciable influence on it. Only in the lower range can the $h$ values be improved substantially by stirring. At higher heat-flow rates the velocities produced by the stirring do not penetrate into the thin thermal boundary layer on the heating surface.

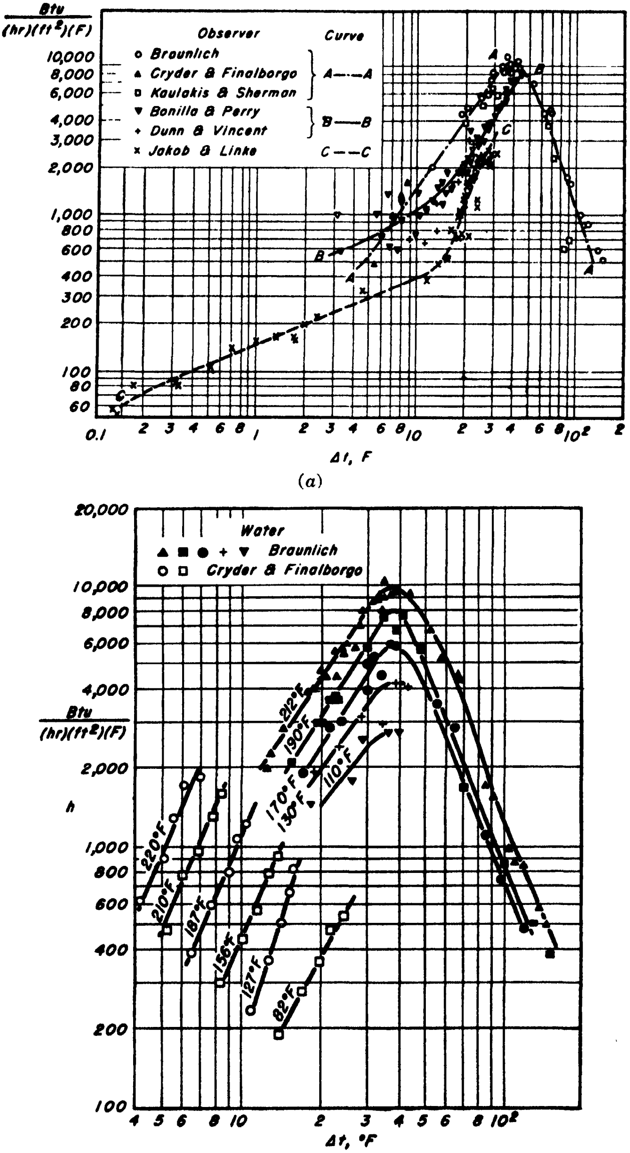

(a)

(b)

FIG. 102. Heat-transfer coefficients for water boiling on horizontal tubes (*A*) and horizontal plates (*B* and *C*). Figure *a* at 1 atm. (*From W. H. McAdams, "Heat Transmission," 2d ed., McGraw-Hill Book Company, Inc., New York, 1942.*)

Evaporators in which the liquid is evaporated inside tubes and which work with forced convection evaporate usually only a few per cent of the circulated liquid. The film heat-transfer value can in this case be calculated using the formulas of flow through tubes without boiling. The stirring action of the vapor bubbles increases the $h$ values by 25 to 40 per cent. Water boiling in tubes under natural convection has heat-transfer values which were summarized by W. Fritz[1] in Table 10. These values are valid for velocities of the liquid less than 3 fps.

TABLE 10. APPROXIMATE VALUES FOR HEAT-TRANSFER COEFFICIENTS TO BOILING WATER AT NORMAL PRESSURE*

| Specific heat flow $q$, Btu/(hr)(ft$^2$) | Horizontal plate, vessels $h$, Btu/(hr)(ft$^2$)(F) | Tube, 1-2 in. diam to 6 ft long, natural circulation $h$, Btu/(hr)(ft$^2$)(F) |
|---|---|---|
| 5,000 | 420 | 550 |
| 10,000 | 660 | 850 |
| 20,000 | 1,100 | 1,350 |
| 30,000 | 1,500 | 1,800 |
| 40,000 | 1,800 | 2,200 |
| 50,000 | 2,150 | 2,600 |
| 60,000 | 2,450 | 2,950 |
| 70,000 | 2,750 | |
| 80,000 | 3,100 | |
| 90,000 | 3,400 | |
| 100,000 | 3,600 | |

* W. Fritz, *Z. Ver. deut. Ing.*, *Beiheft Verfahrenstechnik*, No. 1, 1943, pp. 1–14.

A more extensive treatment of evaporation and a compilation of numerical values for different liquids is found in W. H. McAdams, "Heat Transmission," 2d ed., McGraw-Hill Book Company, Inc., New York, 1942. Local boiling near the surface increases the heat transfer considerably when a liquid cools a surface whose temperature is above the saturation point. Use is made of this cooling method in rockets.[2]

**Example.** As a synopsis of the facts discussed in the chapter on heat transfer by convection, the heating surface of a condenser may be calculated. The condenser is to condense 20,000 lb/hr of water vapor at a pressure of 1.43 lb/in.$^2$ To this pressure there corresponds an evaporation temperature of $t_s = 114$ F. The heating surface may be built up with brass tubes having 1.2-in. internal diameter and 0.04-in. wall thickness. The tube length is 9 ft. The amount of cooling water is $W = 800{,}000$ lb/hr, its temperature $t_{wi} = 80$ F. The velocity of the cooling water in the tubes is 6 fps.

---

[1] W. Fritz, *Z. Ver. deut. Ing.*, *Beiheft Verfahrenstechnik*, No. 1, 1943, pp. 1–14.

[2] F. Kreith and M. Summerfield, *Trans. ASME*, 48-A-38.

The heat of evaporation of water at 1.43 lb/in.$^2$ is 1029 Btu/lb; therefore the heat flow in the condenser is

$$Q = 1029 \times 20{,}000 = 20{,}580{,}000 \text{ Btu/hr}$$

Since this amount of heat must be absorbed by the cooling water, its temperature $t_{we}$ in leaving the condenser can be calculated from the equation

$$Q = W(t_{we} - t_{wi}) \qquad t_{we} = \frac{Q}{W} + t_{wi} = \frac{20{,}580{,}000}{800{,}000} + 80 = 25.7 + 80$$
$$= 105.7 \text{ F}$$

Outside the tubes, the temperature of the steam along the whole heating surface is 114 F (the small influence of the air contained in the steam may be neglected). The logarithmic mean temperature difference is therefore, from Eq. (24) (calculated with Table 2),

$$\Delta t_m = \frac{(t_s - t_{wi}) - (t_s - t_{we})}{\ln(t_s - t_{wi})/(t_s - t_{we})} = \frac{34 - 8.3}{\ln 34/8.3} = 18.2 \text{ F}$$

To calculate the heating surface with Eq. (23), the over-all heat-transfer coefficient must be known. This consists, according to Eq. (11*b*), of the two film heat-transfer coefficients $h$ on both sides of the heating surface and of the value $k/b$ for heat conduction through the tube wall. To calculate the film heat-transfer coefficient $h_w$ from the cooling water to the tube inside, the Reynolds number is constructed:

$$Re = \frac{u_m d}{\nu} = \frac{6 \times (1.2/12)}{0.708 \times 10^{-5}} = 84{,}700$$

The flow therefore is turbulent, and because of $l/d = 90$ it is also fully developed. The film heat-transfer coefficient therefore is to be calculated with Eq. (157). With a Prandtl number $Pr = 4.34$,

$$St = \frac{Nu}{Re\,Pr} = \frac{0.0396 \times 84{,}700^{-1/4}}{1 + 1.6 \times 84{,}700^{-1/8}\,(4.34 - 1)}$$
$$= 0.00101 \qquad \text{and} \qquad Nu = 372$$

With a thermal conductivity $k = 0.363$ Btu/(hr)(ft)(F) there is obtained,

$$h_w = (Nu)\frac{k}{d} = 372\,\frac{0.363 \times 12}{1.2} = 1350 \text{ Btu/(hr)(ft}^2\text{)(F)}$$

The film heat-transfer coefficient on the outside surface of the tubes caused by the condensing steam was calculated in the previous paragraph. It was found that $h_s = 2110$ Btu/(hr)(ft²)(F). The thermal conductivity of brass is $k = 65$ Btu/(hr)(ft)(F). Therefore the over-all heat-transfer coefficient $U$ is given by

$$\frac{1}{U} = \frac{1}{h_w} + \frac{b}{k} + \frac{1}{h_s} = \frac{1}{1{,}350} + \frac{0.04}{12 \times 65} + \frac{1}{2{,}110} = \frac{1}{790}$$

and $U = 790$ Btu/(hr)(ft²)(F). From the equation it can be seen that the greatest thermal resistance which determines the heat flow is that on the water side. The thermal resistance of the brass wall is negligibly small compared with the other resistances. The heating surface $A$ is finally, from Eq. (23),

$$A = \frac{Q}{U\,\Delta t_m} = \frac{20{,}580{,}000}{790 \times 18.2} = 1{,}430 \text{ ft}^2$$

Since the surface of one tube is $\frac{1.2 \times \pi}{12} 9 = 2.82$ ft², 508 tubes are necessary. The film heat-transfer coefficient outside the tubes is greatly diminished by the presence of entrained air in the steam. If entrained air is to be expected, the heating surface must be increased by a certain amount.

## 33. Heat transfer in gases at low densities

In this book the media which transfer heat are considered as continua. This is permissible as long as the volume elements which are used in the calculations still contain a large number of molecules. Even in gases where the distances between the molecules are much larger than in solids or liquids, the mean intermolecular distance is very small as compared with those dimensions with which we are usually concerned in our heat-transfer calculations, and therefore the above condition is well fulfilled. Only at very low pressures and corresponding low densities does the distance between the molecules become comparable with the other dimensions, and then the effect of the molecular structure makes itself felt in flow and heat transfer. The manner in which this occurs will be explained later in this section. The explanation will make it possible to estimate the point at which the ordinary formulas developed in the previous chapters become invalid; however, no equations for the determination of heat flow in gases of low density will be presented.

The knowledge in this field has been very sparse up to now. Only recently, because of the possibility of attaining very high altitudes in the flight of rocket-powered missiles, has research been instigated in this direction.[1]

The tool in dealing with these low-density phenomena is the kinetic theory of gases, developed in a quantitative way first by D. Bernoulli in 1738. This theory considers the gases as consisting of molecules, each of which flies rectilinearly until it collides with another molecule. Their average kinetic energy determines the temperature of the gas. In the collisions the molecules exchange their energies according to the laws of elastic impacts. The average length of the straight-line paths which the molecules follow between the impacts is called the *mean free path*. The velocity of a molecule changes with each impact; therefore, at any specific moment, there are molecules with all sorts of velocities present. Most of them, however, have velocities in the neighborhood of a mean value. Very few have exceedingly small or exceedingly large velocities. The distribution function of the velocities in a gas in equilibrium was calculated by J. C. Maxwell (1859). We will denote the mean molecular velocity by $v$ and the mean free path length by $\lambda$.

One of the early successes of the kinetic theory was that it predicted the astonishing fact that the dynamic viscosity and the thermal conductivity of gases are independent of pressure. This means, for instance, that a certain amount of heat is conducted through a stagnant gas layer under fixed temperature conditions, regardless of the pressure of the gas. Using simplified concepts we will derive approximate expressions for the viscosity and conductivity. The kinetic theory explains the shearing stresses in a flowing gas by the fact that molecules move constantly back and forth between the layers flowing with different velocities. In this way momentum is exchanged between these layers. The same swirling motion of the molecules causes an exchange of their energy when there are temperature differences in the gas. It will be recalled that a similar concept was used in explaining turbulent shearing stresses and heat flow. Figure 62 illustrated the manner in which fluid masses $w'$ were carried by the turbulent motions through an arbitrarily selected plane *aa* and carried with them the temperatures and velocities from planes 1-1 and 2-2 from whence they originated. In this way these fluid masses exchanged heat and momentum.

---

[1] S. A. Schaaf, D. O. Horning, and E. D. Kane, Design and Initial Operation of a Low Density Supersonic Wind Tunnel, Heat Transfer and Fluid Mechanics Institute, Berkeley, Calif., 1949, published by ASME.

Now we consider the laminar flow of a gas parallel to a wall with a velocity and temperature gradient normal to the wall. Molecules pass constantly through an arbitrary plane *aa* parallel to the wall (Fig. 62). During the time interval $d\tau$, molecules with a velocity component $v_\perp$ normal to plane *aa* will pass that plane when they are within a distance $v_\perp d\tau$ of that plane. The number of molecules per unit volume may be $n$. The average velocity component toward plane *aa* of all molecules will be some fraction $i'$ of the mean molecular velocity.[1] Therefore all the molecules within the volume $i'v\,d\tau$ will pass a unit area of the plane. Their number is $i'nv\,d\tau$, and the number of molecules passing a unit area of plane *aa* per unit time from one side is $i'nv$. The molecules carry with them the flow velocity $u$ from their last collision until their next collision. On the average, therefore, they transport the flow velocity from plane 1-1 to plane 2-2 through a distance which must be connected with the mean free path length. We will write for it $j\lambda$ with a numerical factor $j$ which cannot be very different from 1. A molecular stream of equal magnitude passes plane *aa* in the opposite direction and carries the flow velocity $u'$ from plane 2-2 to plane 1-1. The exchange of momentum connected with this process is

$$i'nvm(u - u')$$

with $m$ denoting the mass of one molecule. When the velocity gradient at plane *aa* in a direction normal to that plane is $du/dy$, then $(u - u')$ can be expressed as $j\lambda(du/dy)$. Therefore the exchange of momentum per unit area, or the shearing stress, is

$$\tau = i'jnmv\lambda(du/dy) = inmv\lambda(du/dy)$$

when the product $i'j$ of dimensionless factors is combined into $i$ whose value must be of the order of magnitude 1. On the other hand the viscosity $\mu$ is defined by the equation $\tau = \mu(du/dy)$.

---

[1] More extensive calculations result in $i' = \frac{1}{4}$. See E. H. Kennard, "Kinetic Theory of Gases," p. 60, McGraw-Hill Book Company, Inc., New York, 1938.

Equating both results in

$$\mu = inmv\lambda$$

the product $nm$ is the mass $\rho$ per unit volume. A thorough calculation for spherical molecules by S. Chapman and D. Enskog, which took into account the distribution of velocities and path lengths, gave for the numerical factor $i$ the value 0.499 and therefore for the dynamic viscosity

$$\mu = 0.499\rho v\lambda$$

The kinetic theory shows that the product $\rho\lambda$ is independent of pressure, and for the mean molecular velocity it gives the expression $v = \sqrt{\frac{8gRT}{\pi}}$, where $R$ is the individual gas constant, $T$ is the absolute temperature, and $g$ is the acceleration of gravity). Therefore $\mu$ is, according to the preceding equation, independent of pressure. If the mean free path is known, the viscosity can be calculated from this formula. Normally it is used, however, to calculate the mean free path from measured viscosity values. For air at normal pressure and 68 F, the value $\lambda = 2.5 \times 10^{-6}$ in. is found in this way, and at 900 F, $\lambda = 8.2 \times 10^{-6}$ in.

When a temperature gradient $dt/dy$ is present in the gas, internal thermal energy is exchanged in the same way by the molecules. With $C_m$, the specific heat per molecule, this heat exchange per unit area of plane $aa$ is

$$q = invC_m\lambda(dt/dy)$$

With the specific heat for constant volume, $c_v$, per unit weight $nC_m = \gamma c_v$. On the other hand the thermal conductivity $k$ is defined by the equation $q = k(dt/dy)$. Therefore

$$k = i\gamma c_v v\lambda$$

The exact calculation by S. Chapman determined the numerical factor $i$ for monatomic gases. It is somewhat different from the factor for the viscosity and has the value $i = 5/4$. For molecules with more atoms, A. Eucken developed by plausible deductions the formula $i = \frac{1}{8}(9\kappa - 5)$, in which $\kappa$ is the ratio of specific heats at constant pressure and volume.

Introducing the viscosity into the formula for the thermal conductivity gives

$$k = \frac{9\kappa - 5}{4} g c_v \mu$$

or

$$Pr = \frac{g c_p \mu}{k} = \frac{4\kappa}{9\kappa - 5}$$

Thus the kinetic theory leads to an expression for the Prandtl number which is generally in good agreement with measured values. The kinetic theory also gives an interesting interpretation to the Reynolds number $\frac{\rho V L}{\mu}$. Introducing $\mu$ results in

$$Re = \frac{1}{0.499} \frac{V}{v} \frac{L}{\lambda}$$

The Reynolds number, therefore, is the ratio of the macroscopic flow velocity $V$ to the mean molecular velocity $v$ times the ratio of the characteristic length $L$ to the mean molecular path $\lambda$.

Similarly, from the expression for the sound velocity

$$V_s = \sqrt{g \kappa R T}$$

it follows that $v = \sqrt{\frac{8}{\kappa \pi}}\, V_s$ and therefore

$$Ma = \frac{V}{V_s} = \sqrt{\frac{8}{\kappa \pi}} \frac{V}{v}$$

The Mach number is essentially the ratio $V/v$ of the flow velocity $V$ and the molecular velocity $v$.

Now the conditions within a gas—either stagnant or flowing—with a temperature gradient normal to a wall in the immediate neighborhood of this wall will be studied using the conceptions of the kinetic theory. A stream of molecules, which continuously crosses the control plane *aa* (Fig. 102*c*) situated just in front of the wall in a direction toward the wall, is reflected from the wall and crosses the plane a second time. The gas temperature in the plane *aa* is the average of the temperatures of both molecular streams. Therefore this temperature cannot be equal to the wall temperature even when the reflected molecules have assumed the wall surface temperature since the stream coming from the gas has a higher temperature. There must be a temperature jump at the surface. If the wall is removed and the gas extends

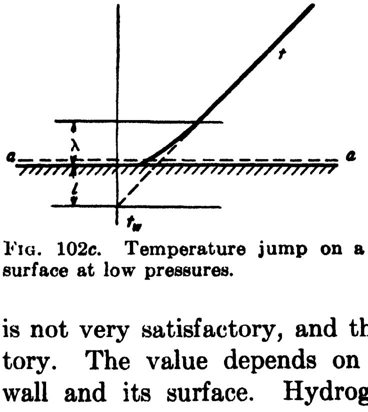

FIG. 102c. Temperature jump on a surface at low pressures.

beyond its surface, then the temperature gradient as found some distance from the wall, where it is not yet affected by the surface, would extend as indicated by the dashed line and the wall temperature would be reached at a distance $l$ from the surface which has approximately the length of the mean free path. This follows immediately from a comparison with Fig. 62 and the considerations which led to the formulas for the viscosity and thermal conductivity. In reality the molecules will not assume exactly the wall temperature in the process of reflection. This fact is expressed by the *accommodation coefficient* as introduced by Knudsen.[1] This coefficient is the ratio $a = (T_i - T_r)/(T_i - T_w)$ where $T_i$ is the temperature of the molecules before they impinge on the wall, $T_r$ is the temperature of the molecules after reflection, and $T_w$ is the wall temperature. The accommodation coefficient is unity when the molecules assume wall temperature upon reflection and less than unity otherwise. Values between 0.1 and 1 have been measured. The accuracy of the measurements, however, is not very satisfactory, and the results are partially contradictory. The value depends on the gas and the nature of the wall and its surface. Hydrogen, for instance, seems to have an especially low accommodation coefficient. More recent experiments by Wiedman[2] gave values of 0.87 to 0.97 for air. The gaskinetic calculation of the length $l$ (Fig. 102c) resulted in

$$l = \frac{2 - a}{a} \frac{1.996\kappa}{\kappa + 1} \frac{2}{Pr}$$

Since in reality the molecules have different path lengths, the temperature field in the gas in the immediate proximity of the wall is influenced within a distance of the order of magnitude of the mean free path length, in the way indicated in Fig. 102c.

The mean free path for air at barometric pressure and normal temperature is $2.5 \times 10^{-6}$ in. It is exceedingly small. Therefore the assumption which has been made in the book that the gas approaches the wall temperature at the surface is well justified at normal pressures. Only at very low pressures does the temperature jump at a surface become recognizable. Its existence was revealed for the first time by experiments of M. Smoluchovsky.[1] It can easily be seen that the heat flow by conduction through a gas layer between two plane walls separated by the distance $L$ is changed by 2 per cent by the temperature jump when the ratio of the length $l$ to the distance $L$ is 0.01. Generally the influence of the temperature jump on the heat flow depends on the ratio of the mean free path $\lambda$ to the characteristic length $L$ of the special problem. This ratio is called *Knudsen number* ($Kn$). It is assumed that the normal heat-flow formulas become inaccurate when the Knudsen number exceeds a value of approximately 0.01. In boundary-layer flow it is apparently opportune to use the boundary-layer thickness as characteristic length. The Knudsen number can be expressed by the Reynolds and Mach numbers. Using the relations on page 189 we find

---

[1] Knudsen, *Ann. Physik*, **34**, 593 (1911).

[2] See H. S. Tsien, *J. Aeronaut. Sci.*, **13**, 653–664 (1946).

$$Kn = \frac{\sqrt{\kappa\pi/8}}{0.499} \frac{Ma}{Re}$$

The limit where the molecular structure of the gas begins to affect the heat transfer can be approached either by high Mach numbers or by low Reynolds numbers. The influence of the temperature jump is felt at comparatively high pressures when the characteristic length $L$ is small, for instance, in heat conduction through gases which fill the open spaces in a pulverized material.

In aerodynamics the assumption is made that the velocities approach the value zero at the surface of a stationary wall. This is not strictly true either, because the molecules which cross a control plane immediately in front of the wall in the direction toward the wall have a finite flow velocity parallel to the wall. Even when they lose this velocity completely upon reflection, the average of the flow velocities of all molecules crossing the reference plane has a finite value. The gas *slips* on the surface of the wall. In reality, the molecules do not lose their flow velocity completely upon reflection. This fact is expressed by the so-called *slip coefficient* $f_s$. This coefficient gives the fraction of momentum in a tangential direction given off by the molecules in the reflection process. The slipping of the flow was found by A. Kundt and E. Warburg (1875) in experiments at low pressures, and the slip coefficient was introduced by T. C. Maxwell (1879) who presented a gaskinetic theory of this phenomenon. Meassured values for the slip coefficient range from 0.8 to 1. The velocity profile looks similar to the temperature profile in Fig. 102*c*. If the trend of the profile at some distance beyond the mean free path is extrapolated it reaches the value zero at a distance $l$ beyond the wall surface. Maxwell's theory gave for this length the formula

---

[1] M. Smoluchovski, *Sitzungsberichte Wiener Akad.*, **107**, 304 (1898); *Anz. Akad. Wiss. Krakau*, A, **5**, 129 (1910).

$$l = 0.998 \frac{2 - f_s}{f_s} \lambda$$

Again the length $l$ and therefore the slip are negligible at normal pressures. When the pressure is lowered it begins to affect the flow at approximately the same values of the Knudsen number as the temperature jump begins to affect the heat transfer. The flow regime (characterized by a certain range of the Knudsen number), where only the immediate neighborhood of solid walls is affected by the molecular structure of the flowing gas in the sense of the above considerations, is called *slip flow regime*.[1] When the pressure is lowered still further the molecular mean free path and the region near the solid surfaces which is influenced grows more and more. Finally the pressure becomes so low that collisions between the molecules are very rare (the mean free path length is large as compared with the characteristic length). This flow regime is called *free molecular flow*. It may be encountered by high-altitude rockets. In this region the calculation of drag and heat transfer becomes possible again. The nature of the calculations has more similarity with radiation calculations since the molecules move on straight paths (collisions with other molecules are neglected) until they hit a solid surface. Heat transfer to surfaces in this flow regime was calculated by Stalder and Jukoff.[2]

---

[1] H. S. Tsien, Superaerodynamics, Mechanics of Rarified Gases. *J. Aeronaut. Sci.*, **13**, 653–664 (1946).

[2] J. R. Stalder and D. Jukoff, Heat Transfer to Bodies Traveling at High Speed in the Upper Atmosphere. *J. Aeronaut. Sci.*, **15**, 381–391 (1948).

# CHAPTER 4

# THERMAL RADIATION

## 34. Basic conceptions

Heated solid bodies and liquids as well as some gases transmit heat also in the form of radiation. The heat rays emitted by such materials are electromagnetic waves. Their nature is the same as that of other electromagnetic waves, such as X rays, visible light, and the waves used in wireless transmission of signals. All these rays differ only in wave length. The human eye is sensitive to rays in the range from 0.35 up to 0.75 μ.[1] Thermal radiation comprises rays with wave lengths 0.3 to 10 μ and more. If radiation impinges upon a body, one part is reflected from the surface and the other part penetrates into the interior of the body. The reflection occurs in such a way that the angle between the reflected beam and the normal to the surface equals the angle made by the impinging beam with the same normal. This reflection is called *specular* or *regular*. On rough surfaces, however, the incident ray is distributed into all directions after reflection. This kind of reflection is called *diffuse reflection*. The radiation penetrating into the body is partially absorbed on its way. The remainder leaves the body through another surface. The ratio of the reflected radiation to the incident radiation is called *reflectivity* and is denoted by $\rho$. The ratio of the absorbed radiation to the incident radiation is the *absorptivity* $\alpha$, and the ratio of the transmitted radiation to the incident radiation is the *transmissivity* $\tau$. Therefore

$$\rho + \alpha + \tau = 1 \tag{210}$$

Solid and liquid bodies absorb practically the entire heat radiation penetrating through the surface into the interior in a very thin layer. Electric conductors need a layer of the order of magnitude 1 μ for this absorption. Electric nonconductors absorb with very few exceptions the entire radiation in layers approximately 0.05 in. in thickness. Since the thicknesses of materials used for industrial purposes are almost always greater, it can be written for these,

---

[1] $1\ \mu = 0.001\ \text{mm} = 3.94 \times 10^{-5}$ in.

$$\rho + \alpha = 1 \tag{211}$$

The laws governing the radiation emitted by a heated body are especially simple if no radiation is reflected from its surface ($\rho = 0$, $\alpha = 1$). Such a body is called *black body.* The name comes from the fact that a surface which absorbs all light rays appears black to the eye. A surface can absorb practically all thermal radiation, however, without absorbing all light rays and therefore without appearing black to the eye. For instance, a whitewashed wall is nearly *black* for thermal radiation. Totally black surfaces do not exist in nature since a certain percentage of the incident radiation is always reflected, but there are surfaces which reflect only a very small portion of the incident radiation. A surface which is very nearly *black* is snow, with an absorptivity of 0.985 for thermal radiation from a body whose temperature is not too high. Although no totally black surfaces exist in nature, the conception of a black body is a useful one because the laws governing its radiation are comparatively simple, and because it can be proved that no surface radiates more heat than a *black* one. This is the content of the Kirchhoff law. To prove this law it is necessary to imagine a hollow space (*hohlraum*) (Fig. 103) whose walls have a uniform temperature. Within this space is situated a body 1 with black surfaces. The body may have the same temperature as the walls. Then the heat radiated by the body must be equal to the heat radiated by the walls and absorbed by the body. If the two amounts of heat were not equal, the body would cool off or heat up. An isolated system of uniform temperature in which there arise spontaneously temperature differences is expressly forbidden by the second law of thermodynamics. The heat which is radiated per unit time from a unit surface is called *emissive power* and is denoted by $e$. If the black body 1 radiates $e_b$, the amount of heat radiated from the surroundings and impinging on a unit surface of body 1 must be $e_b$ as well. Now remove body 1 and replace it with a body 2 of the same shape and magnitude but with an absorptivity $\alpha$. From the

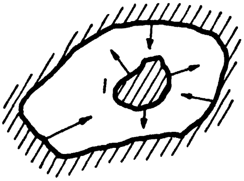

FIG. 103. Derivation of Kirchhoff's law.

walls of the hollow space the same heat $e_b$ as before is radiated against a unit surface of body 2. The body absorbs the amount $\alpha e_b$. The emissive power $e$ of body 2 must have the same magnitude according to the second law of thermodynamics:

$$e = \alpha e_b \tag{212}$$

This is the mathematical expression for the Kirchhoff law. In words we can state that the ratio of the emissive power $e_b$ of a black body to the emissive power $e$ of another body at the same temperature equals the absorptivity of the second body. The ratio of the emissive power of any body to the emissive power of a black body of equal temperature is called *emissivity* $\epsilon$. The Kirchhoff law may also be written in the form

$$\epsilon = \alpha \tag{213}$$

It is therefore only necessary to know either the emissivity or the absorptivity of a surface. For solid and liquid bodies then the reflectivity is also known according to Eq. (211).

For most materials the emissivity $\epsilon$ depends on the temperature. In this case the Kirchhoff law only holds true for a certain temperature. Therefore it gives the absorptivity only for the temperature at which the emissivity was measured. Another limitation to the law must be made when the emissivity and absorptivity differs for different wave lengths. Then Eq. (213) applies strictly only for monochromatic radiation.

## THE EMISSION OF THERMAL RADIATION

### 35. The black body

A surface element of a black body radiates in all directions. The heat flow per unit surface area leaving the body per unit time by this radiation is its emissive power $e$. The heat radiation from unit surface *in a certain direction* can be measured by determining the heat flow $dq$ radiated per unit area of the radiating body and passing through an element of the surface of a sphere constructed with the radius $r = 1$ around the radiating surface element (Fig. 104). The area of such a surface element

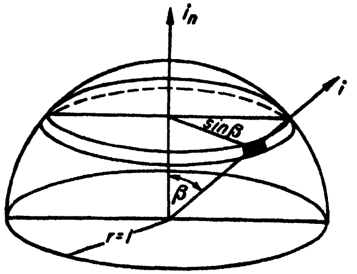

FIG. 104. Determining the radiation in different directions.

on the sphere has the same numerical value as the solid angle $d\omega$. The radiation in the contemplated direction is defined as

$$i = \frac{de}{d\omega} \tag{214}$$

and is called *radiation intensity.* For a black body, the radiation intensity $i_b$ is given by the Lambert cosine law

$$i_b = i_{bn} \cos \beta \tag{215}$$

where $i_{bn}$ is the radiation in direction of the normal to the surface element and $\beta$ is the angle between the radiation $i_b$ and the normal. The total heat radiated per unit of the black surface element, its emissive power, can be found by integration:

$$e_b = \int i_b \, d\omega = 2\pi i_{bn} \int_0^{\pi/2} \cos \beta \sin \beta \, d\beta = \pi i_{bn} \tag{216}$$

Since the radiation intensity $i_b$ is constant in all directions comprised in a conical surface with the opening angle $\beta$ (Fig. 104) a solid angle corresponding to the ring-shaped surface of the sphere $2\pi \sin \beta \, d\beta$ could be used in carrying out the integration. The total heat radiated from the unit surface area of a black body is therefore $\pi$ times the heat radiated in normal direction.

The heat radiated from a body always comprises rays of different wave length. The amount of heat $di$ radiated within an infinitesimally small wave-length range is also an infinitesimally small quantity. The fraction

$$i_\lambda = \frac{di}{d\lambda} \tag{217}$$

however, is a finite quantity and is called *monochromatic radiation intensity.* Calculation of the heat radiated by a black body as a function of the wave length instigated Max Planck to formulate the concept of his famous quantum theory. It so became the origin of modern physics. Planck's law for the monochromatic thermal radiation intensity of a black body in normal direction is

$$i_{\lambda bn} = \frac{2C_1}{\lambda^5(e^{C_2/\lambda T} - 1)} \tag{218}$$

where $T$ is the absolute temperature in degrees Rankine, which is equal to the temperature in degrees Fahrenheit plus 460. Equation (218) is represented in Fig. 105 as a function of the wave length $\lambda$ with the absolute temperature $T$ as parameter. From Fig. 105 it can be seen that at any temperature heat is radiated in a wide range of wave lengths. The maximum value for the radiation moves with increasing temperature to shorter wave lengths. This is described by Wien's law,

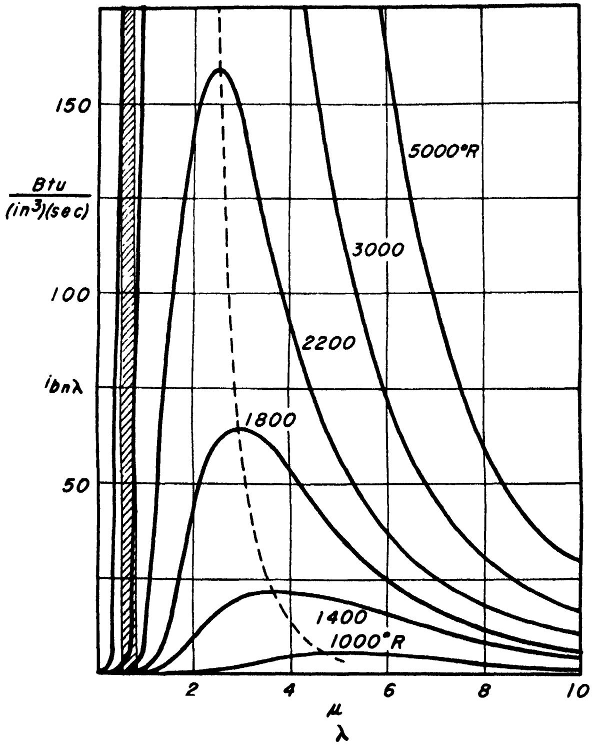

Fig. 105. Black-body radiation as a function of the wave length for different temperatures.

$$\lambda_{max}T = 5{,}190\ \mu \text{ deg R} \tag{219}$$

where $\lambda_{max}$ is the wave length for the maximum of radiation. The visible range of wave lengths is indicated in Fig. 105 as a shaded band. It can be seen that with increasing temperature an increasingly greater part of the whole radiation falls into the visible range. As the human eye can determine very small energies, the small radiation in the visible range at 1800 R, or 1340 F, is seen as dark glowing red. With increasing temperature, the visible part of the radiation becomes greater, and therefore the brightness increases. But even at a temperature of 5000 R this visible part is comparatively small. The filament of a tungsten lamp has this temperature; therefore the efficiency of such a lamp is poor. Only at the temperature of the sun (approximately 10,000 R) does the maximum value of the monochromatic radiation intensity lie within the visible range.

The radiation intensity in the whole range of wave lengths, which is of most interest for industrial calculations, can be found from Planck's law by integration:

$$i_{bn} = \int_0^\infty i_{b\lambda n}\, d\lambda$$

The integration is possible by introducing $x = 1/\lambda$:

$$\begin{aligned} i_{bn} &= 2C_1 \int_0^\infty x^3\left(e^{\frac{C_2}{T}x} - 1\right)^{-1} dx \\ &= 2C_1 \int_0^\infty x^3\left(e^{-\frac{C_2}{T}x} + e^{-\frac{C_2}{T}2x} + e^{-\frac{C_2}{T}3x} + \cdots\right) dx \end{aligned}$$

Each single integral $\int_0^\infty x^3 e^{-\frac{C_2}{T}ix}\, dx (i = 1, 2, 3 \cdots)$ can be solved by partial integration. It gives $6T^4/C_2^4 i^4$. Therefore

$$i_{bn} = \frac{12C_1}{C_2^4} T^4 \left(1 + \frac{1}{2^4} + \frac{1}{3^4} + \cdots\right) = \frac{12C_1}{C_2^4}\frac{\pi^4}{90} T^4 = K_n T^4 \qquad (220)$$

This is the Stephan-Boltzmann law, found experimentally by Stephan and proved theoretically by Boltzmann. According to this law black-body radiation is proportional to the 4th power of the absolute temperature. The emissive power of a black body is $\pi$ times the radiation as presented by Eq. (220). Therefore, it can be written

$$\mathbf{e}_b = \sigma \mathbf{T}^4 \qquad (221)$$

The numerical value of the Boltzmann constant $\sigma$ was determined by very accurate measurements. The resulting value $\sigma = 0.173 \times 10^{-8}$ Btu/(hr)(ft$^2$)(R$^4$) is slightly greater than the value resulting from Eq. (220).

In nature there does not exist an exactly black surface. It can be approached however to any desired degree in the following way. Kirchhoff's law states that a body which absorbs all impinging radiation radiates as a black body. We can realize a black body therefore by using a hollow space in which there is a small opening (Fig. 106) (a *hohlraum*). The walls of the space must be kept at uniform temperature. Radiation which streams through the opening into the hollow space is reflected repeatedly before it leaves the space again through the opening. If the surface of the space has a great absorptivity, then at every reflection the major part of the radiation is absorbed, so that after several reflections almost all radiation is absorbed. The opening of the hollow space therefore acts like a black surface. By decreasing the size of the opening the black body can be approximated as closely as is desired. If the hollow space is heated, then the opening emits black-body radiation according to Kirchhoff's law.

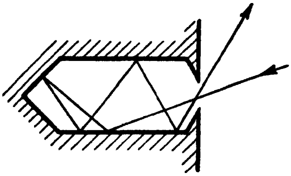

FIG. 106. Radiation of a hollow space.

### 36. Solid and liquid bodies

All solid and liquid bodies reflect a fraction of impinging thermal radiation and therefore according to the Kirchhoff law radiate less heat than the black body. With respect to their thermal radiation properties, there is a principal difference between electric conductors and nonconductors. The conductors reflect the major part of impinging radiation and radiate therefore comparatively little heat. Nonconductors absorb the major part of impinging radiation and radiate comparatively much heat. For both groups, the absorptivity and emissivity change with wave length. Figure 107*a* shows the reflectivity $\rho_\lambda$ of monochromatic radiation for aluminum as an example of metals, and Fig. 107*b* for some nonconducting surfaces of industrial importance, according to W. Sieber.[1] Figure 107*c* represents the absorptivity $\alpha_\lambda$ of water, which was measured by Aschkinass.[2] The polished aluminum surface has a smaller reflectivity for shorter than for longer wave lengths. The reflectivity of metal surfaces as a function of wave length can be calculated by the electromagnetic theory of light. The trend for all metals is the same as that for

[1] W. Sieber, *Z. tech. Physik*, **22**, 130–135 (1941).

[2] E. Aschkinass, *Wied. Ann.*, **55**, 404 (1895).

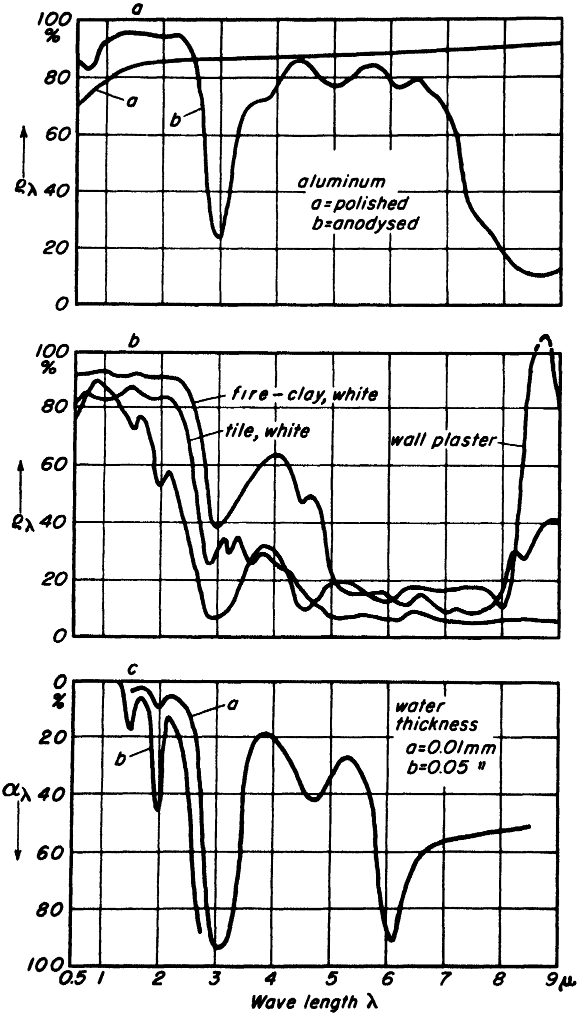

FIG. 107. Reflectivity and absorbtivity as a function of wave length for different materials. [*From W. Sieber, Z. tech. Physik,* **22**, 130–135 (1941).]

aluminum. Equation (211) shows, on the other hand, that the absorptivity of metals is greater at shorter wave lengths. The variation of the reflectivity of electric nonconductors with wave length is much more irregular. The oxide film of the anodized aluminum surface (Fig. 107*a*) corresponds more to the nonconductors. A characteristic feature of nonconductors is the fact that the reflectivity is lower at longer wave lengths. Especially surfaces which have a bright color have high reflectivity at short wave lengths. The reflectivity determines the absorptivity and emissivity according to Eqs. (211) and (213) for any wave length exactly, however, at only one certain temperature.

A surface whose absorptivity is constant for all wave lengths is called a *gray* surface. The surfaces represented in Fig. 107*b* approximate a gray surface but imperfectly. Good approximations of a gray surface are slate, tarboard, and dark linoleum. These materials absorb in the range of wave lengths between 0.5 and 9 $\mu$ from 85 to 92 per cent of the incident radiation.

For industrial calculations, the data for the total radiation integrated over the wave-length range are most important. The absorptivity for the total radiation can be determined from the monochromatic absorptivity in the following way. The distribution of the incident radiation over the wave-length range must be known. Then any ordinate of this curve must be multiplied by the absorptivity $\alpha_\lambda$ belonging to that same wave length. The area under the resulting curve divided by the area of the incident-radiation curve gives the absorptivity $\alpha$. If the radiator is a black body, Fig. 105 gives its distribution curve. Every ordinate of this curve has to be multiplied by the corresponding absorptivity (*e.g.*, taken from Fig. 107). The resulting curve must be planimetered and divided by the area under the radiation curve in Fig. 105. In this way the absorptivity and reflectivity values in Fig. 108 were determined by W. Sieber. In the curves, the difference between electric conductors (represented by aluminum) and nonconductors can be observed. For nonconductors, the absorptivity decreases with increasing temperature; for conductors it increases. Industrial radiators have temperatures between 500 and 2500 R. For such radiation, the absorptivity of nonconductors is much greater than the values for conductors. The sun has a temperature of 10,000 R. At this temperature nonconductors with white surfaces absorb less of the radiation than metal surfaces. Only a few metals, *e.g.*, silver, also have very small absorptivity in the range of visible radiation. Silver has a value for the reflectivity in this range of $\rho = 0.96$.

If the monochromatic absorptivity $\alpha_\lambda$ of a surface for incident black radiation is independent of the surface temperature, the integrated absorptivity $\alpha$ is exactly equal to the total emissivity for radiation radiated by the same surface where it is heated to the temperature of the black radiator. In most cases, however, the absorptivity of a surface depends on its temperature. Then the values of the total absorptivity $\alpha$ (*e.g.*, in Fig. 108) give only a first approximation of the emissivity value.

Lambert's cosine law is not fulfilled exactly for materials present in nature. Figures 109 and 110 show the emissivity in the different directions for a number of electric conductors and nonconductors. If the cosine law were strictly fulfilled, all distribution curves would be semicircles. It can be seen in the figures that nonconductors have smaller emissivities for emission angles in the neighborhood of 90 deg than would be expected from the cosine law. For conductors, the emissivity first increases and afterwards decreases as the emission angle approaches 90 deg. As a consequence of this behavior, the average emissivity $\epsilon$ for radiation in all directions differs somewhat from the emissivity $\epsilon_n$ in the direction normal to the surface. In Table 18 (Appendix) both values are compiled for different materials at room temperature. According to Fig. 108 the emissivity is to be expected to increase with temperature for metals and to decrease for nonconductors. Measured values in a greater temperature range can

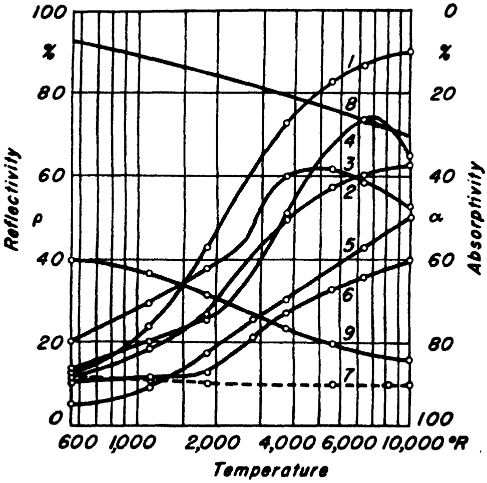

FIG. 108. Reflectivity and absorptivity of different materials as a function of temperature. [*According to W. Sieber, Z. tech. Physik,* **22**, 130–135 (1941).]

(1) white fire clay; (2) asbestos; (3) cork; (4) wood; (5) porcelain; (6) concrete; (7) roof shingles; (8) aluminum; (9) graphite.

be found in a paper by H. Schmidt and E. Furthmann.[1] From the emissivity $\epsilon$ the heat radiated per unit surface area at the absolute temperature $T$—the emissive power $e$—can be calculated by the formula

$$e = \epsilon\sigma T^4 \tag{222}$$

It was mentioned that the absorptivity $\alpha$ cannot be calculated exactly from the emissivity $\epsilon$ with Eq. (213) when it depends on temperature. A detailed investigation[2] shows that for metals the following rule is valid. The absorptivity of a metal surface with the temperature $T_1$ for black-body radiation at the temperature $T_2$ is equal to the emissivity of the same surface at the temperature $T_3 = \sqrt{T_1T_2}$. For nonconducting surfaces the temperature dependency is usually small and can be neglected as long as the temperature is not too high (Fig. 108).

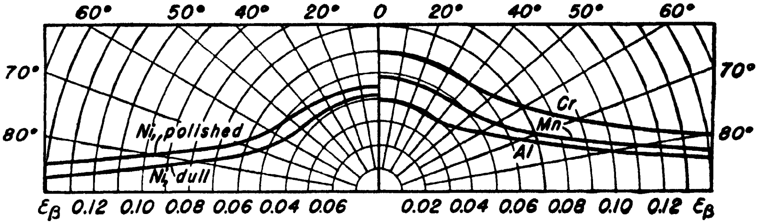

FIG. 109.

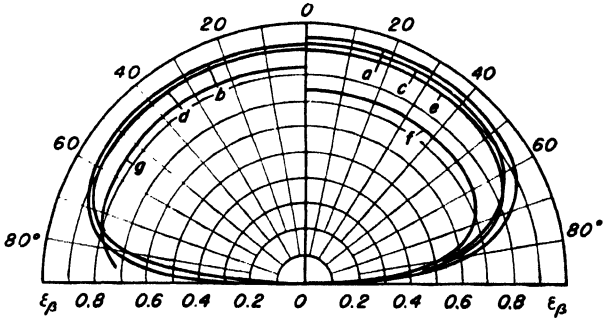

FIG. 110.

FIGS. 109 and 110. Emissivity of materials in different directions. [*From E. Schmidt and E. Eckert, Forsch. Gebiete Ingenieurw.*, **6**, 175–183 (1935).]

(*a*) wet ice; (*b*) wood; (*c*) glass; (*d*) paper; (*e*) clay; (*f*) copper oxide; (*g*) aluminum oxide.

---

[1] H. Schmidt and E. Furthmann, Die Gesamtstrahlung fester Körper, *Mitt. K. Wilhelm Inst. Eisenforschung,* Düsseldorf, 1928.

[2] E. Eckert, *Forsch. Gebiete Ingenieurw.*, **7**, 265–270 (1936).

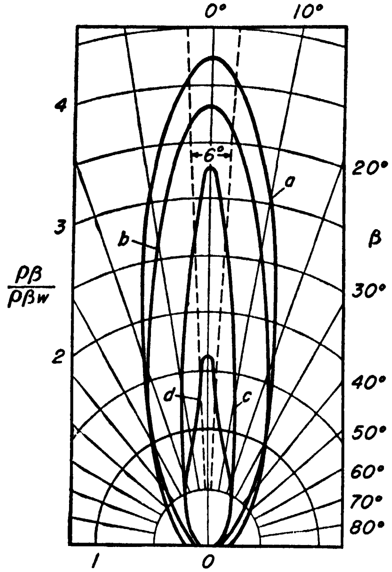

FIG. 111.

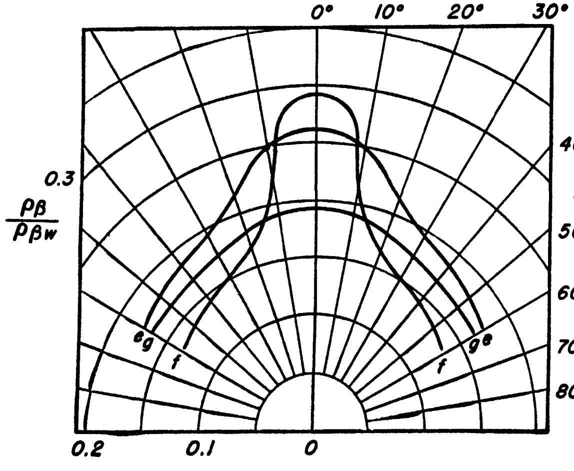

FIG. 112.

FIGS. 111 and 112. Reflectivity of materials for black-body radiation. [*From E. Eckert, Forsch. Gebiete Ingenieurw.*, **1**, 265–270 (1936).]

(*a*) aluminum paint; (*b*) iron scraped; (*c*) black iron; (*d*) copper oxide; (*e*) cast iron; (*f*) clay; (*g*) wood. $\rho_\beta$ measured reflectivity, $\rho_{\beta w}$ reflectivity of a completely diffuse surface with $\alpha = 1$.

With respect to the distribution of reflected radiation there were discerned specular and diffuse reflection. These two conceptions are ideals which are only approximated more or less in reality. Figures 111 and 112 represent measured distribution curves for black-body radiation at 500 F impinging normally on different surfaces. The incident-ray bundle had an opening angle of 6 deg. From Fig. 111 it can be seen that surfaces which appear specular to the eye reflect much more thermal radiation in the proximity of the regularly reflected ray than in the other directions. In Eqs. (211) and (213) the average reflectivity over all directions must be inserted.

## 37. Gases

Some gases absorb and radiate heat. The radiation of the gases originates from oscillations of the atoms within the molecules. The oscillations arise by collisions of the molecules. Since electric charges are associated with the atom, the molecules act as small transmitters of waves. Elementary gases, which consist of atoms all of the same kind, have no free electric charges connected with the atom. Such gases as hydrogen, oxygen, and nitrogen radiate no heat and are perfectly transparent to foreign heat radiation. For industrial calculations, the radiation of carbon dioxide and of water vapor are most important, since these gases are good radiators and are present in combustion gases in high concentration. Carbon monoxide, sulfur dioxide, and methane also radiate well but are generally present only in small concentrations. Figures 113 and 114 show

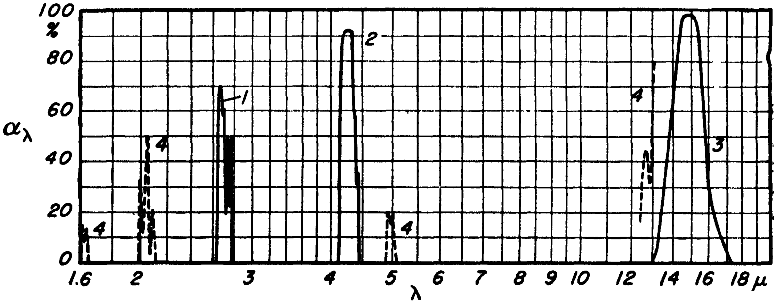

FIG. 113. Absorption bands of carbon dioxide. (*Measurements by E. F. Barker, G. Hertz, C. Schaefer, and B. Philipps.*)

(1) 5-cm; (2) 3-cm; (3) 6.3-cm; (4) 100-cm layers.

the absorption spectra of carbon dioxide and water vapor. It can be seen that gases are different in their behavior from solid and liquid bodies in so far as they radiate and absorb radiation only within certain limited wave-length ranges. For water vapor these ranges lie comparatively close together. The radiation takes place essentially at wave lengths longer than 1 μ; it is, therefore, invisible. From the figures it can also be seen that gases, in contrast to solid and liquid bodies, need great thicknesses to absorb the major part of incident radiation. The monochromatic absorptivity $\alpha_\lambda$ is determined by the following law (Beer's law):

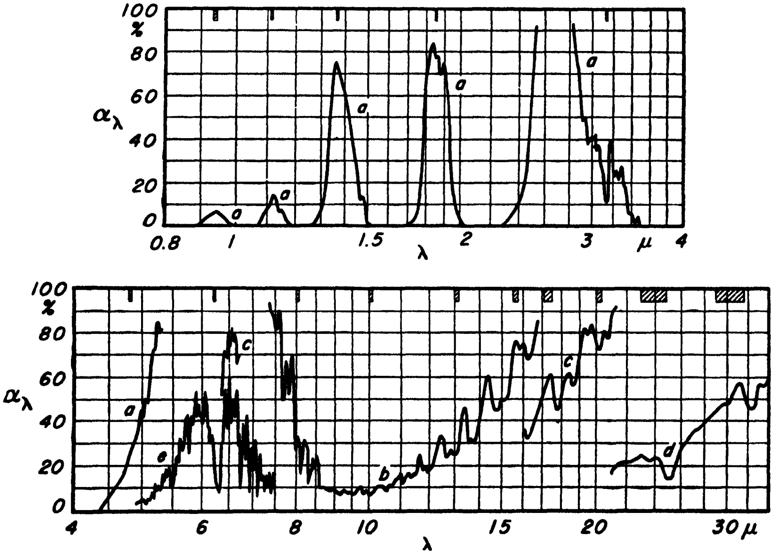

FIG. 114. Absorption bands of water vapor.

(*a*) 127 C and 109 cm; (*b*) 127 C and 104 cm; (*c*) 127 C and 32.4 cm; (*d*) 81 C and 32.4 cm at 4 cm atm; (*e*) room temperature and 220 cm at 7 cm atm. [*From E. Schmidt, Forsch. Gebiete Ingenieurw.*, **3**, 57 (1932).]

$$\alpha_\lambda = 1 - e^{-a_\lambda s} \tag{223}$$

with $s$ as the path length of the radiation in the gas. The value $a_\lambda$ is essentially proportional to the number of molecules per unit volume. Since this number for mixtures of gases is proportional to the partial pressure of the radiating gas, it follows from (223) that the absorptivity and, according to Kirchhoff's law, also the emissivity, are functions of the product of partial pressure times path length. This is the content of Beer's law. This law has exceptions. It does not hold true for very high pressures, and not for all gases. From the monochromatic absorptivity $\alpha_\lambda$, the monochromatic emissivity $\epsilon_\lambda$ can be strictly calculated with Eq. (213) only for that temperature at which the absorptivity was measured.

For industrial heat-transfer calculations, the total radiated heat integrated over all wave lengths is most important. Therefore, a number of extensive experimental investigations were carried out in this field after A. Schack[1] had emphasized the importance of gas radiation for heat transfer in furnaces and steam boilers. Measurements on carbon dioxide were made by H. C. Hottel and H. G. Mangelsdorf[2] and by Eckert.[3] Figure 115 shows the emissivity of carbon dioxide for different temperatures and thicknesses. The emissivity is determined in the same way as for solid bodies, by comparing the radiation of the gas with black-body radiation at the same temperature [Eq. (222)]. E. Eckert made measurements with carbon dioxide–nitrogen mixtures of various partial pressures and thicknesses and proved Beer's law for carbon dioxide. Hottel and Mangelsdorf used carbon dioxide–air mixtures. Both experimental results agree fairly well. Only the extrapolated values for higher temperatures show greater differences. Hottel's values are smaller. Since a theoretical investigation by Schwiedessen showed also that the

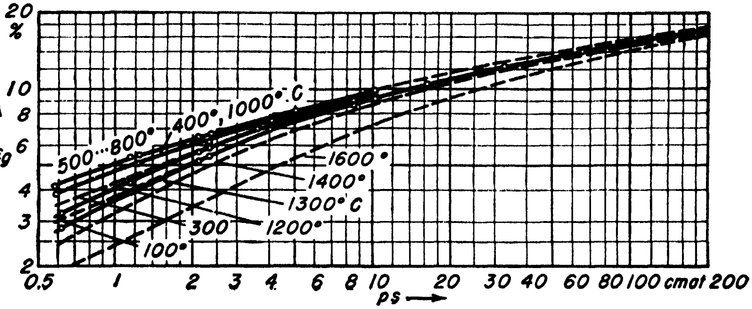

FIG. 115. Emissivity of carbon dioxide. This plot is in the metric system (1 cm = 0.394 in.). (*From E. Eckert, VDI-Forschungsheft* 387, 1937.)

---

[1] A. Schack, *Z. tech. Physik*, **5**, 267–278 (1924).

[2] H. C. Hottel and H. G. Mangelsdorf, *Trans. Am. Inst. Chem. Engrs.*, **31**, 517–549 (1935).

[3] E. Eckert, *VDI-Forschungsheft* 387, 1937.

emissivity decreases at higher temperatures, the curve for 1600 C in Fig. 115 is taken from Hottel's values.

The first measurements on water vapor were done by E. Schmidt.[1] He investigated various thicknesses of pure water vapor. Experiments by Hottel and Mangelsdorf[2] with water vapor–air mixtures of 22-in. thickness agree with Schmidt's values at high partial pressures of the water vapor but are much lower at low partial pressures. Measurements by E. Schmidt and E. Eckert[3] brought out the explanation for these differences. They showed that Beer's law is not valid for water vapor, that the emissivity of this gas at a constant product of partial pressure times thickness is smaller for small partial pressures. This can be accounted for if the emissivity of pure water vapor is multiplied by a reduction factor less than 1 as soon as the partial pressure is less than 1 atm. Figure 116 shows the emissivity of pure water vapor according to the measurements of Schmidt. The small diagram

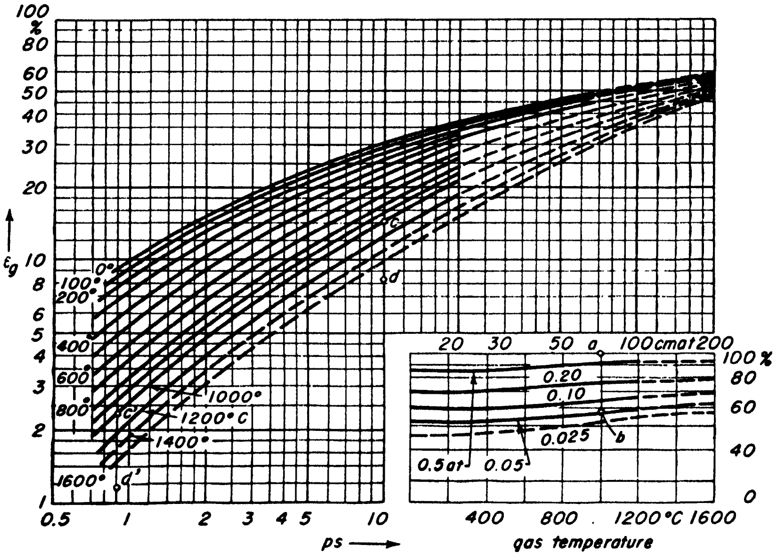

FIG. 116. Emissivity of water vapor. This plot is in the metric system (1 cm = 0.394 in.) (*According to measurements by E. Schmidt, H. Hottel, H. Mangelsdorf, and E. Eckert.*)

---

[1] E. Schmidt, *Forsch. Gebiete Ingenieurw.*, **3**, 57–70 (1932).

[2] H. C. Hottel and H. G. Mangelsdorf, *Trans. Am. Inst. Chem. Engrs.*, **31**, 517–549 (1935).

[3] E. Schmidt and E. Eckert, *Forsch. Gebiete Ingenieurw.*, **8**, 87 (1937).

gives the reduction factor. The measurements of Hottel and Mangelsdorf give higher values for the reduction factor than the measurements of Eckert. The factors in Fig. 116 are mean values derived from a paper by Schwiedessen,[1] who compared all measurements and extrapolated them to higher temperatures. As the scale of the diagram is logarithmic it may be used in the following way. To determine, for instance, the emissivity of water vapor at a partial pressure $p = 0.711$ lb/in.$^2$ $= 0.05$ atm, a thickness of the gas layer $s = 6.56$ ft $= 200$ cm, and a temperature of 1830 F = 1000 C build the product $ps = 10$ cm atm. Pure water vapor would have an emissivity at the same value $ps$ which is determined by point $c$ in the large diagram. The reduction factor is represented in the small diagram. If from this diagram the length $ab$ is taken and plotted in the large diagram downward from point $c$, point $d$ is reached, which determines the emissivity $\epsilon = 0.082$ of water vapor with $p = 0.05$ atm and $s =$ 200 cm. The method used in Fig. 116 assumes that the reduction factor does not depend on the product $ps$. In the range of the full lines in Fig. 116 this was proved by experiments. In the range of the dotted lines no experimental investigations are available. Hottel assumes, from experiments by Eberhardt on a furnace, that at great thicknesses and high temperatures no reduction is necessary.

All measurements were carried out at a total pressure of the mixtures equal to 1 atm. At higher pressures the radiation increases because the number of radiating molecules in a given thickness of the layer increases. It is probable, however, that the radiation of any molecule also increases with pressure. No measurements are available for gas radiation at higher pressures. Radiation at higher pressures is important for analysis of heat transfer in the cylinders of internal-combustion engines and rockets.

The emissivities in Figs. 115 and 116 introduced into Eq. (222) give the amount of heat which is radiated from a volume of gas, with the shape of a hemisphere, to a surface element $dA$, per unit area of this surface (Fig. 117$a$). Only in this case do all rays coming from different directions have the same path length. In all other cases, *e.g.*, in Fig. 117$b$, the path lengths differ in different directions and the radiation must be determined by integration. Such calculations were made by Nusselt, Jakob, E.

---

[1] H. Schwiedessen, *Arch. Eisenhüttenw.*, **14**, 9–14, 145–153, 207–210 (1940).

Schmidt, Hottel, and Eckert. Hottel showed that the radiation from a gas volume of any shape can be replaced by the radiation from a hemisphere with an *equivalent radius.* The values of this *equivalent radius* for different shapes are compiled in Table 11. H. Hausen[1] and F. M. Port[2] found that the formula

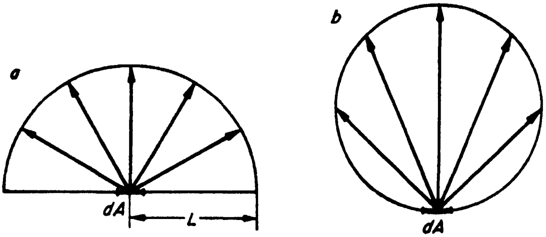

FIG. 117. Equivalent radius for different gas shapes.

$$L_e = 0.9\,\frac{4V}{A}$$

in which $L_e$ is the equivalent radius, $V$ the volume, and $A$ the surface of the gas volume, can be used as a fairly good first

TABLE 11. EQUIVALENT RADII $L_e$ OF GAS VOLUMES OF DIFFERENT SHAPE†

| Shape of gas volume | $L_e$ |
|---|---|
| Circular cylinder: height = diameter = $d$ | |
| Irradiation into the center of the base | $0.77d$ |
| Circular cylinder: height = $\infty$, diameter = $d$ | |
| Irradiation into the convex surface | $0.95d$ |
| Cylinder: height = $\infty$, base semicircle with radius $r$ | |
| Irradiation into the center of the plane rectangular surface | $1.26r$ |
| Sphere: diameter = $d$ | |
| Irradiation into the surface | $0.65d$ |
| Volume between two infinite planes separated by distance $l$ | |
| Irradiation into the planes | $1.8l$ |
| Circular cylinder: height = $\infty$, diameter = $d$ | |
| Irradiation into the center of the base | $0.9d$ |
| Tube bundle:* | |
| In triangular arrangement, $s = d$ | $3.0s$ |
| $s = 2d$ | $3.8s$ |
| In square arrangement, $s = d$ | $3.5s$ |
| Cube: length = $a$ | |
| Irradiation into each surface plane | $0.66a$ |

* $s$ = distance of tubes, $d$ = diameter.

† According to H. C. Hottel and E. Eckert.

---

[1] According to a communication in a letter.

[2] F. M. Port, "Heat Transmission by Radiation from Gases," Sc.D. thesis, Mass. Inst. Technology, 1939.

approximation. The formula is similar to the one giving the hydraulic diameter of a tube.

## HEAT EXCHANGE BY RADIATION

### 38. Black bodies

When different heated bodies are arranged so that they can *see* each other, every body radiates heat to the others and absorbs heat radiated from the other bodies. The hotter bodies lose more heat by radiation than they absorb. For the cooler bodies the inverse is true. In this way a heat flow from the hotter to the cooler bodies arises which will be calculated in the following paragraphs. In this chapter it is assumed that the surfaces of the radiating bodies are black. In Fig. 118, $dA_1$ and $dA_2$ may represent surface elements of two radiating bodies. The distance between them is $s$, and the angles between any of the two normals to the surfaces and the connecting line $s$ are $\beta_1$ and $\beta_2$, respectively. Then the heat $dQ_1$ radiated per unit time from surface $dA_1$ within the solid angle under which $dA_2$ is seen from $dA_1$ is, according to Eqs. (214) and (215),

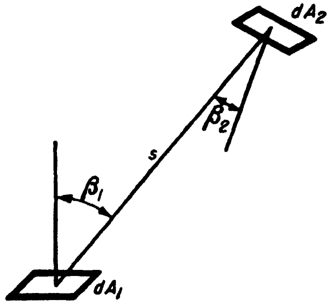

FIG. 118. Heat exchange by radiation of two small surfaces.

$$dQ_1 = i_{n1} \cos \beta_1 \, d\omega_1 \, dA_1 \tag{224}$$

where $i_{n1}$ is the radiation intensity of $dA_1$ in the normal direction, and $d\omega_1$ is the solid angle under which $dA_2$ is seen from $dA_1$. The expression

$$d\omega_1 = \frac{dA_2 \cos \beta_2}{s^2} \tag{225}$$

gives this angle. Equation (224) becomes

$$dQ_1 = i_{n1} \frac{\cos \beta_1 \cos \beta_2}{s^2} dA_1 \, dA_2$$

In the same way the heat $dQ_2$ radiated from $dA_2$ to $dA_1$ is

$$dQ_2 = i_{n2} \cos \beta_2 \, d\omega_2 \, dA_2 = i_{n2} \frac{\cos \beta_1 \cos \beta_2}{s^2} dA_1 \, dA_2 \tag{225a}$$

This amount of heat is absorbed by the black surface $dA_1$. The flow from $dA_1$ to $dA_2$ originated by the exchange of thermal radiation is therefore

$$dQ = dQ_1 - dQ_2 = (i_{n1} - i_{n2}) \frac{\cos \beta_1 \cos \beta_2}{s^2} dA_1 \, dA_2$$

The radiation intensity $i_{n1}$ of the black surface in a direction normal to the surface is given by

$$i_{n1} = \frac{\sigma}{\pi} T_1^4 \tag{226}$$

An analogous equation holds for the radiation intensity $i_{n2}$. Therefore

$$dQ = \frac{\cos \beta_1 \cos \beta_2}{s^2} dA_1 \, dA_2 \frac{\sigma}{\pi} (T_1^4 - T_2^4) \tag{227}$$

By this equation the heat exchange of two small surfaces with arbitrary positions can be calculated. By integration it is possible to calculate the heat exchange of surfaces whose sizes are not small when compared with the distances between them. For simplifying these calculations it is useful to introduce a new conception, the *geometrical factor F*. The geometrical factor $dF_{1-2}$ of $dA_1$ with respect $dA_2$ is the heat $dQ_1/dA_1$ radiated per unit area from $dA_1$ to $dA_2$, divided by the emissive power $e_1$ of $dA_1$. The latter is $e_1 = \pi i_{n1}$. Dividing Eq. (224) by this expression, there is obtained

$$dF_{1-2} = \frac{1}{\pi} \cos \beta_1 \, d\omega_1 \tag{228}$$

Therefore the geometrical factor is fixed by a pure geometrical relation. The heat radiated from $dA_1$ and intercepted by $dA_2$ can now be written as

$$dQ_1 = e_1 \, dF_{1-2} \, dA_1$$

In the same way, the heat radiated from $dA_2$ and intercepted by $dA_1$ is, according to Eqs. (225*a*) and (225),

$$dQ_2 = i_{n2} \cos \beta_1 \, d\omega_1 \, dA_1 = e_2 \, dF_{1-2} \, dA_1$$

and the heat exchange is

$$dQ = (e_1 - e_2) \, dF_{1-2} \, dA_1 = \sigma \, dF_{1-2} \, dA_1 \, (T_1^4 - T_2^4) \tag{229}$$

The calculations can be referred in the same way to the surface element $dA_2$, and thus is obtained

$$dQ = (e_1 - e_2)\, dF_{2-1}\, dA_2 = \sigma\, dF_{2-1}\, dA_2\, (T_1^4 - T_2^4) \qquad (230)$$

The geometrical factor $dF_{2-1}$ of $dA_2$ with respect to $dA_1$ is

$$dF_{2-1} = \frac{1}{\pi} \cos \beta_2\, d\omega_2$$

The heat exchange by radiation between two surfaces whose size is not small when compared with their distance apart can be determined by double integration of Eq. (227). Results of such integrations can be found in the different books dealing with heat transfer.[1] The numerical integration can be replaced by a graphical procedure first mentioned by R. A. Hermann (1900). According to Eq. (228) the geometrical factor of a surface element $dA_1$ with respect to a finite surface $A_2$ is

$$F_{1-2} = \frac{1}{\pi} \int \cos \beta_1\, d\omega_1 \qquad (231)$$

The expression under the integral sign $\cos \beta_1\, d\omega_1$ is the projection of the solid-angle element $d\omega_1$ on the plane of the radiating surface $dA_1$. The integral is the sum of the projections of all solid-angle elements $d\omega_1$, or the projection of the solid angle corresponding to the whole surface $A_2$ on the plane of $dA_1$. From this the following construction arises: we must project by central projection the surface $A_2$ (denoted by 1 in Fig. 119) to the surface of a hemisphere with the radius $R$. This projection 1′ must be projected once more by normal projection to the plane of the radiating surface $dA_1$. The area of this second projection 1″ divided by the area of the circle $R^2\pi$ gives the geometrical factor $F_{1-2}$ as can be seen from Eq. (231). This graphical construction can

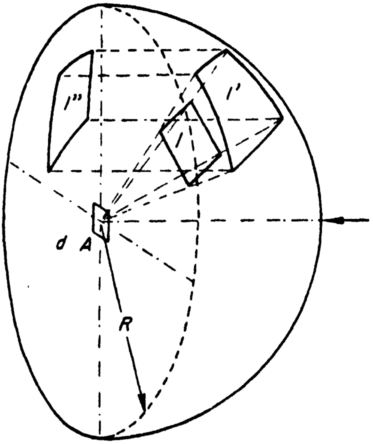

FIG. 119. Determination of the geometrical factor for a surface 1.

---

[1] For example, W. H. McAdams, "Heat Transmission," 2d ed. McGraw-Hill Book Company, Inc., New York, 1942; E. Eckert, "Technische Strahlungsaustauschrechnungen," Berlin, 1937.

be replaced by a simple mechanical integrator[1] or by optical projection.[2] For this purpose a point lamp is arranged in the center of the hemisphere in Fig. 119. The area 1, the geometrical factor of which is to be determined, is made of cardboard and arranged in the proper position. It is projected by the point lamp as shadow to a milk-glass hemisphere. When this hemisphere is photographed from a great distance in direction of the arrow the ratio of the shadow of the cardboard area to the area of the circle representing the glass sphere is the geometrical factor. Figures 120 and 121 show two such photographs. Figure 120 determines the geometrical factor of the radiation cooling surfaces in the furnace of the steam boiler (Fig. 124) as seen from the center of the stoker. Figure 121 determines the geometrical factor of the tungsten spiral as used in an electric bulb. It was produced by arranging the model of the spiral in a short distance before the point lamp.[3] To determine the geometrical factor for a finite surface $A_1$ against a finite surface $A_2$, the surface $A_1$ must be divided into small areas of equal size and the construc-

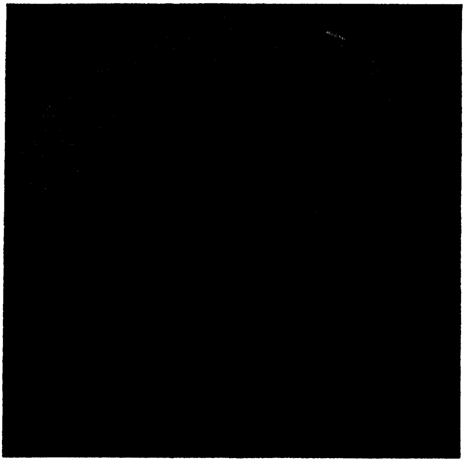

FIG. 120. Photographic determination of the geometrical factor of the radiation cooling surface in the furnace of a steam boiler as seen from the center of the stoker. [*From E. Eckert, Z. Ver. deut. Ing.*, **79**, 1495–1496 (1935).]

---

[1] H. Hottel, *Mech. Eng.*, **52** (1930); V. H. Cherry, D. D. Davis, and L. M. K. Boelter, *Trans. Illum. Eng. Soc.* (*N.Y.*), 1939.

[2] E. Eckert, *Z. Ver. deut. Ing.*, **79**, 1495–1496 (1935).

[3] *Ibid.*

tion shown in Fig. 119 performed for the centers of every one of these areas. The average value of all the geometrical factors determined in this way is the geometrical factor $F_{1-2}$ of $A_1$ against $A_2$. With this factor the heat exchange $Q$ between the two surfaces is

$$\mathbf{Q} = \mathbf{F}_{1-2}\mathbf{A}_1\sigma(\mathbf{T}_1^4 - \mathbf{T}_2^4) \tag{232}$$

The construction can be made also for small areas into which surface $A_2$ is divided. The average value of all the geometrical factors determined in this way gives the geometrical factor $F_{2-1}$ of $A_2$ against $A_1$. Now the heat exchange $Q$ can be written

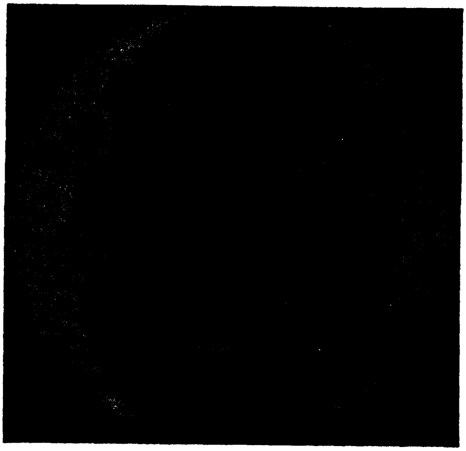

FIG. 121. Photographic determination of the geometrical factor of the tungsten coil in an electric bulb. [*From E. Eckert, Z. Ver. deut. Ing.*, **79**, 1495–1496 (1935).]

$$Q = F_{2-1}A_2\sigma(T_1^4 - T_2^4) \tag{233}$$

Therefore, the heat flow $Q$ can be calculated with either of the surfaces $A_1$ or $A_2$ with the corresponding geometrical factor. It is advantagous to use that one of the two possibilities for which the geometrical factor is easier to calculate. Where, for instance, the surface $A_1$ is completely surrounded by the surface $A_2$ and everywhere convex, it can be stated at once that the geometrical factor $F_{1-2}$ of $A_1$ is equal to one since all heat rays emitted from $A_1$ impinge on the surface $A_2$.

## 39. Solid, liquid, and gaseous bodies

If the surfaces which exchange heat by radiation are not black, conditions become more involved, since part of the thermal radiation is reflected by the surfaces. Some of the radiation travels in this way to and fro between the surfaces until it is finally absorbed. The influence of this action on the heat flow can best be studied with two parallel surfaces whose distance apart is small compared with their size, so that practically all radiation emitted by one surface falls upon the second. The geometrical factor of either surface is therefore one. In Fig. 122, the travel of a heat ray emitted by the surface 1 is traced. The emissive power of the radiation emitted from this surface per unit time and area is $e_1$. From it a part $\alpha_2 e_1$ is absorbed on surface 2, a part $\rho_2 e_1$ is reflected back to surface 1. Here a part $\alpha_1 \rho_2 e_1$ is absorbed; $\rho_1 \rho_2 e_1$ is reflected to surface 2, etc. The amount of heat which left surface 1 per unit time and area is therefore

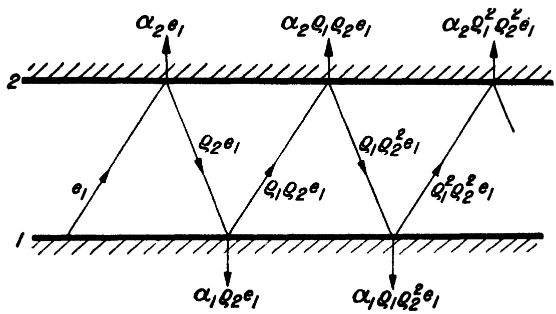

FIG. 122. Radiant heat exchange between two parallel surfaces.

$$
\begin{aligned}
q_1 &= (1 - \alpha_1 \rho_2 - \alpha_1 \rho_1 \rho_2^2 - \alpha_1 \rho_1^2 \rho_2^3 - \cdots)e_1 \\
&= [1 - \alpha_1 \rho_2 (1 + \rho_1 \rho_2 + \rho_1^2 \rho_2^2 + \cdots)]e_1
\end{aligned}
$$

The series within the parentheses gives $1/(1 - \rho_1 \rho_2)$, since $\rho_1$ and $\rho_2$ are smaller than one. Therefore

$$
q_1 = \left(1 - \frac{\alpha_1 \rho_2}{1 - \rho_1 \rho_2}\right) e_1
$$

For bodies opaque to thermal radiation, Eq. (211) holds true, and for thermal radiation generally, Kirchhoff's law, Eq. (213). By substituting the emissivity $\epsilon$ instead of $\alpha$ and $\rho$ the equation is

$$
q_1 = \left[1 - \frac{\epsilon_1 (1 - \epsilon_2)}{\epsilon_1 + \epsilon_2 - \epsilon_1 \epsilon_2}\right] e_1 = \frac{\epsilon_2}{\epsilon_1 + \epsilon_2 - \epsilon_1 \epsilon_2} e_1
$$

On the other hand, surface 2 emits radiation of emissive power $e_2$. From it, $\alpha_1 e_2$ is absorbed by surface 1. The rest is reflected, impinges on surface 2, and is there partly reflected back to surface 1. Here the part $\alpha_1\rho_1\rho_2 e_2$ is absorbed, the rest reflected, etc. By summing up all radiation absorbed by surface 1 there is obtained

$$q_2 = \alpha_1(1 + \rho_1\rho_2 + \rho_1^2\rho_2^2 + \cdot\cdot\cdot)e_2$$

which gives as before,

$$q_2 = \frac{\alpha_1}{1 - \rho_1\rho_2} e_2 = \frac{\epsilon_1}{\epsilon_1 + \epsilon_2 - \epsilon_1\epsilon_2} e_2$$

The heat flowing from surface 1 to surface 2 per unit time and area is

$$q = q_1 - q_2 = \frac{\epsilon_2 e_1 - \epsilon_1 e_2}{\epsilon_1 + \epsilon_2 - \epsilon_1\epsilon_2}$$

The emissive power $e_1$ is

$$e_1 = \epsilon_1\sigma T_1^4$$

and an analogous expression holds true for $e_2$. Introducing these we obtain

$$q = \frac{\sigma}{\dfrac{1}{\epsilon_1} + \dfrac{1}{\epsilon_2} - 1} (T_1^4 - T_2^4) \tag{234}$$

The fraction is called the *interchange factor* and is denoted by $\epsilon_{1-2}$. Therefore

$$q = \epsilon_{1-2}\sigma(T_1^4 - T_2^4) \tag{235}$$

For two parallel walls,

$$\frac{1}{\epsilon_{1-2}} = \frac{1}{\epsilon_1} + \frac{1}{\epsilon_2} - 1 \tag{236}$$

For two coaxial spheres, or cylinders whose surfaces radiate diffusely, the interchange factor was calculated as

$$\frac{1}{\epsilon_{1-2}} = \frac{1}{\epsilon_1} + \frac{A_1}{A_2}\left(\frac{1}{\epsilon_2} - 1\right) \tag{237}$$

where $A_1$ is the surface of the smaller body, and Eq. (235) gives the heat flow leaving this body per unit time and area.[1] When the cylinders or spheres reflect specularly Eq. (236) holds true for them also.

---

[1] E. Eckert, *op. cit.*

For two surfaces whose size is small compared with their distance apart (Fig. 118), the fraction of the reflected radiation which falls back to the radiating surface becomes so small that it can be neglected. The interchange factor then becomes

$$\epsilon_{1-2} = \epsilon_1 \epsilon_2 \tag{238}$$

This equation generally gives a lower limit for the interchange factor. The upper limit is 1.

In a way similar to the radiation exchange between two parallel walls the interchange between a gas and the enclosing walls can be calculated if it is assumed that the walls have *gray* surfaces.[1] The interchange factor $\epsilon_{g-w}$ between the gas and the wall is

$$\frac{1}{\epsilon_{g-w}} = \frac{1}{\epsilon_g} + \frac{1}{\epsilon_{g\infty}\epsilon_w} - \frac{1}{\epsilon_{g\infty}} \tag{239}$$

if $\epsilon_g$ is the emissivity of the gas (see Figs. 115 and 116) and $\epsilon_{g\infty}$ is the emissivity of the same gas with an infinitely thick layer. $\epsilon_{g\infty}$ can be determined in Figs. 115 and 116 by extrapolation. $\epsilon_w$ is the emissivity of the walls. The heat flow per unit wall area is

$$q = \epsilon_{g-w}\sigma T_g^4 - \epsilon_{g-w}\sigma T_w^4 \tag{240}$$

Into the first summand $\epsilon_g$ and $\epsilon_w$ have to be introduced at gas temperature, into the second at wall temperature. When the emissivity of the walls is great (in the neighborhood of 1), the interchange factor can be calculated with the simpler equation

$$\epsilon_{g-w} = \epsilon_g \epsilon_w \tag{241}$$

**Example.** The heat exchange by radiation between the two walls of a Thermos bottle is to be calculated. The walls may be silvered on the sides turned toward each other. The content of the bottle may have a temperature of $t_1 = 212$ F, the ambient temperature is $t_2 = 68$ F. The inner and outer walls have practically also these temperatures. The emissivity of silver is $\epsilon = 0.02$ (see Table 18). As the surfaces reflect specularly, Eq. (236) must be used to determine the interchange factor.

$$\frac{1}{\epsilon_{1-2}} = \frac{1}{0.02} + \frac{1}{0.02} - 1 = \frac{1}{0.01}$$

The heat flow per unit area of the inner wall is

$$q = 0.01 \times 0.173 \times 10^{-8}[(212 + 460)^4 - (68 + 460)^4]$$
$$= 2.19 \qquad \text{Btu/(hr)(ft}^2\text{)}$$

---

[1] E. Eckert, *VDI-Forschungsheft* **387**, 1937, p. 19.

To get the same insulation effect by a cork layer, its thickness must be

$$b = \frac{k}{q}(t_1 - t_2) \text{ with } k = 0.025 \text{ Btu/(hr)(ft)(F)}$$

This gives

$$b = \frac{0.025(212 - 68)}{2.19} = 1.65 \text{ ft}$$

It can be seen that the insulating effect of the Thermos bottle is excellent even though it must be kept in mind that some additional losses by conduction in the glass walls occur. The loss by radiation can be decreased by arranging walls silvered on both sides between the inner and outer wall. With $n$ additional walls the heat loss is decreased by the factor $1/(n + 1)$.

The small radiation exchange between metal surfaces is utilized in Alfol insulation. This insulation is built up from aluminum foils which surround the body to be insulated at approximately ½-in. distance from each other. The total heat flow through the insulation is by radiation, conduction through the air space between the foils, and convection. The convection parts are comparatively small as long as the distance between the foils is kept low enough and the conduction is small since air is a good insulator.

## 40. Radiation of flames

From the emissivity charts for carbon dioxide and water vapor, the radiation of combustion gases after completion of combustion can be calculated, *e.g.*, the heat transfer by radiation within the convective heating surface of water-tube boilers. The radiation of flames is mostly considerably greater than the radiation as computed from the carbon dioxide and water molecules present.

Most fuels burn with a luminous flame. The yellow glow of a flame comes from the hydrocarbons which are evaporated from the fuel and are gradually split up in the flame. Thereby are formed molecules which have an increasing percentage of carbon, and there occur carbon particles which glow in the flame and give it the yellowish color. These particles also emit considerable thermal radiation. All bituminous fuels, *e.g.*, wood, lignite, and the younger coals, and all gasolines burn in this way with luminous flames. Only anthracite, coke, and some gases (generator gas, hydrogen, blast-furnace gas) have nonluminous flames. The faint bluish shine which these flames emit and which is called *chemoluminosity* arises from the chemical reactions within the gaseous components. It is not connected, however, with any thermal radiation worth mentioning as was proved by several investigations. The emission of a luminous flame depends on the number of carbon particles, and this number varies greatly with the conditions under which the combustion occurs. It is influenced, for instance, by the mixing of air and the combustible gases and by the temperatures of both components. As long as these conditions cannot be predicted in a furnace there is no possibility of calculating the radiation of a flame exactly. For a first approximation, the flame may be considered as a black body, and the fact that this is not entirely true may be corrected for by an empirical factor $p$, smaller than 1. This gives for the heat flow $Q$ per unit time to the furnace wall the equation

$$Q = p\epsilon_w\sigma A(T_f^4 - T_w^4) \tag{242}$$

where $\epsilon_w$ is the emissivity (equal to the absorptivity) of the furnace walls, $T_f$ the absolute temperature of the flame, $T_w$ the absolute wall temperature, and $A$ the area of the wall. On the other hand this heat is taken from the enthalpy content of the gas:

$$Q = W(i_{th} - i_f) \tag{243}$$

where $W$ is the gas weight per unit time, $i_{th}$ is the enthalpy content of the gas at the theoretical combustion temperature, and $i_f$ is the enthalpy content at the flame temperature. (It is assumed that the gases leave the furnace with this temperature and that the heat loss of the gases by convection within the furnace can be neglected when compared with the radiated heat.) For such calculations enthalpy-temperature diagrams of combustion gases are very useful.[1]

The empirical factor $p$ depends mainly on the fuel and on the size of the furnace. For large furnaces $p$ is nearly unity. In water-cooled furnaces of steam boilers, the radiation from the flame to the cooling surface is increased by the radiation from the refractory-lined walls and from the fuel layer of the stokers and grates. The factor $p$ therefore is greater in furnaces in which only a small part is water-cooled than in furnaces whose walls are entirely lined with cooling surfaces. In furnaces of usual size, $p$ lies between 0.6 and 1. If the radiation of a cooling surface consisting of a row of tubes before a refractory wall is to be calculated with Eq. (242), there arises the question as to which area is to be used for $A$. Investigations on this difficulty were made by H. C. Hottel[1] and E. Eckert.[2] According to them, the area $A$ is determined by multiplying the area of the furnace walls before which the tubes are arranged by a factor $\psi$. This factor is represented in Fig. 123.

---

[1] R. Fehling, *Z. Ver. deut. Ing.*, **71**, 383 (1927); also "Das I-t Diagram der Verbrennung," Berlin, 1929.

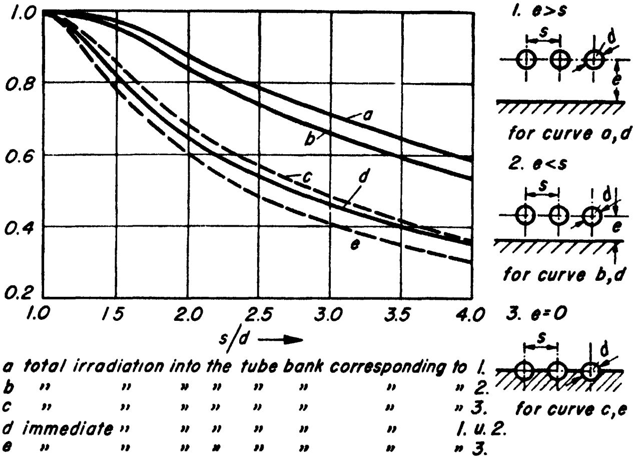

FIG. 123. Radiation factor $\Psi$ for a row of tubes before a refractory wall. [*From E. Eckert, Arch. Waermewirt.*, **13** (1932).]

Different authors, of whom the most important are Wohlenberg[3] and Hottel[4] with their coworkers, give more detailed treatments for radiation calculations in furnaces.

**Example.** The heat absorption by the cooling surface in the combustion chamber of a steam boiler is to be calculated. Figure 124 shows this cooling surface to consist of rows of tubes before the refractory walls. The steam pressure of the boiler may be 1,000 lb/in.$^2$ To this pressure there corresponds a saturation temperature 544.6 F. The external temperature of the tube walls is somewhat higher; it may be assumed to be 600 F. The flame temperature may be 2500 F. The spacings of the tubes along the cooling surface may be $2d$ ($d$ = diameter).

---

[1] H. C. Hottel, *Mech. Eng.*, **52**, 699 (1930); *Trans. ASME*, **53**, 265 (1931).

[2] E. Eckert, *Hauptverein deutscher Ingenieure Mitt.*, 1931, pp. 483–486; *Arch. Wärmewirt.*, **13**, 241 (1932).

[3] W. J. Wohlenberg and H. F. Mullikin, *Trans. ASME*, **57**, 531–540 (1935).

[4] H. C. Hottel, *Trans. ASME*, **53**, 265–273 (1931); *Mech. Eng.*, **52**, 699 (1932).

First of all the surface area $A$ which is to be introduced into Eq. (242) must be calculated. From Fig. 123, on the line $a$ is found $\psi = 0.88$ (the distance of the tubes from the wall may be $> s$). The area of the wall which is lined with cooling tubes is

$$5.25 \times 14.75 + 5.25 \times 17.4 = 168.7 \text{ ft.}^2$$

The surface $A$ is $168.7 \times 0.88 = 148.4$ ft.$^2$ The factor $p$ in Eq. (242) may be 0.87. The emissivity $\epsilon_w$ of the tubes is taken from Table 18 as $\epsilon_w = 0.8$ since the tube surface is covered with the scale in the rolling process and often with slag. Now Eq. (242) gives

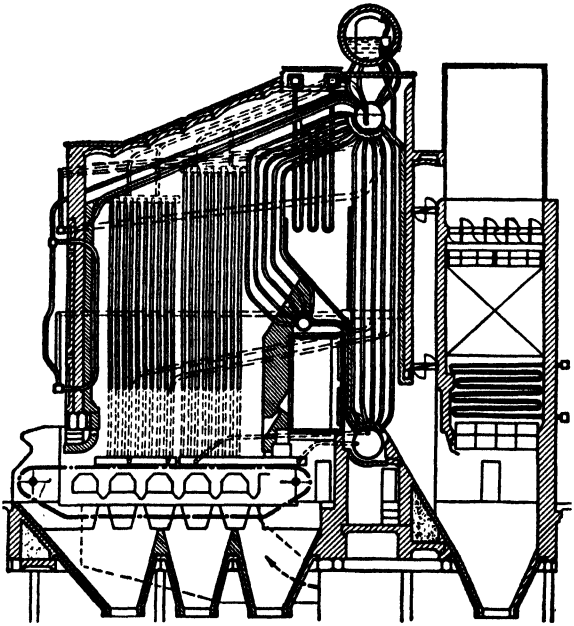

FIG. 124. Steam boiler with radiation heating surface.

$$Q = 0.87 \times 0.8 \times 0.173 \times 10^{-8} \times 148.4[(2500 + 460)^4 - (600 + 460)^4]$$
$$= 13{,}430{,}000 \text{ Btu/hr}$$

The heat of vaporization at 1,000 lb/in.$^2$ is 649.4 Btu/hr. Therefore the cooling surface generates 13,430,000/649.4 = 20,700 lb/hr of steam. The surface of the tubes is greater than the area of the wall which is lined with the tubes by the factor $d\pi/s$. The tube surface therefore is $(\pi/2)168.7 = 265$ ft$^2$, and the steam generation per square foot of the tube surface is 78.2 lb/(hr)(ft$^2$). The heat absorption per square foot of tube surface is 13,430,000/265 = 50,700 Btu/(hr)(ft$^2$).

## 41. The heat-transfer coefficient for radiation

Often heat transfer occurs simultaneously by convection and radiation. As long as the radiation takes place between solid surfaces neither mode of heat transfer interferes with the other. In heat transfer between a gas and a wall exchanging heat by radiation and convection some interference between both ways of heat exchange occurs but it is very difficult to calculate this effect. Therefore usually both parts of the total heat flow are calculated separately and summed up. Since the heat flow by convection is expressed by a film heat-transfer coefficient, it is useful in many cases to build a heat-transfer coefficient $h_r$ for the radiated heat in the same way, by dividing the heat flow per unit area $q$ by the temperature difference:

$$h_r = \frac{q}{t_1 - t_2} = \epsilon_{1-2}\sigma F_{1-2}\frac{T_1^4 - T_2^4}{T_1 - T_2} = \epsilon_{1-2}\sigma F_{1-2}f(T_1, T_2) \qquad (243a)$$

Contrary to the convection heat-transfer coefficient this one depends very much on the temperatures $T_1$ and $T_2$.

The temperature function

$$f(T_1, T_2) = \frac{T_1^4 - T_2^4}{T_1 - T_2}$$

is tabulated in Table 12. This function must be multiplied by the interchange factor $\epsilon_{1-2}$, by the Stephan-Boltzmann constant $\sigma$, and by the geometrical factor $F_{1-2}$ in order to get the radiation heat-transfer coefficient. This coefficient increases very much with the temperatures.

**Example.** The combustion-chamber walls of modern steam boilers are lined with cooling tubes, which absorb heat radiated from the flame and decrease the flame temperature. Through these cooling tubes circulates the boiling water contained in the boiler. Here arises the interesting question as to how the total heating surface must be divided into this cooling surface and the convective surface in order to get the steam generation per unit heating surface as high as possible. To see this it is necessary to calculate the heat-transfer coefficients for the radiation cooling surfaces and the convective surface. The tubes of the boiler may be of 2-in. diameter. For the convective surface these tubes may be arranged on the corners of triangles with equal sides 4-in. long (Fig. 125). Let the velocity of the combustion gases at the entrance of the convective surface be 15 fps, and consider the gases to contain

TABLE 12. TEMPERATURE FACTOR $(T_1^4 - T_2^4)/(T_1 - T_2) \times 10^{-8}$ FOR THE RADIATION HEAT-TRANSFER COEFFICIENT

| $t_2$ F \ $t_1$ F | −460 | −200 | 0 | 200 | 400 | 600 | 800 | 1000 | 1200 | 1400 | 1600 | 1800 | 2000 |
|---|---|---|---|---|---|---|---|---|---|---|---|---|---|
| −460 | 0 | | | | | | | | | | | | |
| −200 | 0.176 | 0.703 | | | | | | | | | | | |
| 0 | 0.973 | 2.011 | 3.894 | | | | | | | | | | |
| 200 | 2.875 | 4.628 | 7.246 | 11.50 | | | | | | | | | |
| 400 | 6.361 | 9.041 | 12.56 | 17.87 | 25.44 | | | | | | | | |
| 600 | 11.91 | 15.72 | 20.29 | 26.81 | 35.75 | 47.64 | | | | | | | |
| 800 | 20.00 | 25.16 | 30.95 | 38.85 | 49.35 | 62.95 | 80.00 | | | | | | |
| 1000 | 31.12 | 37.83 | 44.99 | 54.43 | 66.61 | 82.05 | 101.2 | 124.5 | | | | | |
| 1200 | 45.74 | 54.20 | 62.90 | 74.03 | 88.08 | 105.5 | 126.8 | 152.5 | 183.0 | | | | |
| 1400 | 64.35 | 74.78 | 85.18 | 98.17 | 114.2 | 133.9 | 157.5 | 185.7 | 218.9 | 257.4 | | | |
| 1600 | 87.42 | 100.0 | 112.3 | 127.3 | 145.5 | 167.5 | 193.6 | 224.4 | 260.4 | 302.0 | 349.7 | | |
| 1800 | 115.4 | 130.4 | 144.7 | 161.9 | 182.5 | 206.9 | 235.7 | 269.3 | 308.3 | 353.0 | 404.0 | 461.6 | |
| 2000 | 148.9 | 166.4 | 182.9 | 202.4 | 225.5 | 252.6 | 284.2 | 320.8 | 362.8 | 410.8 | 465.3 | 526.5 | 595.6 |

14 per cent carbon dioxide and 7 per cent water. The surface temperature of the tube walls may be 600 F.

The heat absorption of one tube of the radiation surface is given by Eq. (242). The area $A$ for 1-ft tube length is $\psi s$ ($s$ = distance of tubes). The heat-transfer coefficient by radiation is found by dividing the heat flow $Q$ by the tube surface area and by the difference between the flame temperature $T_f$ and the surface temperature $T_w$ of the tube:

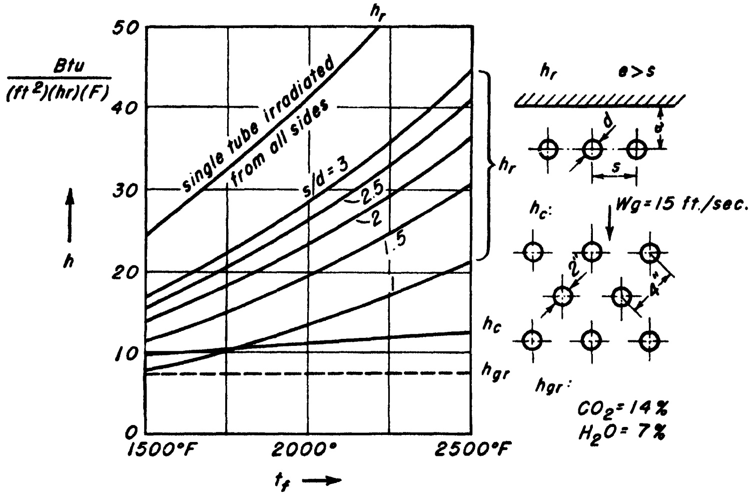

FIG. 125. Comparison of radiation heat-transfer coefficients $h_r$ and convection heat-transfer coefficients $h_c$ as functions of the gas temperature.

$$h_r = \frac{p\epsilon_w\psi s\sigma}{d\pi}\,\frac{T_f^4 - T_w^4}{T_f - T_w}$$

The combustion chamber may be large; therefore $p = 1$ and $\epsilon_w = 0.94$. Otherwise, the same numerical values are used as in the previous example:

$$h_r = \frac{0.94 \times 0.88 \times 0.173 \times 10^{-8} \times 2}{\pi}\,\frac{(2{,}500 + 460)^4 - (600 + 460)^4}{2{,}500 - 600}$$
$$= 36.3 \text{ Btu/(hr)(ft}^2\text{)(F)}$$

By introducing other values for the ratio $r/d$ of tube distance to tube diameter and for the flame temperature, the heat-transfer coefficients $h_r$ in Fig. 125 were determined.

Now the heat-transfer coefficient $h_b$ for the tubes within the convective surface must be calculated. This coefficient comprises heat transfer by gas radiation and heat transfer by convection. For calculating the radiation of carbon dioxide and water in the combustion gases the equivalent length $L$ of the gas layer must be known. From Table 11 take $L = 3d = (3 \times 2)/12 = 0.5$ ft, for the arrangement of tubes used here. The partial pressure of the carbon dioxide is equal to $p = 0.14$ atm for a total pressure of 1 atm; therefore the product $pL$ is 0.07 ft-atm. The gas temperature may be assumed to be 1800 F. From Fig. 115 the emissivity of carbon dioxide at 1800 F is $\epsilon_{CO_2} = 0.06$ and $\epsilon_{CO_2} = 0.055$ for 600 F. The emissivity of the tube wall is $\epsilon_w = 0.8$; therefore, the interchange factor becomes $0.8 \times 0.06 = 0.048$ for 1800 F and

$$0.8 \times 0.055 = 0.044 \text{ for } 600 \text{ F}$$

Now Eq. (240) gives the specific heat flow by the carbon dioxide radiation:

$$q_{CO_2} = 0.173 \times 10^{-8} \times 0.048(1{,}800 + 460)^4 - 0.173 \times 10^{-8} \times 0.044(600 + 460)^4 = 2065 \text{ Btu/(hr)(ft}^2\text{)}$$

For water vapor, the partial pressure is $p = 0.07$ atm; therefore the product $pL = 0.035$ ft atm. From Fig. 116 we take in the small diagram the distance of the curve 0.07 atm at 1800 F from the horizontal 100 per cent line and plot it downward in the main diagram from the intersection between the isotherm 1800 F and 600 F, respectively, and $pL = 0.035$ ft atm. This gives the emissivity $\epsilon_{H_2O} = 0.0156$ for 1800 F, and $\epsilon_{H_2O} = 0.0444$ for 600 F. The interchange factors are $0.8 \times 0.0156 = 0.0125$ and $0.8 \times 0.0444 = 0.0355$. The specific heat flow by water radiation is

$$q_{H_2O} = 0.173 \times 10^{-8} \times 0.0125(1{,}800 + 460)^4 - 0.173 \times 10^{-8} \times 0.0355(600 - 460)^4 = 487 \text{ Btu/(hr)(ft}^2\text{)}$$

and therefore the total heat flow by gas radiation is

$$487 + 2{,}065 = 2552 \text{ Btu/(hr)(ft}^2\text{)}$$

and the heat-transfer coefficient by gas radiation is

$$h_{gr} = \frac{2{,}552}{1{,}800 - 600} = 2.12 \text{ Btu/(hr)(ft}^2\text{)(F)}$$

The heat-transfer coefficient by convection can be calculated with Eq. (180) and the values in Table 9. It is found to be

$$h = 8.14 \text{ Btu/(hr)(ft}^2\text{)(F)}$$

Therefore, the total heat-transfer coefficient for the convective surface is $h_c = 2.12 + 8.14 = 10.26$ Btu/(hr)(ft²)(F) for 1800 F gas temperature. For other gas temperatures the values are found in Fig. 125.

A comparison between the values $h_r$ for the radiation cooling surface and the values $h_c$ for the convective surface in Fig. 125 shows that only for very small ratios of $s/d$ (tube distance to tube diameter) and flame temperatures under 1800 F does the convective surface have greater heat-transfer coefficients than the radiation cooling surface. It is therefore advantageous to line the whole combustion chamber with narrowly spaced cooling tubes as long as other considerations (difficulties in ignition, etc.) do not prevent this.

## CHAPTER 5

# THE EXCHANGE OF MASS

### 42. Basic equations for mixtures of two components

When some moist material is dried by an air stream flowing over it, the vapor rising from the surface is carried away with the air. But first the vapor must penetrate the boundary layer of the air. This process has great similarity to the exchange of heat from a solid body to a liquid or gas flow, and it has proved very useful to use this similarity in calculating the transfer of matter connected with the described drying process or with similar processes (absorption, dissolving of a solid body in a liquid, combustion of solid fuels, etc). In this chapter only the absorption of humidity by a solid body from an air stream and the evaporation of humidity into an air stream will be dealt with. First, the basic equations of humid air are compiled.

Humid air may be regarded as a mixture of air and water vapor. At normal pressures both components behave as ideal gases. For a mixture of ideal gases which do not react chemically, Dalton's law applies: where different gases are present in the same room, every gas fills the whole room as if the other gases were not present. The pressure which any of the gases creates according to the gas law is its *partial pressure.* The total pressure of the mixture of gases equals the sum of all partial pressures. If the partial pressure of air is denoted by $p_a$ and the partial pressure of the water vapor by $p_v$, the total pressure $p$ of the humid air is

$$p = p_a + p_v \tag{244}$$

Now consider a volume $V$ in which the air weight $W_a$ and the vapor weight $W_v$ are present at the temperature $T$. For air, according to Dalton's law the following equation is valid:

$$p_a V = W_a R_a T = W_a \frac{\mathcal{R}}{M_a} T \tag{245}$$

in which $R_a$ is the gas constant for air, $\mathcal{R}$ the universal gas constant, and $M_a$ the molecular weight of air. In the same way, for the water vapor, which may also be considered as an ideal gas,

$$p_v V = W_v R_v T = W_v \frac{\mathcal{R}}{M_v} T \tag{246}$$

where $R_v$ and $M_v$ are the gas constant and the molecular weight of water vapor, respectively. The universal gas constant has the numerical value $\mathcal{R} = 1{,}545.4$ ft-lb/lb mole, F.

For calculations with humid air it is useful to base all equations on one pound of dry air as the water-vapor content changes. The weight of water vapor per pound of dry air is called *specific humidity* and it is denoted by $s$.

From the above equation follows,

$$s = \frac{W_v}{W_a} = \frac{M_v}{M_a} \frac{p_v}{p_a} \tag{247}$$

The molecular weight of water vapor is 18; the molecular weight of air 29. Therefore

$$s = 0.622 \frac{p_v}{p_a} = 0.622 \frac{p_v}{p - p_v} \tag{248}$$

At a certain temperature, air can hold only a certain maximum content of water vapor. Air with this maximum content is said to be saturated. The saturation point is fixed by the condition that the partial pressure of the water vapor cannot be greater than the saturation pressure of water vapor corresponding to the air temperature. The saturation pressure belonging to different temperatures can be found in the *s-i* diagram Fig. *A* (page 254). The specific humidity of saturated air is fixed by the equation

$$s_s = 0.622 \frac{p_s}{p - p_s} \tag{249}$$

where $p_s$ denotes the saturation pressure.

The humidity of the air is often expressed by the ratio of the actual vapor pressure $p_v$ to the saturation pressure $p_s$ at the air temperature. This ratio is called *relative humidity* and denoted by $r$:

$$r = \frac{p_v}{p_s} \tag{250}$$

Sometimes the ratio of the specific humidities is used instead of the ratio of the partial pressures. This ratio,

$$\rho = \frac{s}{s_s} \tag{251}$$

can be expressed by the partial pressures of the water vapor. At low temperatures, the partial pressure of the vapor is very small as compared with the total barometric pressure. It can then be written instead of Eq. (248):

$$s \approx 0.622 \frac{p_v}{p}$$

and for saturated air

$$s_s \approx 0.622 \frac{p_s}{p}$$

Therefore

$$\rho = \frac{s}{s_s} \approx \frac{p_v}{p_s} = r$$

At low temperatures there is therefore no difference between the two ratios $r$ and $\rho$.

An amount of water exceeding the specific humidity at saturation can be held in the air only in liquid form as water droplets (fog) or in solid form as snow. The amount of water in 1 lb of dry air is $(s - s_s)$.

For the following calculations the enthalpy of moist air is needed. As long as the specific humidity does not exceed the saturation point, the enthalpy of moist air consists of the enthalpy of the dry air and the enthalpy of the water vapor. Now there arises the difficulty that commonly the temperature 0 F is used as a datum for air; however, the melting point (32 F) of ice is used as a datum point for water vapor. We will use here the temperature $t_0 = 32$ F as a datum for both air and water vapor. With the specific heat $c_{pa}$ of air at constant pressure the enthalpy of the dry air is $i_a = c_{pa}(t - t_0)$. The enthalpy $i_v$ of water vapor at low temperatures can be expressed in the form

$$i_v = c_{pv}(t - t_0) + i_{v,0}$$

with $c_{pv}$ the specific heat of water vapor at constant pressure, and $i_{v,0}$ the heat of vaporization at 32 F. The enthalpy of moist air is

$$i = i_a + s i_v = c_{pa}(t - t_0) + s[c_{pv}(t - t_0) + i_{v,0}] \tag{252}$$

with the numerical values $c_{pa} = 0.240$ Btu/(lb)(F), $c_{pv} = 0.44$ Btu/(lb)(F), and $i_{v,0} = 1076$ Btu/lb. When the air is supersaturated with water vapor the enthalpy of the liquid water $i_f = t - t_0$ must be added. This gives

$$i = c_{pa}(t - t_0) + s_s[c_{pv}(t - t_0) + i_{v,0}] + (s - s_s)(t - t_0) \quad (253)$$

The enthalpy of ice is $i_i = -i_{s,0} + c_i(t - t_0)$ with the heat of fusion $i_{s,0}$ equal to 143 Btu/lb, and the specific heat of ice $c_i$ equal to 0.5 Btu/(lb)(F). The enthalpy of ice has a negative value since the enthalpy of liquid water at 32 F is fixed to be zero. The enthalpy of air with ice fog is

$$i = c_{pa}(t - t_0) + s_s[c_{pv}(t - t_0) + i_{v,0}] - (s - s_s)[i_{s,0} - c_i(t - t_0)] \quad (254)$$

Equation (252) must be applied as long as $s < s_s$. For $s > s_s$ and $t > 32$ F Eq. (253) must be used, and for $s > s_s$ and $t < 32$ F Eq. (254) holds true.

In nonsaturated air, the water vapor is present in a superheated condition, since the vapor pressure is smaller than the saturation pressure corresponding to the air temperature. Under special conditions air may hold an amount of water vapor greater than that belonging to the saturation point. This is possible, for instance, if the air is cooled very rapidly (by adiabatic expansion, *e.g.*, in a nozzle) or if the air does not contain any solid particles (dust, soot) on which the formation of droplets could start. This condition is called *supersaturated.* For industrial calculations this condition is of minor importance. We will assume therefore in the following calculations that no supersaturation occurs.

## 43. The s-i diagram for humid air

Drying and moistening processes are usually studied with the help of the psychrometric chart of humid air. In this chart the temperature (dry-bulb temperature) is used as abscissa and the specific humidity as ordinate. R. Mollier[1] introduced another diagram which uses the enthalpy instead of the temperature. This diagram has the advantage that processes of mixing two or more air streams or of admixing moisture as water or water vapor to air can be solved exactly by simple geometrical constructions in this diagram, whereas such constructions give only approximate solutions in the psychrometric chart. Moreover such Mollier diagrams can be generalized for mixtures of two materials other than air and water. In the original Mollier diagram the specific humidity is the abscissa and the enthalpy the ordinate. We shall turn it around so that the enthalpy is the abscissa and the specific humidity the ordinate. In this presentation the diagram is very similar to the psychrometric chart, the only difference being that the lines of constant temperature which are vertical in the chart are straight lines slightly inclined by varying angles in the Mollier diagram. In the following pages this diagram for humid air will be developed.

---

[1] R. Mollier, *Z. Ver. deut. Ing.*, **67**, 869–872 (1923); **73**, 1009–1013 (1929).

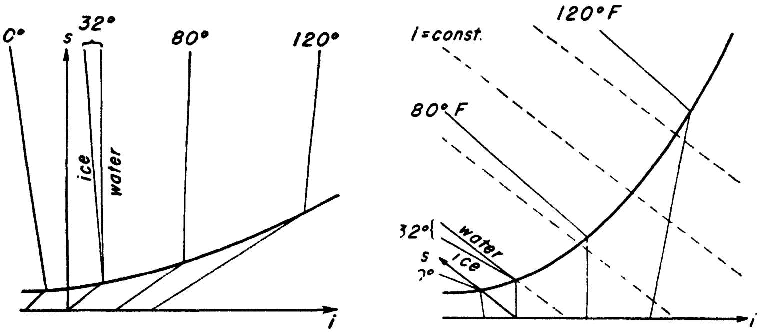

(a) (b)

FIG. 126. Specific-humidity–enthalpy diagram for moist air. (*According to R. Mollier.*)

If the specific humidity $s$ is used as ordinate and the enthalpy $i$ as the abscissa, Fig. 126*a* arises. In the figure are shown some isotherms, which are composed of straight lines. The isotherm for $t = 32$ F has, for example, in the range of unsaturated air the inclination 1076 Btu/lb toward the ordinate up to the saturation limit. For higher humidities $s$, the isotherm is a vertical line according to Eq. (253). If the superfluous water is contained in the air as ice, the isotherm above the saturation limit is given by Eq. (254). It has therefore a negative inclination of 143 Btu/lb toward the ordinate. The isotherms for positive temperatures are inclined toward the right; the 32 F isotherm for foggy air ($s$ greater than $s_s$) is vertical. The isotherms for negative temperatures are inclined toward the left. By connecting all points which correspond to the saturation limit at different temperatures the saturation curve in the diagram arises. As the saturation humidity depends on the total pressure according to Eq. (249), this curve, and therefore the whole diagram, holds only for a certain pressure.

The saturation curve separates the regions of unsaturated and foggy state. At the point of intersection with the 32 F isotherm, the saturation curve has a slight break since for temperatures above 32 F it is fixed by the equilibrium between water and its vapor, and for temperatures below 32 F by the equilibrium between ice and water vapor. In the form shown in Fig. 126*a* the diagram has the disadvantage that the region of unsaturated air is comparatively small. This can be avoided by using a system of oblique-angled coordinates. Mollier proposed to give the $s$ axis such a direction that the 32 F isotherm is vertical in the unsaturated range. Such a diagram is shown in Fig. 126*b*. The lines $i$ = constant are in this diagram a group of parallel oblique lines. Such a diagram on an increased scale is added to the book as an Appendix.

This diagram will now be used to work some examples. The condition of humid air at a certain pressure is given by two state functions, *e.g.*, by the temperature $t_1$ and the specific humidity $s_1$. In Fig. 127 this fixes the point of state 1. We can immediately determine the value $\rho$ by following the isotherm $t_1$ up to the point of intersection with the saturation curve and reading the saturation humidity $s_{s1}$. The value is $\rho_1 = s_1/s_{s1}$. For not too high temperatures, the relative humidity $r$ has the same value. For higher temperatures it must be determined from the partial pressures. The $s$-$i$ diagram (page 254) shows curves $r$ = constant. When air with the state 1 is cooled, its humidity does not change as long as the air is not saturated. This means that in the diagram the state moves on a horizontal line. The relative humidity increases with decreasing temperature and at point 2 saturation is reached. This point is called the dew point and the corresponding temperature, dew-point temperature. When the air is cooled to still lower temperatures part of the water vapor condenses in form of small droplets (fog). At state point 3 the

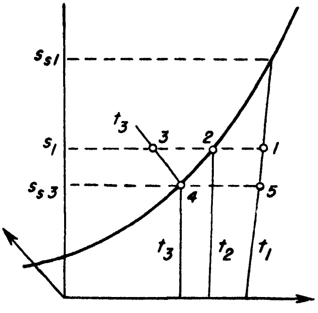

Fig. 127. Determination of the state of moist air in the Mollier $s$-$i$ diagram.

temperature $t_3$ is reached. Of the total humidity $s_1$, a part $s_{s3}$ is present as vapor, the rest as liquid. The vapor part $s_{s3}$ is fixed by the intersection of the isotherm through point 3 with the saturation line. The liquid part of the water can be removed from the air, for instance, by waiting until the droplets sink to the ground. In this way the humidity of the air has been decreased from $s_1$ to $s_{s3}$. The corresponding state point in the diagram is point 4. In this way, therefore, air can be dried. If, for instance, air with the state 1 must be dried to the specific humidity $s_{s3}$, the air must be cooled to the temperature $t_3$. By this the dew point is first reached, and afterwards point 4 when the liquid water is separated. Now the air can be heated again to the initial temperature so that the final state 5 has the same temperature but a lower humidity than the original state 1. This method is applied very often in air conditioning.

As a second example, the state may be determined which arises by mixing two amounts of air with different temperatures and humidities. The weight of air $W_1$ may have a temperature $t_1$ and a specific humidity $s_1$; the weight of air $W_2$ may have a temperature $t_2$ and a specific humidity $s_2$.

By mixing there results a weight of air $W$ with a temperature $t$ and a specific humidity $s$. The following equations hold true:

$$W_1 + W_2 = W \text{ (weight balance for air)} \tag{255}$$

$$W_1 s_1 + W_2 s_2 = Ws \text{ (weight balance for water)} \tag{256}$$

$$W_1 i_1 + W_2 i_2 = Wi \text{ (heat balance)} \tag{257}$$

where the values $i$ are the enthalpies of the moist air. They can be read from the diagram. By eliminating $W$ with the help of the first equation there is obtained

$$W_1(s - s_1) = W_2(s_2 - s)$$
$$W_1(i - i_1) = W_2(i_2 - i)$$

and by division

$$\frac{s - s_1}{i - i_1} = \frac{s_2 - s}{i_2 - i} \tag{258}$$

From this equation it follows that in the $s$-$i$ diagram the state point $M$ for the mixture must be situated on a straight line 1-2 connecting the two initial points (Fig. 128). The location of point $M$ on the line follows from the equation

$$\frac{W_1}{W_2} = \frac{s_2 - s}{s - s_1} \tag{259}$$

The ratio of the distance $M$-2 in Fig. 128 to the distance $M$-1 must therefore be equal to the ratio of the weights $W_1/W_2$. If air with the state 3 is mixed with air of the state 4 the resulting state of the mixture lies on line 3-4 (Fig. 128). It can be seen that the mixture may lie in the foggy range. A very common example of this fact is the visibility of the exhaled air in cold weather. The warm, wet air from the lungs mixes with the cold outside air and there arise supersaturated mixtures whose water content is visible as fog.

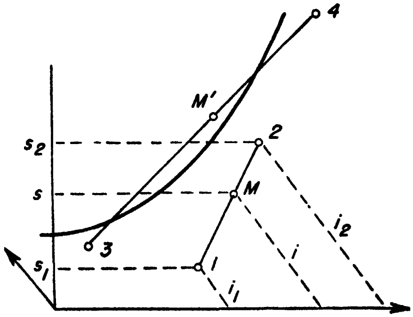

FIG. 128. Mixing of air streams in the Mollier $s$-$i$ diagram.

Another example is the moistening of air with liquid water or with steam. The initial state of the air may be determined by its amount $W_1$, its temperature $t_1$, and its humidity $s_1$. The water weight mixed with the air may be $W$ and its enthalpy $i_w$. Then

$$W_1(s - s_1) = W \text{ (weight balance)} \tag{260}$$
$$W_1(i - i_1) = Wi_w \text{ (heat balance)} \tag{260a}$$

By dividing both equations there is obtained

$$\frac{i - i_1}{s - s_1} = i_w \tag{261}$$

By this equation, the direction is fixed in which the state of the air moves in the $s$-$i$ diagram during moistening. The ratio of the enthalpy change $(i - i_1)$ to the change $(s - s_1)$ in specific humidity must be equal to the enthalpy $i_w$ of the water. This gives the angle $\alpha$ a certain value. In order to find this direction easily in the Mollier diagram (Fig. 129), a scale is inserted along the edge. The rays of this scale originate in point 32 F and $s = 0$ and are denoted by the corresponding enthalpy. If a straight line is drawn through point 1 giving the state of the air before the humidification in the direction which is taken from the edge scale, this line gives the change of the state of the air. The final state on this line is fixed by the amount of water admixed. Equation (260) gives

$$s - s_1 = \frac{W}{W_1} \tag{262}$$

and fixes the final point of state. The enthalpy of steam has the order of magnitude 1000 Btu/lb. From the large $s$-$i$ diagram it can be seen that the direction of this change of state is approximately vertical. If unsaturated air is humidified with steam its temperature changes therefore only very little. Foggy air is heated by steam. The enthalpy of water equals its temperature. The direction of a change of state produced by injecting water into air has a strong inclination to the left. In the unsaturated range air therefore cools by injection of water. It may seem strange at first that air can be cooled by injection of water also where the water is warmer than the air. The reason is that the water evaporates and takes its heat of evaporation from the air. Other examples for the use of the diagram are given in the following paragraphs. For mixtures of two materials other than air and water similar diagrams have proved very useful.[1]

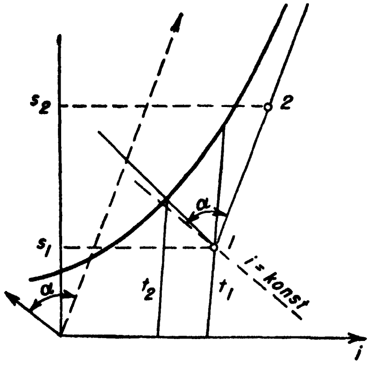

FIG. 129. Moistening of air with steam or water in the Mollier $s$-$i$ diagram.

## 44. Diffusion

When a wet surface is dried by an air flow, the vapor escaping from the surface is carried away in the air flow by convection.

---

[1] A description of the construction and use of such diagrams is found in F. Bošnjaković, "Technische Thermodynamik," Vol. 2, Dresden, 1937.

First, however, it must penetrate the boundary layer on the surface by diffusion. The mass flow arising by diffusion is given by *Fick's law,* which is much the same as the heat-conduction equation. We will acquaint ourselves with this law by describing a simple experiment. A glass tube closed on one end may be filled at the bottom with a little water (Fig. 130). Over the open end of the tube an air flow is blown with a certain concentration of water vapor. The air velocity may be small. The total pressure within the tube is then constant and equal to the outside pressure. The partial pressure of the water vapor outside the tube is generally different from that over the water surface. The partial pressure of the water vapor over the water surface equals the saturation pressure at the surface temperature.[1] The partial pressure at the upper end of the tube is fixed by the partial pressure in the air flow. Within the tube the partial pressure may be as shown in Fig. 130. The weight flow of water vapor per unit of the area 1-1, the weight velocity connected with the diffusion process is, according to Fick's law,

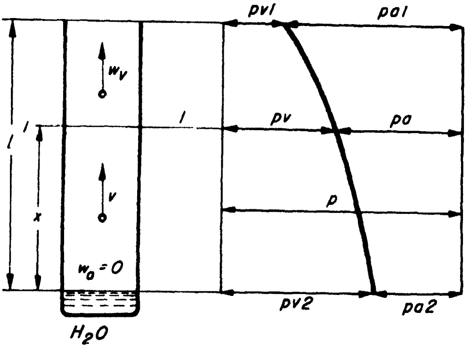

FIG. 130. Diffusion of water vapor through air.

$$\mathbf{w}_v = -\mathbf{D}\frac{\mathbf{dc}_v}{\mathbf{dx}} \tag{263}$$

---

[1] Theoretically the vapor pressure over the surface is slightly lower than the saturation pressure as soon as a mass flow from the surface occurs, but the difference is very small and can be neglected in industrial calculations. On the other hand the evaporation uses up heat, which must, in many cases, flow from inside the liquid to the surface. This results in a temperature gradient in the liquid near the surface and a surface temperature lower than the average liquid temperature.

where $c_v$ is the concentration of the vapor (in pounds per cubic foot), $D$ the diffusion coefficient, and $dc_v/dx$ the gradient of the concentration along the tube axis. The diffusion coefficient depends on both masses which diffuse into each other. Accurate values for this coefficient are scarce. Some are tabulated in the Appendix. The best known is the diffusion coefficient for water vapor in air.[1] The dimension of the diffusion coefficient is, in accordance with Eq. (263), square feet per hour.

The concentration $c_v$ can be expressed by the partial pressures $p_v$ using the values introduced in the previous paragraphs in the following way:

$$c_v = \frac{W_v}{V} = \frac{p_v}{R_v T} \tag{264}$$

With this Fick's law becomes

$$\mathbf{w}_v = -\frac{\mathbf{D}}{\mathbf{R}_v\mathbf{T}}\frac{\mathbf{dp}_v}{\mathbf{dx}} \tag{265}$$

Only in this form Fick's law is also valid for great temperature differences. At extremely high temperature differences there is added to the diffusion given by Eq. (265) a second kind of diffusion which arises at constant partial pressure, and which is called *thermodiffusion.*

Since the partial pressure of the water vapor $p_v$ and the partial pressure of the air $p_a$ add up to the total pressure $p$, and since the total pressure is constant, there corresponds to a gradient of the vapor pressure a gradient of the partial pressure of the air. As Eq. (265) must also be valid for the air, a mass flow of the air must arise which is in the opposite direction to the vapor flow. No air can leave the tube at the bottom, however, as it is closed there. Therefore a convective flow in an upward direction must be present within the tube, which compensates for the diffusive air flow. The velocity of this convective flow may be $v$. The amount of vapor which is transported by this convective flow through the cross section 1-1 per unit area and time is $vc_v$. Therefore the whole weight velocity of the water vapor in the cross section 1-1 is

$$w_v = -\frac{D}{R_v T}\frac{dp_v}{dx} + v\frac{p_v}{R_v T} \tag{266}$$

---

[1] R. Schirmer, *Z. Ver. deut. Ing., Beiheft Verfahrenstechnik,* 1938, pp. 170–177.

The same relation must be valid for the resulting air flow. Since the flow is zero the resulting equation is

$$w_a = -\frac{D}{R_aT}\frac{dp_a}{dx} + v\frac{p_a}{R_aT} = 0$$

This equation gives the velocity:

$$v = \frac{D}{p_a}\frac{dp_a}{dx} \tag{267}$$

The partial pressure of the air can be expressed by

$$p_a = p - p_v \qquad \frac{dp_a}{dx} = -\frac{dp_v}{dx}$$

This gives

$$v = -\frac{D}{p - p_v}\frac{dp_v}{dx} \tag{267a}$$

and for the weight velocity of the vapor,

$$\mathbf{w}_v = -\frac{\mathbf{D}}{\mathbf{R}_v\mathbf{T}}\frac{\mathbf{p}}{\mathbf{p} - \mathbf{p}_v}\frac{\mathbf{dp}_v}{\mathbf{dx}} \tag{268}$$

This equation is called *Stefan's law.*[1]

When the cross section of the tube is constant over $x$, Eq. (268) can be integrated, since $w_v$ is then independent of $x$. Also the velocity $v$ is then constant. By separating the variables there results

$$\frac{dp_v}{p - p_v} = -\frac{w_v}{D}\frac{R_vT}{p}dx$$

and by integration between $x = 0$ and $x = l$,

$$ln\frac{p - p_{v1}}{p - p_{v2}} = w_v\frac{l}{D}\frac{R_vT}{p}$$

or

$$\mathbf{w}_v = \frac{\mathbf{D}}{\mathbf{l}}\frac{\mathbf{p}}{\mathbf{R}_v\mathbf{T}}\ln\frac{\mathbf{p} - \mathbf{p}_{v1}}{\mathbf{p} - \mathbf{p}_{v2}} \tag{269}$$

**With this equation the weight velocity can be calculated from the partial pressures at both ends of the tube when the diffusion coefficient is known. Inversely, such an experiment can be used to determine the diffusion coefficient by measuring the partial pres-**

---

[1] **Stefan, *Wiener Berichte,* 68, 385–425 (1874).**

sures and the weight evaporated per hour. As long as the difference in the partial pressures is small when compared with the total pressure, Eq. (269) can be simplified into

$$w_v = \frac{D}{l}\,\frac{1}{R_vT}\,(p_{v2} - p_{v1}) \tag{270}$$

This equation has exactly the same form as Eq. (2) for heat conduction in a plane wall. In the same way Stephan's law, Eq. (268), transforms into Fick's law, Eqs. (265) and (263) respectively, at small partial pressure differences, and then has the same shape as the general equation for heat conduction, Eq. (31).

The previous calculations were made for the evaporation of a liquid in order to connect them with a concrete example. They can be applied generally, however, to the diffusion of two gases. Only for Eqs. (266) and (269) must the condition be fulfilled that through the interface (in the above case the surface of the liquid) there penetrates only one of the gases (in our case the vapor).

There are cases where both gases penetrate the interface. For instance, during the combustion of solid carbon, the oxygen diffuses to the surface of the fuel and the carbon monoxide or carbon dioxide generated by the combustion on the surface diffuses away from it.

**Example.** A vertical tube with 0.775 in.$^2$ cross section is filled with water at the bottom. The distance from the water surface to the open end of the tube is 2.527 in. Over the open end a flow of perfectly dried air is blown and the tube is held at a constant temperature of 87.5 F. The water evaporated is measured by weighing and is found to be $5.165 \times 10^{-5}$ lb/hr. From this experiment the diffusion coefficient of water vapor in air is to be calculated.

The weight velocity is

$$w_v = \frac{5.615 \times 10^{-5} \times 144}{0.775} = 1.043 \times 10^{-2} \qquad \text{lb/(hr)(ft}^2\text{)}$$

The saturation pressure of water vapor at 87.5 F can be found in the steam tables. It is $p_{v1} = 0.6453$ lb/in.$^2$ The gas constant of water vapor is obtained from its molecular weight $M = 18.016$ and the universal gas constant $\mathcal{R} = 1545.4$ ft-lb/(lb-mole)(R):

$$R_v = \frac{\mathcal{R}}{M_v} = \frac{1{,}545}{18.02} = 85.80 \qquad \text{ft-lb/(lb)(R)}$$

Solving Eq. (269) for $D$ gives

$$D = \frac{w_v\, l R_v T}{p \ln p/(p - p_{v2})}$$
$$= \frac{1.043 \times 10^{-2} \times 2.527 \times 85.80 \times (459.7 + 87.5)}{12 \times 14.22 \times 144 \times \ln 14.22/(14.22 - 0.6453)} = 1.097 \qquad \text{ft}^2/\text{hr}$$

Two facts must be watched, which may falsify the result of the experiment. The temperature of the water surface may be lower than the surrounding and there may occur free convection within the tube, since humid air is not so heavy as dry air, so that the air in the bottom is lighter than near the upper end. Both errors can be kept small by using a tube with a small diameter.

## 45. The boundary-layer equations of mass transfer

When the air above the wet surface is not in a state of rest as in the example considered in the preceding paragraph but flows along the surface, humidity is also transported away by convection. The diffusion process is then confined to a small zone in the proximity of the surface. The process is essentially analogous to a heat-transfer process where the heat is transported by conduction through the thermal boundary layer and outside it by convection. The zone within which a measurable gradient in partial vapor pressure arises may be called the boundary layer for mass transfer. At the same time there is on the surface a boundary layer of the velocity field. The thicknesses of these boundary layers may be different. Very often a heat flow takes place simultaneously with the mass transfer. In drying processes, for instance, heat is afforded to evaporate the liquid and this heat must be transported to the surface. We have therefore often three boundary layers superimposed—the velocity boundary layer, the thermal boundary layer, and the mass-transfer boundary layer. The last can be calculated with an equation similar to the momentum equation and the heat-flow equation for the two other boundary layers. The velocity field and the temperature field near the surface are changed by the mass transfer. There will be considered here only two-dimensional problems of forced convection. Consider an elementary volume with the dimensions $dx$ and $l$ near the surface from which the mass flow originates (Fig. 131). Normal to the plane of the drawing the dimension may be 1. The length $l$ may be greater than any of the boundary-layer thicknesses. The state of the air outside the boundary layer is fixed by its velocity $u_s$ (in $x$ direction), the temperature $t_s$, the partial pressure of the vapor $p_{vs}$, or the vapor concentration $c_{vs}$. On the surface the velocity is zero ($u = 0$). The temperature may be $t_w$, the vapor pressure $p_{vw}$, and the vapor concentration $c_{vw}$, respectively. At the distance $y$ from the surface, within the boundary layer, the respective values may be $u$, $t$, $p_v$, and $c_v$. The total pressure $p$ can again be assumed constant on any normal to the surface within the boundary layer because of the small boundary-layer thickness.

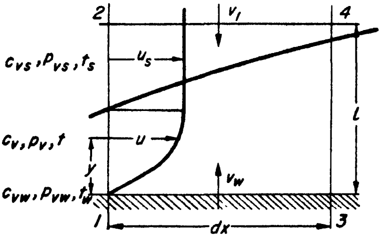

FIG. 131. Deriving the boundary-layer equations of mass transfer.

First the continuity equation may be set up for the volume element. The mass flow through the area 1-2 is $\int_0^l \rho u\,dy$. Through the length $dx$ it changes by the amount $\frac{d}{dx}\left(\int_0^l \rho u\,dy\right)dx$. In steady state this same amount must enter the volume through the areas 1-3 and 2-4. On the surface (area 1-3) there exists a normal velocity $v_w$, whose magnitude was calculated in the previous section. The velocity through the area 2-4 may be $v_1$; therefore the continuity demands

$$v_1 = \frac{d}{dx}\int_0^l u\,dy - v_w \qquad (271)$$

It is assumed that the density $\rho$ is constant in the whole field. The equation of momentum (Sec. 15) is now

$$\frac{d}{dx}\int_0^l \rho u^2\,dy - \rho v_1 u_s = -\tau_w - l\,\frac{dp}{dx}$$

By introducing the continuity equation there is obtained

$$\rho\,\frac{d}{dx}\int_0^l (u_s - u)\,u\,dy - \rho v_w u_s - \rho\,\frac{du_s}{dx}\int_0^l u\,dy = \mu\left(\frac{du}{dy}\right)_w + l\,\frac{dp}{dx} \qquad (272)$$

The shearing stress on the wall is substituted by the velocity gradient with the equation $\tau_w = \mu(du/dy)_w$. The equation of momentum has changed as compared with Eq. (111) by the summand $\rho v_w u_s$. The assumption that the density may be regarded as constant is fulfilled when the two diffusing components differ little in specific weight. For the mixing of water vapor with air this holds true.

To write the mass-flow equation for the vapor the fact must be expressed that in steady state the difference between the vapor mass carried by the flow into the volume element through area 1-2, and out of it through 3-4, must come into the volume by area 1-3 and 2-4. The weight velocity of the vapor on the solid surface may be $w_{vw}$. This gives

$$w_{vw} = \frac{d}{dx}\int_0^l c_v u\, dy - v_1 c_{vs}$$

Expressing the velocity $v_1$ by the continuity equation (271) and using the partial pressures instead of the concentration gives

$$\frac{d}{dx}\int_0^l (p_{vs} - p_v) u\, dy - v_w p_{vs} = -R_v T w_{vw}$$

For the introduction of the partial pressures into the equation it was assumed that the temperature differences are small compared with the absolute temperatures. Elimination of the weight velocity $w_{vw}$ of the vapor on the solid surface by Eq. (266) leads to

$$\frac{d}{dx}\int_0^l (p_{vs} - p_v) u\, dy = D\left(\frac{dp_v}{dy}\right)_w + v_w(p_{vs} - p_{vw}) \qquad (273)$$

and with the velocity $v_w$ in Eq. (267*a*),

$$\frac{d}{dx}\int_0^l (p_{vs} - p_v) u\, dy = D\,\frac{p - p_{vs}}{p - p_{vw}}\left(\frac{dp_v}{dy}\right)_w \qquad (274)$$

The heat-flow equation is found in the same way by a heat balance in the volume element. The heat flow per unit area of the solid surface is $q_w$. Then

$$\frac{d}{dx}\int_0^l C_p t u\, dy - C_p t_s v_1 = q_w$$

Heat is transferred from the solid surface not only by conduction but also by convection with the evaporating component.

Therefore

$$q_w = -k\left(\frac{dt}{dy}\right)_w + C_p t_w v_w \tag{275}$$

Here the specific heat $C_p$ at constant pressure per unit volume is used. Assuming it to be constant and introducing $v_1$ from the continuity equation gives

$$\frac{d}{dx}\int_0^l (t_s - t)u\,dy = \alpha\left(\frac{dt}{dy}\right)_w + (t_s - t_w)v_w \tag{276}$$

The boundary-layer equations (273) and (276) for mass transfer differ from the corresponding equation for heat transfer alone by the addition of the summand with the velocity $v_w$. The equations can be solved in the same way as in Sec. 19 by introducing proper expressions for the velocity, the temperature, and the partial-pressure profile, and calculating the boundary-layer thicknesses. In order to increase the accuracy of this approximate solution it is usefull to fulfill for the assumed profiles the boundary conditions on the solid surface which are valid for the real profiles. In Sec. 19, the fact that the second derivative of the temperature to the wall distance must be constant on the solid surface was derived from the condition that $q_w$ is constant in the immediate proximity of the wall. For the heat flow during mass transfer Eq. (275) holds true. Again, in the immediate proximity of the wall the heat flow $q_w$ must be constant. Therefore

$$\left(\frac{dq}{dy}\right)_w = v_w c_p\left(\frac{dt}{dy}\right)_w - k\left(\frac{d^2t}{dy^2}\right)_w = 0 \tag{277}$$

For the weight velocity of the vapor Eq. (266) is valid. Also the weight flow must be constant in the proximity of the wall. By differentiating Eq. (266) in which $x$ must be replaced here by $y$, there is obtained

$$\begin{aligned} -D\left(\frac{d^2p_v}{dy^2}\right)_w + \frac{D}{T}\left(\frac{dp_v}{dy}\right)_w\left(\frac{dt}{dy}\right)_w - v_w\frac{p_v}{T}\left(\frac{dt}{dy}\right)_w& \\ + v_w\left(\frac{dp_v}{dy}\right)_w = 0& \qquad (278) \end{aligned}$$

If the temperature is constant, which means that only mass transfer occurs, Eq. (278) simplifies to

$$D\left(\frac{d^2p_v}{dy^2}\right)_w - v_w\left(\frac{dp_v}{dy}\right)_w = 0 \tag{279}$$

For the shearing stress $\tau_w$ without diffusion, Eq. (109) holds true. If a mass flow originates from the wall this equation changes. Imagine a plane in the proximity of the solid surface and parallel to it; then, within this plane a shearing stress arises by the viscosity of the air flowing along the surface. But in addition, there exists a virtual shearing stress caused by the transport of momentum with the vapor passing the plane. This shearing stress has the same magnitude as the one which arises by turbulent mixing and which was calculated in Sec. 23. The total shearing stress therefore is

$$\tau = \mu\frac{du}{dy} - \frac{w_v}{g}u$$

where $g$ is the acceleration of gravity. This shearing stress must again be constant in the immediate proximity of the wall. So its derivative to $y$ at the wall is zero:

$$\mu\left(\frac{d^2u}{dy^2}\right)_w - \frac{w_v}{g}\left(\frac{du}{dy}\right)_w = 0 \tag{280}$$

The calculations become much simpler when the partial-pressure differences within the boundary layer are small compared with the average pressure of the air. In this case the velocity $v_w$ normal to the wall is small and can be neglected in Eqs. (272), (273), and (276). The equation of momentum (272) and the heat-flow equation (276) have then the same shape as for heat transfer alone (Secs. 15 and 19). This means that the flow and the heat transfer are not influenced by the mass transfer. For the calculation of the mass transfer Eq. (273) holds true; but this equation need not be solved, because the result can be determined directly by similarity conditions.[1]

A calculation of mass transfer without heat transfer for the flow along a plane surface in the range of the laminar boundary layer by solution of the above equations was given by E. Eckert and V. Lieblein.[1]

---

[1] The similarity considerations were given by E. Schmidt, *Gesundh. Ing.*, **52**, 525–529 (1929), and W. Nusselt, *Z. angew. Math. Mech.*, **10**, 105–121 (1930). G. Ackermann, *VDI-Forschungsheft* **382**, 1937, gave approximate correction values for high partial pressures.

The calculation shows that the mass transfer depends on two dimensionless values. The first is $A = (D/\nu)(M_v/M)$ with $D$ the diffusion coefficient, $\nu$ the kinematic viscosity, $M$ the molecular weight of the mixture between the vapor and the gas passing by, and $M_v$ the molecular weight of the vapor evaporated or absorbed by the plane surface. Since for the derivation of the above equations it was assumed that the molecular weights of both components do not differ greatly, the value $A$ is essentially the same as the ratio $D/\nu$ which occurs again in the following paragraph. The second dimensionless value $B = \dfrac{p_{vs} - p_{vw}}{p - p_{vw}}$ is the ratio of the difference in partial vapor pressures outside the boundary layer (in the free stream) and on the plane surface to the difference between the total pressure and the partial vapor pressure on the surface. The numerical computations were made for evaporation or absorption of water vapor from a surface in an air stream, the flowing air being at 68 F and 14.2 lb/in.$^2$ pressure. The dimensionless value $A$ is 1.04. From the results, Figs. 132 and 133 are presented here. Figure 132 shows the velocity profile and the partial-pressure profile for the water vapor in the boundary layer. $\delta$ means the thickness of the boundary layer for the velocity profile and the thickness of the mass-transfer boundary layer for the partial-pressure profile, respectively. The characteristic values $K$ for the velocity profile, and $K_p$ for the partial-pressure profile are the following functions of the dimensionless values $A$ and $B$:

$$K_p = 3 - \frac{4 - 2\sqrt{4 - 6B}}{B} \qquad K = \frac{3A(2 - \sqrt{4 - 6B})\,\delta/\delta_p}{A(2 - \sqrt{4 - 6B})\,\delta/\delta_p - 4}$$

where $\delta$ is the boundary-layer thickness for the velocity, and $\delta_p$ the boundary-layer thickness for the partial pressures. The ratio $\delta/\delta_p$ of the two boundary-layer thicknesses is unity for evaporation of the water from the wall and increases up to 2 for absorption of the steam by the wall with great partial-pressure differences. For mass transfer from the wall (evaporation) $K$ has positive values, and for mass transfer to the wall (absorption) negative values. The line for $K = 0$ gives the velocity profile for the flow along the wall without mass transfer and approximately the velocity and the partial-pressure profiles for very small partial-pressure differences. It can be seen from the figure that both the velocity and the partial-pressure profile change considerably at higher partial-pressure differences. The line $K = K_p = 3$ is valid for a partial pressure of the air equal to zero at the wall, which means for a boiling-water surface. The mass flow from or to the wall can be determined with Fig. 133. The value $h_D$ on the ordinate gives the mass-transfer coefficient, which is analogous to the heat-transfer coefficient and will be explained in detail in the next section. The value $h_D x/D$ is the dimensionless mass-transfer coefficient and corresponds to the

---

[1] E. Eckert and V. Lieblein, *Forsch. Gebiete Ingenieurw.*, **16**, No. 2 (1949).

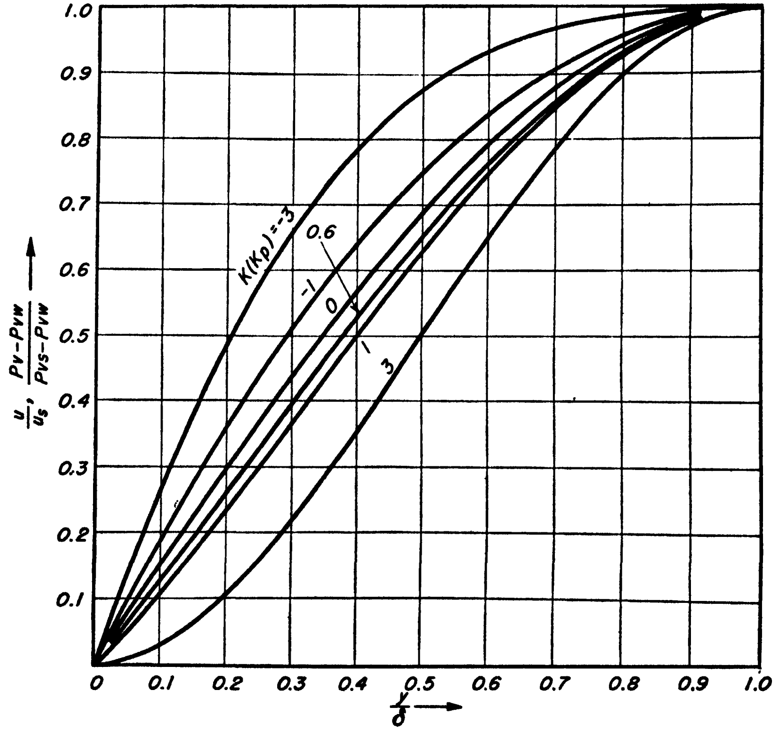

FIG. 132. Velocity and partial-pressure profile in the laminar boundary layer on a flat surface absorbing or evaporating water into an air flow. (*According to E. Eckert and V. Lieblein, Forsch. Gebiete Ingenieurw.*, 1949.)

Nusselt number in heat transfer. This value increases with the square root of the Reynolds number. The same relation was valid for heat transfer in flow along a plate with laminar boundary layer. As a parameter, the ratio of the partial pressure ($p - p_{vw}$) of the air at the wall to the total pressure $p$ arises. Only the curves above the dashed line have any physical reality. The values for the mass-transfer coefficient at low partial-pressure differences lie on the vertical line $K_p = 0$. It can be seen that the mass transfer depends considerably on the value $K_p$, which means on the partial-pressure differences. Positive values of $K_p$ hold for evaporation, negative values for absorption of the steam on the wall.

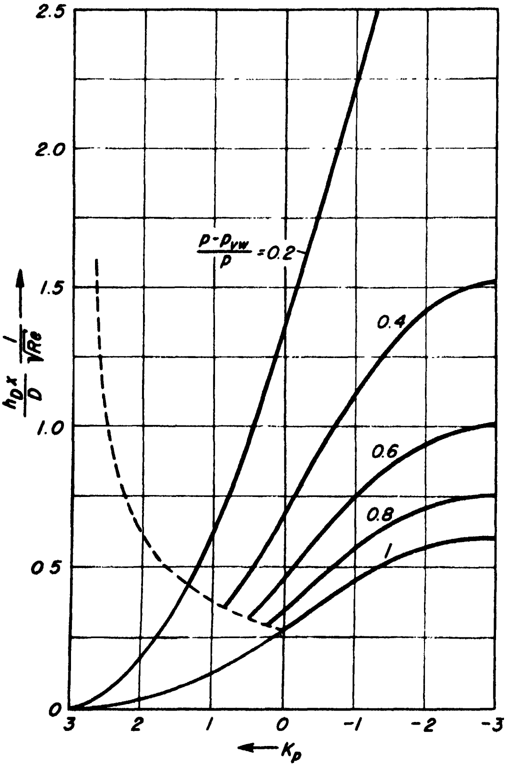

FIG. 133. Dimensionless mass-transfer coefficient for a flat surface absorbing or evaporating water into a laminar air flow. (*According to E. Eckert and V. Lieblein, Forsch. Gebiete Ingenieurw.*, 1949.)

## 46. Similarity relations for mass transfer[1]

As long as the differences in partial pressures are small compared with the total pressure the summand with the velocity $v_w$ can be neglected in Eqs. (273) and (276). Both equations then appear in the same form as the heat-flow equation (135). This can be seen from the following comparison.

Heat-flow equation:

$$\frac{d}{dx}\int_0^l (t_s - t)u\,dy = \alpha\left(\frac{dt}{dy}\right)_w$$

Mass-flow equation:

$$\frac{d}{dx}\int_0^l (p_{vs} - p_v)u\,dy = D\left(\frac{dp_v}{dy}\right)_w$$

As a consequence of their similar form the solutions for both equations must also be similar. There is obtained, therefore, from the solution of the heat-flow equation, the solution of the mass-transfer equation when the partial pressure $p_v$ is substituted for the temperature $t$, and the diffusion coefficient $D$ for the thermal diffusivity $\alpha$. There is also an analogy to the general heat-flow equation (171) in mass transfer:

$$u\frac{\partial p_v}{\partial x} + \cdots = D\frac{\partial^2 p_v}{\partial x^2} + \cdots$$

In Sec. 27 it was derived that the temperature fields in the neighborhood of similar bodies transmitting heat by forced convection can be represented in the following way:

$$\vartheta' = f\left(y', Re, \frac{\nu}{\alpha}\right) = f(y', Re, Pr) \tag{281}$$

where $\vartheta'$ is a dimensionless value giving the difference between the temperature $t$ of a point with the dimensionless distance $y'$ from a surface and the temperature of any arbitrary reference point $t_r$ divided by any arbitrary reference temperature difference, as, for instance, the difference between the temperature $t_s$ of the flowing medium at a great distance from the body and the temperature $t_w$ of the body. *Re* is the Reynolds number and $\nu/\alpha$ the Prandtl number. For the same body we get the partial-pressure field by substituting partial pressures for the temperatures $\left(p_v' = \frac{p_v - p_{vw}}{p_{vs} - p_{vw}}\right)$ and the diffusion coefficient $D$ for the thermal diffusivity $\alpha$:

---

[1] **These relations were first derived simultaneously by E. Schmidt, *loc. cit.*, and by W. Nusselt, *loc. cit.***

$$p'_v = f\left(y', Re, \frac{\nu}{D}\right) = f\,(y', Re, Sc) \tag{282}$$

The dimensionless value $\nu/D$ is called the Schmidt number. The function $f$ has the same form in both Eqs. (281) and (282).

In heat-transfer problems, we are primarily interested in the specific heat flow $q_w$ per unit of the surface area of the body. It can be calculated from the film heat-transfer coefficient $h$ by the equation

$$q_w = h(t_s - t_w)$$

On the other hand there is the equation

$$q_w = -k\left(\frac{\partial t}{\partial y}\right)_w$$

Therefore

$$h(t_s - t_w) = k\left(\frac{\partial t}{\partial y}\right)_w \tag{283}$$

In an analogous manner, the mass flow per unit area is characterized by a mass-transfer coefficient $h_D$ defined by the equation

$$w_{v,w} = h_D(c_{vs} - c_{vw})$$

The dimension of the mass-transfer coefficient is feet per hour. By introducing the partial pressures instead of the concentrations, the above equation becomes

$$w_{vw} = \frac{h_D}{R_vT}\,(p_{vs} - p_{vw}) \tag{284}$$

This equation was first used by E. Dalton (1788). On the other hand, the mass flow per unit area is described by the equation

$$w_{vw} = -\frac{D}{R_vT}\left(\frac{\partial p_v}{\partial y}\right)_w$$

Neglecting the minus sign it follows that

$$h_D(p_{vs} - p_{vw}) = D\left(\frac{\partial p_v}{\partial y}\right)_w \tag{285}$$

From Eq. (283) the dimensionless film heat-transfer coefficient becomes

$$\frac{hl}{k} = \left(\frac{\partial \vartheta'}{\partial y'}\right)_w$$

with the dimensionless temperature difference $\vartheta'$ and the dimensionless distance $y' = y/l$ from the solid surface. According to Eq. (281) the last equation becomes

$$\frac{hl}{k} = f(Re, Pr) \tag{286}$$

In the same way, a dimensionless mass-transfer coefficient can be built up by dividing the partial pressure $p_v$ in Eq. (285) by the difference $(p_{vs} - p_{vw})$, and by dividing the coordinate $y$ by the reference length $l$.

$$\frac{h_D l}{D} = \left(\frac{\partial p'_v}{\partial y'}\right)_w \tag{287}$$

By differentiating Eq. (282) with respect to $y'$, there is given at the distance $y = 0$,

$$\frac{h_D l}{D} = f\left(Re, \frac{\nu}{D}\right) = f(Re, Sc) \tag{288}$$

The functions in both Eqs. (286) and (288) have the same shape.

Any of the equations in Chapter 3 for heat transfer, therefore, gives also the solution for a corresponding mass-transfer problem if the Nusselt number $hl/k$ is replaced by the dimensionless mass-transfer coefficient $h_D l/D$, and the Prandtl number $\nu/\alpha$ by the dimensionless value $\nu/D$.[1]

If, for a gas mixture, the diffusion coefficient $D$ equals the thermal diffusivity $\alpha$, the two dimensionless transfer coefficients are equal for a given Reynolds number. By substituting for the diffusion coefficient $D$, the thermal diffusivity $\alpha = k/\gamma c_p = k/C_p$ ($C_p$ = specific heat per unit volume at constant pressure) we get

$$h_D = h\frac{D}{k} = h\frac{\alpha}{k} = \frac{h}{C_p} \tag{289}$$

This law was derived by *Lewis*[2] and is therefore called the Lewis relation. For turbulent exchange according to Fig. 134, the following conditions apply. $V'$ denotes the gas volume exchanged between the two planes 1 and 2 per unit time and area, and $t$ and

---

[1] This law was verified by a number of experiments. See, for example, T. K. Sherwood, *Trans. Am. Inst. Chem. Engrs.*, **36**, 817–840 (1940); also A. P. Colburn, *Ind. Eng. Chem.*, **22**, 967–970 (1930).

[2] W. K. Lewis: *Trans. Am. Inst. Chem. Engrs.*, **20**, 9 (1927).

$t'$ or $c_v$ and $c'_v$, respectively, the temperatures and concentrations in both planes. Then the heat flow per unit area from plane 1 to plane 2 associated with the turbulent exchange is

$$q_t = V'C_p(t - t')$$

If this heat flow is characterized by a turbulent film heat-transfer coefficient $h_t$, it may be written

$$h_t(t - t') = V'C_p(t - t') \qquad (290)$$

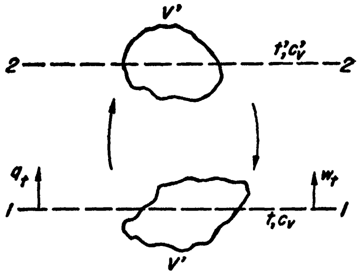

FIG. 134. Simplified picture of turbulent mass transfer.

In the same way, the mass flow $w_t$ per unit area associated with the turbulent exchange is

$$w_t = V'(c_v - c'_v)$$

and expressed in terms of a turbulent mass-transfer coefficient $h_{Dt}$, is

$$h_{Dt}(c_v - c'_v) = V'(c_v - c'_v) \qquad (291)$$

Dividing Eqs. (290) and (291) by each other gives

$$h_{Dt} = \frac{h_t}{C_p} \qquad (292)$$

One can see that the Lewis relation holds true in turbulent flow regardless of whether the ratio $\alpha/D$ equals 1 or not. For the laminar sublayers which always arise in turbulent flow in the immediate neighborhood of solid surfaces, the Lewis relation is valid only for $\alpha/D = 1$.

Heat transfer by free convection can be represented by the following equation, according to Sec. 27:

$$Nu = f(Gr, Pr) \qquad (293)$$

where $Nu$ is the dimensionless heat-transfer coefficient $hl/k$, $Gr$ the Grashof number $g\beta\Theta l^3/\nu^2$, and $Pr$ the Prandtl number $\nu/\alpha$. In the Grashof number, the product of the thermal expansion coefficient $\beta$ and a reference-temperature difference $\Theta$ took the place of the ratio of the specific weights $(\gamma_s - \gamma_w)/\gamma_w$. As for diffusion processes, where the buoyancy forces are generated by the difference in specific weight of the different mixtures, the

Grashof number for mass transfer has the form

$$Gr_D = \frac{gl^3}{\nu^2}\left(\frac{\gamma_s}{\gamma_w} - 1\right)$$

where $\gamma_w$ is the specific weight of the gas mixture at the solid wall and $\gamma_s$ is the specific weight outside the boundary layer. The same deductions used for forced convection now lead to the following expression for the mass-transfer coefficient:

$$\frac{h_D l}{D} = f\left(Gr_D, \frac{\nu}{D}\right) = f(Gr_D, Sc) \tag{294}$$

The function $f$ is again the same as for the corresponding heat-transfer problem. If on the same surface, heat and mass transfer occur simultaneously, it is not possible to calculate the mass-transfer coefficient from the solution of the corresponding problem with heat transfer alone as long as $D \neq \alpha$.[1]

**Example.** Along a horizontal water surface an air stream with a velocity $u_s = 10$ fps is flowing. The amount of water evaporated per hour per square foot from the water surface is to be calculated. The temperature of the water on the surface is 59 F, the air temperature is 68 F, and the partial pressure of the water vapor in it is

$$p_{vs} = 0.1130 \text{ lb/in.}^2$$

corresponding to a relative humidity $r = 33.3$ per cent. The water surface in the wind direction has a length of $x = 4$ in.

The Reynolds number for the air flow is

$$Re_x = \frac{u_s x}{\nu} = \frac{10 \times (4/12)}{16.8 \times 10^{-5}} = 19{,}830$$

with $\nu = 16.8 \times 10^{-5}$ ft²/sec from the Appendix. The flow therefore is laminar and the average heat-transfer coefficient is given by Eqs. (140) and (141), $Nu_x = 0.662 \sqrt[3]{Pr}\sqrt{Re_x}$. The mass-transfer coefficient is determined by the analogous equation $h_D x/D = 0.662 \sqrt[3]{\nu/D}\sqrt{Re_x}$ The diffusion coefficient is $D = 1.023$ ft²/hr (see Appendix). Therefore $\frac{\nu}{D} = \frac{16.8 \times 10^{-5} \times 3600}{1.023} = \frac{0.605}{1.023} = 0.591$. This gives

$$\frac{h_D x}{D} = 0.662 \sqrt[3]{0.591}\sqrt{19{,}830} = 78.4$$

---

[1] E. Schmidt, *loc. cit.*

and

$$h_D = 78.4 \times 1.023 \times {}^{12}/_{4}$$

If it is desired to use the Lewis relation the heat-transfer coefficient must first be determined, with $Pr = 0.710$ for air,

$$Nu = 0.662 \sqrt{19{,}830} \times \sqrt[3]{0.710} = 83.3$$

and $h = Nu(k/x) = 83.3 \times 0.0148 \times {}^{12}/_{4} = 3.7$ Btu/(hr)(ft²)(F). For air at 68 F and 14.22 lb/in.², the specific heat per unit volume is $= 0.0175$ Btu/(ft³)(F). Therefore $h_D = 3.7/0.0175 = 211$ ft/hr. This value is too small by 14 per cent because the assumption $\alpha/D = 1$ under which the Lewis relation holds true is not quite fulfilled here. For approximate calculations on evaporation of water in air, however, the Lewis relation is very useful.

The partial pressure of the water vapor over the water surface is the saturation pressure at the water-surface temperature,

$$p_{vw} = 0.2473 \text{ lb/in.}^2$$

Therefore the amount of water evaporated per square foot per hour is [Eq. (284)]

$$w_{vw} = \frac{h_D}{R_v T}(p_{vw} - p_{vs}) = \frac{240}{85.9 \times 519}(0.2473 - 0.1130)144$$
$$= 0.104 \text{ lb/(hr)(ft}^2\text{)}$$

## 47. The evaporation of water into air

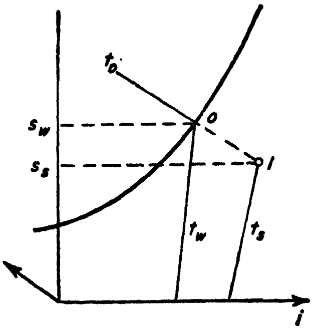

FIG. 135. Determining the humidity of air with a dry- and a wet-bulb thermometer.

When evaporation of water into air or condensation of water from moist air takes place on a surface, the Lewis relation can be used for approximate calculations, since the ratio of thermal diffusivity to the diffusion coefficient has the value 0.835 at 68 F, which is not greatly different from the value 1. In Sec. 43, processes with moist air were studied with the enthalpy-specific-humidity diagram. Therefore, it is useful to transform Eq. (284) into a relationship which contains the specific humidities instead of the partial pressures. According to Sec. 42

$$s = \frac{M_v}{M_a}\frac{p_v}{p_a}$$

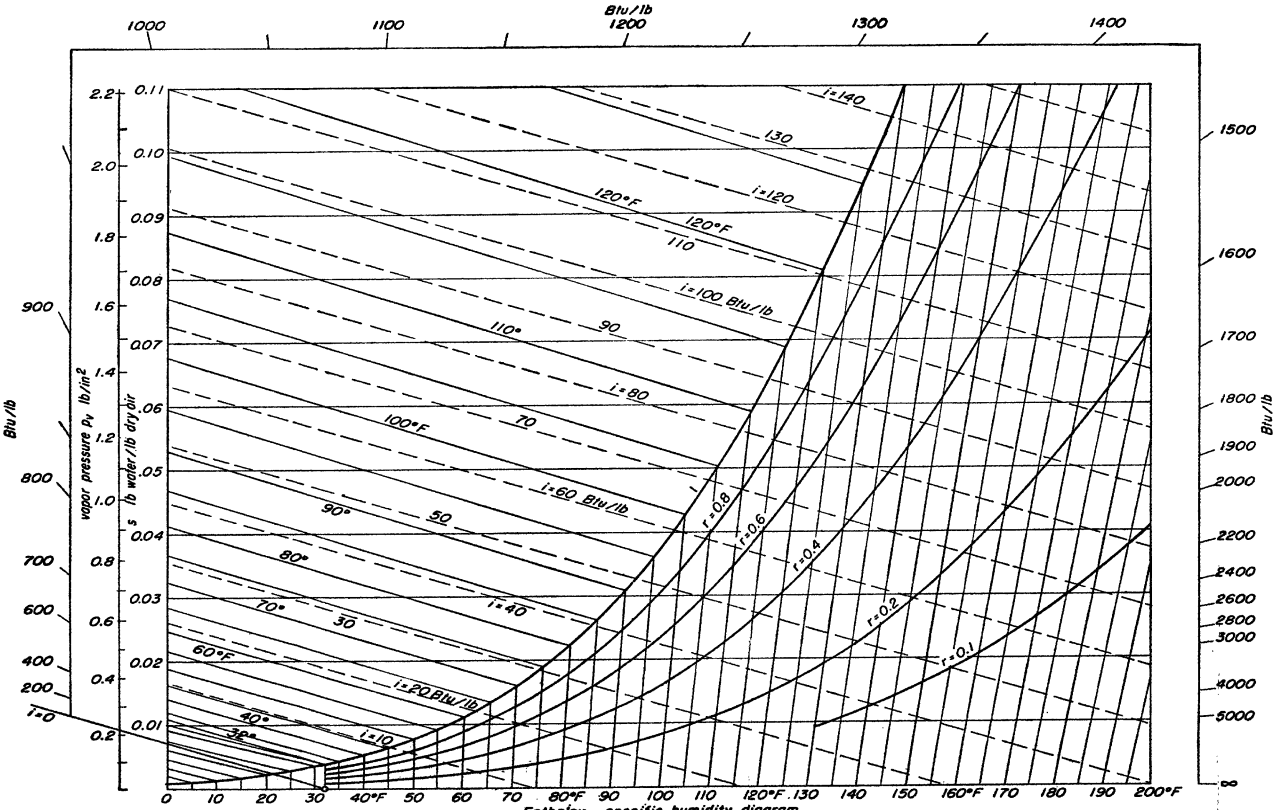

Enthalpy – specific humidity diagram
total pressure p = 14.696 lb/in²

Fig. A.

For small partial pressures of the water vapor it may be written

$$s \approx \frac{M_v}{M_a} \frac{p_v}{p}$$

The range of states represented in the accompanying enthalpy-specific-humidity diagram (see Fig. *A*) comprises only states with a vapor pressure smaller than 2.2 lb/in.$^2$ Within this range the above relation gives an error of less than 6 per cent. If we assume this to be tolerable we may write Eq. (284) in the form

$$w_{vw} = \frac{h_D}{R_v} \frac{p}{T} \frac{M_a}{M_v} (s_s - s_w)$$

The gas constant $R_v$ of the water vapor may be expressed by the universal gas constant $\mathcal{R}$ and the molecular weight $M_v$ of the water vapor $R_v = \mathcal{R}/M_v$. This gives

$$w_{vw} = h_D \frac{p}{R_a T} (s_s - s_w) = h_D \gamma_a (s_s - s_w)$$

where $\gamma_a$ is the specific weight of the dry air. The product $h_D \gamma_a$ is called the evaporation coefficient and is denoted by $\sigma$. The dimension of the evaporation coefficient is pounds per hour per square foot. The above equation assumes the simple form

$$w_{vw} = \sigma(s_s - s_w) \tag{295}$$

The Lewis relation for the evaporation coefficient becomes

$$\sigma = \mathbf{h}_D \gamma_a = \frac{\mathbf{h} \gamma_a}{\mathbf{C}_p} = \frac{\mathbf{h}}{\mathbf{c}_p} \tag{296}$$

The numerical value for the specific heat per pound of air can be inserted as 0.24 Btu/(lb)(F). Experiments by different scientists confirmed the above Lewis relation very well for turbulent flow,[1] but for laminar flow the agreement is not so good (see the above example).

Of special importance for evaporation processes is the temperature which a moist body assumes in an air stream where it exchanges heat only by convection with the air stream. Such a body assumes a temperature which is lower than the air temperature since, for the evaporation, heat is used up which must be transferred from the air to the body. This temperature can be calculated by the Lewis relation and is called the wet-bulb temperature since it is assumed by a thermometer whose bulb is covered with a wet cloth. The mass flow $w_w$ and the heat flow $q_w$ per unit surface area are described by the equations

---

[1] E. Kirschbaum, *Chem. Fabrik*, **14**, 171–181 (1941).

$$\begin{aligned} w_w &= \sigma(s_s - s_w) \\ q_w &= h(t_s - t_w) \end{aligned}$$

When the body gets the whole amount of heat necessary for the evaporation from the air by convection, $q_w = w_w r$, with $r$ as heat of evaporation per pound of water.
Then

$$\frac{t_s - t_w}{s_s - s_w} = r\frac{\sigma}{h} = \frac{r}{c_p} \tag{297}$$

By this equation, the direction of the line is fixed which connects in the enthalpy-specific-humidity diagram the point 0 ($s_w$, $t_w$) for the state of the air immediately over the surface, with point 1 ($s_s$, $t_s$) representing the state of the air at a great distance from the body. R. Mollier[1] showed that the wet-bulb temperature $t_w$ is found in the diagram by finding the isotherm in the supersaturated region whose prolongation hits point 1.[2]

The moisture content of air is conveniently measured by the psychrometric method. A psychrometer consists of an ordinary or *dry-bulb* thermometer, and a *wet-bulb* thermometer whose bulb is covered with a moist cloth. The air whose moisture is to be measured must be blown with sufficient velocity over the thermometers so that the heat exchange by radiation with the surroundings can be neglected as compared with the heat exchange by convection. By looking up the point in the enthalpy-specific-humidity diagram where the dry-bulb isotherm and the prolonged wet-bulb isotherm intersect, the state point of the air and its humidity are fixed.

**Example.** A measurement in air at 14.7 lb/in.$^2$ with a psychrometer gave a dry-bulb temperature of 68 F, and a wet-bulb temperature of 50 F. The specific humidity of the air is to be determined.

---

[1] R. Mollier, "Stodola-Festschrift," Leipzig, 1929; F. Bošnjaković, "Technische Thermodynamik," Vol. 2, p. 43, Dresden, 1937; E. Kirschbaum, *Chem. Fabrik*, **14**, 171–181 (1941).

[2] This method is not quite correct, but it agrees very well with experiments.

In the enthalpy-specific-humidity diagram the isotherm 50 F in the supersaturated region must be prolonged until it intersects the isotherm 68 F. The point of intersection gives the state of the moist air. Its specific humidity can be read from the ordinate scale as $s = 0.0037$ *lb* of water per pound of dry air. If the enthalpy-specific-humidity diagram contains lines of constant relative humidity, this value for the investigated air can be read immediately. Otherwise it is necessary to calculate the partial pressure of the water vapor of the investigated air and the partial pressure of water vapor of saturated air at 68 F from the specific humidities with Eq. (249) or to take the values from steam tables or the accompanying $s$-$i$ diagram. The ratio of the two partial pressures is the relative humidity $r = 0.245$.

# APPENDIX

## CONTENTS

PAGE
Introduction . . . . . . . . . . . . . . . . . . . . . . . . . . . . . . . . . . . . . . . . . . . . . . . . 261
Table 13. Property Values, Metals . . . . . . . . . . . . . . . . . . . . . . . . . . . . . . . . 266
Table 14. Property Values, Nonmetals . . . . . . . . . . . . . . . . . . . . . . . . . . . . . 270
Table 15. Property Values, Liquids . . . . . . . . . . . . . . . . . . . . . . . . . . . . . . . . 271
Table 16. Property Values, Gases . . . . . . . . . . . . . . . . . . . . . . . . . . . . . . . . . 274
Table 17. Coefficients of Diffusion . . . . . . . . . . . . . . . . . . . . . . . . . . . . . . . . 276
Table 18. Emissivities . . . . . . . . . . . . . . . . . . . . . . . . . . . . . . . . . . . . . . . . . 277
Fig. 136. Specific Weight of Water Vapor . . . . . . . . . . . . . . . . . . . . . . . . . . 262
Fig. 137. Expansion Coefficient, Water and Water Vapor . . . . . . . . . . . 263
Fig. 138. Specific Heat, Water and Water Vapor . . . . . . . . . . . . . . . . . . . 263
Fig. 139. Viscosity, Water and Water Vapor . . . . . . . . . . . . . . . . . . . . . . 264
Fig. 140. Viscosity, Water Vapor . . . . . . . . . . . . . . . . . . . . . . . . . . . . . . . . 264
Fig. 141. Thermal Conductivity, Water and Water Vapor . . . . . . . . . . 265
Fig. 142. Thermal Conductivity, Water Vapor . . . . . . . . . . . . . . . . . . . . 265
Fig. 143. Prandtl number, Water and Water Vapor . . . . . . . . . . . . . . . . 269
References for Property Values . . . . . . . . . . . . . . . . . . . . . . . . . . . . . . . . . 278

# APPENDIX

By

**ROBERT M. DRAKE, Jr.**

The Appendix is intended primarily to support the text and not to fulfill the requirements of a handbook; thus the accent is on brevity and simplicity. The reader or researcher desiring more detailed or additional material should consult any of the excellent and extensive publications listed here.

Table 15 gives the property values of a number of liquids at saturation pressures. Excluding the region in the neighborhood of the critical state, the variation with pressure of the property values listed is small, so that the values in the tables can be universally used. The viscosity is shown as the kinematic viscosity $\nu$. This is done because in the use of the dynamic viscosity $\mu$ there is always a possibility for confusion, as in the literature these values are given side by side in both the gravitational system and in the absolute system. This confusion does not exist in the use of the kinematic viscosity since the dimensions contain neither force nor mass.

Table 16 presents the property values of important gases at atmospheric pressure. Excluding again the region of the critical state, the property values for other pressures can be obtained from those given in the following way. The specific weight can be determined using the ideal-gas equation $\gamma = p/RT$. From this, it follows that at any temperature the specific weight is $\gamma = \gamma_0(p/p_0)$, where $p_0 = 14.22$ lb/in.$^2$ and $\gamma_0$ is the value of the specific weight as listed in the tables for the temperature in question. Further, the specific heat $c_p$ is practically independent of pressure for gases for a fairly wide range. This independence of pressure is true also for the thermal conductivity $k$, the dynamic viscosity $\mu$, and thus the Prandtl modulus *Pr*. The kinematic viscosity $\nu$ and the thermal diffusivity $\alpha$ are inversely proportional to the specific weight and therefore, for a certain temperature, they are inversely proportional to the pressure. In this way, property values for other pressures can be found from the ones listed in the tables.

The dependency of the property values on pressure and temperature in the neighborhood of the critical state is shown in the Figs. 136 to 143 for water. A similar dependence for other materials and, therefore, the deviations from the values calculated as proposed above may be approximately determined from the fact that the percentage variation of any value in the region of the critical state has the same order of magnitude for all materials at corresponding distances from the critical state (equal values of $p/p_c$ and $T/T_c$, where $p_c$ and $T_c$ represent the critical pressure and critical temperature respectively).

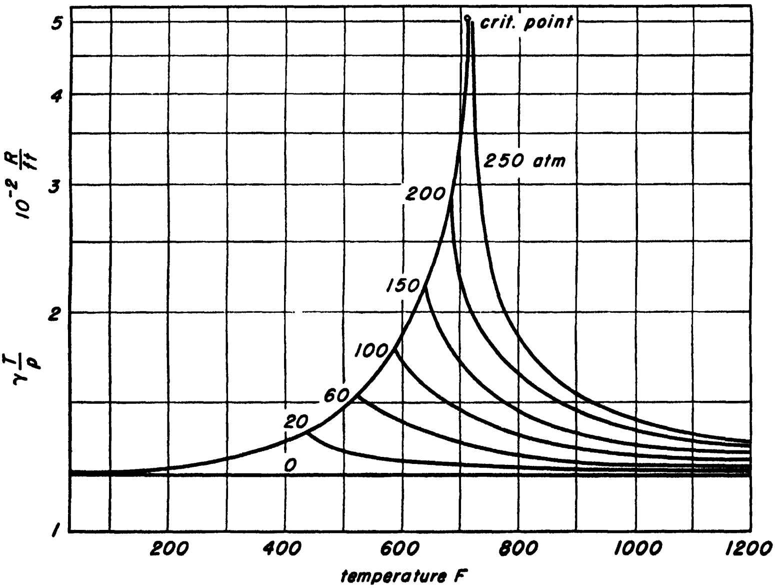

FIG. 136. The specific weight of water vapor showing the dependency upon pressure and temperature.

Tables 13, 15, and 16 are taken from the book "Hauptwerte des Wärmeaustauches," by B. Koch (as yet unpublished), with the kind permission of the author. The values are converted herein from the metric to the English system of units. The values for air in the range 500 to 3000 F are prepared from "Gas Tables," by J. H. Keenan and J. Kaye. The thermal conductivities and

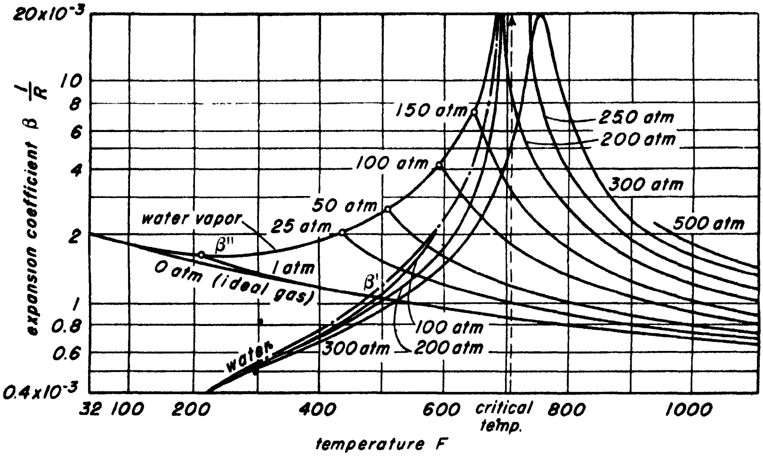

FIG. 137. The expansion coefficient $\beta = (1/v)(\partial v/\partial T)$ of water and water vapor.

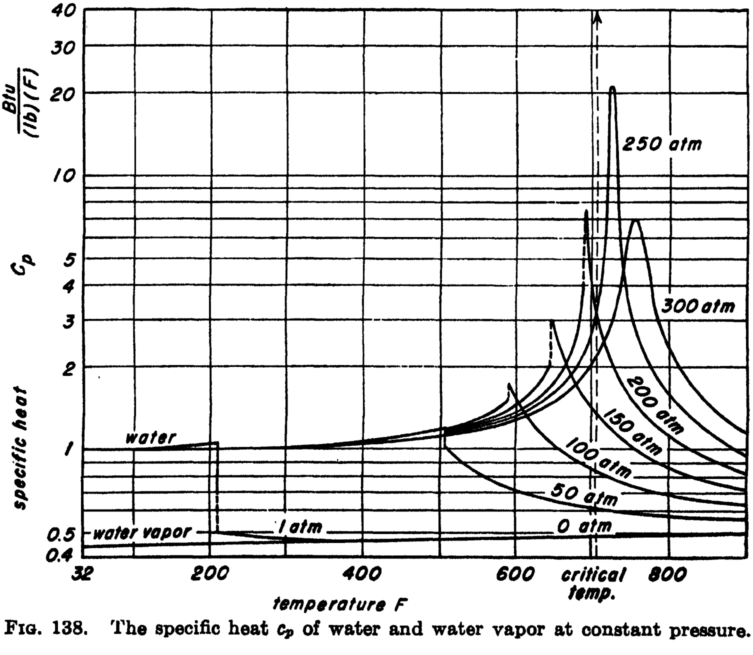

FIG. 138. The specific heat $c_p$ of water and water vapor at constant pressure.

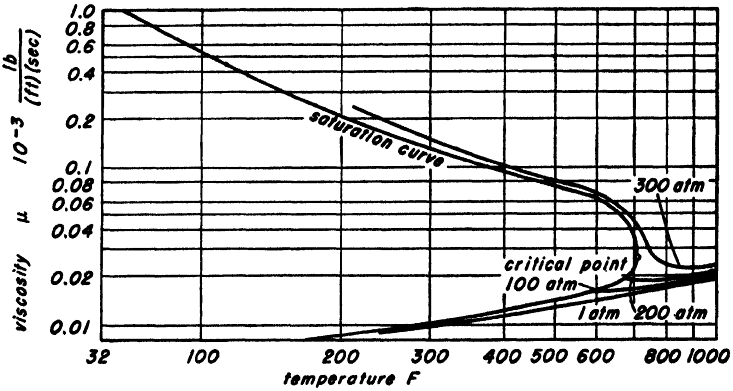

Fig. 139. The dynamic viscosity $\mu$ of water and water vapor.

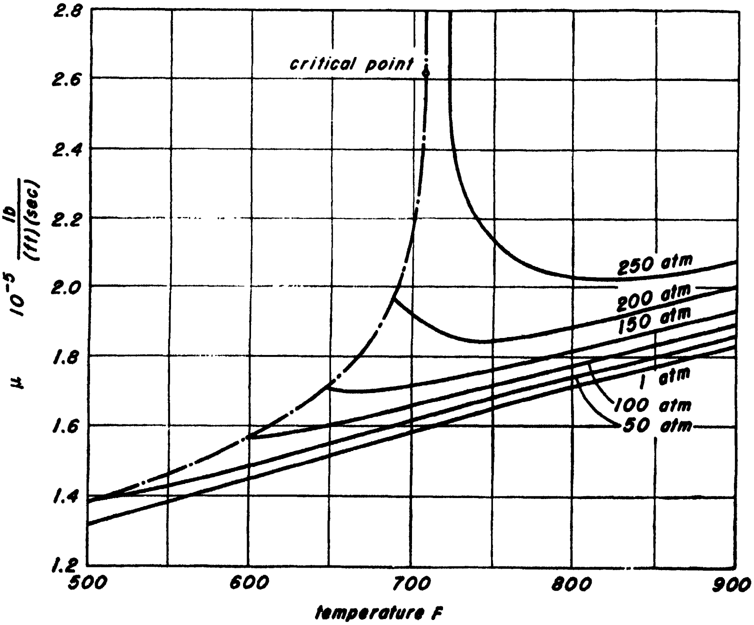

**Fig. 140.** The dynamic viscosity $\mu$ of water vapor.

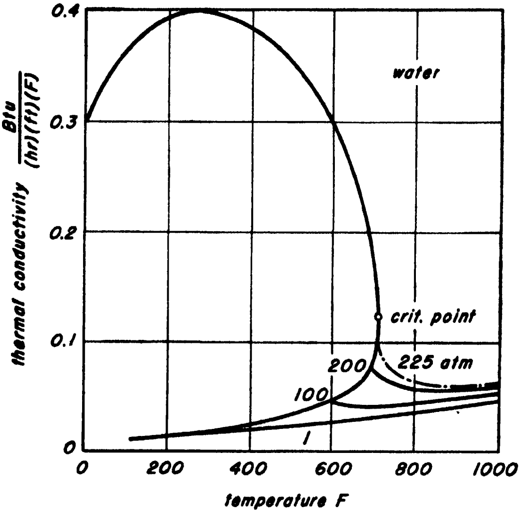

FIG. 141. The thermal conductivity $k$ of water and water vapor in superheated and saturated state.

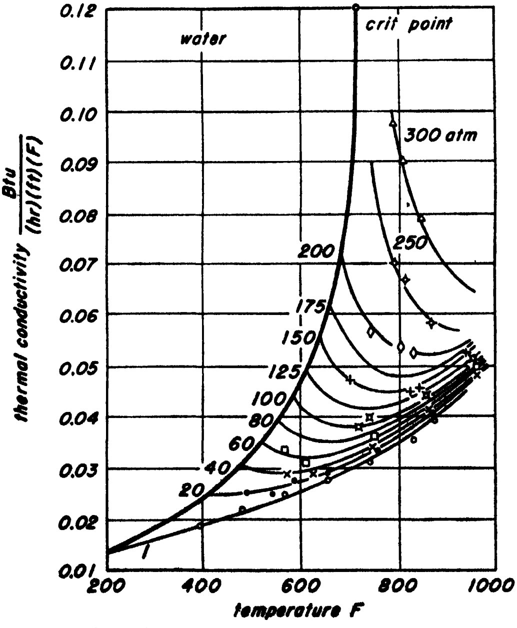

FIG. 142. The thermal conductivity $k$ of water vapor showing the dependence upon pressure and temperature. (*The Experimental Points from Timrot and Vargaftik.*)

### TABLE 13. PROPERTY VALUES

| Metals | Properties at 68 F | | | | $k$, thermal conductivity, Btu/(hr)(ft)(F) | | | | | | | | | |
|---|---|---|---|---|---|---|---|---|---|---|---|---|---|---|
| | $\gamma$ lb/ft³ | $c_p$ $\frac{\text{Btu}}{\text{(lb)(F)}}$ | $k$ $\frac{\text{Btu}}{\text{(hr)(ft)(F)}}$ | $\alpha$ $\frac{\text{ft}^2}{\text{hr}}$ | −148 F −100 C | 32 F 0 C | 212 F 100 C | 392 F 200 C | 572 F 300 C | 752 F 400 C | 1112 F 600 C | 1472 F 800 C | 1832 F 1000 C | 2192 F 1200 C |
| **Aluminum:** | | | | | | | | | | | | | | |
| Pure | 169 | 0.214 | 132 | 3.665 | 134 | 132 | 132 | 132 | 132 | | | | | |
| Al-Cu (Duralumin) 94–96 Al, 3–5 Cu, trace Mg | 174 | 0.211 | 95 | 2.580 | 73 | 92 | 105 | 112 | | | | | | |
| Al-Mg (Hydronalium) 91–95 Al, 5–9 Mg | 163 | 0.216 | 65 | 1.860 | 54 | 63 | 73 | 82 | | | | | | |
| Al-Si (Silumin) 87 Al, 13 Si | 166 | 0.208 | 95 | 2.773 | 86 | 94 | 101 | 107 | | | | | | |
| Al-Si (Silumin, copper bearing) 86.5 Al; 12.5 Si; 1 Cu | 166 | 0.207 | 79 | 2.311 | 69 | 79 | 83 | 88 | 93 | | | | | |
| Al-Si (Alusil) 78–80 Al; 20–22 Si | 164 | 0.204 | 93 | 2.762 | 83 | 91 | 97 | 101 | 103 | | | | | |
| Al-Mg-Si 97 Al; 1 Mg; 1 Si; 1 Mn | 169 | 0.213 | 102 | 2.859 | ..... | 101 | 109 | 118 | | | | | | |
| **Lead** | 710 | 0.031 | 20 | 0.924 | 21.3 | 20.3 | 19.3 | 18.2 | 17.2 | | | | | |
| **Iron:** | | | | | | | | | | | | | | |
| Pure | 493 | 0.108 | 42 | 0.785 | 50 | 42 | 39 | 36 | 32 | 28 | 23 | 21 | 20 | 21 |
| Wrought iron (C < 0.5 %) | 490 | 0.11 | 34 | 0.634 | ..... | 34 | 33 | 30 | 28 | 26 | 21 | 19 | 19 | 19 |
| Cast iron (C ≈ 4 %) | 454 | 0.10 | 30 | 0.666 | | | | | | | | | | |
| Steel (C max ≈ 1.5 %) | | | | | | | | | | | | | | |
| Carbon steel C ≈ 0.5 % | 489 | 0.111 | 31 | 0.570 | ..... | 32 | 30 | 28 | 26 | 24 | 20 | 18 | 17 | 18 |
| 1.0 % | 487 | 0.113 | 25 | 0.452 | ..... | 25 | 25 | 24 | 23 | 21 | 19 | 17 | 16 | 17 |
| 1.5 % | 484 | 0.116 | 21 | 0.376 | ..... | 21 | 21 | 21 | 20 | 19 | 18 | 16 | 16 | 17 |
| Nickel steel Ni ≈ 0 % | 493 | 0.108 | 42 | 0.785 | | | | | | | | | | |
| 10 % | 496 | 0.11 | 15 | 0.279 | | | | | | | | | | |
| 20 % | 499 | 0.11 | 11 | 0.204 | | | | | | | | | | |
| 30 % | 504 | 0.11 | 7 | 0.118 | | | | | | | | | | |
| 40 % | 510 | 0.11 | 6 | 0.108 | | | | | | | | | | |
| 50 % | 516 | 0.11 | 8 | 0.140 | | | | | | | | | | |
| 60 % | 523 | 0.11 | 11 | 0.182 | | | | | | | | | | |
| 70 % | 531 | 0.11 | 15 | 0.258 | | | | | | | | | | |
| 80 % | 538 | 0.11 | 20 | 0.344 | | | | | | | | | | |
| 90 % | 547 | 0.11 | 27 | 0.452 | | | | | | | | | | |
| 100 % | 556 | 0.106 | 52 | 0.892 | | | | | | | | | | |
| Invar Ni = 36 % | 508 | 0.11 | 6.2 | 0.108 | | | | | | | | | | |

| | | | | | | | | | | | | | |
|---|---|---|---|---|---|---|---|---|---|---|---|---|---|
| Chrome steel Cr = 0 % | 493 | 0.108 | 42 | 0.785 | 50 | 42 | 39 | 36 | 32 | 28 | 23 | 21 | 20 | 21 |
| 1 % | 491 | 0.11 | 35 | 0.645 | ..... | 36 | 32 | 30 | 27 | 24 | 21 | 19 | 19 | |
| 2 % | 491 | 0.11 | 30 | 0.559 | ..... | 31 | 28 | 26 | 24 | 22 | 19 | 18 | 18 | |
| 5 % | 489 | 0.11 | 23 | 0.430 | ..... | 23 | 22 | 21 | 21 | 19 | 17 | 17 | 17 | 17 |
| 10 % | 486 | 0.11 | 18 | 0.344 | ..... | 18 | 18 | 18 | 17 | 17 | 16 | 16 | 17 | |
| 20 % | 480 | 0.11 | 13 | 0.258 | ..... | 13 | 13 | 13 | 13 | 14 | 14 | 15 | 17 | |
| 30 % | 476 | 0.11 | 11 | 0.204 | | | | | | | | | | |
| Cr-Ni (chrome-nickel): 15 Cr; 10 Ni | 491 | 0.11 | 11 | 0.204 | | | | | | | | | | |
| 18 Cr; 8 Ni (V2A) | 488 | 0.11 | 9.4 | 0.172 | ..... | 9.4 | 10 | 10 | 11 | 11 | 13 | 15 | 18 | |
| 20 Cr; 15 Ni | 489 | 0.11 | 8.7 | 0.161 | | | | | | | | | | |
| 25 Cr; 20 Ni | 491 | 0.11 | 7.4 | 0.140 | | | | | | | | | | |
| Ni-Cr (nickel-chrome): 80 Ni; 15 Cr | 532 | 0.11 | 10 | 0.172 | | | | | | | | | | |
| 60 Ni; 15 Cr | 516 | 0.11 | 7.4 | 0.129 | | | | | | | | | | |
| 40 Ni; 15 Cr | 504 | 0.11 | 6.7 | 0.118 | | | | | | | | | | |
| 20 Ni; 15 Cr | 491 | 0.11 | 8.1 | 0.151 | ..... | 8.1 | 8.7 | 8.7 | 9.4 | 10 | 11 | 13 | | |
| Cr-Ni-Al: 6 Cr; 1.5 Al; 0.5 Si (Sicromal 8) | 482 | 0.117 | 13 | 0.237 | | | | | | | | | | |
| 24 Cr; 2.5 Al; 0.5 Si (Sicromal 12) | 479 | 0.118 | 11 | 0.194 | | | | | | | | | | |
| **Manganese steel** Ma = 0 % | 493 | 0.118 | 42 | 0.784 | | | | | | | | | | |
| 1 % | 491 | 0.11 | 29 | 0.538 | | | | | | | | | | |
| 2 % | 491 | 0.11 | 22 | 0.376 | ..... | 22 | 21 | 21 | 21 | 20 | 19 | | | |
| 5 % | 490 | 0.11 | 13 | 0.247 | | | | | | | | | | |
| 10 % | 487 | 0.11 | 10 | 0.194 | | | | | | | | | | |
| **Tungsten steel** W = 0 % | 493 | 0.108 | 42 | 0.785 | | | | | | | | | | |
| 1 % | 494 | 0.107 | 38 | 0.720 | | | | | | | | | | |
| 2 % | 497 | 0.106 | 36 | 0.677 | ..... | 36 | 34 | 31 | 28 | 26 | 21 | | | |
| 5 % | 504 | 0.104 | 31 | 0.591 | | | | | | | | | | |
| 10 % | 519 | 0.100 | 28 | 0.527 | | | | | | | | | | |
| 20 % | 551 | 0.093 | 25 | 0.484 | | | | | | | | | | |
| Silicon steel Si = 0 % | 493 | 0.108 | 42 | 0.785 | | | | | | | | | | |
| 1 % | 485 | 0.11 | 24 | 0.451 | | | | | | | | | | |
| 2 % | 479 | 0.11 | 18 | 0.344 | | | | | | | | | | |
| 5 % | 463 | 0.11 | 11 | 0.215 | | | | | | | | | | |

TABLE 13. PROPERTY VALUES.—(*Continued*)

| Metals | Properties at 68 F |  |  |  | $k$, thermal conductivity, Btu/(hr)(ft)(F) |  |  |  |  |  |  |  |  |  |
|---|---|---|---|---|---|---|---|---|---|---|---|---|---|---|
|  | $\gamma$ lb/ft³ | $c_p$ $\frac{\text{Btu}}{(\text{lb})(\text{F})}$ | $k$ $\frac{\text{Btu}}{(\text{hr})(\text{ft})(\text{F})}$ | $\alpha$ $\frac{\text{ft}^2}{\text{hr}}$ | −148 F −100 C | 32 F 0 C | 212 F 100 C | 392 F 200 C | 572 F 300 C | 752 F 400 C | 1112 F 600 C | 1472 F 800 C | 1832 F 1000 C | 2192 F 1200 C |
| **Copper:** |  |  |  |  |  |  |  |  |  |  |  |  |  |  |
| Pure | 559 | 0.0915 | 223 | 4.353 | 235 | 223 | 219 | 216 | ..... | 210 | 204 |  |  |  |
| Aluminum bronze 95 Cu; 5 Al | 541 | 0.098 | 48 | 0.903 |  |  |  |  |  |  |  |  |  |  |
| Bronze 75 Cu; 25 Sn | 541 | 0.082 | 15 | 0.333 |  |  |  |  |  |  |  |  |  |  |
| Red brass 85 Cu; 9 Sn; 6 Zn | 544 | 0.092 | 35 | 0.699 | ..... | 34 | 41 |  |  |  |  |  |  |  |
| Brass 70 Cu; 30 Zn | 532 | 0.092 | 64 | 1.322 | 51 | ..... | 74 | 83 | 85 | 85 |  |  |  |  |
| German silver 62 Cu; 15 Ni; 22 Zn | 538 | 0.094 | 14.4 | 0.290 | 11.1 | ..... | 18 | 23 | 26 | 28 |  |  |  |  |
| Constantan 60 Cu; 40 Ni | 557 | 0.098 | 13.1 | 0.237 | 12 | ..... | 12.8 | 15 |  |  |  |  |  |  |
| **Magnesium:** |  |  |  |  |  |  |  |  |  |  |  |  |  |  |
| Pure | 109 | 0.242 | 99 | 3.762 | 103 | 99 | 97 | 94 | 91 |  |  |  |  |  |
| Mg-Al (electrolytic) 6–8 % Al; 1–2 % Zn | 113 | 0.24 | 38 | 1.397 | ..... | 30 | 36 | 43 | 48 |  |  |  |  |  |
| Mg-Mn 2 % Mn | 111 | 0.24 | 66 | 2.473 | 54 | 64 | 72 | 75 |  |  |  |  |  |  |
| **Molybdenum** | 638 | 0.060 | 79 | 2.074 | 80 | 79 | 79 |  |  |  |  |  |  |  |
| **Nickel:** |  |  |  |  |  |  |  |  |  |  |  |  |  |  |
| Pure (99.9 %) | 556 | 0.1065 | 52 | 0.882 | 60 | 54 | 48 | 42 | 37 | 34 |  |  |  |  |
| Impure (99.2 %) | 556 | 0.106 | 40 | 0.677 | ..... | 40 | 37 | 34 | 32 | 30 | 32 | 36 | 39 | 40 |
| Ni-Cr 90 Ni; 10 Cr | 541 | 0.106 | 10 | 0.172 | ..... | 9.9 | 10.9 | 12.1 | 13.2 | 14.2 |  |  |  |  |
| 80 Ni; 20 Cr | 519 | 0.106 | 7.3 | 0.129 | ..... | 7.1 | 8.0 | 9.0 | 9.9 | 10.9 | 13.0 |  |  |  |
| **Silver:** |  |  |  |  |  |  |  |  |  |  |  |  |  |  |
| Purest | 657 | 0.0559 | 242 | 6.601 | 242 | 241 | 240 | 238 |  |  |  |  |  |  |
| Pure (99.9 %) | 657 | 0.0559 | 235 | 6.418 | 242 | 237 | 240 | 216 | 209 | 208 |  |  |  |  |
| **Tungsten** | 1208 | 0.0321 | 94 | 2.430 | ..... | 96 | 87 | 82 | 77 | 73 | 65 | 44 |  |  |
| **Zinc, pure** | 446 | 0.0918 | 64.8 | 1.591 | 66 | 65 | 63 | 61 | 58 | 54 |  |  |  |  |
| **Tin, pure** | 456 | 0.0541 | 37 | 1.505 | 43 | 38.1 | 34 | 33 |  |  |  |  |  |  |

the values derived therefrom in this range are extrapolated values and are therefore subject to some uncertainty. It is believed, however, that it is preferable to present the data here in extrapolated form, even though it is not too accurate, than to leave the extrapolation up to the reader. Figures 136 to 138 are prepared from "Steam Tables," and Figs. 139 and 140 are from measurements by K. Sigwart [*Forschung. Ing. Wes.* **7**, 215–230 (1936)] with some changes in the superheated region to bring the values into agreement with other measurements. Figures 141 and 142 are from W. Fritz and B. Koch, "*Wärme- und Kältetechnik,*" **42**, 113–117 (1940).

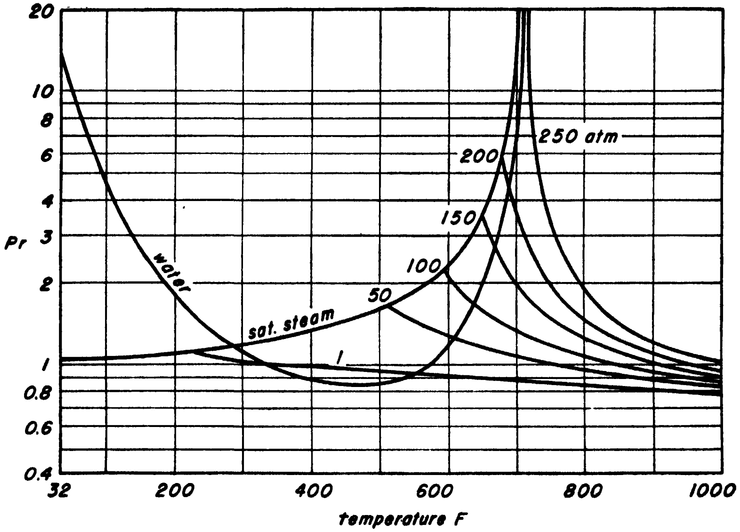

FIG. 143. The Prandtl number of water and water vapor.

With respect to Figs. 136 to 140, the designation atm, indicating atmospheres pressure, is the value generally occurring in the metric system and is equivalent to 14.22 lb/in.$^2$ in the English system of units.

TABLE 14. CHARACTERISTICS FOR SOME NONMETALS

| Material | $t$ F | $\gamma$ lb/ft$^3$ | $c_p$ $\frac{\text{Btu}}{(\text{lb})(\text{F})}$ | $k$ $\frac{\text{Btu}}{(\text{hr})(\text{ft})(\text{F})}$ | $\alpha$ $\frac{\text{ft}^2}{\text{hr}}$ |
|---|---|---|---|---|---|
| Aerogel, silica | 248 | 8.5 | ..... | 0.013 | |
| Asbestos | −328 | 29.3 | ..... | 0.043 | |
| Asbestos | 32 | 29.3 | ..... | 0.090 | |
| Asbestos | 32 | 36.0 | ..... | 0.087 | |
| Asbestos | 212 | 36.0 | ..... | 0.111 | |
| Asbestos | 392 | 36.0 | ..... | 0.120 | |
| Asbestos | 752 | 36.0 | ..... | 0.129 | |
| Asbestos | −328 | 43.5 | ..... | 0.090 | |
| Asbestos | 32 | 43.5 | ..... | 0.135 | |
| Brick, dry | 68 | 110–113 | 0.20 | 0.22–0.30 | 0.011–0.013 |
| Bakelite | 68 | 79.5 | 0.38 | 0.134 | 0.0044 |
| Cardboard, corrugated | ..... | ....... | ..... | 0.037 | |
| Clay | 68 | 91.0 | 0.21 | 0.739 | 0.039 |
| Concrete | 68 | 119–144 | 0.21 | 0.47–0.81 | 0.019–0.027 |
| Coal, anthracite | 68 | 75–94 | 0.30 | 0.15 | 0.005–0.006 |
| Coal, powdered | 86 | 46 | 0.31 | 0.067 | 0.005 |
| Cotton | 68 | 5 | 0.31 | 0.034 | 0.075 |
| Cork, board | 86 | 10 | ..... | 0.025 | |
| Cork, expanded scrap | 68 | 2.8–7.4 | 0.45 | 0.021 | 0.006–0.017 |
| Cork, ground | 86 | 9.4 | ..... | 0.025 | |
| Diatomaceous earth | 100 | 20.0 | ..... | 0.036 | |
| Diatomaceous earth | 1600 | 20.0 | ..... | 0.082 | |
| Earth, coarse gravelly | 68 | 128 | 0.44 | 0.30 | 0.0054 |
| Felt, wool | 86 | 20.6 | ..... | 0.03 | |
| Fiber, insulating board | 70 | 14.8 | ..... | 0.028 | |
| Fiber, red | 68 | 80.5 | ..... | 0.27 | |
| Glass plate | 68 | 169 | 0.2 | 0.44 | 0.013 |
| Glass, borosilicate | 86 | 139 | ..... | 0.63 | |
| Glass, wool | 68 | 12.5 | 0.16 | 0.023 | 0.011 |
| Granite | ..... | ..... | ..... | 1.0–2.3 | |
| Ice | 32 | 57 | 0.46 | 1.28 | 0.048 |
| Marble | 68 | 156–169 | 0.193 | 1.6 | 0.054 |
| Rubber, hard | 32 | 74.8 | ..... | 0.087 | |
| Sandstone | 68 | 135–144 | 0.17 | 0.94–1.2 | 0.041–0.049 |
| Silk | 68 | 3.6 | 0.33 | 0.021 | 0.017 |
| Wood, oak radial | 68 | 38–50 | 0.57 | 0.10–0.12 | 0.0043–0.0047 |
| Wood, fir (20% moisture) radial | 68 | 26.0–26.3 | 0.65 | 0.08 | 0.0048 |

### TABLE 15. PROPERTY VALUES

Fluids in saturated state

| $t$ F | $\gamma$ lb/ft³ | $c_p$ $\frac{\text{Btu}}{(\text{lb})(\text{F})}$ | $\nu$ ft²/sec | $k$ $\frac{\text{Btu}}{(\text{hr})(\text{ft})(\text{F})}$ | $\alpha$ $\frac{\text{ft}^2}{\text{hr}}$ | $Pr$ | $\beta$ $\frac{1}{R}$ |
|---|---|---|---|---|---|---|---|
| | | | | Water ($H_2O$) | | | |
| 32 | 62.57 | 1.0074 | $1.925 \times 10^{-5}$ | 0.319 | $5.07 \times 10^{-3}$ | 13.6 | |
| 68 | 62.46 | 0.9988 | 1.083 | 0.345 | 5.54 | 7.02 | $0.10 \times 10^{-3}$ |
| 104 | 62.09 | 0.9980 | 0.708 | 0.363 | 5.86 | 4.34 | |
| 140 | 61.52 | 0.9994 | 0.514 | 0.376 | 6.02 | 3.02 | |
| 176 | 60.81 | 1.0023 | 0.392 | 0.386 | 6.34 | 2.22 | |
| 212 | 59.97 | 1.0070 | 0.316 | 0.393 | 6.51 | 1.74 | |
| 248 | 59.01 | 1.015 | 0.266 | 0.396 | 6.62 | 1.446 | |
| 284 | 57.95 | 1.023 | 0.230 | 0.395 | 6.68 | 1.241 | |
| 320 | 56.79 | 1.037 | 0.204 | 0.393 | 6.70 | 1.099 | |
| 356 | 55.50 | 1.055 | 0.186 | 0.390 | 6.68 | 1.004 | |
| 392 | 54.11 | 1.076 | 0.172 | 0.384 | 6.61 | 0.937 | |
| 428 | 52.59 | 1.101 | 0.161 | 0.377 | 6.51 | 0.891 | |
| 464 | 50.92 | 1.136 | 0.154 | 0.367 | 6.35 | 0.871 | |
| 500 | 49.06 | 1.182 | 0.148 | 0.353 | 6.11 | 0.874 | |
| 537 | 46.98 | 1.244 | 0.145 | 0.335 | 5.74 | 0.910 | |
| 572 | 44.59 | 1.368 | 0.145 | 0.312 | 5.13 | 1.019 | |
| | | | | Ammonia ($NH_3$) | | | |
| −58 | 43.93 | 1.066 | $0.468 \times 10^{-5}$ | 0.316 | $6.75 \times 10^{-3}$ | 2.60 | |
| −40 | 43.18 | 1.067 | 0.437 | 0.316 | 6.88 | 2.28 | |
| −22 | 42.41 | 1.069 | 0.417 | 0.317 | 6.98 | 2.15 | |
| −4 | 41.62 | 1.077 | 0.410 | 0.316 | 7.05 | 2.09 | |
| 14 | 40.80 | 1.090 | 0.407 | 0.314 | 7.07 | 2.07 | |
| 32 | 39.96 | 1.107 | 0.402 | 0.312 | 7.05 | 2.05 | |
| 50 | 39.09 | 1 126 | 0.396 | 0.307 | 6.98 | 2.04 | |
| 68 | 38.19 | 1.146 | 0.386 | 0.301 | 6.88 | 2.02 | $1.36 \times 10^{-3}$ |
| 86 | 37.23 | 1.168 | 0.376 | 0.293 | 6.75 | 2.01 | |
| 104 | 36.27 | 1.194 | 0.366 | 0.285 | 6.59 | 2.00 | |
| 122 | 35.23 | 1.222 | 0.355 | 0.275 | 6.41 | 1.99 | |
| | | | | Carbon dioxide ($CO_2$) | | | |
| −58 | 72.19 | 0.44 | $0.128 \times 10^{-5}$ | 0.0494 | $1.558 \times 10^{-3}$ | 2.96 | |
| −40 | 69.78 | 0.45 | 0.127 | 0.0584 | 1.864 | 2.46 | |
| −22 | 67.22 | 0.47 | 0.126 | 0.0645 | 2.043 | 2.22 | |
| −4 | 64.45 | 0.49 | 0.124 | 0.0665 | 2.110 | 2.12 | |
| 14 | 61.39 | 0.52 | 0.122 | 0.0635 | 1.989 | 2.20 | |
| 32 | 57.87 | 0.59 | 0.117 | 0.0604 | 1.774 | 2.38 | |
| 50 | 53.69 | 0.75 | 0.109 | 0.0561 | 1.398 | 2.80 | |
| 68 | 48.23 | 1.2 | 0.098 | 0.0504 | 0.860 | 4.10 | $3.67 \times 10^{-3}$ |
| 86 | 37.32 | 8.7 | 0.086 | 0.0406 | 0.108 | 28.7 | |

TABLE 15. PROPERTY VALUES.—(*Continued*)

| $t$<br>F | $\gamma$<br>lb/ft$^3$ | $c_p$<br>$\frac{\text{Btu}}{(\text{lb})(\text{F})}$ | $\nu$<br>ft$^2$/sec | $k$<br>$\frac{\text{Btu}}{(\text{hr})(\text{ft})(\text{F})}$ | $\alpha$<br>$\frac{\text{ft}^2}{\text{hr}}$ | $Pr$ | $\beta$<br>$\frac{1}{R}$ |
|---|---|---|---|---|---|---|---|
| | | | Sulfur dioxide ($SO_2$) | | | | |
| −58 | 97.44 | 0.3247 | $0.521 \times 10^{-5}$ | 0.140 | $4.42 \times 10^{-3}$ | 4.24 | |
| −40 | 95.94 | 0.3250 | 0.456 | 0.136 | 4.38 | 3.74 | |
| −22 | 94.43 | 0.3252 | 0.399 | 0.133 | 4.33 | 3.31 | |
| −4 | 92.93 | 0.3254 | 0.349 | 0.130 | 4.29 | 2.93 | |
| 14 | 91.37 | 0.3255 | 0.310 | 0.126 | 4.25 | 2.62 | |
| 32 | 89.80 | 0.3257 | 0.277 | 0.122 | 4.19 | 2.38 | |
| 50 | 88.18 | 0.3259 | 0.250 | 0.118 | 4.13 | 2.18 | |
| 68 | 86.55 | 0.3261 | 0.226 | 0.115 | 4.07 | 2.00 | $1.08 \times 10^{-3}$ |
| 86 | 84.86 | 0.3263 | 0.204 | 0.111 | 4.01 | 1.83 | |
| 104 | 82.98 | 0.3266 | 0.186 | 0.107 | 3.95 | 1.70 | |
| 122 | 81.10 | 0.3268 | 0.174 | 0.102 | 3.87 | 1.61 | |
| | | | Methylchloride ($CH_3Cl$) | | | | |
| −58 | 65.71 | 0.3525 | $0.344 \times 10^{-5}$ | 0.124 | $5.38 \times 10^{-3}$ | 2.31 | |
| −40 | 64.51 | 0.3541 | 0.342 | 0.121 | 5.30 | 2.32 | |
| −22 | 63.46 | 0.3564 | 0.338 | 0.117 | 5.18 | 2.35 | |
| −4 | 62.39 | 0.3593 | 0.333 | 0.113 | 5.04 | 2.38 | |
| 14 | 61.27 | 0.3629 | 0.329 | 0.108 | 4.87 | 2.43 | |
| 32 | 60.08 | 0.3673 | 0.325 | 0.103 | 4.70 | 2.49 | |
| 50 | 58.83 | 0.3726 | 0.320 | 0.099 | 4.52 | 2.55 | |
| 68 | 57.64 | 0.3788 | 0.315 | 0.094 | 4.31 | 2.63 | |
| 86 | 56.38 | 0.3860 | 0.310 | 0.089 | 4.10 | 2.72 | |
| 104 | 55.13 | 0.3942 | 0.303 | 0.083 | 3.86 | 2.83 | |
| 122 | 53.76 | 0.4034 | 0.295 | 0.077 | 3.57 | 2.97 | |
| | | | Dichlorodifluoromethane (Freon)($CCl_2F_2$) | | | | |
| −58 | 96.56 | 0.2090 | $0.334 \times 10^{-5}$ | 0.039 | $1.94 \times 10^{-3}$ | 6.2 | $1.4 \times 10^{-3}$ |
| −40 | 94.81 | 0.2113 | 0.300 | 0.040 | 1.99 | 5.4 | |
| −22 | 92.99 | 0.2139 | 0.272 | 0.040 | 2.04 | 4.8 | |
| −4 | 91.18 | 0.2167 | 0.253 | 0.041 | 2.09 | 4.4 | |
| 14 | 89.24 | 0.2198 | 0.238 | 0.042 | 2.13 | 4.0 | |
| 32 | 87.24 | 0.2232 | 0.230 | 0.042 | 2.16 | 3.8 | |
| 50 | 85.17 | 0.2268 | 0.219 | 0.042 | 2.17 | 3.6 | |
| 68 | 83.04 | 0.2307 | 0.213 | 0.042 | 2.17 | 3.5 | |
| 86 | 80.85 | 0.2349 | 0.209 | 0.041 | 2.17 | 3.5 | |
| 104 | 78.48 | 0.2393 | 0.206 | 0.040 | 2.15 | 3.5 | |
| 122 | 75.91 | 0.2440 | 0.204 | 0.039 | 2.11 | 3.5 | |

TABLE 15. PROPERTY VALUES.—(*Continued*)

| $t$ F | $\gamma$ lb/ft$^3$ | $c_p$ $\frac{\text{Btu}}{\text{(lb)(F)}}$ | $\nu$ ft$^2$/sec | $k$ $\frac{\text{Btu}}{\text{(hr)(ft)(F)}}$ | $\alpha$ $\frac{\text{ft}^2}{\text{hr}}$ | $Pr$ | $\beta$ $\frac{1}{R}$ |
|---|---|---|---|---|---|---|---|
| | | | Eutectic calcium chloride solution (29.9 % $CaCl_2$) | | | | |
| −58 | 82.39 | 0.623 | $39.13 \times 10^{-5}$ | 0.232 | $4.52 \times 10^{-3}$ | 312 | |
| −40 | 82.09 | 0.6295 | 26.88 | 0.240 | 4.65 | 208 | |
| −22 | 81.79 | 0.6356 | 18.49 | 0.248 | 4.78 | 139 | |
| −4 | 81.50 | 0.642 | 11.88 | 0.257 | 4.91 | 87.1 | |
| 14 | 81.20 | 0.648 | 7.49 | 0.265 | 5.04 | 53.6 | |
| 32 | 80.91 | 0.654 | 4.73 | 0.273 | 5.16 | 33.0 | |
| 50 | 80.62 | 0.660 | 3.61 | 0.280 | 5.28 | 24.6 | |
| 68 | 80.32 | 0.666 | 2.93 | 0.288 | 5.40 | 19.6 | |
| 86 | 80.03 | 0.672 | 2.44 | 0.295 | 5.50 | 16.0 | |
| 104 | 79.73 | 0.678 | 2.07 | 0.302 | 5.60 | 13.3 | |
| 122 | 79.44 | 0.685 | 1.78 | 0.309 | 5.69 | 11.3 | |
| | | | Glycerin [$C_3H_5(OH)_3$] | | | | |
| 32 | 79.66 | 0.540 | 0.0895 | 0.163 | $3.81 \times 10^{-3}$ | $84.7 \times 10^3$ | |
| 50 | 79.29 | 0.554 | 0.0323 | 0.164 | 3.74 | 31.0 | |
| 68 | 78.91 | 0.570 | 0.0127 | 0.165 | 3.67 | 12.5 | $0.28 \times 10^{-3}$ |
| 86 | 78.54 | 0.584 | 0.0054 | 0.165 | 3.60 | 5.38 | |
| 104 | 78.16 | 0.600 | 0.0024 | 0.165 | 3.54 | 2.45 | |
| 122 | 77.72 | 0.617 | 0.0016 | 0.166 | 3.46 | 1.63 | |
| | | | Ethylene glycol [$C_2H_4(OH_2)$] | | | | |
| 32 | 70.59 | 0.548 | $61.92 \times 10^{-5}$ | 0.140 | $3.62 \times 10^{-3}$ | 615 | |
| 68 | 69.71 | 0.569 | 20.64 | 0.144 | 3.64 | 204 | $0.36 \times 10^{-3}$ |
| 104 | 68.76 | 0.591 | 9.35 | 0.148 | 3.64 | 93 | |
| 140 | 67.90 | 0.612 | 5.11 | 0.150 | 3.61 | 51 | |
| 176 | 67.27 | 0.633 | 3.21 | 0.151 | 3.57 | 32.4 | |
| 212 | 66.08 | 0.655 | 2.18 | 0.152 | 3.52 | 22.4 | |
| | | | Engine oil (unused) | | | | |
| 32 | 56.13 | 0.429 | 0.0461 | 0.085 | $3.53 \times 10^{-3}$ | 47100 | |
| 68 | 55.45 | 0.449 | 0.0097 | 0.084 | 3.38 | 10400 | $0.39 \times 10^{-3}$ |
| 104 | 54.69 | 0.469 | 0.0026 | 0.083 | 3.23 | 2870 | |
| 140 | 53.94 | 0.489 | $0.903 \times 10^{-3}$ | 0.081 | 3.10 | 1050 | |
| 176 | 53.19 | 0.509 | 0.404 | 0.080 | 2.98 | 490 | |
| 212 | 52.44 | 0.530 | 0.219 | 0.079 | 2.86 | 276 | |
| 248 | 51.75 | 0.551 | 0.133 | 0.078 | 2.75 | 175 | |
| 284 | 51.00 | 0.572 | 0.086 | 0.077 | 2.66 | 116 | |
| 320 | 50.31 | 0.593 | 0.060 | 0.076 | 2.57 | 84 | |
| | | | Mercury (Hg) | | | | |
| 32 | 850.78 | 0.0335 | $0.133 \times 10^{-5}$ | 4.74 | $166.6 \times 10^{-3}$ | 0.0288 | |
| 68 | 847.71 | 0.0333 | 0.123 | 5.02 | 178.5 | 0.0249 | $1.01 \times 10^{-4}$ |
| 122 | 843.14 | 0.0331 | 0.112 | 5.43 | 194.6 | 0.0207 | |
| 212 | 835.57 | 0.0328 | 0.0999 | 6.07 | 221.5 | 0.0162 | |
| 302 | 828.06 | 0.0326 | 0.0918 | 6.64 | 246.2 | 0.0134 | |
| 392 | 820.61 | 0.0375 | 0.0863 | 7.13 | 267.7 | 0.0116 | |
| 482 | 813.16 | 0.0324 | 0.0823 | 7.55 | 287.0 | 0.0108 | |

Table 16. Property Values

Gases at a pressure, $p = 14.22$ lb/in.$^2$

| $t$<br>F | $\gamma$<br>lb/ft$^3$ | $c_p$<br>$\frac{\text{Btu}}{\text{(lb)(F)}}$ | $\nu$<br>ft$^2$/sec | $k$<br>$\frac{\text{Btu}}{\text{(hr)(ft)(F)}}$ | $\alpha$<br>ft$^2$/hr | $Pr$ |
|---|---|---|---|---|---|---|
| | | | Air | | | |
| $-328$* | 0.1260 | 0.245 | $2.88 \times 10^{-5}$ | 0.0040 | 0.128 | 0.81 |
| $-238$ | 0.1743 | 0.247 | 3.35 | 0.0068 | 0.159 | 0.76 |
| $-148$ | 0.1237 | 0.244 | 6.42 | 0.0095 | 0.314 | 0.74 |
| $-58$ | 0.0959 | 0.241 | 10.23 | 0.0118 | 0.507 | 0.721 |
| 32 | 0.0783 | 0.240 | 14.77 | 0.0140 | 0.747 | 0.712 |
| 122 | 0.0662 | 0.240 | 19.89 | 0.0162 | 1.02 | 0.701 |
| 212 | 0.0573 | 0.241 | 25.59 | 0.0185 | 1.34 | 0.690 |
| 392 | 0.0452 | 0.245 | 38.59 | 0.0226 | 2.04 | 0.678 |
| 572 | 0.0373 | 0.249 | 53.21 | 0.0267 | 2.88 | 0.668 |
| 752 | 0.0318 | 0.255 | 69.66 | 0.0308 | 3.80 | 0.661 |
| 932 | 0.0276 | 0.261 | 87.51 | 0.0345 | 4.80 | 0.658 |
| 1112 | 0.0245 | 0.266 | 107.2 | 0.0385 | 5.89 | 0.655 |
| 1292 | 0.0220 | 0.271 | 127.7 | 0.0419 | 7.03 | 0.655 |
| 1472 | 0.0199 | 0.276 | 149.4 | 0.0451 | 8.22 | 0.655 |
| 1652 | 0.0182 | 0.279 | 173.1 | 0.0483 | 9.51 | 0.655 |
| 1832 | 0.0168 | 0.283 | 196.7 | 0.0515 | 10.8 | 0.655 |
| 2012 | 0.0156 | 0.285 | 222.5 | 0.0543 | 12.2 | 0.655 |
| 2192 | 0.0145 | 0.288 | 249.4 | 0.0573 | 13.7 | 0.655 |
| 2372 | 0.0136 | 0.291 | 277.4 | 0.0606 | 15.3 | 0.655 |
| 2552 | 0.0128 | 0.293 | 305.3 | 0.0637 | 16.8 | 0.655 |
| 2732 | 0.0121 | 0.295 | 334.3 | 0.0658 | 18.4 | 0.655 |
| 2912 | 0.0114 | 0.296 | 365.5 | 0.0680 | 20.1 | 0.655 |
| | | | Ammonia ($NH_3$) | | | |
| $-58$† | 0.0239 | 0.525 | $2.04 \times 10^{-4}$ | 0.0099 | 0.796 | 0.93 |
| 32 | 0.0479 | 0.520 | 1.31 | 0.0127 | 0.524 | 0.90 |
| 122 | 0.0392 | 0.520 | 1.89 | 0.0151 | 0.744 | 0.91 |
| 212 | 0.0338 | 0.534 | 2.56 | 0.0171 | 0.950 | 0.97 |
| 302 | 0.0298 | 0.553 | 3.31 | 0.0188 | 1.14 | 1.05 |
| 392 | 0.0266 | 0.572 | 4.17 | 0.0201 | 1.32 | 1.13 |

* At saturation pressure $p = 6.09$ lb/in.$^2$

† At saturation pressure $p = 5.93$ lb/in.$^2$

TABLE 16. PROPERTY VALUES.—(*Continued*)

| $t$ F | $\gamma$ lb/ft$^3$ | $c_p$ $\frac{\text{Btu}}{\text{(lb)(F)}}$ | $\nu$ ft$^2$/sec | $k$ $\frac{\text{Btu}}{\text{(hr)(ft)(F)}}$ | $\alpha$ ft$^2$/hr | $Pr$ |
|---|---|---|---|---|---|---|
| Carbon dioxide ($CO_2$) | | | | | | |
| −58 | 0.1476 | 0.185 | $5.15 \times 10^{-5}$ | 0.0064 | 0.228 | 0.81 |
| 32 | 0.1197 | 0.196 | 7.75 | 0.0083 | 0.354 | 0.79 |
| 122 | 0.1009 | 0.208 | 10.86 | 0.0103 | 0.490 | 0.79 |
| 212 | 0.0873 | 0.219 | 14.30 | 0.0123 | 0.645 | 0.80 |
| 302 | 0.0768 | 0.229 | 18.17 | 0.0143 | 0.815 | 0.80 |
| 392 | 0.0687 | 0.239 | 22.36 | 0.0163 | 0.997 | 0.81 |
| Hydrogen ($H_2$) | | | | | | |
| −328 | 0.0204 | 2.56 | $1.11 \times 10^{-4}$ | 0.030 | 0.571 | 0.70 |
| −148 | 0.0086 | 3.14 | 4.78 | 0.067 | 2.49 | 0.69 |
| 32 | 0.00544 | 3.41 | 10.3 | 0.101 | 5.48 | 0.67 |
| 212 | 0.00399 | 3.45 | 17.42 | 0.132 | 9.65 | 0.65 |
| 392 | 0.00314 | 3.47 | 25.80 | 0.159 | 14.62 | 0.64 |
| 572 | 0.00260 | 3.48 | 35.91 | 0.181 | 19.03 | 0.63 |
| Steam ($H_2O$) | | | | | | |
| 212 | 0.0362 | 0.510 | $2.38 \times 10^{-4}$ | 0.0140 | 0.759 | 1.12 |
| 392 | 0.0283 | 0.46 | 3.96 | 0.0189 | 1.457 | 0.978 |
| 572 | 0.0233 | 0.48 | 5.82 | 0.0246 | 2.209 | 0.948 |
| 752 | 0.0198 | 0.49 | 7.80 | 0.0318 | 3.289 | 0.876 |
| 932 | 0.0172 | 0.52 | 10.48 | 0.0434 | 4.859 | 0.777 |

TABLE 17. COEFFICIENTS OF DIFFUSION ($D$)

Water ($H_2O$) in air: $D$ (in ft²/hr) $= 0.892(p_0/p)(T/T_0)^{1.81}$

Ammonia ($NH_3$) in air: $D$ (in ft²/hr) $= 0.763(p_0/p)(T/T_0)^{1.81}$

($p_0 = 14.22$ lb/in.², $T_0 = 460$ R)

| Classification | Diffusing material | Medium of diffusion | Temperature, F | Diffusion coefficient $D$ | Schmidt number $Sc = \frac{\nu}{D}$ |
|---|---|---|---|---|---|
| Solids..... | Cu | Al | 864 | $9.1 \times 10^{-9}$ ft²/day | |
| | Hg | Pb | 351 | $2.1 \times 10^{-9}$ ft²/day | |
| | | | 387 | $5.4 \times 10^{-9}$ ft²/day | |
| Liquids... | HCl | $H_2O$ | 32 | 0.000024 ft²/sec | 0.81 |
| | $NH_3$ | $H_2O$ | 39.2 | 0.000013 ft²/sec | 1.5 |
| Gases (at 29.9 in. Hg).... | $NH_3$ | Air | 32 | 0.000233 ft²/sec | 0.634 |
| | $CO_2$ | $H_2$ | 64.4 | 0.000651 ft²/sec | 0.158 |
| | Hg | $N_2$ | 66.2 | 0.035 ft²/sec | 0.00424 |
| | $O_2$ | $N_2$ | 53.6 | 0.000218 ft²/sec | 0.681 |
| | $H_2O$ | Air | 60.8 | 0.000303 ft²/sec | 0.488 |
| | $H_2$ | $O_2$ | 57.2 | 0.000834 ft²/sec | 0.182 |
| | $H_2$ | $N_2$ | 54.5 | 0.000794 ft²/sec | 0.187 |
| | $C_6H_6$ | Air | 32 | 0.0000807 ft²/sec | 1.83 |
| | $C_6H_6$ | $CO_2$ | 32 | 0.0000567 ft²/sec | 1.37 |
| | $C_6H_6$ | $H_2$ | 32 | 0.000316 ft²/sec | 3.26 |
| | Ethyl alcohol | Air | 32 | 0.000109 ft²/sec | 1.36 |

### TABLE 18. EMISSIVITIES $\epsilon_n$ OF THE RADIATION IN THE DIRECTION OF THE NORMAL TO THE SURFACE AND $\epsilon$ OF THE TOTAL HEMISPHERICAL RADIATION FOR VARIOUS MATERIALS FOR THE TEMPERATURE $t$

From measurements of E. Schmidt and E. Eckert

In the case of metals, the emissivities rise with rising temperature, but in the case of nonmetallic substances (metal oxides, organic substances) this rule is sometimes not correct. In the instances where the exact measurements are not given, take for bright metal surfaces an average ratio $\epsilon/\epsilon_n = 1.2$, and for other substances with smooth surfaces $\epsilon/\epsilon_n = 0.95$ and in the case of rough surfaces use $\epsilon/\epsilon_n = 0.98$.

| Surface | $t$, F | $\epsilon_n$ | $\epsilon$ |
|---|---|---|---|
| Gold, polished | 266 | 0.018 | |
| Gold, polished | 752 | 0.022 | |
| Silver | 68 | 0.020 | |
| Copper, polished | 68 | 0.030 | |
| Copper, lightly oxidized | 68 | 0.037 | |
| Copper, scraped | 68 | 0.070 | |
| Copper, black oxidized | 68 | 0.78 | |
| Copper, oxidized | 268 | 0.76 | 0.725 |
| Aluminum, bright rolled | 338 | 0.039 | 0.049 |
| Aluminum, bright rolled | 932 | 0.050 | |
| Aluminum paint | 212 | 0.20–0.40 | |
| Silumin, cast, polished | 302 | 0.186 | |
| Nickel, bright matte | 212 | 0.041 | 0.046 |
| Nickel, polished | 212 | 0.045 | 0.053 |
| Manganin, bright rolled | 245 | 0.048 | 0.057 |
| Chrome, polished | 302 | 0.058 | 0.071 |
| Iron, bright etched | 302 | 0.128 | 0.158 |
| Iron, bright abrazed | 68 | 0.24 | |
| Iron, red rusted | 68 | 0.61 | |
| Iron, hot rolled | 68 | 0.77 | |
| Iron, hot rolled | 266 | 0.60 | |
| Iron, hot cast | 212 | 0.80 | |
| Iron, heavily rusted | 68 | 0.85 | |
| Iron, heat-resistant oxidized | 176 | 0.613 | |
| Iron, heat-resistant oxidized | 392 | 0.639 | |
| Zinc, gray oxidized | 68 | 0.23–0.28 | |
| Lead, gray oxidized | 68 | 0.28 | |
| Bismuth, bright | 176 | 0.340 | 0.366 |
| Corundum, emery rough | 176 | 0.855 | 0.84 |
| Clay, fired | 158 | 0.91 | 0.86 |
| Lacquer, white | 212 | 0.925 | |
| Red lead | 212 | 0.93 | |
| Enamel, lacquer | 68 | 0.85–0.95 | |
| Lacquer, black matte | 176 | 0.970 | |
| Bakelite lacquer | 176 | 0.935 | |
| Brick, mortar, plaster | 68 | 0.93 | |
| Porcelain | 68 | 0.92–0.94 | |
| Glass | 194 | 0.940 | 0.876 |
| Ice, smooth, water | 32 | 0.966 | 0.918 |
| Ice, rough crystals | 32 | 0.985 | |
| Waterglass | 68 | 0.96 | |
| Paper | 203 | 0.92 | 0.89 |
| Wood, beech | 158 | 0.935 | 0.91 |
| Tar paper | 68 | 0.93 | |

## REFERENCES FOR PROPERTY VALUES

1. "International Critical Tables," McGraw-Hill Book Company, Inc., New York, 1929.
2. "L. S. Marks, "Mechanical Engineers' Handbook," McGraw-Hill Book Company, Inc., 1941.
3. V. D'Ans and E. Lax, "Taschenbuch für Chemiker und Physiker," Springer-Verlag, Berlin, 1943.
4. F. Henning, "Wärmetechnische Richtwerte," VDI-Verlag, Berlin, 1938.
5. W. H. McAdams, "Heat Transmission," 2d ed., McGraw-Hill Book Company, Inc., 1942.
6. "Landolt-Börnstein: Physikalisch Chemische Tabellen," Springer-Verlag, Berlin, 1923, and Edwards Bros., Ann Arbor, 1943.
7. J. H. Keenan and J. Kaye, "Gas Tables," J. Wiley & Sons, Inc., New York, 1945.
8. J. H. Keenan and F. G. Keyes, "Thermodynamic Properties of Steam," J. Wiley & Sons, Inc., New York, 1936.

# INDEX

A

Absorptivity, 193
Accommodation coefficient, 190
Ackermann, G., 245
Adiabatic wall temperature, 152
Aeroengines, 34
Airplane cooler, 109
Airplanes, 32, 157
Arithmetic mean temperature difference, 12
Aschkinass, E., 199
Atomic power plant, 114
Average heat-transfer coefficient, 93

B

Beckmann, W., 162, 171
Beer's law, 206
Benke, R., 145
Bernoulli, D., 61, 186
Biot number, 49
Black body, 194
Blasius, 73
Blasius' law, 81
Blast furnace, 54
Boehm, J., 104
Boelter, L., 115, 121, 124, 125, 214
Boiling liquid, 179
Boltzmann constant, 198
Bošnjakovíc, F., 236, 256
Boundary layer, 63
  thermal, 86
  turbulent, 64
Brick wall, 48
Bühne, W., 112
Bulk temperature, 100

C

Carbon dioxide radiation, 205
Carbon monoxide radiation, 205
Carslaw, H., 48
Chapman, R., 88
Chapman, S., 188
Chemoluminosity, 219
Cherry, V., 214
Cigarette smoke, 64
Colburn, 16, 102, 251
Cold period regenerator, 55
Combustion chamber, 220, 223
Combustion engine, 1, 53
Composite-wall heat conduction, 5
Concentration, 238
Concrete wall in steady heat flow, 48
Condensation, dropwise, 177
  filmwise, 172
Condenser, 183
Conduction, 2, 19
Conductivity, heat, 3
Conductor, electric, 20
Construction business, 38
Convection, 2, 59
Convection thickness, boundary-layer, 119
Counterflow, 9
Critical distance, 64
Critical Reynolds number, plate, 65
  tube, 66
Crocco, L., 93, 152
Crossflow, 9, 83
Cube, heat-conduction, 49
Curved tube, heat-transfer, 115
Cylinder, 49, 83
Crossflow, heat-transfer, 95

D

Dalton's equation, 250
Dalton's law, 228
Daily fluctuation temperature, 53
Dam, 38
Davis, D., 214
Dead water, 83, 85
Deformation, velocity profile, 101
Developed flow, 65
Dew point, 233
Diffuse reflection, 193
Diffusion, 236
Diffusion coefficient, 238
Diffusivity, thermal, 42
Dimensional analysis, 128
Displacement thickness, 71
Dissipation heat, 150
Dittus, F., 115
Dow, W., 94, 117
Drag coefficient, 85
  of a cylinder, 85
Drake, R., 98
Drewitz, O., 155
Dropwise condensation, 177
Dry-bulb temperature, 231
Ducted cooler, 109
Dynamic viscosity, 62

E

Eberhardt, 209
Eckert, E., 95, 96, 115, 139, 152, 154, 167, 169, 203, 207, 213, 218, 221, 246
Economizer, 34
Eddy diffusivity, 121
Effectiveness of fins, 32
Ehret, L., 100
Electric conductors, 193, 199
Electric generator, 38
Electric model, 21
Electric nonconductors, radiation of, 193, 199
Electrolytic trough, 22
Electromagnetic waves, 193
Electromotor, 38
Emissive power, 194
Enskog, D., 188
Enthalpy, moist-air, 230
Entrance length, 65
Equivalent radius, radiation of, 210
Erk, S., 48, 49, 52
Eucken, A., 188
Evaporation coefficient, 255
Expansion coefficient, 137

F

Fehling, R., 220
Fick's law, 237
Film, heat-transfer, 6
Film heat-transfer coefficient, 7
Filmwise condensation, 172
Fin, optimum shape, 36
  rectangular, 30
  short, 31
  triangular, 35
Finned heating surface, 29
Fischer, W., 156
Flachsbarth, L., 84
Flame temperature, 220
Flames, 219
Flat plate, 64
Flow, laminar and turbulent, 63
  near stagnation point, 95
  separation, 83
Fluctuation, daily, 53
  yearly, 53
Focke, R., 35
Forced convection, 59
Form resistance, 85
Fourier, J., 3, 43
Fourier number, 49
Franz, A., 154
Free convection, 59
Free molecular flow, 192
Friction coefficient, laminar, plate, 72
  tube, turbulent, 81
Frictionless flow, 61
Fritz, W., 179, 183
Frössling, 97
Furthmann, E., 203

G

Gas constant, 229
Gas turbine, 2, 109, 157
Geometrical factor, 212
Geometrically similar bodies, 132
Gradient, 19
Graetz, L., 100
Grashof number, 137
Gray surface, 201
Grele, M., 93
Grigull, U., 175
Grimison, E., 145, 146, 147
Groeber, H., 48, 49, 52
Ground, temperature fluctuations in, 53

H

Hahnemann, H., 100
Half-value time, 50
Hausen, H., 54, 58, 105, 115, 210
Hawkins, G., 159
Heat capacity, 10
Heat conduction, 19
Heat of dissipation, 150
Heat flow, 7
  unsteady, 40
Heat-flow equation, 86
Heating period regenerator, 54
Heat sources, 37
Heat-transfer coefficient, 7
Hermann, R., 164, 213
High velocities, 150
Hilpert, R., 142, 144
Hoffman, E., 112, 114
Horning, D., 186
Hottel, H., 207–209, 214, 221
Hydraulically smooth, defined, 78

I

Impulse thickness, 119
Inflow region, 79
Instability, boundary-layer, 75
Insulation, 21, 24
Intake, 11, 79
Intake length, thermal, 103
Intensity radiation, 196
Interchange factor, 217
Interconnection, flow and heat transfer by, 59
Interference photo, 139, 167, 168, 170
Interferometer, 166

J

Jaeger, T., 48
Jakob, M., 94, 117, 159, 179, 209
Jodlbauer, K., 164
Johnson, H., 94, 118, 150, 156
Jonassen, F., 121, 124, 125
Jukoff, D., 192

K

Kane, E., 186
Kármán, von, T., 66, 82, 83, 85, 106, 120
Keevil, C., 101
Kennard, R., 169, 187
Kinetic theory of gases, 186
Kirchhoff's law, 194
Kirschbaum, E., 255, 256
Knudsen, 190
Kraussold, H., 104
Kreith, F., 183
Kroujiline, G., 88, 97
Kundt, A., 192

L

Lambert's law, 196
Laminar flow, 63
Laminar sublayer, 73
Langmuir, J., 164
Law of momentum, 66
Leidenfrost, 181
Lewis, W., 251
Lieblein, V., 246
Lieneweg, F., 51
Liepmann, H., 150
Liquid-film theory, 172
Locomotives, 109
Logarithmic mean temperature difference, 12

Lorisch, W., 140, 148
Low-density gases, 185
Lowdermilk, W., 93
Low Prandtl numbers, 113
Low-temperature operations, 54
Luminous flame, 219

M

McAdams, W., 48, 79, 81, 101, 182, 183, 213
Mach number, 138, 150
Mangelsdorf, H., 207, 208
Martinelli, R., 82, 114, 121, 124, 125, 127, 128
Mass-transfer coefficient, 251
Maxwell, J., 186, 192
Mean free path, 186
Mean radius, 23
Mean temperature difference, 11
Meier, A., 53
Mercury thermometer, 28, 50
Metals, molten, 114
Methane, radiation, 205
Missile, 157, 186
Model, electric, 21
Modulus, Reynolds, 64
Molecular weight, 229
Molecules, 186
Mollier, R., 231, 256
Momentum, equation, 68
  law, 66
Monochromatic radiation, 196
Motorcar, 109, 116
Motzfeld, 82
Mueller, 16

N

Nagle, 16
Navier-Stokes equation, 133
Nessi, A., 47
Newton, 7, 61, 173
Nikuradse, 16, 83
Nisolle, L., 47
Norris, H., 35, 156
Nusselt, W., 13, 100, 104, 128, 138, 139, 172, 209, 245
Nusselt number, 92

O

Ohm, 4
Optimum height of fin, 34
Optimum shape of fin, 35
Oscillations, 47
Over-all heat-transfer coefficient, 8

P

Parallel flow, 9
Partial pressure, 228
Peclet number, 130
Periodic temperature fluctuations, 51
Pfriem, H., 47, 60
Physically similar, 132
Pipe inlet, 65, 79
Piston engine, 53
Planck, M., 196
Plate, 49
  heat transfer, laminar, 88
Pohlhausen, E., 152, 162
Port, F., 210
Potential, electric, 21
Prandtl, L., 63, 66, 73, 74, 78, 81, 82, 106, 112, 124
Prandtl number, 90
Psychrometric chart, 231
Puckett, A., 150

Q

Quasi-stationary heat flow, 47

R

Radiation, 2, 193
Radiation intensity, 196
Radiator, 116
Rate of heat flow, 3
Recovery factor, 153
Rectangular fin, 30
Recuperator, 57
Reference temperature, 93, 115, 159
Reflection, diffuse, 193
  regular, 193
  specular, 193

Reflectivity, 193
Regenerator, 54
Regular reflection, 193
Reichardt, H., 83, 127
Relative humidity, 229
Resistivity, electric, 21
Reynolds' O., 63, 106, 107
Reynolds, analogy, 107
Reynolds number, 64
Rice, C., 164
Rocket, 156, 157, 183, 186, 192, 209
Rod, 25
Rohonczy, G., 81
Rough surface, 65, 78
Rubesin, M., 88, 94, 118, 150, 156

S

Saturated air, 229
Saturation curve, 233
Saunders, A., 164, 169
Schaaf, S., 186
Schack, A., 207
Schardin, H., 166
Schiller, L., 79
Schirmer, R., 238
Schlichting, H., 75
Schlieren method, 165
  photograph, 166
Schmidt, E., 35, 43, 98, 141, 162, 165, 171, 177, 203, 208, 245, 253
Schmidt, H., 203
Schmidt number, 250
Schmidt plot, 44
Schuh, 82
Schultz-Grunow, F., 74
Schurig, W., 177
Schwiedessen, 207, 209
Sellschopp, W., 177
Separation, flow, 83
  of gases, 54
Shearing-stress velocity, 82
Sherwood, T., 251
Short fin, 32
Sieber, W., 199
Sieder, E., 81, 104, 115
Similarity, 132
Slip, gas on a surface, 191
Slip coefficient, 192
Slip flow regime, 192
Smoke, cigarette, 64
Smoluchovski, M., 191
Soehngen, E., 139, 167, 169
Specific humidity, 229
Specific rate of heat flow, 4
Specific resistance, 5
Specular reflection, 193
Sphere, 25, 49
Spofford, W., 35
Squire, 95, 158, 163
Stagnation point, 83
Stalder, J., 192
Static state, 150
Steam boiler, 54, 109, 149, 207, 214, 221
Steam engines, 1, 53
Steel industry, 54
Stephan-Boltzmann law, '98
Stephan's law, 239
Sublayer, laminar, 73
Sulfur dioxide radiation, 205
Summerfield, M., 183
Supersaturation, 231
Surface element, 19

T

Tate, G., 81, 104, 115
Taylor, G., 106, 112, 124
Temperature, gradient, 19
  jump, 190
  measurement, 28
  profiles, turbulent, 113
Ten Bosch, 28, 112, 116, 140
Thermal boundary layer, 86
Thermal conductivity, 3
Thermal diffusivity, 42
Thermal radiation, 193
Thermal resistance, 5
Thermodiffusion, 238
Thermometer, 28, 50
Thermos bottle, 219
Thoma, H., 148
Tollmien, W., 75
Total state, 150
Touloukian, Y., 159

Transformer, 40
  coil, 40
Transmissivity, 193
Triangular fin, 35
Tsien, H., 190, 192
Tube, bundles, 16, 145
  in crossflow, heat transfer, 142
  flow in, 79
  insulated, 22
Turbulent boundary layer, 64
Turbulent flow, 63
Turbulent mixing motions, 106
Turbulent shearing stress, 107

U

Universal-temperature profile, 128
Universal-velocity profile, 83
Unsteady heat flow, 40

V

van der Hegge-Zynen, B., 77
Velocity profile, laminar, plate, 70
  turbulent, plate, 73
Velox boiler, 109, 157
Venant, D. S., and Wantzel's formula, 151
Viscosity, 62
Visualization of flow, 148
Vortex wake, 85
Vortices, 83

W

Wall, 3, 37, 44, 52
Warburg, 192
Warm-water heating, 34
Water equivalent, 10
Water vapor, radiation of, 205
Weight rate of flow, 10
Weinig, F., 36
Weise, W., 152
Well, 28
Wenner, K., 98, 141
Wet-bulb temperature, 256
Wiedmann, 190
Wien's law, 197
Wires in free convection, 164
Wohlenberg, W., 221

Y

Yamagata, K., 102
Yearly fluctuations, 53

Z

Zehnder-Mach interferometer, 166
Zobel, T., 169